

# Potential of refrigerant based district heating and cooling networks

THÈSE N° 6935 (2016)

PRÉSENTÉE LE 4 MARS 2016

À LA FACULTÉ DES SCIENCES ET TECHNIQUES DE L'INGÉNIEUR  
LABORATOIRE D'ÉNERGÉTIQUE INDUSTRIELLE  
PROGRAMME DOCTORAL EN ENERGIE

ÉCOLE POLYTECHNIQUE FÉDÉRALE DE LAUSANNE

POUR L'OBTENTION DU GRADE DE DOCTEUR ÈS SCIENCES

PAR

**Samuel HENCHOZ**

acceptée sur proposition du jury:

Dr J. Van Herle, président du jury  
Prof. F. Maréchal, Prof. D. Favrat, directeurs de thèse  
Prof. B. Elmegaard, rapporteur  
Dr P. Richner, rapporteur  
Prof. J. R. Thome, rapporteur



ÉCOLE POLYTECHNIQUE  
FÉDÉRALE DE LAUSANNE

Suisse  
2016





There is no energy crisis, only a crisis of ignorance.  
— R. Buckminster Fuller

On ne révolutionne pas en révolutionnant. On révolutionne en solutionnant.  
— Le Corbusier

A mes parents, ma famille, mes amis et à Soumaya.



# Remerciements

Je tiens à remercier le Prof. François Maréchal pour m'avoir accueilli dans son groupe de recherche (IPESE) et qui m'a permis de réaliser ce travail de façon très autonome, m'accordant une totale confiance et me laissant une liberté d'action peu commune et fort appréciée.

Mes remerciements vont aussi au Prof. Daniel Favrat qui m'a accueilli au Laboratoire d'Énergétique Industrielle (LENI) et a co-supervisé cette thèse. Dans les faits le Prof. Favrat est à l'origine du sujet de cette recherche et il a été mon principal interlocuteur pour les questions liées au contenu scientifique de cette thèse, mais aussi en ce qui concerne la gestion du projet de recherche dans son ensemble. Je lui suis extrêmement reconnaissant pour m'avoir fait partagé son expertise scientifique dans le domaines de l'énergie et de la thermodynamique et sa grande expérience pratique en matière de systèmes de conversion d'énergie. Je lui suis aussi reconnaissant pour la liberté d'action qu'il m'a laissé dans la réalisation de cette thèse ainsi que pour les coups de pouce lors des périodes où "tout n'allait pas tout seul."

Je me dois aussi de remercier la Commission pour la Technologie et l'Innovation d'avoir financé ce projet de recherche ainsi que les entreprises partenaires, soit le bureau d'ingénieur Amstein & Walthert et les services industriels de Genève - SIG. En particulier, je remercie Céline Weber de chez Amstein & Walthert et Laurent Rami des SIG pour m'avoir assisté dans le travail. Mes remerciements vont aussi à leur supérieur respectif, Messieurs Matthias Achermann et Michel Monnard, qui ont permis la mise en place du projet de recherche.

Je remercie aussi Pierre-Alain Giroud et Romain Rouffet de l'entreprise Zero-C. Ils ont permis la réalisation concrète du banc d'essai et ont fait montre d'une efficacité exemplaire. Avoir recours à Zero-C a été indéniablement une des meilleures décisions prises durant ce projet.

J'ai eu l'immense chance de pouvoir travailler avec quatre étudiants de Génie Mécanique, Silvio Giacomini, Simon Gailledrat, Zeli Zhang et Patrick Chatelan dans le cadre de projets de semestre, de diplômes et même pour deux d'entre eux en qualité d'ingénieurs. Ils ont participé activement aux réflexions liées au développement et à la réalisation du banc d'essai, mais aussi dans des aspects plus théoriques au cours desquels ils ont démontré l'excellence et l'étendue de leur capacités. Ils ont en outre été mes yeux, oreilles, mains et *pieds-au-cul* sur le site d'implantation du banc d'essai. Sans eux et tout le travail qu'ils ont abattu, cette thèse n'existerait tout simplement pas.

## Remerciements

---

Je remercie aussi les collègues que j'ai eu la chance de côtoyer au cours de ces cinq années de thèse, que ce soit au Laboratoire d'Énergétique Industrielle (LENI) ou, dans l'air post-LENI, au groupe d'Ingénierie des Procédés et Systèmes Énergétiques Intégrés (IPESE) et au Centre de l'Énergie de l'EPFL. L'ambiance excellente qui règne au sein de ces trois unités a été une source d'oxygène pour moi et il va sans dire que sans toute cette clique tout aurait été bien moins évident.

En parlant de clique, je remercie les camarades d'études de génie mécanique, l'équipe du cinéma de Cossonay, la troupe de théâtre dans laquelle j'ai eu le plaisir de jouer durant plus d'une décennie et tous mes autres amis. Ces personnes et les activités qui y sont liées m'ont permis de conserver un équilibre de vie qui a été plusieurs fois salvateur au cours de ces cinq années.

Je remercie aussi mes parents Claude et Marianne, ma sœur Sabine, mes frères, Gautier, Guillaume, Léonard et mon beau-frère Jean-Pierre qui m'ont soutenu durant tout ce temps et sur lesquels je prends régulièrement exemple lorsque je ressens le besoin de garder les pieds sur terre.

Enfin, *last but not least*, je remercie Soumaya et son soutien indéfectible dans les meilleurs moments comme dans les pires. En outre, je lui suis infiniment reconnaissant de m'avoir aidé autant qu'elle l'a fait pour la correction de cette thèse.

Lausanne, février 2016

S. H.

# Abstract

Urban areas represent an ever increasing challenge in terms of energy use and environmental impact associated with it. Projections from the United Nation expect this number to reach 66% by 2050. In Europe 40% of the final energy consumption and 36% of the emissions of greenhouse gases are caused by buildings. The building sector is also one of the area where there is a great potential of reduction of the greenhouse gases emissions and of the dependence on fossil fuels. Among the measures that can help realise this potential, efficient energy conversion technologies supplying thermal energy services could play an important role.

The present thesis aims at demonstrating the potential of a new type of district network, capable of delivering indistinctly cooling and heating services using a two-pipe network and in which the transfer of energy across the network is done by exploiting the evaporation/condensation of a refrigerant.

The main research question that this thesis attempts to answer is the following:

*Is it possible to build and operate safe, reliable, energy efficient and economically profitable district heating and cooling networks that use a refrigerant as a transfer fluid?*

The demonstration follows three axes, the first being a thermoeconomic analysis. This analysis focuses on a test case area in Geneva's city centre where 5 variants of refrigerant based district heating and cooling networks, one cold water network and the mix of conversion technologies currently in use are compared on the basis of their energy and exergy performances and on the economic profitability. Considerations on economic uncertainty, safety and technical issues are also included in the analysis. The key findings are:

- All the variants of network can potentially reduce the final energy consumption of over 80% as compared to the current situation.
- All the variants of network have rather similar exergy efficiencies comprised between 39.5% and 45%.
- The most profitable variant uses CO<sub>2</sub> as a transfer fluid and an open cycle CO<sub>2</sub> heat pump at the central plant. It costs initially between 27 and 35 mio €, reaches break-even in 4 to 6 years and the net present value after 40 years is comprised between 40 and 80 mio €.

## Abstract

---

- A cold water network is the second best option, although more expensive initially and thus less profitable, it has several advantages in terms of safety and availability of components.
- The CO<sub>2</sub> variants exhibit a much better compactness than the cold water network.

The second axis is the design, construction and testing of a lab scale refrigerant network. First a description of the design process and of the test facility is provided. It is followed by a presentation of the results of the test campaign. The tests aimed at demonstrating the practical feasibility of the concept, mostly by assessing the controllability of the network. Overall the good behaviour of the test facility and its ability to be smoothly and automatically controlled could be demonstrated, which further improved confidence in the practicality of the concept.

The third axis is the development of dynamic models of simulation. These models are described in the present manuscript. They include, heat exchangers, pipes, pumps and valves. A short comparison between experimental and simulation results is also provided. The comparison between experiment and simulation showed that at their current stage of development the models cannot simulate accurately enough a refrigerant based network. There are also issues in terms of numerical stability.

Key words: district heating and cooling, urban energy system, refrigerant, heat pump, thermoeconomic analysis, experimental facility, dynamic models of simulation

## Résumé

Les villes représentent un défi toujours plus grand en matière d'énergie et d'impact environnemental. Les nations unies prévoient que d'ici 2050 deux tiers de la population mondiale vivra dans les villes. En outre, actuellement en Europe le secteur du bâtiment engendre 40% de la consommation d'énergie finale et 36% des émissions de gaz à effet de serre. Il s'avère que ce secteur représente un potentiel important en matière de réduction des émissions de gaz à effet de serre et par la même de réduction de la dépendance aux énergies fossiles. Parmi les mesures pouvant contribuer à réaliser ce potentiel, les technologies efficaces de conversion d'énergie assurant les services énergétiques de chauffage et de refroidissement pourraient jouer un rôle prépondérant.

La thèse présentée ici, vise à démontrer le potentiel d'un nouveau type de réseau de distribution de chaleur et de froid à distance, ne nécessitant que deux conduites et dont la particularité est d'utiliser l'évaporation/la condensation d'un fluide frigorigène pour assurer les transferts d'énergie à travers le réseau.

La question à laquelle cette thèse tente de répondre est la suivante :

*Est-il possible de construire et opérer des réseaux de chaleur et de froid à distance basés sur l'utilisation d'un réfrigérant, d'une façon sûre, fiable, efficiente et économique ?*

La démonstration proposée dans cette thèse suit trois axes principaux, le premier étant une analyse thermoéconomique sur un quartier test du centre de Genève, où 5 variantes de réseaux à réfrigérants, un réseau à eau froide et le mix de systèmes de conversion actuellement utilisés sont comparés sur la base de leur performance énergétique et exergetique, ainsi que sur leur rentabilité économique. Des considérations de nature technique, mais aussi concernant la sécurité et les incertitudes économiques sont aussi prises en compte. Les résultats principaux sont :

- Toutes les variantes de réseau proposées permettraient une économie d'énergie finale supérieure à 80%.
- Ces variantes de réseaux ont des rendements exergetiques compris entre 39.5% et 45%.
- La variante la plus prometteuse utilise le CO<sub>2</sub> comme fluide de transfert et une pompe à chaleur au CO<sub>2</sub> à la centrale du réseau. Elle coûte initialement entre 27 et 35 mio. €, le point de début de rentabilité économique est situé entre 4 et 6 ans après la mise en service et la valeur actuelle nette après 40 ans est comprise entre 40 et 80 mio. €.

## Abstract

---

- Un réseau à eau froide et la seconde meilleure option qui, bien que plus chère, présente des avantages en termes de sécurité et de disponibilité des composants.
- Un réseau CO<sub>2</sub> est beaucoup plus compact qu'un réseau à eau froide.

Le second axe concerne la conception, la réalisation et l'expérimentation d'un réseau à réfrigérant à échelle réduite. Tout d'abord une description est faite du processus de conception de l'installation d'essai et de ces caractéristiques principales. Les résultats des essais sont ensuite discutés. Ces essais se sont focalisés sur la démonstration de la faisabilité du concept, principalement en ce qui concerne son contrôle automatique. Les essais ont montré le bon comportement de l'installation et ont validé le concept de contrôle automatique et ont donc permis de renforcer la confiance dans les aspects pratiques du concept de réseau CO<sub>2</sub>.

Le troisième axe consiste en la réalisation de modèles de simulation dynamiques. Ces modèles qui incluent des échangeurs de chaleur, des tuyaux, des pompes et des vannes sont décrits dans ce manuscrit. Une comparaison sommaire entre les résultats expérimentaux et de simulation est aussi fournie. La comparaison entre la simulation et les résultats expérimentaux ont mis en évidence que les modèles, dans leur états actuels ne permettent pas de rendre compte du fonctionnement d'un réseau à réfrigérant de façon adéquate. En outre des problèmes de stabilité numérique sont survenus.

Mots clefs : chauffage et refroidissement à distance, systèmes énergétiques urbains, réfrigérant, pompe à chaleur, analyse thermo-économique, installation expérimentale, modèles de simulation dynamique.



# Contents

<b>Remerciements</b>	<b>i</b>
<b>Abstract (English/Français)</b>	<b>iii</b>
<b>List of figures</b>	<b>xi</b>
<b>List of tables</b>	<b>xv</b>
<b>Nomenclature</b>	<b>xvii</b>
<b>Introduction</b>	<b>1</b>
<b>1 Thermoeconomic analysis</b>	<b>5</b>
1.1 Introduction . . . . .	5
1.2 Urban area studied . . . . .	7
1.3 Thermal energy needs . . . . .	9
1.4 Conversion technologies: An energy comparison . . . . .	14
1.4.1 Currently used technology . . . . .	16
1.4.2 Refrigerant based networks . . . . .	22
1.4.3 Cold water based district energy networks . . . . .	50
1.4.4 Exergy loss and efficiency . . . . .	57
1.4.5 Comparison and intermediate conclusion . . . . .	68
1.5 Conversion technologies: Evaluation of the investment . . . . .	72
1.5.1 Currently used technologies - Boilers and chillers . . . . .	72
1.5.2 CO <sub>2</sub> based networks . . . . .	73
1.5.3 R1234yf and R1234ze based networks . . . . .	77
1.5.4 Cold water network . . . . .	77
1.5.5 Comparison of the required investment . . . . .	78
1.6 Conversion technologies: An economic profitability analysis . . . . .	79
1.6.1 Maximisation of the net present value . . . . .	83
1.6.2 Evolution of the NPV for the different technologies . . . . .	87
1.6.3 Safety and its impact on the profitability . . . . .	89
1.6.4 Cost of the fluid and its impact on the profitability . . . . .	96
1.6.5 Intermediate conclusion from the profitability analysis . . . . .	98
1.7 Conversion technologies: Economic robustness . . . . .	100

## Contents

---

1.7.1	Simulation of the Rues Basses test case using stochastic processes: Modelling . . . . .	101
1.7.2	Simulation of the Rues Basses test case using stochastic processes: Results	111
1.8	CO <sub>2</sub> vs. cold water: On technical issues. . . . .	116
1.8.1	Compactness . . . . .	117
1.8.2	Availability of the equipment . . . . .	120
1.9	Conclusion from the thermoeconomic analysis . . . . .	122
<b>2</b>	<b>Experimental facility and test campaign</b>	<b>127</b>
2.1	Design process . . . . .	127
2.2	Description of the normal operation . . . . .	134
2.3	Test campaign: Stationary tests and fitting of a heat transfer correlation . . . . .	138
2.4	Test campaign: Assessment of dynamic behaviour and controllability. . . . .	142
2.4.1	Stationary tests and example of a heat load step reduction. . . . .	142
2.4.2	Example of pressure setpoint step change (50-52 bar) . . . . .	143
2.4.3	Example of pressure setpoint change, 3 min ramp (50-52 bar) . . . . .	145
2.4.4	Example of pressure setpoint downward change, 2 min ramp (58-54 bar) . . . . .	150
2.4.5	On other dynamic tests . . . . .	153
2.4.6	Tests assessing the risks linked to hydro-acoustic phenomena . . . . .	156
2.4.7	Mishaps, or why the full certification was in the end useful . . . . .	158
2.5	Conclusion on the experimental facility and test campaign . . . . .	159
<b>3</b>	<b>Dynamic Modelling and Simulation</b>	<b>163</b>
3.1	Introduction . . . . .	163
3.2	State of the art . . . . .	163
3.3	Condenser and evaporator: Modelling approach . . . . .	165
3.3.1	Refrigerant channel . . . . .	167
3.3.2	Water channel . . . . .	171
3.3.3	Wall . . . . .	172
3.3.4	Water side heat transfer coefficient and friction factor . . . . .	172
3.3.5	Refrigerant side heat transfer coefficient . . . . .	172
3.3.6	Thermodynamic and transport properties . . . . .	173
3.3.7	Discretization scheme . . . . .	174
3.4	Pipes: Modelling approach . . . . .	174
3.4.1	Refrigerant pipe . . . . .	174
3.4.2	Refrigerant side heat transfer coefficient and friction factor . . . . .	176
3.4.3	Thermodynamic and transport properties . . . . .	177
3.4.4	Discretization scheme . . . . .	177
3.5	Pump model . . . . .	177
3.6	Valve model . . . . .	178
3.7	Example of results: Cooling user substation . . . . .	179
3.8	Example of results: Comparison of the test bench dynamics and a simulation . . . . .	182
3.9	Conclusion on the dynamic modelling and simulation . . . . .	185

<b>Conclusion</b>	<b>191</b>
<b>A Centrifugal compressors</b>	<b>195</b>
<b>B Cost functions</b>	<b>199</b>
<b>C Description of the safety concept</b>	<b>205</b>
<b>Bibliography</b>	<b>219</b>
<b>Curriculum Vitae</b>	<b>221</b>



# List of Figures

1.1	Test case area: Rues Basses . . . . .	9
1.2	Daily thermal energy demand . . . . .	12
1.3	Test case area load curve . . . . .	15
1.4	Comparison of modeled and statistical values of heat expense indices . . . . .	16
1.5	Installed heating capacity in the test case area . . . . .	17
1.6	Seasonal exergy efficiency of water cooled chillers . . . . .	20
1.7	Current tech. - heating oil and electricity consumption . . . . .	21
1.8	Schematic representation of a refrigerant based district energy network . . . . .	24
1.9	CO <sub>2</sub> network: Representation of the decentralized heat pump cycles . . . . .	29
1.10	Efficiency map of the decentralized heat pump compressors . . . . .	32
1.11	CO <sub>2</sub> network: Central plant heat pump cycles . . . . .	37
1.12	Layout of the CO <sub>2</sub> network studied for the test case area. . . . .	38
1.13	CO <sub>2</sub> network with CO <sub>2</sub> central HP: Electricity consumption. . . . .	40
1.14	CO <sub>2</sub> network with CO <sub>2</sub> central HP: Electric load curve. . . . .	41
1.15	R1234yf/ze network with open cycle heat pumps. . . . .	43
1.16	R1234yf/ze network: Representation of the decentralized heat pump cycles . . . . .	44
1.17	R1234yf/ze network: Representation of the centralized heat pump cycle . . . . .	45
1.18	R1234yf network: Electricity consumption. . . . .	47
1.19	R1234yf network: Electric load curve. . . . .	48
1.20	R1234ze network: Electric load curve. . . . .	49
1.21	Cold water network schematics . . . . .	53
1.22	Cold water network: heat pump cycles . . . . .	54
1.23	Cold water network: Electricity consumption. . . . .	56
1.24	Cold water network: Electric load curve. . . . .	57
1.25	Exergy analysis: Control volume. . . . .	59
1.26	Exergy analysis: Transformation exergy of liquid water. . . . .	61
1.27	Exergy analysis: Boilers + Chillers supply & demand . . . . .	62
1.28	Exergy analysis: CO <sub>2</sub> network supply & demand . . . . .	63
1.29	Exergy analysis: R1234ze network supply & demand . . . . .	64
1.30	Exergy analysis: Cold water network supply & demand . . . . .	65
1.31	Exergy analysis: Efficiency vs. duration . . . . .	67
1.32	Exergy analysis: Exergy loss reduction . . . . .	68
1.33	CO <sub>2</sub> network with CO <sub>2</sub> HP: Max NPV . . . . .	86

## List of Figures

---

1.34 CO <sub>2</sub> network with NH <sub>3</sub> HP: Max NPV . . . . .	87
1.35 CO <sub>2</sub> network with R1234yf HP: Max NPV . . . . .	88
1.36 R1234yf network: Max NPV . . . . .	89
1.37 R1234ze network: Max NPV . . . . .	90
1.38 Cold water network: Max NPV . . . . .	91
1.39 CO <sub>2</sub> network with CO <sub>2</sub> HP: Inv. vs. operating costs . . . . .	92
1.40 R1234yf network: Inv. vs. operating costs . . . . .	92
1.41 Cold water network: Inv. vs. operating costs . . . . .	93
1.42 Evolution of the NPV over the lifetime . . . . .	94
1.43 Stochastic modelling of inflation rates . . . . .	107
1.44 Boilers and chillers: Distribution of NPV . . . . .	113
1.45 CO <sub>2</sub> network: Distribution of NPV . . . . .	115
1.46 Boilers and chillers: Distribution of NPV . . . . .	116
1.47 Compactness comparison of the various networks . . . . .	119
1.48 Representation of a sectioning valve room for a refrigerant network. . . . .	121
2.1 PFD of the test bench - state april 2015 . . . . .	131
2.2 View of the test bench - central plant side . . . . .	132
2.3 View of the test bench - user side . . . . .	133
2.4 Detail of the central plant . . . . .	135
2.5 CO <sub>2</sub> evaporation/condensation heat transfer coef. - relative error . . . . .	140
2.6 CO <sub>2</sub> evaporation/condensation heat transfer coef. vs mass velocity . . . . .	140
2.7 CO <sub>2</sub> average void fraction as function of the temperature . . . . .	141
2.8 Control of pressure and superheat . . . . .	144
2.9 CO <sub>2</sub> massflow and control of delta P . . . . .	144
2.10 CO <sub>2</sub> massflow and value of the PID output signal to valve 3002 . . . . .	146
2.11 Pressure step (up) change: Control of pressure and superheat . . . . .	146
2.12 Pressure step (up) change: Control of superheat and $\Delta P$ . . . . .	147
2.13 Pressure step (up) change: CO <sub>2</sub> mass flowrates and CO <sub>2</sub> pump frequency . . . . .	148
2.14 Pressure step (up) change: condenser subcooling and valves opening . . . . .	149
2.15 Pressure ramp (up) change: Control of pressure and superheat . . . . .	151
2.16 Pressure ramp (up) change: Control of superheat and $\Delta P$ . . . . .	151
2.17 Pressure ramp (up) change: CO <sub>2</sub> mass flowrates and CO <sub>2</sub> pump frequency . . . . .	152
2.18 Pressure ramp (up) change: condenser subcooling and valves opening . . . . .	152
2.19 Pressure ramp (down) change: Control of pressure and superheat . . . . .	154
2.20 Pressure ramp (down) change: Control of superheat and $\Delta P$ . . . . .	154
2.21 Pressure ramp (down) change: CO <sub>2</sub> mass flowrates and CO <sub>2</sub> pump frequency . . . . .	155
2.22 Pressure ramp (down) change: condenser subcooling and valve opening . . . . .	155
2.23 Pressure ramp (down) change: Mass of CO <sub>2</sub> processed and mas imbalance . . . . .	161
2.24 Liquid hammer after a quick valve closure at high load . . . . .	161
2.25 Burst fitting, close view . . . . .	162
3.1 Plate heat exchangers geometry . . . . .	165

3.2	Dynamic model of evaporator/condenser: Sub-models and their interfacing. .	166
3.3	Dynamic model of evaporator/condenser: Refrigerant channel control volume.	167
3.4	Schematic representation of a free cooling substation . . . . .	179
3.5	Free cooling substation: Response to mass flowrate perturbation . . . . .	181
3.6	Free cooling substation: Response to enthalpy perturbations . . . . .	181
3.7	Free cooling substation: Response to pressure perturbations . . . . .	182
3.8	Comparison experiment vs. dynamic simulation: Case 1 . . . . .	186
3.9	Comparison experiment vs. dynamic simulation: Case 4 . . . . .	187
3.10	Comparison experiment vs. dynamic simulation: Case 3 . . . . .	188
3.11	Pressure ramp (up) change - simulation vs. experiment: pressure and superheat	189
3.12	Pressure ramp (up) change - simulation vs. experiment: subcooling and delta P	189
A.1	CO <sub>2</sub> network: Central plant heat pump compressor characteristics . . . . .	197
A.2	CO <sub>2</sub> network: Central plant heat pump compressor geometry . . . . .	198
B.1	Cost function: Brine-water heat pumps . . . . .	201
B.2	Cost function: Compressors . . . . .	202
B.3	Cost function: Heat exchangers . . . . .	203
B.4	Cost function: Water pumps . . . . .	204





# List of Tables

1.1	Thermoeconomic factors . . . . .	6
1.2	ERA of the Rues Basses test case . . . . .	10
1.3	Yearly energy and thermal loss coef. of buildings . . . . .	11
1.4	Numerical parameters - Current conversion technology . . . . .	20
1.5	Thermodynamic and transport properties for CO <sub>2</sub> ,R1234yf/ze . . . . .	26
1.6	Specifications of the decentralized heat pump compressors . . . . .	31
1.7	Maximum liquid velocities in pipe . . . . .	33
1.8	CO <sub>2</sub> network: Values of the various numerical parameters . . . . .	39
1.9	R1234yf and R1234ze networks: Values of the various numerical parameters . . . . .	46
1.10	Cold water network: Values of the various numerical parameters . . . . .	58
1.11	Energy indicators for the various technologies . . . . .	71
1.12	List of the cost functions used . . . . .	74
1.13	Detail of the investment required - Part 1. . . . .	80
1.14	Detail of the investment required - Part 2. . . . .	81
1.15	Possible damages caused by a refrigerant network . . . . .	97
1.16	Water quality required in district heating networks . . . . .	98
1.17	Potential of improvement of buildings . . . . .	108
2.1	Design specifications for the test facility . . . . .	129
3.1	Conditions of the simulation: Initial conditions, and final values of the perturbations . . . . .	180



# Nomenclature

## Latin letters

$\Delta T_{min}$	Minimum approach of temperature difference [K]
$\dot{G}$	Mass velocity [ $\text{kg s}^{-1} \text{m}^{-2}$ ]
$\dot{m}$	Mass flowrate [ $\text{kg s}^{-1}$ ]
$A$	Area [ $\text{m}^2$ ]
$C$	Velocity [ $\text{m s}^{-1}$ ]
$c$	Specific heat capacity [ $\text{J kg}^{-1} \text{K}^{-1}$ ]
$COP$	Coefficient of performance [-] for heating ( $h$ ), cooling ( $c$ ) or both ( $h+c$ )
$D_H$	Hydraulic diameter [m]
$E$	Electric, mechanical energy or Exergy [J]
$E$	Isothermal bulk modulus (Chapter 2) [ $\text{N m}^{-2}$ ]
$e$	Thickness [m]
$E_y$	Transformation exergy [J]
$F$	Force [N]
$f$	Friction factor [-]
$h$	Specific enthalpy [ $\text{J kg}^{-1}$ ]
$j$	Imaginary number [-]
$k$	Specific coenthalpy [ $\text{J kg}^{-1}$ ]
$K_v$	Valve flow factor [-]
$L$	Exergy loss [J]
$l$	Length [m]

## Nomenclature

---

$M$	Mass [kg]
$n$	Generic quantity (number of plates, blades, connections...) [-]
$P$	Pressure [ $\text{N m}^{-2}$ ]
$Q$	Heat energy [J]
$s$	Specific entropy [ $\text{J kg}^{-1} \text{K}^{-1}$ ]
$T$	Temperature [ $^{\circ}\text{C}$ ]
$T_a$	Ambient temperature [ $^{\circ}\text{C}$ ]
$U$	Internal energy (Chapter 3) [J]
$U$	Overall heat transfer coefficient [ $\text{W m}^{-2} \text{K}^{-1}$ ]
$V$	Volume [ $\text{m}^3$ ]
$v$	Specific volume [ $\text{m}^3 \text{kg}^{-1}$ ]
$w$	Width [m]
$Y$	Transformation energy [J]
$Y$	Young's modulus (Chapter 2) [ $\text{N m}^{-2}$ ]

## Greek letters

$\alpha$	Heat transfer coefficient [ $\text{W m}^{-2} \text{K}^{-1}$ ]
$\chi$	Boilers: load factor [-]
$\epsilon$	Relative error [-]
$\epsilon$	Void fraction (Chapter 2) [-]
$\epsilon_n$	Boilers: first law efficiency at full load [-]
$\eta$	Exergy efficiency [-]
$\eta_{Cs}$	Compressor isentropic efficiency [-]
$\eta_C$	Compressor efficiency [-]
$\eta_p$	Pump efficiency [-]
$\kappa$	Roughness [m]
$\lambda_0$	Boilers: residual consumption at idling condition [-]

$\nu$	Frequency [ $s^{-1}$ ]
$\Phi$	Area enhancement factor (Chapter 3) [-]
$\phi$	Diameter [m]
$\Pi$	Perimeter [m]
$\rho$	Density [ $kg\ m^{-3}$ ]
$\tau$	Inflation rate [-]
$\theta$	Angle [rad]

**Indices**

<i>a</i>	Ambient
<i>AC</i>	Air conditioning
<i>air</i>	Cooling air for chillers
<i>booster</i>	booster pump/compressor
<i>c</i>	Cold stream (Chapter 3)
<i>c, out</i>	Evaporator - chilled water outlet
<i>CDC</i>	Cooling of data centres
<i>cond</i>	Condensation
<i>condensate</i>	condensate extraction pump
<i>connect</i>	Connections: Network main line - users
<i>CP</i>	Central plant
<i>cycle</i>	Thermodynamic cycle
<i>DHW</i>	Domestic hot water
<i>dissip</i>	Heat dissipation
<i>ERA</i>	Energy reference area
<i>evap</i>	Evaporation
<i>f</i>	Heating oil
<i>H</i>	Space heating
<i>h</i>	Hot stream (Chapter 3)

## Nomenclature

---

<i>h, out</i>	Condenser - cooling water outlet
<i>HEX</i>	Heat exchanger
<i>HP</i>	Heat pumping
<i>in</i>	Inlet
<i>lake</i>	Lake water
<i>liq</i>	Liquid
<i>max</i>	Maximum
<i>MDAC</i>	Mechanical draught air cooler
<i>min</i>	Minimum
<i>N</i>	Network
<i>n</i>	Nominal
<i>out</i>	Outlet
<i>pipe</i>	Pipe
<i>plate</i>	Plate (of a heat exchanger)
<i>R</i>	Refrigeration (for commercial use)
<i>rad</i>	Radiator (heat emitter)
<i>ref</i>	Reference conditions
<i>refr</i>	Refrigerant
<i>ren</i>	Renovated
<i>rr</i>	Heat exchange: Refrigerant/refrigerant
<i>rw</i>	Heat exchange: Refrigerant/water
<i>s</i>	Isentropic process
<i>sat</i>	Saturation
<i>SC</i>	Subcooling
<i>service</i>	Energy service
<i>SH</i>	Superheat
<i>summer</i>	Summer conditions (cooling season)

<i>tot</i>	Total
<i>vap</i>	Vapour
<i>w</i>	Water
<i>winter</i>	Winter conditions (heating season)
<i>ww</i>	Heat exchange: Water/water

### Superscripts

+	Positive entering the system
–	Positive leaving the system

### Acronyms

CEPCI	Chemical engineering plant cost index
ERA	Energy reference area
ESEER	European seasonal energy efficiency ratio
GWP	Global warming potential, expressed in mass of CO <sub>2</sub> equivalent per unit mass
HEI	Heat expense index
HFC	Hydrofluorocarbon (family of synthetic refrigerants)
HFO	Hydrofluoroolefin (family of synthetic refrigerants)
LMTD	Logarithmic mean temperature difference
MAO	Major accident ordinance
PLC	Programmable logic controllers
YDD	Yearly degree-days

### Conventions

$\bar{X}$	Average value of the quantity X
$\Delta X$	Difference between two values of the quantity X
$\dot{X}$	First time derivative of the quantity X





# Introduction

Urban areas represent an ever increasing challenge in terms of energy use and environmental impact associated with it. According to the World Bank [1], the share of the world population living in urban areas rose steadily from 34% to 53% over the period 1961-2013, and projections from the United Nation expect this number to reach 66% by 2050. In Switzerland the current figure is 73%, which is on parity with the value in Europe. According to URBACT [2] the building sector in the European Union accounts for 40% of the final energy consumption and 36% of the emissions of greenhouse gases. It also considers that energy efficiency in buildings located in urban areas represents one of the greatest potential to cut down greenhouse gases emissions and reduce the impact of the European society on the climate. According to the Swiss Federal Office for Energy [3], the final energy consumption associated to thermal energy services in the sectors of households, services, industries are 87.6%, 71.5% and 68% respectively. Therefore, in order to realize the potential of energy savings in urban areas, it appears crucial to develop efficient energy conversion technologies dedicated to the thermal services. Obviously, other measures have to be taken jointly in order to reach the full potential of savings in the urban building sector. Measures such as the improvement on the envelope of buildings, the management of solar and internal gains or a better integration of electrical and thermal energy services.

Among the technologies particularly suited to supply thermal energy services to urban areas, district heating and cooling networks are well placed.

## Historical development and current trends in district energy networks

The oldest known use of water to deliver heat via network dates back to 1334 in *Chaudes-Aigues*, France. Geothermal spring water was brought to houses via a network of wooden pipes, the local lord charged users with a fee for the concession [4]. Over the centuries the system evolved and expanded providing heat for the buildings, workshop and mills of the town. Operation ceased in 2009 when it was decided to use the geothermal water in a hydrothermal therapy centre.

The first district heating as it is understood today started operation in 1877 in New-York, distributing steam to the customers, where it was condensed and then brought back to the central plant to be re-vaporized in a boiler.

## Introduction

---

In 2011, countries members of Euroheat and power [5] had over 482'000 km of district heating in operation, 2/3 of which for Russia and China only, they provided 3'276 TWh of heat for the final users. The share of the population connected to district heating networks in all these countries is in average 28.6%. Two major technological shifts have occurred over the twentieth century with regard to the technology of district heating. The first shift concerns the supply temperature that gradually decreased as new networks were being built. Networks built in the early 1900's typically distribute steam at about 300°C, while those built between 1930 and 1970 rely on superheated water supplied at more than 120°C and more recent networks operate with water at 80°C. The trend toward lower supply temperatures continues as networks at 50°C are considered for the supply of energy efficient building areas [6, 7, 8]. For instance, since 1985 space heating is delivered to the campus of EPFL by two networks, one with a supply temperature of 65°C (at  $T_a = -10^\circ\text{C}$ ) feeding the oldest buildings and one at 50°C for the newer constructions. The second shift concerns the conversion technologies used in these networks. Initially, fossil fuelled heat-only producing boilers were the only technology, but over the years, and especially after the oil crises of 1973 and 1979, steam cycle based cogeneration plants became widespread. In 2011 and for the OECD countries the share of district heat provided by cogeneration plants reached 79% [9]. One also has to mention the successful integration in district heating of biomass or municipal solid wastes fired boilers/CHP plants, of gas turbines either in single or combined cycles, of electric or absorption heat pumps and of solar thermal collectors [10, 11, 12, 13, 14].

Since the 1980's, district cooling networks have also been in use [15], they consist in distributing cold water to the customers through a network of pipes, either in a closed or open loop. The cold water can be directly pumped from a river, a lake or a sea and sent trough the network or it can also be used in a heat exchanger at the central plant to cool down the water from the network. Finally, if the water from the source is not cold enough, centralized water cooled chillers are used. Where both district heating and cooling networks coexist, heat pumps at the central plant are sometimes used to provide both services simultaneously [15]. Another trend of development is the use of a single network to provide heating and cooling services. It has been proposed to use a district heating network to deliver heat to the hot side of absorption chillers installed at the users end, allowing the delivery of cooling services which reduce the relative thermal loss during the hot season. The use, at the user's end, of absorption heat pumps and/or small cogeneration units based on ORCs is also a mean to increase the energy efficiency when an existing high temperature district heating networks is used to provide heat to modern buildings equipped with low temperature hydronic loops [16, 17]. In some cold water networks, essentially built for cooling purposes, decentralized electric heat pumps are sometimes used to deliver heating services [15]. The major interest of using decentralized heat pumps is to supply heat at a temperature adapted to each user, thus reducing the electricity consumption when the stock of buildings is heterogeneous as compared to a centralized solution with a single supply temperature fixed by the most demanding consumer. There is a maximum limit to the use of decentralized heat pumps in networks where the users are connected in series (no return line) to avoid freezing in the pipes. For a network with the users connected between a supply and a return line, there is no such limit, the maximum

amount of decentralized heat pumping being mostly linked to the maximum flowrate and the supply temperature. For instance, at the time of writing, a 28 MW district heating network relying on a cold water loop feeding decentralized heat pumps started operating in 2015 in “La Tour-de-Peilz” (Switzerland) [18]. Over the last decade, concepts of enhanced networks have been proposed. They are able to supply heating and cooling at temperatures adapted to each building. They also allow the recovery of waste heat emitted by cooling users for valorisation at the heating users. These concepts operate at similar temperatures, between 5°C and 15°C, allowing the use of direct cooling for most of the cooling services and provide heat via the extensive use of decentralized heat pumps. Furthermore they all use a small or no temperature difference between the two pipes they rely on. The main topological difference that can be identified is the use of water vs. refrigerant fluids as heat transfer media. The water based advanced district energy networks seem to have appeared in Switzerland over the last 5 years, in the German speaking part they are referred to as “Anergienetze”. To the author’s knowledge, three such networks are in operation [19, 20, 21], the largest one, on the campus of ETHZ – Honggerberg, is part of a set of measures that allows the campus to reach the per capita targets of 2 kW average primary energy consumption and 1 ton/year emission of CO<sub>2</sub> equivalent [19]. Refrigerant based district energy networks are still at the research stage, they rely on the latent heat of evaporation/condensation of a refrigerant to collect and transfer heat across the network [22, 23, 24, 25, 26]. Until recently, the focus was exclusively on the use of CO<sub>2</sub> as a refrigerant, as it is the only non toxic, non flammable one among the natural refrigerants available [27]. However CO<sub>2</sub> still presents some challenges and the recent appearance of HFO refrigerants made the question of the choice of the heat transfer media worth reinvestigating [28].

### Scope of the thesis and organisation of the manuscript

This thesis is part of a research project, cofunded by the Swiss Commission for Technology and Innovation, the engineering firm Amstein & Walthert and Geneva’s utility company, SIG. The goal was to pursue the research on district heating and cooling networks that use refrigerants as heat transfer media with a strong focus on application. The research question that motivated this work can be summed up as follows:

*Is it possible to build and operate safe, reliable, energy efficient and economically profitable district heating and cooling networks that use a refrigerant as a transfer fluid?*

It resulted in three following major topics, a thorough thermoeconomic analysis, the development/testing of a lab scale network and the development of a dynamic model of the technology. These three topics constitute the three chapters of the present manuscript.

**Chapter 1: Thermoeconomic analysis** In this analysis, a test case urban area is described and the models predicting the heat and cooling demand are presented. Then models

of seven different energy conversion technologies are described. These technologies comprise the conversion technologies currently used in the area, 5 versions of refrigerant based networks and a cold water network. These technologies are each considered for the supply of the thermal energy services to the test case area. The analysis compares the technologies with the following criteria:

- Energy performance
- Exergy performance
- Initial investment required
- Profitability based on the net present value
- Robustness regarding uncertain economic conditions
- Technology and safety related considerations

**Chapter 2: Experimental facility** In this chapter, first the design requirements of the test facility are described, then a description of the test facility is provided and finally the results of the various tests are presented.

**Chapter 3: Dynamic Modelling and Simulation** In this last chapter, a description of the dynamic models developed for the heat exchangers and network pipes is first provided. Then the models of pump and valves are shortly described, and finally two examples of results are provided. This includes a succinct comparison between the dynamic simulation and the experimental tests.

# 1 Thermoeconomic analysis

## 1.1 Introduction

Globally, energy systems, as the rest of man-made constructions, are part of a very intricate, highly non linear socio-economic system, subject to physical and environmental constraints. The dynamics of these systems and of their coupling with the rest of the socio-economic system and its environment is also very complex, in the sense that some of the time constants might well be in the order of a few seconds, as for instance blackout events in the electric grid, to at least centuries when it comes to the climatic response to the increase in concentration of greenhouse gases in the atmosphere. In particular, energy systems are part of what can be considered the heavy infrastructure of the socio-economic system. They are crucial to the rest and are to be taken very seriously as their effects can be very far reaching and might last over very long periods of time.

When a new energy system is to be envisaged, either as an entirely new piece of infrastructure or as a retrofit/extension, a methodology to compare the various options is required. First, a methodology and a set of metrics should be defined and applied to the various proposed technologies. Special care must be taken in order to keep the comparison unbiased. Second, an assessment of the response of the proposed technologies to changing framework conditions should be carried out to check how the proposed technologies cope with variations that can be treated in a probabilistically sound way. As said earlier, the variety of the implications, influential factors and impacts of energy systems are very diverse and when it comes to compare several options a wise choice of metrics is a key element to obtain meaningful results. As long as the process is to be of a scientific kind, ethical integrity should prevail and provide a certain confidence in the pertinence of the analysis. However the aforementioned variety of factors at play in energy systems makes it virtually impossible to cover the entire picture, or at least within the time for one person to do a PhD. In the present study, whenever it was felt necessary, the limitations of the approach used are discussed. Some of the elements at play in energy systems are listed in Table 1.1. Some metrics that can be used to assess these elements are also mentioned.

## Chapter 1. Thermoeconomic analysis

---

In the perspective of developing the technology of district energy networks based on refrigerants the following research questions were formulated and constitute the backbone of the present thermoeconomic analysis:

- What are the typical characteristics of the thermal energy needs in urban areas?
- How does the energy conversion technology currently in place perform?
- What are the possible working fluid for a refrigerant based network?
- How would such networks perform in these urban areas?
- How would they perform relatively to each other?
- How would the closest competing technology perform?
- How would performances be affected by the uncertainties associated to the framework conditions?

Table 1.1 – Typical influential factors that can be included in an energy systems analysis

Factor	Metrics
Energy performance	Final energy consumption 1st law efficiency 2nd law efficiency
Economic performance	Net present value Payback time Capital expenditure
Environmental impact	Life cycle analysis Embodied energy Extended exergy analysis
Safety and security	Probabilistic risk assessment Security of supply
Technology readiness Social impact	Technology readiness level

Of the factors mentioned in Table 1.1 only, the energy performance and the economic performance have been quantitatively kept in the analysis. The "safety and security" criterion was taken into account only qualitatively and mostly to narrow down the number of possible working fluids.

The following criteria have been dropped out of the analysis:

**Environmental impact** It was dropped out of the current study based on intuition and on the finding from former studies [22, 23]. These studies showed that a district heating and cooling network solely relying on heat pumping to provide heating and mostly

on free cooling to provide the cooling services, would lead to much lower final energy consumption and emission of greenhouse gases. However, a rigorous environmental impact assessment should be done for the proposed technology. The life cycle assessment (LCA) based method from Gerber could be used [29] as well as the extended exergy analysis as defined by Rocco et al. in [30].

**Technology readiness** The technology readiness of the proposed technology was at the beginning of this work, in 2010, at TRL 1<sup>1</sup> to TRL 2<sup>2</sup> according to [31]. The main goal of the present thesis was to advance in the development from the early conceptual stage to a stage corresponding roughly to TRL 5<sup>3</sup>. The next step then would be the design and construction of an engineering scale pilot network. In the present thermoeconomic analysis the several variants of refrigerant based network that will be presented are similar enough, to be considered at a same level of development, hence their technology readiness level will not be useful to discriminate between the different variants of network. However, the level of readiness of the closest competing technology is much higher since several commercial networks exist already. This will be retained in the analysis of the results.

**Social impact** The social impact of the various technologies that will be presented in this study has been neglected. The social impact of the proposed networks could take various forms, such as modifications in the housing prices, improvement of the air quality and subsequent positive effects on the population health, influences on the local HVAC equipments installers and retailers. It could also encompass the study of the public acceptance of refrigerant based networks. How are they perceived? How could the perception be positively changed? Which business/sales model would lead to the widest social acceptance? How should these models be changed if refrigerant based networks were to be installed in an other region/country?

All these questions are worth investigating. However the competences required to treat them are not those of an engineering PhD student. Furthermore the author believes that the energy and economic potential of district energy networks using refrigerants should be assessed in priority, as these two aspects are sufficient to determine whether there is an interest in pursuing with the development of the technology. If the energy and economic perspectives are promising, then the environmental and social impacts should be integrated in the design process of the technology.

## 1.2 Urban area studied

Since the two industrial partners involved in the project are both located in Geneva, Switzerland, the test case area was logically chosen within this city. The area of "Rues Basses" was chosen at an early stage of the project. Initially it was viewed as a good potential candidate for

---

<sup>1</sup>TRL 1: Basic principles observed and reported.

<sup>2</sup>TRL 2: Technology concept and/or application formulated.

<sup>3</sup>TRL 5: Laboratory/bench scale, similar system validation in relevant environment

## Chapter 1. Thermo-economic analysis

---

a first implementation of a full scale pilot network. However a study, carried out by one of the industrial partners, the engineering company Amstein & Walthert, showed later on that some practical considerations made it a poor choice:

- The area is large in terms of size and energy demand for a first full scale prototype. The risk involved was deemed as being too important.
- The potential customers are too numerous and some key ones are likely not to accept relying on an untested technology (banks, insurance and international trading firms).
- A large number of public transportation lines pass through these streets and their rerouting during the construction period would be very difficult.
- Initially it was assumed that an existing utility tunnel passing below the streets could be used but is much too deep in the ground to be of any interest.

Nevertheless, the thermo-economic analysis was done using this area as a test case, since data such as the energy reference area (ERA) and the types of buildings had been made available at an early stage by Geneva's cantonal office for energy [32].

The area is located on the South bank of Lake Geneva at its outlet where the water flows into the Rhône river. It is approximately 900 m long and 200 m wide. The buildings in the area have mixed affectations, comprising in term of energy reference area (ERA) 23% of commercial surface, 60% of office and 17% of residential. The total ERA of the test case area is 687'843 m<sup>2</sup>. The population density in this area varies from 1'600 inhabitants km<sup>-2</sup> at the north-western end to around 3'200 inhabitants km<sup>-2</sup> at the south-west. This is a low value as compared to some areas of Geneva in excess of 25'000 inhabitants km<sup>-2</sup>. It is caused by the large share of commercial and office buildings in the area.

Fig. 1.1 shows a map of the area studied. The area was divided in 32 groups of buildings for which the six following possible types were considered:

- Commercial - Shop
- Commercial - Restaurant
- Office - Individual offices
- Office - Open space offices
- Residential - built before 1990
- Residential - built after 1990

Table 1.2 shows the ERA for the groups of buildings depicted in Fig. 1.1. It shows also the repartition between the six possible affectation considered in this study.



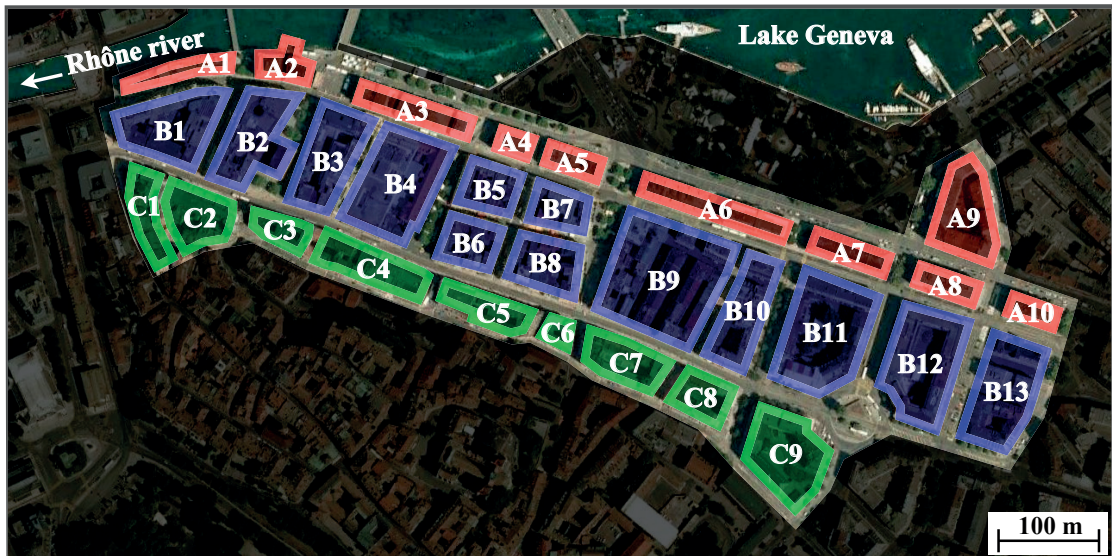


Figure 1.1 – Map of the test case area of "Rues Basses" showing the subdivision used for the various groups of buildings.

### 1.3 Thermal energy needs

As the urban area considered encompasses a relatively broad mix of buildings affectations, the thermal energy services required are similarly broad. For the present study it has been decided to consider the following ones.

- Space heating
- Air conditioning
- Hot water preparation
- Refrigeration (for commercial use)
- Cooling of data centres.

For each of the six categories of buildings affectation, the yearly energy required for a given service was computed using the Swiss standards of 1988 [33] and the literature [34]. It is worth noticing that the buildings in the area considered are in general relatively old. It is the reason why the Swiss standards of 1988 was used, rather than the latest version of 2009. The results are shown in Table 1.3.

In order to evaluate the daily energy requirements, while taking into account the effect of the varying atmospheric temperature on space heating and air conditioning demands, the

## Chapter 1. Thermoeconomic analysis

Table 1.2 – Energy Reference Area (ERA) in the various zones and per type of buildings affectation considered for the test case area "Rues Basses."

Zone		Commerical		Offices		Residential	
		Shops	Restaurants	Individual	Open space	post-1990	pre-1990
A	1	2'030	226	4'209	4'209	148	590
	2	913	101	3'549	3'549	0	0
	3	2'655	295	6'551	6'551	428	1'714
	4	1'144	127	2'739	2'739	0	0
	5	2'269	252	3'543	3'543	0	0
	6	2'083	231	2'065	2'065	1'429	5'715
	7	1'659	184	5'529	5'529	0	0
	8	1'351	150	5'804	5'804	0	0
	9	3'446	383	8'244	8'244	799	3'197
	10	1'077	120	2'350	2'350	736	2'944
B	1	4'113	457	18'713	18'713	0	0
	2	3'173	353	16'470	16'470	0	0
	3	7'015	779	10'337	10'337	0	0
	4	34'358	3'818	1'454	1'454	0	0
	5	3'436	382	6'827	6'827	136	544
	6	3'820	424	7'565	7'565	195	781
	7	3'368	374	7'781	7'781	225	902
	8	4'163	463	5'203	5'203	1'122	4'489
	9	9'281	1'031	13'809	13809	3'708	14'834
	10	3'807	423	9'094	9'094	578	2'313
	11	3'293	366	5'628	5'628	2'035	8'142
	12	5'781	642	22'481	22'481	1'227	4'907
	13	1'706	190	4'968	4'968	1'075	4'298
C	1	4'222	469	948	948	2'277	9'107
	2	7'838	871	5'806	5'806	581	2'323
	3	4'541	505	0	0	2'605	10'422
	4	5'095	566	8'580	8'580	0	0
	5	5'086	565	1'860	1'860	759	3'035
	6	1'562	174	445	445	578	2'312
	7	2'229	248	5'408	5'408	1'151	4'603
	8	3'615	402	1'458	1'458	1'210	4'840
	9	2'156	240	6'797	6'797	464	1'857
<b>All</b>		142'283	15'809	206'208	206'208	23'467	93'868
<b>Total: 687'843 m<sup>2</sup></b>							

following equation was used:

$$Q_{ERA} = \frac{UA}{ERA} \cdot \int (T_{service} - T_a) dt \quad (1.1)$$

### 1.3. Thermal energy needs

In the case of space heating,  $Q_{ERA}$  is the yearly space heating demand per  $m^2$  of Energy Reference Area - ERA. It is derived from statistics and it aggregates the effect of the various heat sources (solar and internal heat gains) and heat sinks (thermal losses through the envelope and preheating of the air renewal.) In this study it was assumed that an equivalent loss coefficient -  $UA/ERA$  - could be used, linking linearly the flow of thermal energy to the temperature difference between the room and the outside air only. This is also known as an energy-signature model [35]. The integral can be replaced by the yearly heating, respectively cooling degree-days. Hence the coefficient of loss becomes:

$$\frac{UA}{ERA} = \frac{1000}{24} \cdot \frac{Q_{ERA}}{YDD} \quad (1.2)$$

The value of the coefficient of loss for the six buildings affectations is shown on Table 1.3. The annual value for Geneva is 2937 degree-days in heating. This value is obtained using a base temperature of 20°C and considering that space heating systems are shutdown whenever the average daily atmospheric temperature exceeds 12°C. An identical method is used to evaluate the loss coefficient applicable to air conditioning. In that case, the annual value is 384 cooling degree-days. It assumes a base temperature of 18°C and the method used is the UKMO method [36]. It has to be mentioned that in Switzerland and unlike for heating, no national standard defines how to compute cooling degree-days. The values for the various loss coefficients found are shown in Table 1.3.

Table 1.3 – Yearly energy requirement per  $m^2_{ERA}$  and thermal loss coefficients for the six different types of building considered

	Units	Shop	Rest.	Offices indiv.	Offices open S.	Resid. >1990	Resid. <1990
Space heating	[kWh $m^{-2}$ $yr^{-1}$ ]	124.6	66	55	55	37.5	70.6
Heating loss coef	[W $K^{-1}$ $m^{-2}$ ]	1.768	0.936	0.78	0.78	0.532	1.001
Air conditioning	[kWh $m^{-2}$ $yr^{-1}$ ]	70	-	72	45	-	-
Cooling loss coef.	[W $K^{-1}$ $m^{-2}$ ]	7.605	-	7.822	4.889	-	-
Hot water prep.	[kWh $m^{-2}$ $yr^{-1}$ ]	7.4	66	-	-	12.5	21.4
Refrigeration	[kWh $m^{-2}$ $yr^{-1}$ ]	30	10	-	-	-	-
Data centres cooling	[kWh $m^{-2}$ $yr^{-1}$ ]	-	-	8	45	-	-

The total thermal energy required annually is 102'572 MWh. 51.8% of which are for heating and 48.2% for cooling. Fig. 1.2 shows the energy required for each service throughout the year on a daily basis. The heating peak occurs in February at a load of 19.23 MW, the ratio between maximum and minimum heating requirement is 38.9. The minimum heating demand occurs in summer when the only heat demand is for hot water preparation. The cooling peak occurs in August at a load of 33.0 MW and the ratio between maximum and minimum cooling demand is 18.9. Space heating is required for the totality of the 687'843  $m^2$  of ERA, it represents a load

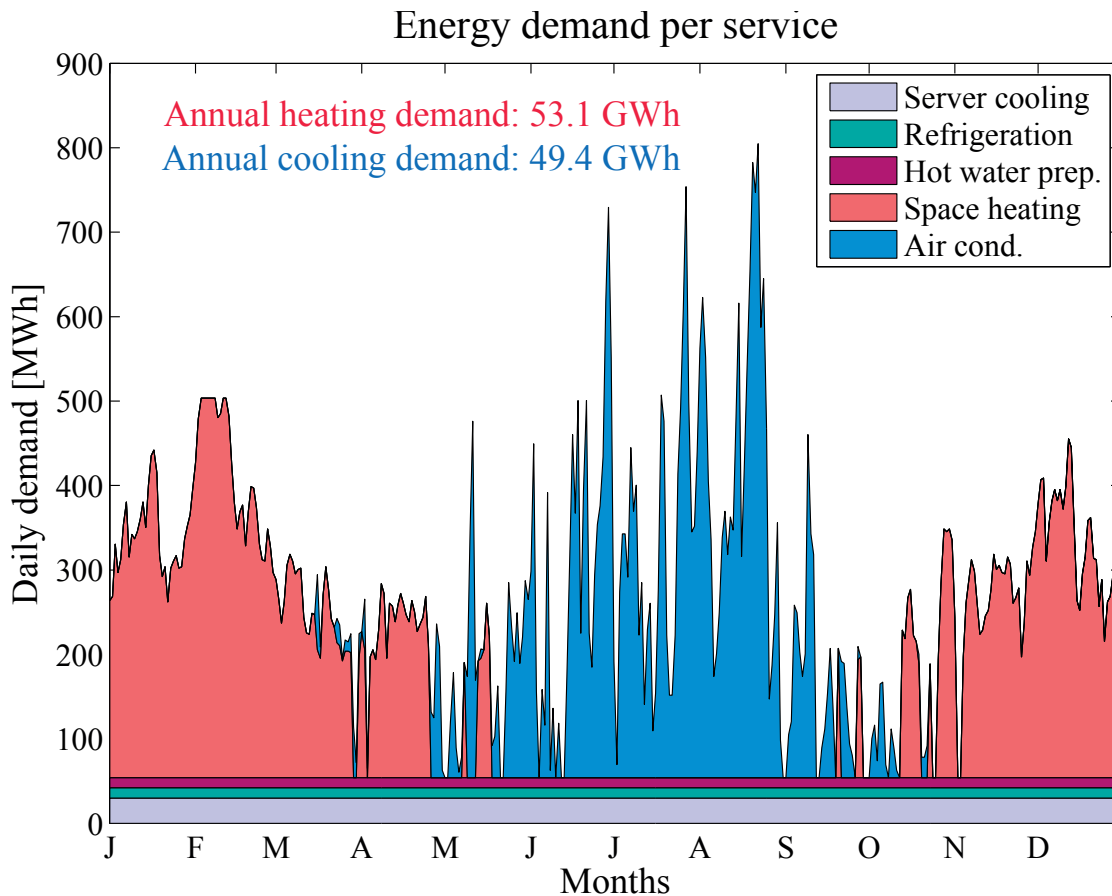


Figure 1.2 – Daily demand of the various thermal energy services considered in the test area of "Rues Basses"

of 18.74 MW at design conditions ( $T_a = -7^{\circ}\text{C}$ ). The capacity required for the preparation of domestic hot water is 0.50 MW. Since air conditioning equipment is forbidden in residential building in Geneva, the air conditioning area is reduced from the initial 687'843 m<sup>2</sup> of ERA to 570'800 m<sup>2</sup>, and leads to a required cooling capacity of 44.44 MW at design conditions ( $T_a = 30^{\circ}\text{C}$ ). The required cooling capacity for refrigeration and the cooling of data centres is 0.50 MW (143.1 tons) and 1.24 MW (353.8 tons) respectively. Obviously, it can be concluded that the dominant services are space heating and air conditioning. To clearly illustrate the relative importance of the various services, the load curve is shown at Fig.1.3, where negative heating loads have positive values and cooling loads negative ones. In this particular figure the cooling load curves have been flipped from left to right to express the fact that in general peak heating demand and peak cooling demand are not simultaneous. However some comments are required on that matter.

Under the hypothesis made, the preparation of domestic hot water, refrigeration and the cooling of data centres are simultaneous all over the year. On daily averaged basis it is true, on an intraday level however, domestic hot water is typically prepared over periods of 3 to

6 hours, consequently the required heating load is 2 to 4 times the daily average. Regarding refrigeration, even though the demand is relatively constant, the type of technology used for the compressors can introduce fairly large intra-day fluctuations, especially if operated in "on/off" mode. For economic reasons it is not interesting to operate a data centre at part load but it is likely that they exhibit variations in computation load that affect their cooling demand. All these factors have been neglected in the present study. For what concerns the services of space heating and air conditioning, very little simultaneity occurs between these two services. It can be seen at Fig.1.2 that only during the last two weeks of March and on one day at the end of September that such a situation happens. It is in part due to the difference between the two different methods used to compute degree-days as the method used for cooling [36] takes into account the *min* and *max* values of the ambient temperature, while the method used for the heating degree-days doesn't. It is also worth mentioning that depending on the building's orientation and if they have large and unshaded windows, heating is sometimes still required for the rooms facing North while the ones facing South need air conditioning to avoid overheating.

The quasi absence of simultaneity between air conditioning and space heating, combined with neglecting the load variations for the services of domestic hot water preparation, refrigeration and cooling of data centres, renders the representation shown at Fig. 1.3 a fair approximation. It also has the merit to be a didactic way to represent the demand and is widely used in the HVAC community. However, it should be kept in mind that such a representation makes sense only if the *time varying* cooling and heating services are almost exclusively non simultaneous.

Regarding the distribution of the loads, Fig. 1.3 shows some differences between space heating and air conditioning. For space heating the sudden jump is due to the fact that in the heating degree-days method used it is assumed that no heating is needed when the outside temperature exceeds 12°C. For air conditioning instead, there is no jump in demand since the daily maximum outside air temperature has to exceed the base temperature used ( $T_{base} = 18^\circ\text{C}$ ) to start having a non-zero value. For outside air temperatures higher than 18°C, the function is continuous with respect to the *min*, *max* and *average* outside air temperature. Had the method used for cooling [36] also been used for heating<sup>4</sup>, the jump in demand would have disappeared. However, it would also have led to an additional heat demand during periods when the outside temperature exceeds 12°C, ultimately adding roughly 18% to the annual space heating demand. In the present study it was assumed that the buildings are well managed and therefore space heating systems are fully shut down according to the standards, hence justifying the choice of the heating degree-days method used. Note that the demand predicted for  $T_a < 12^\circ\text{C}$  would show in average a difference of 2.1% only, which indicates that the two methods are fairly equivalent.

It is important to note the difference in *equivalent full load operating hours* between the services of space heating and air conditioning. Indeed space heating occurs over a period more than twice as long as air conditioning. Moreover, there are 28 days during which space heating exceeds 75% of the maximum predicted load, while in the case of air conditioning

---

<sup>4</sup>Assuming that the base temperature of 20°C used for space heating in Switzerland is kept.

the figure is only 8. The sharp peak characterising cooling is significant, particularly when it comes to the sizing of equipment and as a result it tends to affect negatively the economic performance of the system.

A verification of the model used to compute the various thermal energy demand of the building was carried out. Geneva's cantonal authorities have made mandatory for heated buildings owners to compute the annual consumption of final energy agents for space heating and domestic hot water preparation normalized to 1 m<sup>2</sup> of ERA. The indicator is called *heat expense index* (HEI)<sup>5</sup>. For each of the 32 zones an equivalent HEI was computed using the model described above. In the area considered, the services of space heating and domestic hot water preparation are provided almost exclusively by combustion boilers. In that case the HEI is basically the energy content of the combustion agents consumed annually over a given zone divided by its ERA. A correction was necessary as the HEI available from Geneva's database is for the year 2014 and the models presented here use the reference year 2012. The correction consists in dividing the heating oil consumption for space heating by the ratio of the yearly degree days for 2012 and 2014 respectively. Note that the definition of the degree days used by the cantonal authorities differs from [37] the one used in this study. The result is visible at Fig.1.4. It is clear from the figure that the model used in this study almost always underestimates the HEI and as a consequence the overall heat demand in the test case area. The distribution of the actual HEI also spans over a larger scale than the one resulting from the model which lead to the conclusion that the heterogeneity between the various zones is greater in reality than what the model predicts. Since the present comparison was only made at the very end of the thesis it was not possible to redo all the analysis with more accurate thermal loss predictions.

### 1.4 Conversion technologies: An energy comparison

This section deals with the definition of the models used to evaluate the energy performance of the various energy conversion technologies compared within the framework of the present study.

The various conversion technologies are all considered as a replacement for the currently used technologies over the entire urban area of "Rues Basses" described previously. Many conversion technologies could have been included in the comparison, however for time reasons only the following ones have been studied:

**Currently used technology** In order to characterize the current situation in the area of "Rues Basses", a model of the energy conversion technology currently in operation was defined. It assumes that the entire heat demand of space heating and domestic hot water is provided by decentralized boilers fuelled with light heating oil. It also assumes that all the cooling needs are satisfied through, air cooled, electrically driven compression

---

<sup>5</sup>In french: Indice de dépense de chaleur - IDC



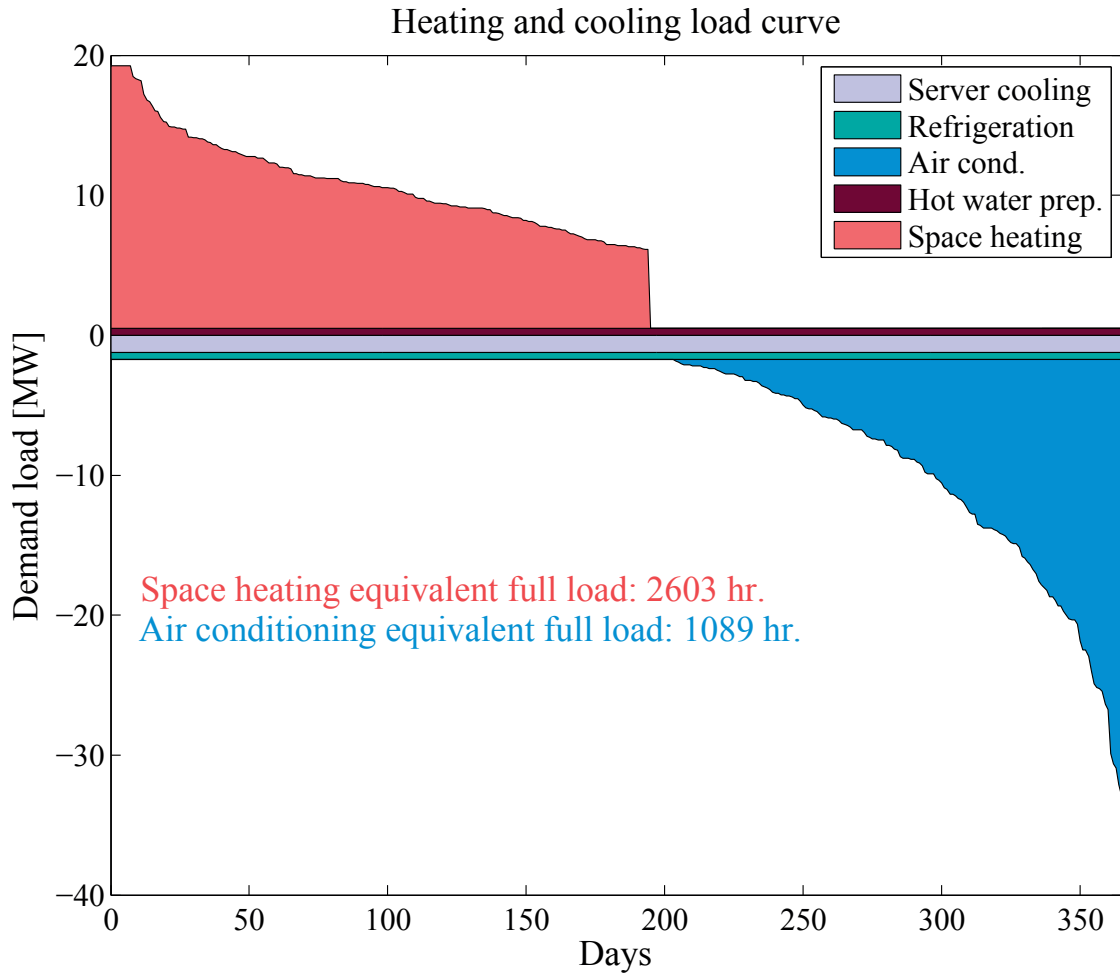


Figure 1.3 – Load curve for the various services in the test area of "Rues Basses". The cooling parts have been flipped from left to right in order to emphasize that space heating and air conditioning are in general not simultaneous.

chillers.

**Refrigerant based networks** As they represented the main focus of the present research study, several variants of district energy network using refrigerants as a transfer fluid have been proposed. All of them rely on a *two-pipes* network capable of satisfying the heating needs through a combination of centralized and decentralized heat pumps and the cooling needs mostly via free cooling but not exclusively. All these variants exploit the latent heat of vaporisation of a refrigerant fluid to transfer heat across the network.

**Water based network** The only water network studied is of a very similar type to the refrigerant based ones. It also uses two pipes, a combination of centralized and decentralized heat pumps for heating and free cooling for most of the cooling. The major difference is in the use of the sensible heat of water instead of the latent heat. This particular type of water network is often referred to as an *anergy* network. It was decided to limit the

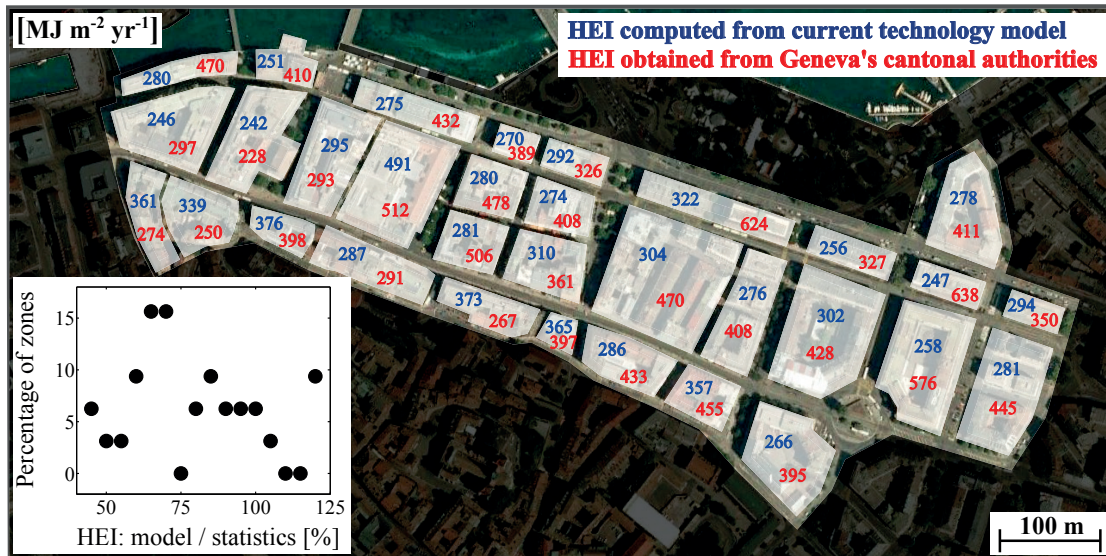


Figure 1.4 – Comparison of the real heat expense index obtained from Geneva’s authorities [38] with the one computed using the model of buildings and boilers described in this study. Insert: histogram of the ratio of the HEI modeled over actual

study on water based networks only to the energy network since it is likely to be a very - if not the most - serious competitor to refrigerant based networks.

Obviously there is a very wide range of possible energy conversion technologies that could supply the thermal services to an urban area. However the scope of this study was to investigate in detail the concept of refrigerant based networks, hence the comparison with other technologies was limited to two benchmarks, one representing the current situation in the area of "Rues Basses" and the other representing what is believed to be the closest competitor.

### 1.4.1 Currently used technology

As said earlier the heat demand is considered to be exclusively satisfied using oil fuelled boilers. Air cooled, electrically driven vapour compression chillers are assumed to provide all the cooling services.

Regarding boilers this early hypothesis was proven relatively inaccurate since a new database of the existing heating equipment [38] shows that the share of heating oil boilers in the test case area represents only 51.4% of the total installed capacity. The two other technologies are natural gas boilers that account for 39.9% and *bi-fuel* boilers<sup>6</sup> that represent the last 8.7%. A map of the boiler capacity installed per zone and boiler type in the "Rues Basses" area can be seen at Fig.1.5. Note that in spite of the extensive used of natural gas in the area of "Rues Basses", the model of conversion technology developed in the present study considers only oil fuelled boilers. It was estimated that the imprecision caused by not considering natural gas

<sup>6</sup>Normally fuelled on natural gas except during peak demand where they switch to oil instead



## 1.4. Conversion technologies: An energy comparison

would not significantly affect the evaluation of the energy performance. However, it leads to overestimating total costs and greenhouse gas emissions. There isn't any equivalent database for the cooling equipment and thus it is not possible to proceed to a similar verification.

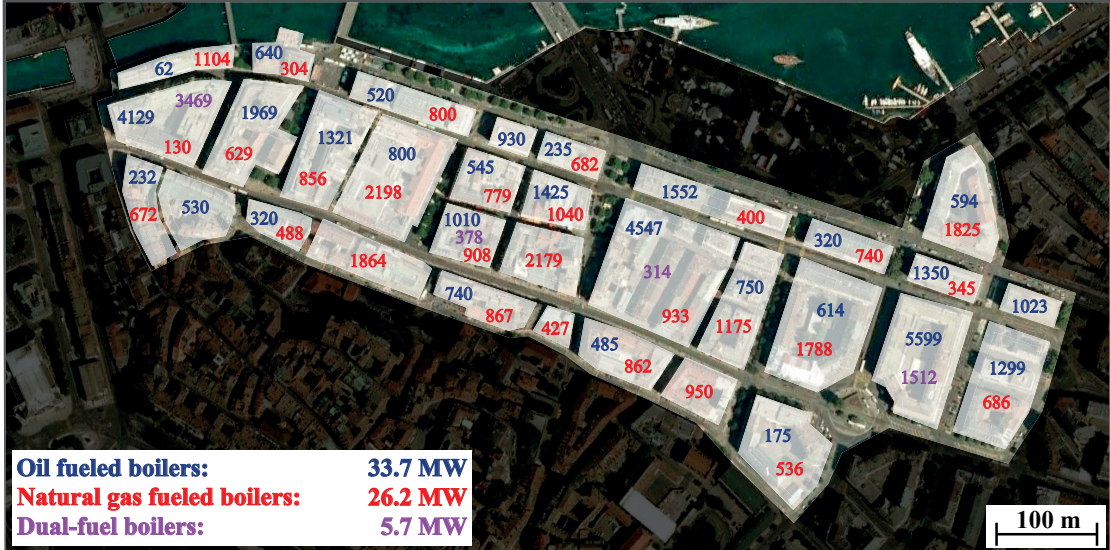


Figure 1.5 – Installed capacity for the various boiler types in the 32 zones of the test case area. The values correspond to the sum of the burners capacity and are expressed in kW.

The boilers are considered to operate following a pulse width modulation by alternating between full load and idle periods of variable duration. The design atmospheric temperature was set to  $-7\text{ }^{\circ}\text{C}$  [34]. The part load energy efficiency of the boilers is computed as follows:

$$\epsilon = \left( \frac{1}{\epsilon_n} + \frac{\lambda_0}{\chi} - \lambda_0 \right)^{-1} \quad (1.3)$$

Where the parameter  $\epsilon_n$  is the first law efficiency [39] at nominal load and the parameter  $\lambda_0$  is the residual consumption at idling condition, as a fraction of the delivered nominal load. The independent variable  $\chi$  is the load factor<sup>7</sup>. In the present work the value of the load factor is obtained by the ratio of the actual heat rate demand on a given day to the nominal heat rate capacity of the boiler.

The value chosen for  $\epsilon_n$  corresponds to the legal limit of 7% of flue gas losses<sup>8</sup> imposed by the Swiss Federal Ordinance on Air Pollution Control (OAPC) [40] to which the radiation and convection losses are added. For these losses the value chosen is 0.9% and is typical of a 500 kW pulse width modulating oil fuelled boiler<sup>9</sup>[41]. The value used for  $\lambda_0$  is assumed to be equal to the radiation and convection losses, and so the same value of 0.9% was used.

<sup>7</sup>Fraction of time during which the boiler operates at full load

<sup>8</sup>for boilers equipped with *forced draught burners with single-stage operation*

<sup>9</sup>the average nominal combustion heat rate of the boilers in this study is 646 kW

## Chapter 1. Thermo-economic analysis

---

The performance of the vapour compression chillers is approximated using ideal Carnot heat pump cycles multiplied by a constant exergy efficiency. Since air-cooling is considered, the parasitic power consumption of the fans was accounted for. Hence, the electric power required is computed as follows:

$$\dot{E} = \dot{E}_{cycle} + \dot{E}_{MDAC} \quad (1.4)$$

With the first term on the right hand side given by:

$$\dot{E}_{cycle} = \frac{\dot{Q}_{evap}}{\eta} \frac{T_{h,out}}{T_{c,out}} \left( 1 - \frac{T_{c,out}}{T_{h,out}} \right) \quad (1.5)$$

Where  $\dot{Q}_{evap}$  is the cooling load,  $\eta$  the exergy efficiency,  $T_{h,out}$  the absolute temperature of the cooling water at the condenser outlet and  $T_{c,out}$  the absolute temperature of the chilled water at the evaporator outlet. These two temperatures are computed through:

$$T_{h,out} = T_a + \Delta T_{air} + \Delta T_{min} \quad (1.6)$$

$$T_{c,out} = T_{service} \quad (1.7)$$

The second term on the right hand side of eq. (1.4) corresponds to the electric power consumed by the fans for the air-cooling of the condenser. It is given by the following equation [42]:

$$\dot{E}_{MDAC} = \frac{0.605 (\dot{Q}_{evap} + \dot{E}_{cycle})}{(\Delta T_{air} + \Delta T_{min})^{0.9937}} \quad (1.8)$$

In the expressions (1.6), (1.7) and (1.8),  $\Delta T_{air}$  is the temperature increase in the cooling air passing through the air cooler,  $\Delta T_{min}$  is the minimum approach temperature difference in the air cooler. In the present study it has been assumed that the chillers themselves are cooled through a water loop linking the chiller with the air cooler. Obviously, the loop represents an inefficiency as the condenser pressure is necessarily higher than in the case of a condenser that is directly air cooled. This choice is motivated by the tendency from the authorities to favour indirect systems as they have a reduced inventory of refrigerant and a reduced exposed

#### 1.4. Conversion technologies: An energy comparison

length of refrigerant pipes. The aim being to limit the leaks in the environment of substances having a high global warming potential (GWP).

A survey of a total of 1918 water cooled chillers certified by Eurovent [43] was carried out in order to define a realistic value for the exergy efficiency  $\eta$  in eq. (1.4). A seasonal performance indicator is defined in Europe as the *European Seasonal Energy Efficiency Ratio* or *ESEER*, it is a weighted average of the coefficient of performance in cooling -  $COP_c$  - at the following standardized measurement points:

- 100% cooling load, cold source 12/7°C, hot source 30/35°C, 3% of the time
- 75% cooling load, cold source 12/7°C, hot source 26/31°C, 33% of the time
- 50% cooling load, cold source 12/7°C, hot source 22/27°C, 41% of the time
- 25% cooling load, cold source 12/7°C, hot source 18/23°C, 23% of the time

An equivalent ideal *ESEER* under the same conditions was defined as follows:

$$\begin{aligned}
 ESEER_{ideal} = & 0.03 \frac{308.15}{280.15} \left(1 - \frac{280.15}{308.15}\right) + 0.33 \frac{304.15}{280.15} \left(1 - \frac{280.15}{304.15}\right) \\
 & + 0.41 \frac{300.15}{280.15} \left(1 - \frac{280.15}{300.15}\right) + 0.23 \frac{296.15}{280.15} \left(1 - \frac{280.15}{296.15}\right) = 13.92 \quad (1.9)
 \end{aligned}$$

The ratio between the actual *ESEER* and its ideal counterpart -  $ESEER_{ideal}$  - was then computed for all the chillers surveyed, the results are shown at Fig. 1.6. The average value - 40.2% - was used as the representative exergy efficiency for the chillers considered in this study.

The values used for the various parameters in eq. (1.3)-(1.8) are listed in Table 1.4.

Using the demand for the various services defined in the previous section and the model of the current conversion technologies, the final energy consumption was computed on a daily basis for each zone in the test case area.

The annual total amount is 66.42 GWh, 87.4% of which is heating oil and 12.6% electricity. The maximum combustion heat rate of the boilers reaches 20.88 MW corresponding to the installed capacity. It is due to a 6 days cold snap in February 2012 during which the atmospheric temperature plummeted below the sizing temperature of -7°C.

The annual share of electricity used in the water cooled chillers is 72.0% and the consumption of the air coolers fans accounts for 28%. The maximum electric load occurs in August at 7.885 MW, which is significantly below the installed capacity of 12.81 MW suggesting that

## Chapter 1. Thermo-economic analysis

Table 1.4 – Numerical parameters used for the conventional energy conversion technologies and temperature of the various cooling services.

Parameter	Value
$\epsilon_n$	92.1%
$\lambda_0$	0.9%
$\eta$	40.2%
$\Delta T_{air}$	12°C
$\Delta T_{min}$	2.5°C
<b>Energy Service</b>	<b>Temperature</b>
Air conditioning	18°C
Refrigeration	5°C
Cooling of data centres	28°C

the sizing criterion used - an atmospheric temperature of 30°C - is a bit excessive. The daily consumption of heating oil, respectively electricity for the different services is shown on Fig. 1.7. The yearly energy efficiency in heating, for the considered area and the current energy conversion technologies is 0.915. The yearly effectiveness in cooling is 5.90.

Similarly to what was done for the heating services needs in the test case area, a comparison between the predicted installed capacity of boilers with the actual installed capacity given at Fig. 1.5 was done. It shows an overcapacity of 44.9 MW, or an oversizing factor of 3.17. Oversizing boilers in building applications is a common practice, as for that technology it does

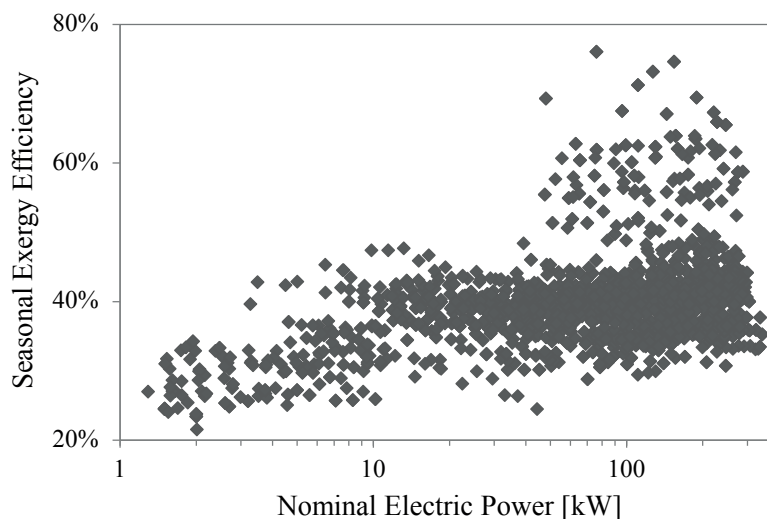


Figure 1.6 – Seasonal exergy efficiency of certified chillers [43]. It is based on the european seasonal energy efficiency ratio as defined in [44], the reference ideal process is defined in eq. (1.9).

#### 1.4. Conversion technologies: An energy comparison

not cause too much of a cost penalty. Note that, as shown for the heat expense index at Fig. 1.4, the prediction of the heat demand done by the model underestimates the real demand by around 33%. Accounting for that, the boilers capacity installed in that area still exceeds around 2.4 times what is required. In reality it is likely that the combination of a low average load factor due to the overcapacity and higher idling losses cause the annual efficiency to be lower than the value of 0.915 found with the model of boiler. Regarding cooling equipments, it is likely that the real installed capacity matches the real demand quite well, since cooling systems can be installed only after the need for them has been demonstrated to the cantonal authorities. As a consequence every system installed can be supposed to have been sized reasonably well. However, even if the cooling systems are generally not oversized, a field measurement campaign [45, 46] has shown that cooling effectiveness can reach a very low value in poorly managed systems. As a result, the yearly effectiveness in cooling of 5.90 found here is likely to be overestimated.

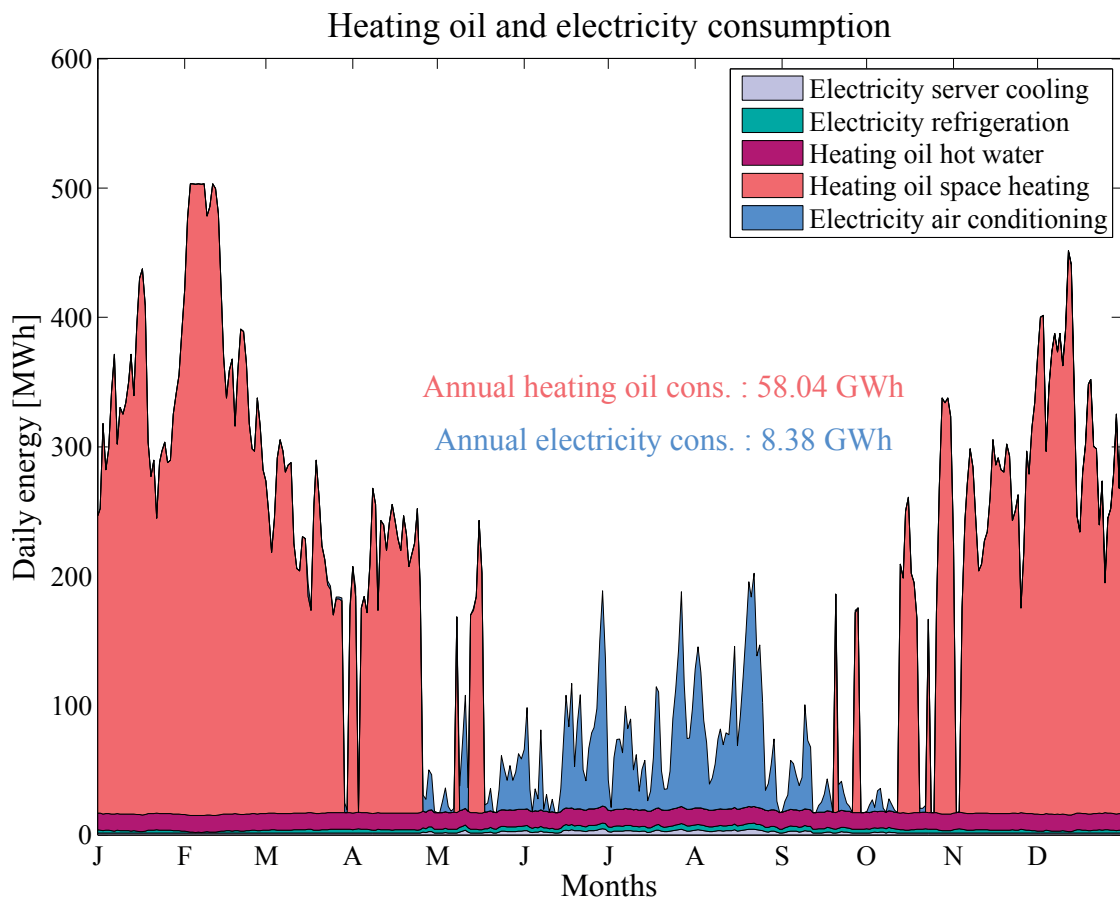


Figure 1.7 – Daily heating oil and electricity consumption of the currently used technologies for the test case area of "Rues Basses"

### 1.4.2 Refrigerant based networks

In this section the concept of a district energy network using a refrigerant as a transfer fluid will be defined. Afterwards, a description of the models will be provided.

District heating and cooling networks have been used to deliver energy in urban areas for many decades. Generally, these networks rely on centralized energy conversion technologies supplying heating and/or cooling to the users through a water network. In most of the cases, the supply temperature of these networks is selected, at best, according to the most demanding consumer connected. Thus all the other users are supplied at a temperature beyond their needs - often far beyond their needs. Furthermore, when heating and cooling have to be supplied, two independent water loops are used. Finally, most of the time, heat discharged by the cooling users in the district cooling network is not transferred to the district heating network, and thus not recovered.

To overcome the shortcomings of the aforementioned district heating and cooling networks, a new type of district energy network is being investigated. It is based on the use of a refrigerant as a heat transfer fluid. The latent heat of vaporization is used, instead of the sensible heat, to store and transfer heat across the network. The pressure of the network is selected such that evaporation/condensation takes place at a desired temperature. That temperature should be low enough to allow for free cooling to be used in most of the cooling applications. Wherever free cooling can be applied the electricity consumption is drastically reduced even when compared to compression chillers with the highest efficiency.

Even with a temperature of the network low enough to satisfy a large share of free cooling, the network can still be used to deliver space heating and produce domestic hot water using decentralized heat pumps installed at the user end. In those two cases the network is used as a cold source. Generally speaking, the network in spite of being relatively cold remains a fairly high temperature heat source for these heat pumps, resulting in an improved heating capacity<sup>10</sup> and a better  $COP_h$ . Decentralized heat pumps also allow each heating user to be supplied at the required temperature and not more. In the case of a very heterogeneous area, populated with buildings having different temperatures of heat distribution, it represents a serious advantage as each machine operates at the best possible ideal  $COP_h$ . In comparison, a fully centralized solution will be constrained by the *worst* user in terms of supply/return temperature and as in this case all buildings are supplied at the same temperature, it results that a centralized heat pump is forced to operate at the lowest possible ideal  $COP_h$ . Obviously, the real  $COP_h$  is the parameter of interest and its value is strongly influenced by the exergy efficiency of the machines. In practice large industrial heat pumps have 55 - 65% exergy efficiency and residential machines have generally 45-50% efficiency. However some machines of the latest generation reach almost 60% [47, 48]. It appears that using decentralized heat pumps to supply heat at a temperature adapted to each user is advantageous from the efficiency point

---

<sup>10</sup>The higher density of the refrigerant at the compressor suction port causes a higher mass flowrate in the whole circuit. Especially for scroll and screw compressors in which the suction volume flowrate is only marginally influenced by the inlet and outlet thermodynamic states



#### 1.4. Conversion technologies: An energy comparison

---

of view, if this temperature is in average lower than the supply temperature from a centralized heat pump. To give an idea of how much lower the supply temperature needs to be to for a decentralized solution to be worthwhile energetically, a rule of thumb is that the supply temperature must be at least 1 - 1.5°C lower for every percentage points of exergy efficiency decrease of the decentralized as compared to the centralized heat pump. As the efficiency gap between centralized and decentralized heat pumps is closing, decentralized heat pumping solutions are becoming more and more attractive.

The proposed network requires only two pipes. Cooling users discharge waste heat into the network causing refrigerant drawn from the liquid pipe to evaporate. Heating users extract heat from the network by condensing refrigerant from the vapour pipe. This process allows the recovery of waste heat inside the network.

Obviously, the heat required by the heating users may, most of the time, not be strictly equal to the waste heat discharged by the cooling users. Hence, a central plant is needed to balance the overall network by taking or releasing heat into the environment, for instance a lake. A schematic view of a refrigerant based network, is provided in Fig. 1.8. Note the presence of a condenser-evaporator at the interface between the network and the decentralized heat pump. Condenser-evaporators are necessary whenever a different refrigerant from that of the network is used in decentralized heat pumps. If the refrigerant is the same but the decentralized heat pumps are equipped with lubricated compressors, condenser-evaporators might be used to isolate hydraulically the refrigerant circuit from the network, to ensure the proper lubrication of the compressor and avoid contaminating the parts of the network that can be oil-free. In order to avoid the presence of liquid in the vapour line of the network, the flow of refrigerant entering the evaporators at the cooling users must be controlled such that the fluid is fully evaporated and even slightly superheated. Similarly, the frequency of the circulation pumps at the heating users must be controlled in order to avoid cavitation at their inlet by ensuring a certain degree of subcooling on the condensing side of the condenser-evaporators. During some transients, or if a valve is malfunctioning, one can expect some spillage of liquid into the vapour line of the network. This issue could be remedied by installing liquid traps that would collect the spilled liquid and where it could be sent back to the liquid line or vaporized. For readability reasons these traps are not shown in Fig. 1.8. The concept, as initially imagined, was described by Weber and Favrat in Refs. [23, 22, 49]. A list of possible energy services and associated conversion technologies that can be included in a refrigerant based network was done by Henchoz et al. in Ref. [24]. An initial thermoeconomic analysis of the concept of a refrigerant network using CO<sub>2</sub> as a working fluid was done by Henchoz et al. in Ref. [25], later it was largely refined and published in [26]. The methodology used in this last article is very similar to the one followed in the present chapter. Finally a comparison of the energy performance of two refrigerant based networks, CO<sub>2</sub> and HFO R1234yf, and one cold water (anergy) network can be found in Ref. [28], these variants are very similar to the ones about to be presented in this chapter.

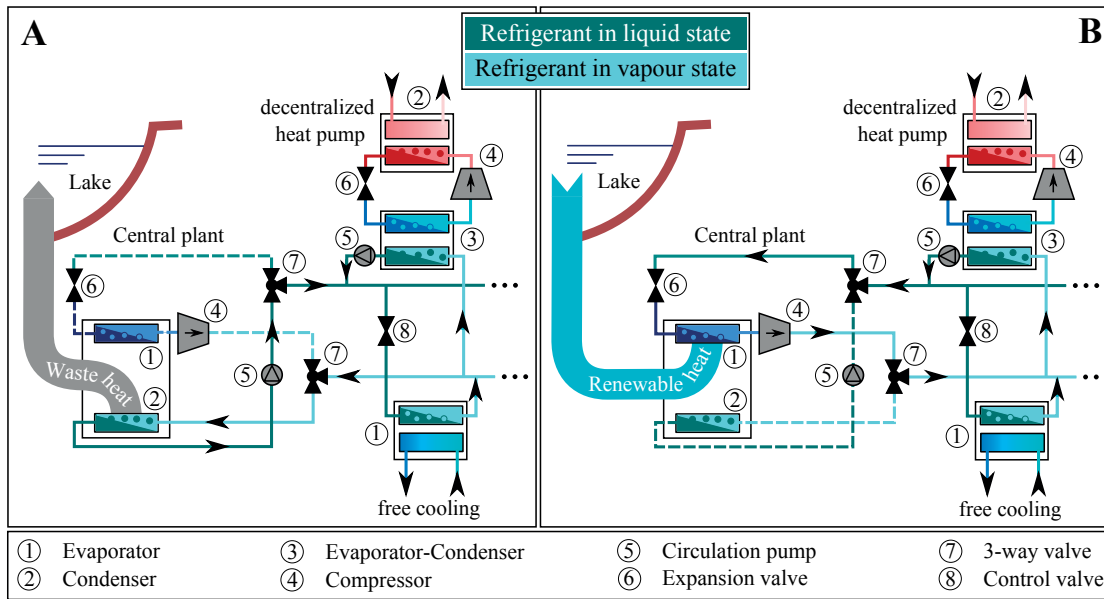


Figure 1.8 – Schematic representation of a refrigerant based district energy network. Side A - net cooling operation. Side B - net heating operation. Note: The refrigerant in the decentralized heat pump and in the network are different.

**Safety & environmental considerations and their impact on the potential fluids**

Before going any further in the description of refrigerant based networks, it is wise to discuss the question of the safety and environmental regulations to which these networks will have to comply. In particular, how would these considerations impact the choice of the refrigerant? It was decided to consider the question of safety and environmental regulations early in the process, in order to narrow down the choice of possible refrigerant as much and as quick as possible. A reverse approach might have been considered, such as carrying out a thermo-economic analysis of all the different topologies of network combined with all the possible refrigerants, and then rule out the infeasible ones based on safety and environmental considerations. However, the method of first ruling out and then do the thermo-economic analysis was preferred as it was clear from the beginning that the choice would ultimately come down to only a handful of fluids.

Selecting an appropriate working fluid is a key factor in the development of energy efficient, safe, environmentally sound and cost effective refrigeration, air conditioning and heat pump-equipments. The Montreal protocol, regulating the phase-out of ozone depleting CFC and HCFC refrigerants has been a major boost in the development of machines using HFCs. More recently however, the global warming potential of refrigerants has become an issue that led to a renewed interested towards natural fluids and the development of the new HFO synthetic fluids [50, 51]. Recently, the trend of more restricting the use of HFC refrigerants has gained momentum worldwide [52]. In Switzerland, a new federal ordinance sets very stringent limits to the use of HFC refrigerants [27]. In essence only natural refrigerants and



## 1.4. Conversion technologies: An energy comparison

---

the new HFOs are allowed in installations with more than 600 kW of cooling/heating capacity. For these fluids the only condition imposed by the new ordinance is that the installations must fulfil the appropriate safety requirements, which in the perspective of a refrigerant based district energy network, limits further the number of possible fluids. The proposed concept of district energy networks would require large charges of refrigerants, typically ranging from several tens of tons to a few hundred tons, they are also considered for densely populated areas. Contrarily to industrial and large commercial refrigeration plants the environment cannot be considered fully under control. Moreover, it can be assumed that the average person present on site will not be aware of the existence of a refrigerant network. All these elements render the criteria of non-toxicity and non-flammability *sine qua non* conditions for a fluid to be accepted as potential candidate for use in a refrigerant based district energy network. Currently, and under the aforementioned constraints, only CO<sub>2</sub>, and the two HFOs, R1234yf and R1234ze, can be envisaged.

The thermodynamic and transport properties of these three fluids are listed in Table 1.5. The values are computed for a temperature of 15°C which is representative of the temperature at which a refrigerant based network would operate. A comparison of the parameters for network branches that are 1 km long and that have a heating/cooling capacity of 1, 10 and 30 MW is also provided in Table 1.5. The sizing constraint chosen is a maximum tolerable drop in saturation temperature of 1°C along the lines, which translates into a maximum pressure drop. The main reason for this choice is to avoid generating a significant amount of two-phase flows in the lines that could impede the operation or deteriorate some components of the network. When comparing the size of the pipes for the three fluids, it appears clearly that CO<sub>2</sub> allows for much smaller pipes for the three capacities considered. Two reasons explain this: First, the density of the CO<sub>2</sub> in vapour state is more than 5 times greater than that of the two HFOs. Second, the maximum tolerable pressure drop is 8, respectively 10 times higher than for the two HFOs. Overall it results that the heat rate density<sup>11</sup> for CO<sub>2</sub> is around 3.8 and 4.3 times higher than for the R1234yf and R1234ze respectively. It is worth mentioning that although the heat rate density changes significantly with respect to the branch capacity, the relative value between the three different refrigerants remains almost constant.

Considering the applicable safety and environmental regulations as well as the global trend towards more restrictions in the use of HFC refrigerants, it was consequently decided to limit the case studies on refrigerant based networks using CO<sub>2</sub>, HFO R1234yf or HFO R1234ze as heat transfer fluids.

### CO<sub>2</sub> based networks: Description of the models

This subsection provides the description of the set of technologies required and the associated models needed to evaluate the performance of a CO<sub>2</sub> based district energy network.

Each branch of a CO<sub>2</sub> network consists of two lines, one containing CO<sub>2</sub> in a liquid state

---

<sup>11</sup>Defined as the branch capacity over the sum of the cross-sectional area of the vapour and of the liquid pipe

## Chapter 1. Thermo-economic analysis

Table 1.5 – Thermodynamic properties, transport properties and example of network branches for the three possible refrigerants and with three different heat rate capacities

Thermodynamic properties at $T_N = 15^\circ\text{C}$			CO <sub>2</sub> (R744)	R1234yf	R1234ze
Saturation pressure	[bar]		50.87	5.10	3.64
Reduced pressure	[-]		0.689	0.15	0.1
Latent heat of evaporation	[kJ kg <sup>-1</sup> ]		176.65	153.05	174.08
Liquid phase density	[kJ m <sup>-3</sup> ]		821.21	1127.2	1195.0
Vapour phase density	[kJ m <sup>-3</sup> ]		160.73	28.27	19.36
Transport properties at $T_N = 15^\circ\text{C}$					
Sat. Liq.	Dynamic viscosity	[Nm <sup>2</sup> s <sup>-1</sup> ]	74.43 · 10 <sup>-6</sup>	174.93 · 10 <sup>-6</sup>	224.48 · 10 <sup>-6</sup>
	Thermal conductivity	[Wm <sup>-1</sup> K <sup>-1</sup> ]	91.86 · 10 <sup>-3</sup>	66.73 · 10 <sup>-3</sup>	77.86 · 10 <sup>-3</sup>
	Surface tension	[Nm <sup>-1</sup> ]	1.95 · 10 <sup>-3</sup>	7.40 · 10 <sup>-3</sup>	10.16 · 10 <sup>-3</sup>
Sat. Vap.	Prandtl number	[-]	2.76	3.53	3.89
	Dynamic viscosity	[Nm <sup>2</sup> s <sup>-1</sup> ]	16.95 · 10 <sup>-6</sup>	11.81 · 10 <sup>-6</sup>	11.81 · 10 <sup>-6</sup>
	Thermal conductivity	[Wm <sup>-1</sup> K <sup>-1</sup> ]	27.96 · 10 <sup>-3</sup>	13.00 · 10 <sup>-3</sup>	12.76 · 10 <sup>-3</sup>
Prandtl number	[-]	1.96	0.91	0.87	
Conditions at $T_N = 15^\circ\text{C}$ for a 1 MW capacity pipeline (pipe rugosity: 0.3 mm, max. $T_{sat}$ drop: 1°C.)					
Liquid pipe	Pressure drop	[bar m <sup>-1</sup> ]	1.21 · 10 <sup>-3</sup>	0.15 · 10 <sup>-3</sup>	0.12 · 10 <sup>-3</sup>
	Refrigerant charge	[kg m <sup>-1</sup> ]	9.90	18.13	18.71
	Heat rate density	[MW m <sup>-2</sup> ]	51.39	13.33	11.87
	<b>Required diameter</b>	<b>[mm]</b>	<b>93</b>	<b>137</b>	<b>136</b>
	Flow velocity	[m s <sup>-1</sup> ]	1.01	0.39	0.33
Vapour pipe	<b>Required diameter</b>	<b>[mm]</b>	<b>127</b>	<b>277</b>	<b>298</b>
	Flow velocity	[m s <sup>-1</sup> ]	2.78	3.84	4.26
Conditions at $T_N = 15^\circ\text{C}$ for a 10 MW capacity pipeline (pipe rugosity: 0.3 mm, max. $T_{sat}$ drop: 1°C.)					
Liquid pipe	Pressure drop	[bar m <sup>-1</sup> ]	1.21 · 10 <sup>-3</sup>	0.15 · 10 <sup>-3</sup>	0.12 · 10 <sup>-3</sup>
	Refrigerant charge	[kg m <sup>-1</sup> ]	43.82	106.26	108.17
	Heat rate density	[MW m <sup>-2</sup> ]	89.19	23.04	20.50
	<b>Required diameter</b>	<b>[mm]</b>	<b>223</b>	<b>330</b>	<b>327</b>
	Flow velocity	[m s <sup>-1</sup> ]	1.76	0.68	0.57
Vapour pipe	<b>Required diameter</b>	<b>[mm]</b>	<b>305</b>	<b>666</b>	<b>717</b>
	Flow velocity	[m s <sup>-1</sup> ]	4.82	6.64	7.35
Conditions at $T_N = 15^\circ\text{C}$ for a 30 MW capacity pipeline (pipe rugosity: 0.3 mm, max. $T_{sat}$ drop: 1°C.)					
Liquid pipe	Pressure drop	[bar m <sup>-1</sup> ]	1.21 · 10 <sup>-3</sup>	0.15 · 10 <sup>-3</sup>	0.12 · 10 <sup>-3</sup>
	Refrigerant charge	[kg m <sup>-1</sup> ]	101.18	245.97	250.89
	Heat rate density	[MW m <sup>-2</sup> ]	116.00	29.79	26.52
	<b>Required diameter</b>	<b>[mm]</b>	<b>339</b>	<b>502</b>	<b>498</b>
	Flow velocity	[m s <sup>-1</sup> ]	2.29	0.88	0.74
Vapour pipe	<b>Required diameter</b>	<b>[mm]</b>	<b>463</b>	<b>1015</b>	<b>1092</b>
	Flow velocity	[m s <sup>-1</sup> ]	6.28	8.57	9.51

#### 1.4. Conversion technologies: An energy comparison

---

and the other CO<sub>2</sub> in a vapour state. Both lines are operated very close to saturation and the pressure is maintained at a level that enables the use of free cooling in most of the cooling applications. As a consequence, the temperature of the network during "summer" operation is simulatenously constrained by the temperature of the cold source, the lake water, and the temperature of the coldest cooling service to be provided by free cooling, in this case the return from air conditioning at 18°C. Consequently, the limits for the temperature of the network -  $T_N$  - during summer operations are defined as follows:

$$\begin{aligned} T_{N,min,summer} &= T_{lake} + \Delta T_{lake} + \Delta T_{min,rw} = 10^{\circ}\text{C} \\ T_{N,max,summer} &= T_{AC} - \Delta T_w - \Delta T_{min,rw} = 12.5^{\circ}\text{C} \end{aligned} \tag{1.10}$$

The limit during winter operations is set by the temperature required for the free cooling of data centres, and is defined as follows:

$$T_{N,max,winter} = T_{CDC} - \Delta T_w - \Delta T_{min,rw} = 22.5^{\circ}\text{C} \tag{1.11}$$

Where  $T_{AC}$  and  $T_{CDC}$  are the temperatures for the services of air conditioning and the cooling of data centres respectively.  $T_{lake}$  is the temperature of the water from the lake. Note that the water from the lake is assumed to be taken deep enough so that its temperature can be considered constant throughout the year.  $\Delta T_{lake}$  is the minimum achievable temperature rise for the water from the lake when passing through the heat exchanger at the central plant.  $\Delta T_{min,rw}$  is the minimum approach of temperature assumed for the heat exchangers operating with refrigerant on one side and water on the other. The values used for these parameters are detailed in Table. 1.8. Strictly speaking there is no constraint on the minimum temperature of the network during winter operation. In this study however the same value than  $T_{N,min,summer}$  was used, as it appeared that a low temperature of the network in winter is penalizing from an economic point of view. The optimal choice of the temperature of the network for summer and winter operations will be discussed in another section using an economic criterion. The bounds set in eq. (1.10) and eq. (1.11) will however remain applicable. Consistently with these bounds, the pressure in the CO<sub>2</sub> network would have to be maintained between 47 and 61 bar. Finally, the use of free cooling implies that the pressure in the liquid line is maintained slightly above the one in the vapour line (1 bar), allowing the CO<sub>2</sub> to flow naturally in the evaporators.

The decentralized conversion technologies chosen to supply the various energy services at the user end are the following:

- Heat exchangers for air conditioning and the cooling of data centres.
- CO<sub>2</sub> vapour compression chillers for refrigeration. Liquid CO<sub>2</sub> is expanded from the network to the required saturation temperature and evaporated; the vapour produced is then compressed back to the network.
- Intermediate heat pumps for space heating and hot water preparation. (Heat from the CO<sub>2</sub> condensation is transferred to the refrigerant through a condenser-evaporator.)

### Free cooling substations

The free cooling substations did not require any particular model of technology. It is assumed that the heat exchanger of a substation receives CO<sub>2</sub> in a saturated liquid state. The massflow of water is assumed to be adapted such that the temperature of the water from the hydronics is always constant in and out of the evaporator, and the massflow of CO<sub>2</sub> is assumed to be adapted such that CO<sub>2</sub> leaves the evaporator in a superheated vapour state with  $\Delta T_{SH} = 2K$ . The evaporator is also assumed to have negligible pressure drops and to be perfectly thermally insulated from the ambient.

### CO<sub>2</sub> vapour compression chillers for refrigeration

As refrigeration represents a small share of the total demand in the test case area considered, it was chosen to model the CO<sub>2</sub> open cycle refrigeration plants using Carnot cycles corrected of an energy efficiency. It is very similar than what was done for the compression chillers in the model of the currently used mix of conversion technologies (see eq. 1.5) except that the hot source temperature is the temperature of the network. Hence,  $T_{h,out} = T_N$  in eq. 1.5. Obviously there is no air cooler and as consequently no parasitic power consumption to drive the fans.

### Decentralized heat pumps

A preliminary study has shown that decentralized heat pumps are the largest electricity consumers of a CO<sub>2</sub> based network [25], for that reason it was decided to improve the level of detail in the model of these heat pumps. The computation of the electrical consumption of the decentralized heat pumps is made with a model based on the real thermodynamic cycle, namely a reverse Rankine cycle. A representation of the cycle considered is shown at Fig. 1.9. Note that rigorously two different diagrams should have been used, one of the thermodynamic cycle using a standard  $T-s$  diagram and one "pinch diagram" for representing the two heat exchanges. For compactness reasons however, it was decided to represent the cycle and the heat exchanges in a single  $T-s^*$  diagram, where  $s^*$  denotes that the entropy is different for the different substances at play (here, CO<sub>2</sub>, water and R1234yf). Such a representation is also used in [39].

Based on the new ordinance on refrigerants [53] the fluid chosen for the decentralized heat

#### 1.4. Conversion technologies: An energy comparison

pumps is R1234yf, even if only about one third of the zones in the test case area need more than 600 kW heating capacity.

Since the first law efficiency ( $COP_h$ ) of heat pumps depends strongly on the temperature level at which they deliver heat and since the majority of buildings are equipped with a hydronic distribution loop, it is necessary to consider a realistic heating curve. It was decided to use one which results from an aggregation of data collected for many buildings in Geneva [34]. This heating curve is typical of hydronics equipped with wall mounted radiators, the most widespread technology in Switzerland.

$$T_H [^\circ\text{C}] = 55 - 1.47(T_a + 6) \quad \forall T_a \leq 16.4^\circ\text{C} \quad (1.12)$$

The cycle is calculated for every day of the heating season ( $T_a < 12^\circ\text{C}$ ). The temperature supplied to the buildings follows the heating curve described by eq. (1.12). The temperature at the cold source of the heat pump corresponds to the temperature of the network and can vary between the bounds set in eq. (1.10) and eq. (1.11). The minimum approach temperature difference, the temperature rise of the cooling water through the condenser, the superheat of R1234yf at compressor inlet and the subcooling of the condensed  $\text{CO}_2$  are all assumed constant. Their value and the relations between these various temperatures are shown at Fig. 1.9.

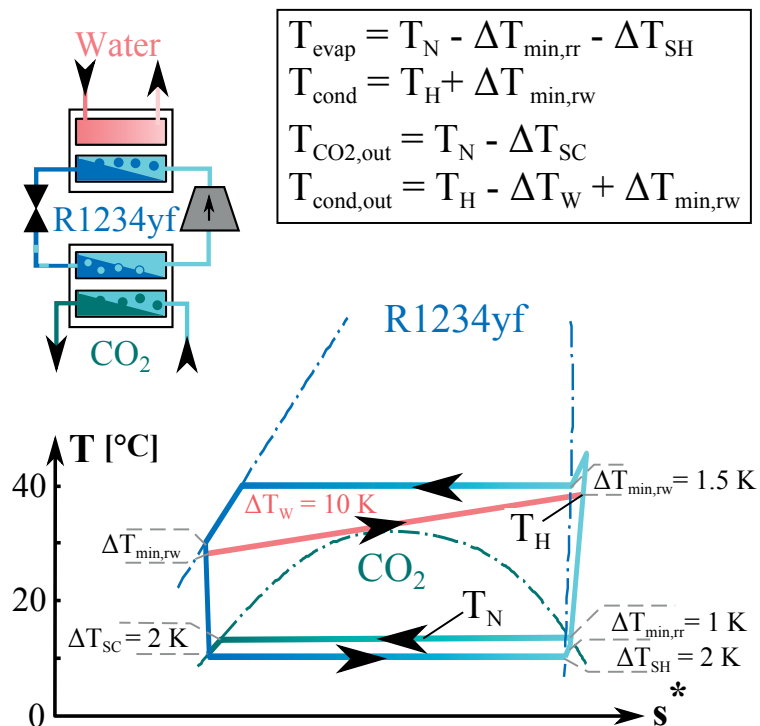


Figure 1.9 –  $\text{CO}_2$  network: Representation of the decentralized heat pump cycles and how the relevant temperatures are calculated.

As the temperature of the hot source varies throughout the heating season, it was considered necessary to have a realistic evaluation of the isentropic efficiency in the compression process for all the operating points. Inspired by a commercially available water-water heat pump [54] with a heating capacity of around 340 kW @ W15W55 that appeared to be the largest machine for which cost information could be obtained. It was decided to consider twin screw compressors for the model of the decentralized heat pumps. Obviously, this choice could be made, because this particular machine has a capacity well within the range of what is required in the test case area.

The efficiency of fixed built-in volume ratio compressors - to which twin screw compressors belong to - varies rather strongly with the operating point. It is caused essentially by the throttling loss due to the mismatch between the real and the built-in pressure ratio. Using information from the selection software of a manufacturer of compressors [55] it was possible to select a model of compressor that closely matched the one of the machine that inspired the model [54]. The characteristics was implemented and integrated as part of the model, thus allowing an accurate evaluation of the energy performance at all the required operating points.

Note that the heat pump that inspired the model uses HFC R134a. However, as it was decided to consider HFO R1234yf instead and that no commercial screw compressor designed for this latter fluid could be found at the time, an approximation was made by selecting a compressor model for HFC R134a. Since R1234yf was developed as a replacement for R134a, it can be reasonably assumed that the performance in term of efficiency will not differ too significantly. Standard test conditions and performance reports for compressors are defined in the European standard EN 12900 [56], it includes polynomial fits giving massflow and electric power as functions of evaporation and condensing temperature. These polynomial coefficients are available in the selection software [55] and have been used to compute the efficiency of the compressor using the following method:

The massflow processed by the compressor and the electric power consumed are represented by the following polynomials where  $\dot{y}$  denotes indifferently of the massflow or the power:

$$\begin{aligned} \dot{y} = & C_1 + C_2 T_{evap} + C_3 T_{cond} + C_4 T_{evap}^2 + C_5 T_{evap} T_{cond} + C_6 T_{cond}^2 \\ & + C_7 T_{evap}^3 + C_8 T_{cond} T_{evap}^2 + C_9 T_{evap} T_{cond}^2 + C_{10} T_{cond}^3 \quad (1.13) \end{aligned}$$

The polynomial coefficients are fitted from data obtained through standardized tests [56]. An important parameter is the superheat at compressor inlet; for halocarbons and hydrocarbons<sup>12</sup>, the standard requires the superheat to be maintained at a value of 10 K for all the points. Note that the difference in efficiency caused by the difference in superheat from the standard 10 K value to the value of 2 K assumed in this study was neglected. As the twin screw compressor chosen is semi-hermetic and adiabatic, one can assume that all the heat result-

---

<sup>12</sup>Including refrigerant blends

## 1.4. Conversion technologies: An energy comparison

ing from the dissipation is transferred to the working fluid (assuming a perfectly thermally insulated compressor casing), thus the enthalpy difference between inlet and outlet can be computed as:

$$\Delta h = \frac{\dot{E}}{\dot{m}} \quad (1.14)$$

The suction and discharge pressure  $P_{in}$  and  $P_{out}$  are computed from the value of  $T_{evap}$  and  $T_{cond}$  using REFPROP [57]. The enthalpy change corresponding to the isentropic process is then computed as follows using REFPROP:

$$s_{in} = (P_{in}, T_{evap} + 10) \quad (1.15)$$

$$\Delta h_s = h(P_{out}, s_{in}) - h(P_{in}, s_{in}) \quad (1.16)$$

Finally the isentropic efficiency is obtained by the ratio of 1.16 over 1.14:

$$\eta_{Cs} = \frac{\Delta h_s}{\Delta h} \quad (1.17)$$

The resulting efficiency map for the compressors used in the model of decentralized heat pump is represented at Fig. 1.10. The characteristics of the compressor used in the present study for the decentralized heat pumps are presented in Table 1.6.

Table 1.6 – Specifications of the compressor used in the model of the decentralized heat pumps

Compressor specifications										
Manufacturer:	Bitzer Kühlmaschinenbau GmbH									
Type:	Twin screw semi-hermetic									
Model:	CSH8573-140Y-40P									
Refrigerant:	HFC R134a									
Swept volume:	410 m <sup>3</sup> h <sup>-1</sup> @ 2900 rpm									
Motor voltage:	380-415 V PW-3-50 Hz									
Poly. coef. [EN12900]:	C <sub>1</sub>	C <sub>2</sub>	C <sub>3</sub>	C <sub>4</sub>	C <sub>5</sub>	C <sub>6</sub>	C <sub>7</sub>	C <sub>8</sub>	C <sub>9</sub>	C <sub>10</sub>
Power [W]:	31630.76	765.97	343.16	17.028	-18.382	2.5474	0.1624	-0.2612	0.1930	0.1087
Massflow [kg h <sup>-1</sup> ]:	5505.41	191.43	-0.3971	2.8029	0.2848	0.0569	0.0202	-0.0035	-0.0044	-0.0036

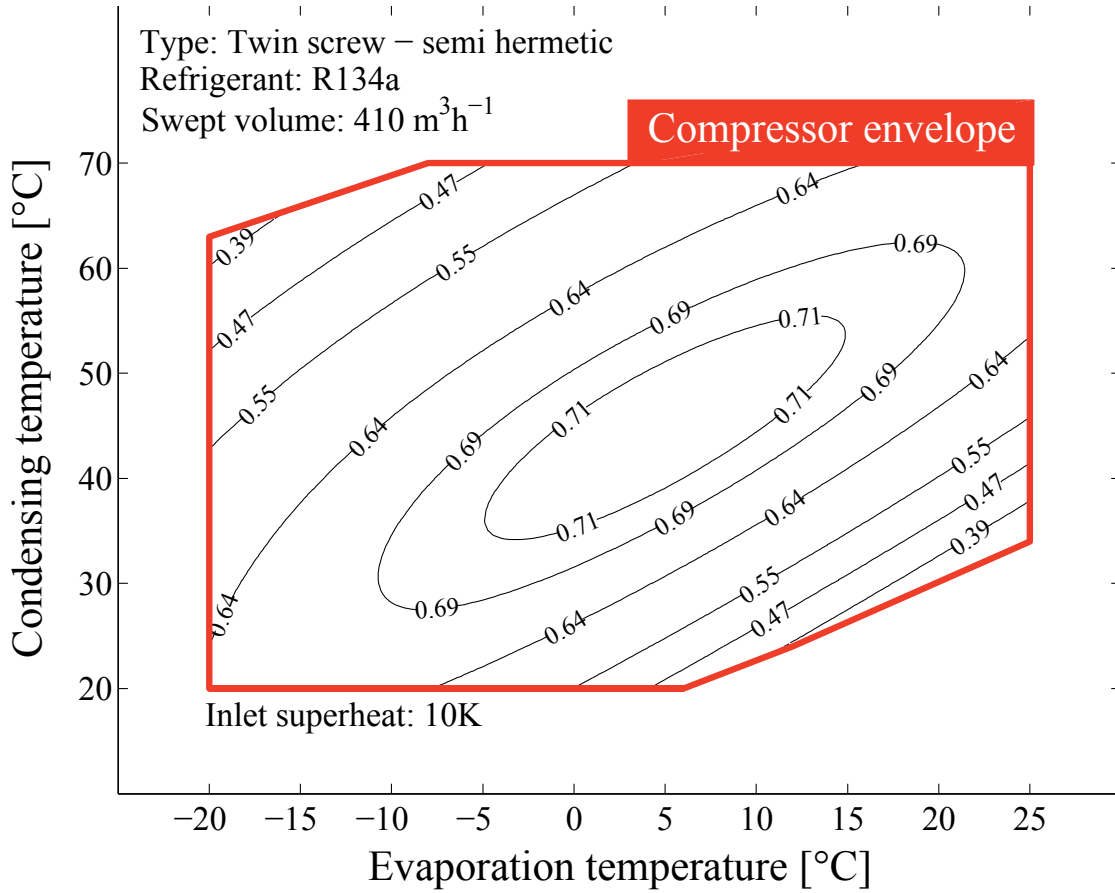


Figure 1.10 – Envelope and isentropic efficiency map of the compressor used in the model of the decentralized heat pumps

**Massflow of CO<sub>2</sub>, velocity constraint and pumping losses**

Knowing the energy required for each service, the specific enthalpies of the CO<sub>2</sub> in the liquid and vapour lines and taking into account the conversion technologies defined above, particularly with respect to their electricity consumption, it was possible to evaluate the massflow of liquid CO<sub>2</sub>, consumed by each of the 32 zones in the test case area:

$$\dot{m}_{liq} = \frac{\dot{Q}_{evap} - \dot{Q}_{cond}}{h_{vap} - h_{liq}} \tag{1.18}$$

In which  $\dot{Q}_{evap}$  and  $\dot{Q}_{cond}$  are computed as follows:

$$\dot{Q}_{evap} = \dot{Q}_{AC} + \dot{Q}_{CDC} + \dot{Q}_R \tag{1.19}$$



$$\dot{Q}_{cond} = \dot{Q}_H + \dot{Q}_{DHW} \quad (1.20)$$

A positive value of  $\dot{m}_{liq}$  implies that the cooling loads in the zone exceed the heat consumed at the cold source of the heat pumps installed in that zone. The massflow of vapour is simply the opposite of the massflow computed with eq. (1.18).

Subsequently, the massflow along the liquid and vapour lines are computed for each individual segment (length of pipeline between two zones).

According to Recknagel et al. [58] the velocity of liquid flow in pipelines must remain below a certain threshold, the value of which depends on the diameter of the pipes. These threshold values have been listed in Table 1.7. The goal of this particular criterion is to limit the risks associated with abrasion and cavitation erosion of the pipes, as well as avoiding excessive noise. Though developed for water pipelines, the criterion of maximum velocity can be considered to apply to a CO<sub>2</sub> network as well. Indeed, the energy of a CO<sub>2</sub> spherical cavitation bubble can be up to 85% that of a water cavitation bubble of the same size (in fact the ratio of the density of the two fluids). Using the maximum liquid velocity criterion, the massflow and the density of the liquid CO<sub>2</sub>, the diameter of the liquid pipes can be computed. Only then, pressure drops can be calculated, in the present study with the correlation of Churchill [59]. The diameter of the vapour pipes is not submitted to a similar constraint, therefore it can be a decision variable, the value of which should be selected adequately, for instance as a result of an optimization procedure.

Table 1.7 – Maximum liquid flow velocities in pipes according to Recknagel et al. [58]

Pipe outside diameter [mm]	Maximum liquid velocity [m s <sup>-1</sup> ]
50	1
100	1.4
150	1.6
200	2.1
300	2.5
≥ 500	3

Pressure drops along the lines have to be compensated by the use of booster pumps and compressors the power consumption of which is computed as follows:

$$\dot{E}_{C,booster} = \frac{1}{\eta_{C,booster}} \sum_{i=1}^n |\dot{m}_i| \frac{\Delta P_i}{\rho_{vap}} \quad (1.21)$$

$$\dot{E}_{p,booster} = \frac{1}{\eta_{p,booster}} \sum_{i=1}^n |\dot{m}_i| \frac{\Delta P_i}{\rho_{liq}} \quad (1.22)$$

Where the terms on the right hand side of eq. (1.21) and (1.22) are the sum of the pumping losses on each segment. Obviously  $\eta_C$  and  $\eta_p$  are the efficiencies of the booster compressors and pumps respectively. It has to be mentioned that in the case of a CO<sub>2</sub> network, pressure drops do not only affect the energy efficiency of the system, but they also cause the appearing of two-phase flows in both liquid and vapour lines. In the case of CO<sub>2</sub>, an isenthalpic expansion starting in a saturated liquid or vapour state leads to entering the saturation dome as the pressure goes down. Two-phase flows in the pipes should be avoided or at least limited for the sake of operational reliability. Consequently, the number and location of the booster pumps/compressors was selected such that pressure drops never exceed 1 bar between two of them. Note that adding more boosters in more locations when the total pressure drop increases is rather specific to refrigerant based networks. In comparison, standard high temperature water based district heating networks will tend to use boosters generating higher heads before adding more of them.

As mentioned earlier the liquid line is at a higher pressure than the vapour line which enables the use of free cooling. However it also implies an additional pumping power consumption for all the heating users. The expression is the following:

$$\dot{E}_{p,condensate} = \frac{1}{\eta_{p,condensate}} \frac{\Delta P_{liq-vap}}{\rho_{liq}} \sum_{i=1}^n \dot{m}_i \quad (1.23)$$

Where the sum denotes the total massflow of CO<sub>2</sub> pumped from the vapour line to the liquid line by the heating users. The total pumping power for the network is the sum of eq. (1.21)-(1.23).

### **Central plant variants**

As already mentioned earlier in the text, the proposed type of network requires a central plant to be balanced. Typically, in winter the central plant will inject heat into the network as the waste heat from the cooling users will not be enough to satisfy the need of the heating users<sup>13</sup> In summer, the situation is opposite, as the combination of low heat and high cooling demand asks for a central plant able to remove the excess heat out of the network. Summer operation is straightforward, as the temperature of the network -  $T_N$  - is constrained between 10°C and 12.5°C (see eq. (1.10)), the lake is cold enough to directly cool down the condenser of the central plant. Another peculiarity of summer operation is that the central plant does

---

<sup>13</sup>The heat demand of the heating users minus the electric consumption of the decentralized heat pumps.

#### 1.4. Conversion technologies: An energy comparison

not consume electricity since the pumping power needed to circulate the fluid is considered separately.

During winter operation the situation is more complex as several technologies/combinations of technologies can be envisaged to deliver heat efficiently to the network, they include heat pumps - electrically or thermally driven, various types of cogeneration systems, low temperature geothermal energy, thermal storages of different size and kind... For the sake of simplicity it was decided to focus the present thesis exclusively on central plants equipped with large electrically driven heat pumps. Note that the pertinence of a conversion technology for the central plant largely depends on conditions that are site specific and time dependent, particularly regarding the availability of the various energy resources and the nature of the framework conditions.

The dissipative heat exchanger at the central plant and used during summer operation is modelled in a similar way to the free cooling heat exchangers at the users. The dissipated heat rate is computed as:

$$\dot{Q}_{CP,dissip} = (h_{vap} - h_{liq}) \max\left(0, \sum_{i=1}^n \dot{m}_{liq,i}\right) \quad (1.24)$$

Where  $\dot{m}_{liq,i}$  is the massflow of liquid CO<sub>2</sub> drawn by each of the 32 zones computed from eq. (1.18). The heat rate to be provided by the central plant to the network during winter operation is computed as:

$$\dot{Q}_{CP,HP} = (h_{liq} - h_{vap}) \min\left(0, \sum_{i=1}^n \dot{m}_{liq,i}\right) \quad (1.25)$$

Note that eq.(1.24) and (1.25) use the function *max* and *min* to represent the transition between the heat dissipation mode and the heat pumping mode.

The amount of heat to be provided to the network by the heat pump at the central plant is computed using eq.(1.25), then the next step is to compute the electricity consumed.

As heat pumping at the central plant appeared to be the second largest electricity consumption, it was also decided to spend some effort on developing a relatively accurate model of it. It is based on computing the real thermodynamic cycle, rather similarly to what was done for the decentralized heat pumps. The following variants of heat pumps have been considered:

- Open cycle, single stage, using the CO<sub>2</sub> from the network as a working fluid.
- Closed cycle, single stage, using ammonia as a working fluid.

- Closed cycle, single stage, using R1234yf as a working fluid.

The cycles are schematically represented at Fig. 1.11, together with the way the various relevant temperatures are computed. Side A shows the CO<sub>2</sub> open cycle heat pump and side B the ammonia (NH<sub>3</sub>) closed cycle heat pump. The R1234yf version is not represented as it is topologically similar to the ammonia cycle. The decision to consider also other working fluids than CO<sub>2</sub> for the heat pump at the central plant came from the fact that the CO<sub>2</sub> being at high reduced pressure and its saturation dome being relatively flat, it causes a relatively important temperature rise during compression and a large desuperheating is required before the fluid starts condensing. Moreover the entropy generated in the expansion valve is comparatively large. All these factors render a CO<sub>2</sub> based heat pump less exergy efficient, than its ammonia or R1234yf counterparts, in spite of the added condenser exergy loss. In the present work the temperature of the water from the lake is considered constant throughout the year and during summer and respectively winter operation, the temperature of the network is considered constant. It results that the compressors at the central plant operate under a constant pressure ratio imposed by the temperature defined at Fig. 1.11. The key challenge for these compressors is that they have to be able to operate from virtually no flow to the design capacity of the plant, at a good efficiency, particularly at high loads. The detailed design of these compressors is beyond the scope the present work, however based on some preliminary considerations and at the time these lines are being written, the preference goes to a combination of several centrifugal compressors installed in parallel equipped with some kind of capacity control mechanism - under the form of variable speed drives and/or variable inlet guide vanes and diffuser vanes. More information is provided in the appendix about these compressors and how they have been modelled. Based on the typical efficiency range found and since parallel operation is considered, which allows at any load to run the right number of compressors at the right frequency for maximizing the overall efficiency. It was decided to consider a constant efficiency throughout the year for the compression process in the model of heat pump at the central plant. The values chosen for the efficiency are:

- for CO<sub>2</sub>:  $\eta_{C_s,CP} = 0.79$
- for NH<sub>3</sub>:  $\eta_{C_s,CP} = 0.79$
- for R1234yf:  $\eta_{C_s,CP} = 0.83$

### CO<sub>2</sub> based networks: Application to the test case area

In this paragraph, a CO<sub>2</sub> network is considered as alternative to the oil fuelled boilers and the air cooled compression chillers currently in place. The services to be provided remain the same in term of temperature levels and energy. In other words no refurbishment of the envelope of buildings or of their heating/cooling hydronics is considered. The configuration

## 1.4. Conversion technologies: An energy comparison

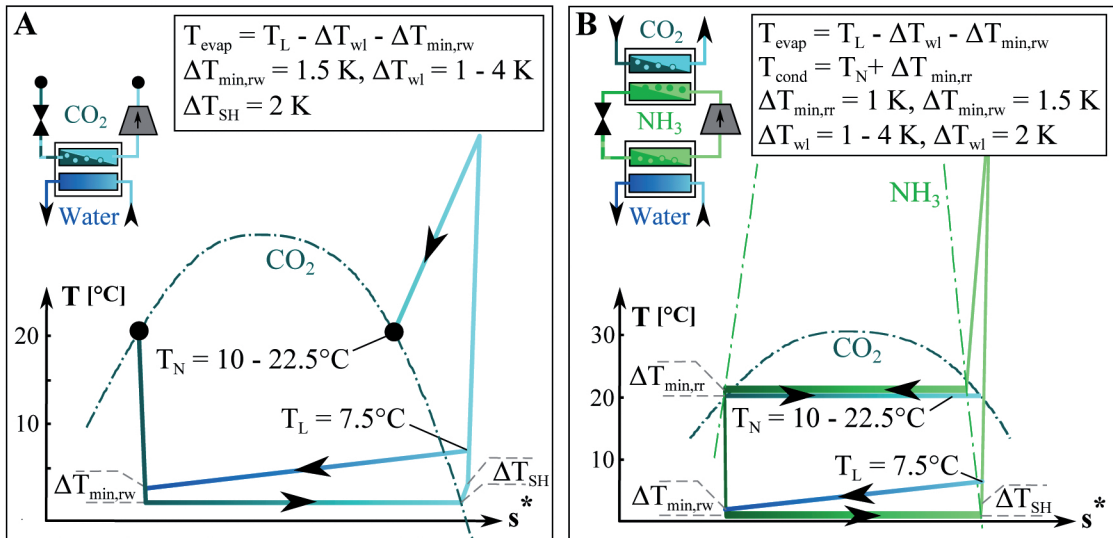


Figure 1.11 – Schematic representation of the heat pump cycle variants for the CO<sub>2</sub> network's central plant, Side A - CO<sub>2</sub> open cycle heat pump. Side B - Closed cycle heat pump using ammonia as a working fluid (the R1234yf version is not represented)

of the proposed network is shown at Fig. 1.12. It consists of two branches, 900 and 940 m long respectively. 18 segments were considered; their length corresponding to the distance from one group of buildings to another. Note that some of the closest groups have been lumped together to reduce the number of segments. Besides, the massflows coming from the groups B1 to B13 (See Fig. 1.1) have been split equally between the two branches of the network. The balancing of the network is done with a central plant that takes heat or releases heat in the nearby lake, through heat pumping or direct cooling respectively. The proposed CO<sub>2</sub> network is evaluated for the three variants of central plant's heat pump. A list of the relevant parameters and their value is provided at Table 1.8.

In the present application a diameter of 280 mm for the liquid lines is sufficient to satisfy the maximum velocity criterion. The diameter of the vapour lines, and the temperature of the network in winter and summer have been selected for maximizing the net present value at the end of the lifetime. A detailed description of the process will be given in a next chapter. For the vapour line diameter the optimal value found is 330 mm and it is not influenced by the type of heat pump used at the central plant. Note that connection lines of 30 m have been considered for the zones A1 - A10 and C1 to C9. Two connections of 30 m each were considered for the zone B1-B13, to share equally the load between the southern and northern branch of the network. The diameter of the liquid connection line is 110 mm and that of the vapour connection line 130 mm.

The optimal temperature in summer is 12°C and is also not influenced by the heat pump at the central plant, as during summer operation the plant work as a heat sink. For winter operation and a central plant equipped with the CO<sub>2</sub> open cycle heat pump the optimal is 20.5°C. For the variants with NH<sub>3</sub> and R1234yf central heat pumps, the optimal winter network's temperature



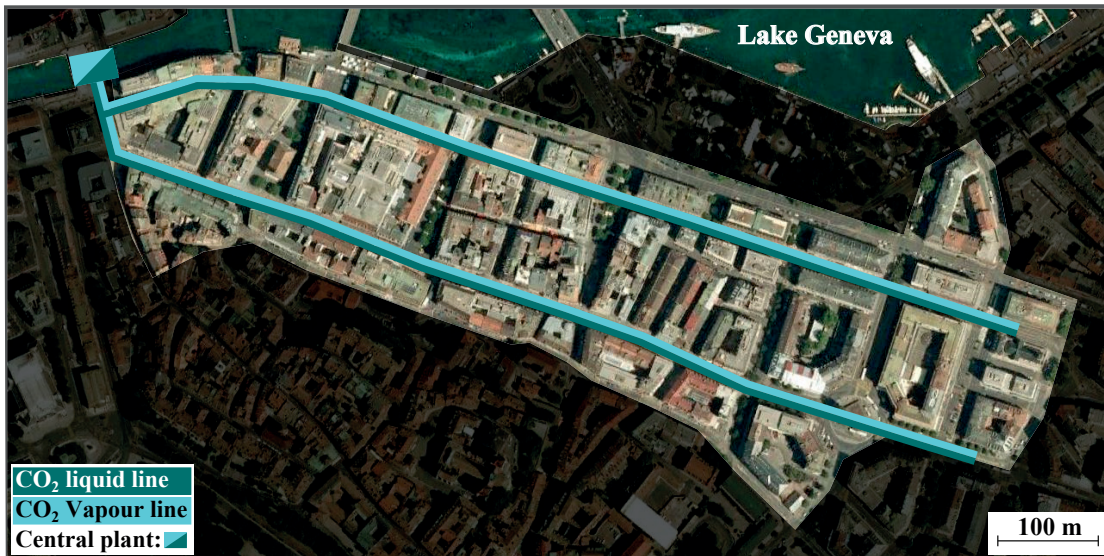


Figure 1.12 – Layout of the CO<sub>2</sub> network studied for the “Rues Basses” test case area.

reaches the upper bound defined in eq. (1.11) at 22.5°C. The difference is consistent with the higher exergy efficiency of the two latter variants, displacing the optimal trade-off between centralized and decentralized heat pumping towards a higher temperature of the network. The daily electricity consumption for the network equipped with the CO<sub>2</sub> central plant's heat pump is visible at Fig. 1.13. The annual electricity consumption is 11.66 GWh, with a peak electric load occurring in February during the cold snap at 5.61 MW. Overall the decentralized heat pumps<sup>14</sup> are the largest electricity consumers at 6.94 GWh per year they represent 59.50% of the annual consumption. The central plant's heat pump with 4.00 GWh is the second largest consumption and corresponds to 34.28% of the total. Refrigeration accounts for 5.87% and the pumping energy only accounts for the remaining 0.35%. The minimum load occurs during interseason when simultaneously the only electricity demand linked to the heating services is for domestic hot water, the central plant is used as a heat dissipater and the pumping energy is reduced to its minimum as the demand for air conditioning is low. The lowest electrical load is 153 kW, Note that during the 170 days period that the central plant operates as heat dissipater, the electrical load never exceeds 242 kW. The maximum pumping load occurs in august and is due to the peak demand for air conditioning, it corresponds to an electrical load of 89 kW or 36.8% of the consumption for that particular day.

The electricity consumption exhibit very clearly the two different types of operation characteristic of the proposed concept of network. To better illustrate these modes of operation the electric load curve is provided at Fig.1.14. Though limited to the same caveats than those applying to the demand load curve (Fig. 1.3, it also features the same didactic qualities. Note that on Fig. 1.14 the pumping power requirement have been separated for winter and summer

<sup>14</sup>Including the electricity required to pump the CO<sub>2</sub> from the condenser-evaporator back into the liquid line.

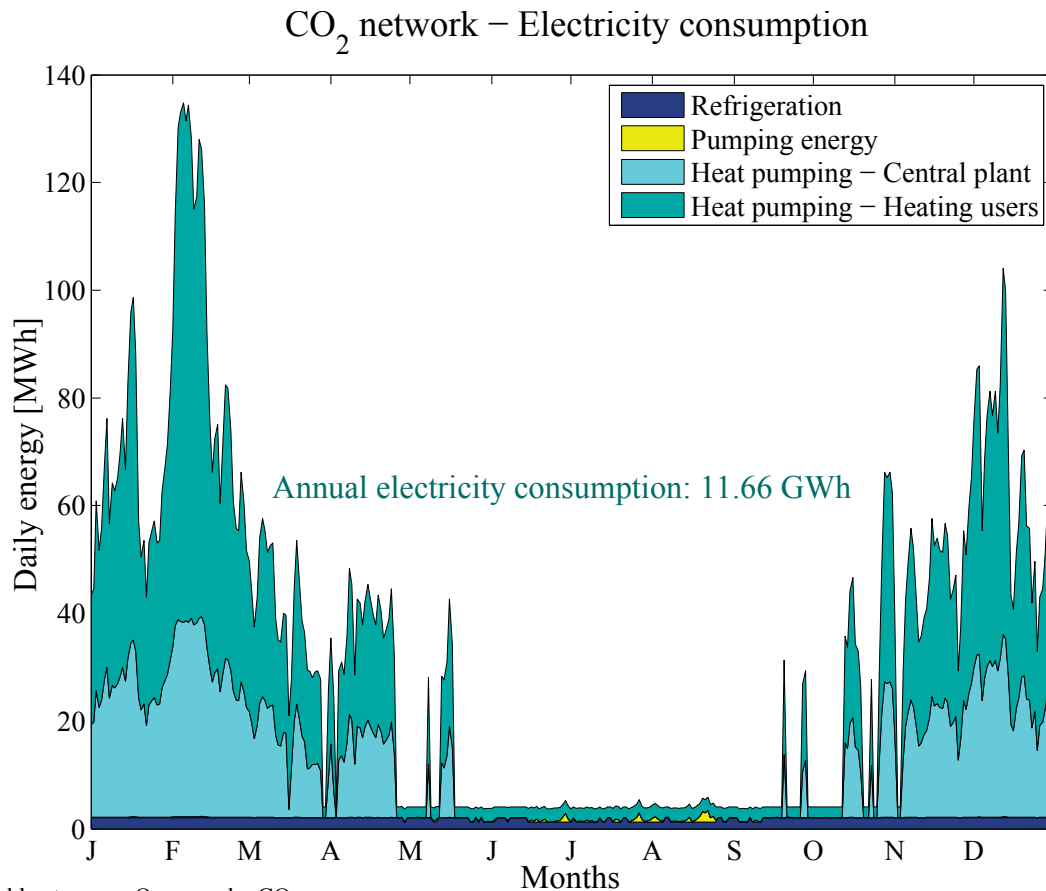
## 1.4. Conversion technologies: An energy comparison

Table 1.8 – CO<sub>2</sub> network: Values of the various numerical parameters.

Description	Parameters	Values		
Heat pump type at the central plant		CO <sub>2</sub> , open cycle	NH <sub>3</sub> , closed cycle	R1234yf, closed cycle
T, lake water	$T_{lake}$	7.5°C	7.5°C	7.5°C
T, network in winter	$T_{N,winter}$	20.5°C	22.5°C	22.5°C
T, network in summer	$T_{N,summer}$	12°C	12°C	12°C
Compressors isentropic efficiency at CP	$\eta_{Cs,CP}$	0.79	0.79	0.83
Delta T lake water in winter at CP	$\Delta T_{lake,winter}$	4 K		
Delta T lake water in summer at CP	$\Delta T_{lake,summer}$	3 K		
Inside diameter of the liquid lines	$\phi_{liq}$	280 mm		
Inside diameter of the vapour lines	$\phi_{vap}$	330 mm		
Diameter of the liquid connections	$\phi_{liq,connect}$	110 mm		
Diameter of the vapour connections	$\phi_{vap,connect}$	130 mm		
Length per connection	$l_{connect}$	30 m		
Number of connections	$n_{connect}$	45		
Pressure differential, liquid to vapour line	$\Delta P_{liq-vap}$	1 bar		
Max pressure drop over the length of network	$\Delta P_{max}$	1 bar		
Min. approach of temperature, refr. - water	$\Delta T_{min,rw}$	1.5 K		
Min. approach of temperature, refr. - refr.	$\Delta T_{min,rr}$	1 K		
Efficiency of booster compressors	$\eta_{C,booster}$	0.7		
Efficiency of booster pumps	$\eta_{p,booster}$	0.7		
Efficiency of CO <sub>2</sub> condensate pumps	$\eta_{p,condensate}$	0.25		
Pipe roughness	$\kappa_{pipe}$	0.3 mm		
Refrigerant charge (pipelines)	$M_{refr}$	130 tons		

operations, based on the criterion of whether the central plant provides or retrieve heat from the network. The reason behind it lies in the fact that pumping power shows a peak in summer, but also in winter, although the latter is much smaller than the first one. Finally at Fig. 1.14 the summer pumping load curve was flipped from left to right, as it is not simultaneous with the other loads that are all winter peaking. Comparing Fig. 1.14 with Fig. 1.3 one can sum up the behaviour of the system in winter as that of a two stage heat pumping system with a little bit of waste heat recovery, while in summer it behaves mostly like a free cooling network with a few heat pumps and compression chillers installed where needed. Furthermore, the values of the average combined heating and cooling coefficient of performance shown on Fig. 1.14 are characteristic of a heat pumping and of a free cooling system in winter and summer respectively. When comparing the load curve for the central and decentralized heat pumps it is worth noticing that the centralized heat pump as a much smoother evolution than the decentralized ones. In fact it has a very similar shape to that of the space heating load curve of Fig. 1.3. This can be explained by the fact that the  $COP_h$  of the centralized heat pump is constant, as the temperature of the lake and networks are assumed constant as well as the efficiency of the compressors. In fact the electric load of the centralized heat pump exceeds 75% of the maximum for 32 days in the year, which is rather similar to the 28 days in the case of space heating demand. For decentralized heat pumps the sharp increase of the electric load explains itself by the decrease of the  $COP_h$  due to the higher supply temperature required as the days get colder.<sup>15</sup> The decentralized machines see their electric load exceed 75% of the maximum only during 12 days per year. Note that the year 2012 chosen as reference in this

<sup>15</sup>See the heating curve defined by eq. (1.12).



Central heat pump: Open cycle, CO<sub>2</sub>

Figure 1.13 – Daily electricity consumption per type of use for a CO<sub>2</sub> network equipped with an open cycle CO<sub>2</sub> central heat pump.

study was colder than average, and during normal years without cold snaps these figures will be significantly smaller. The small numbers of days during which the systems operate at more than 75% capacity also apply to the summer operation, but since the only affected electricity consumption is the pumping energy, the effect on the total load is small. However one has to mention that the pumping power load exceeds 75% of the maximum only during 4 days in the year, which is half the value for the air conditioning demand, but can be explained by the non linearity of the pumping power with the cooling load<sup>16</sup>. Finally, the jump that can be observed in the electric load curve when both the decentralized heat pumps and the one at the central plant start operating as its origin in the degree-days method used, which is entirely similar to what was observed for Fig.1.3.

The annual electricity consumption of the variant equipped with a NH<sub>3</sub> closed cycle heat pump is 11.02 GWh, which represents an improvement of 5.5% over the CO<sub>2</sub> open cycle version. The improvement is mostly due to the consumption reduction for heat pumping at the central

<sup>16</sup>In fact with the flowrate, but in the present study the inlet and outlet thermodynamic state of the free cooling evaporators are constant, hence cooling load and flowrate vary proportionally



#### 1.4. Conversion technologies: An energy comparison

plant, from 4.00 GWh down to 3.53 GWh, and to the increased  $COP_h$  in decentralized heat pumping thanks to the higher temperature of the network in winter, causing its consumption to decrease from 6.94 to 6.71 GWh. Note that these improvements, are slightly compensated by an increase in the winter consumption for refrigeration due to the higher temperature of the network and also from a minor increase in pumping energy. The variant with an R1234yf heat pump at the central plant exhibit the same trend, leading to a total electricity consumption of 10.97 GWh, 6.0% lower compared to the variant with the  $CO_2$  heat pump and 1% compared to the  $NH_3$  one. The peak electricity consumption reaches 5.27 MW for the variant of network equipped with the  $NH_3$  heat pump, for the one with the R1234yf central plant the figure is 5.25 MW.

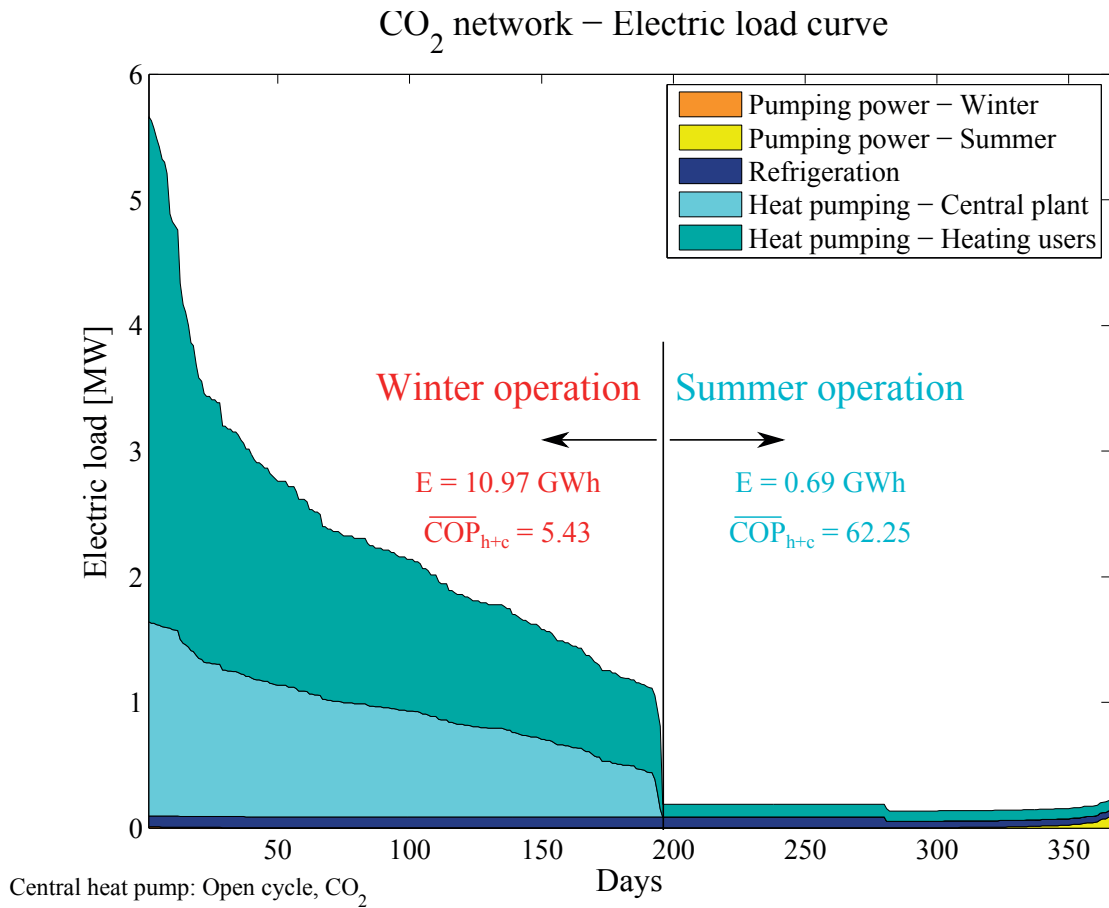


Figure 1.14 – Electricity load curve consumption per type of use for a  $CO_2$  network equipped with an open cycle  $CO_2$  central heat pump. The winter and summer types of operation are clearly visible. The total electricity consumption and average combined heating and cooling COP are given for the two types of operation respectively.

### R1234yf and R1234ze based networks: Description of the models

At the time of writing and as was discussed in section 1.4.2 various environmental, safety and legal considerations leave only CO<sub>2</sub> and HFO refrigerants R1234yf and R1234ze as potential fluids to be used in refrigerant based district energy networks. Compared to CO<sub>2</sub> both HFOs present the advantage of a much lower pressure. Typically for temperatures within the same constraints as those formulated for the CO<sub>2</sub> network in eq. (1.10) and (1.11), it correspond to a pressure of 4.4 - 6.4 bar and 3.1 - 4.6 bar for R1234yf and R1234ze respectively. These low pressures, as compared to the 45 - 60 bar for CO<sub>2</sub> in the same conditions represent a technical advantage and was the prime reason that motivated the study of HFO refrigerant based district energy networks. The general concept is identical to the CO<sub>2</sub> version - to use the latent heat of a refrigerant fluid to transfer heat across a combined district heating and cooling network in which cooling demand is mostly satisfied through free cooling and heating demand through decentralized heat pumping. The only topological difference come from the HFO refrigerants reduced pressure at network's temperature, that renders possible the use of the same refrigerant in the decentralized heat pumps in an open cycle. A schematic representation of the proposed variant of refrigerant network is provided at Fig. 1.15. Open cycle heat pumps pose some technical challenges particularly regarding the lubrication of the compressor, indeed it is very likely that only oil-free compressors could allow this kind of cycle to be implemented. If lubrication is necessary, then the use of decentralized heat pumps connected to the network through a condenser-evaporator is probably the most practical solution. In the latter eventuality an R1234yf/ze network becomes topologically similar to a CO<sub>2</sub> network (See Fig. 1.8).

For R1234yf and R1234ze networks, the decentralized conversion technologies used to supply the various thermal energy services are the following:

- Heat exchangers for air conditioning and cooling of data centres.
- R1234yf/ze vapour compression chillers for refrigeration. Liquid refrigerant is expanded from the network to the required saturation temperature and evaporated; the vapour produced is then compressed back to the network vapour line.
- Intermediate heat pumps for space heating and hot water preparation. The compressor of these machines is directly fed with refrigerant from the network. After the expansion valve the liquid refrigerant is sent back to the network's liquid line.

The models for the air conditioning, cooling of data centres and refrigeration systems are identical to that of the CO<sub>2</sub> networks. The way massflows, pressure drops and pumping power are computed is also identical to what was done for the CO<sub>2</sub> network. For more details the reader should refer to paragraph 1.4.2.

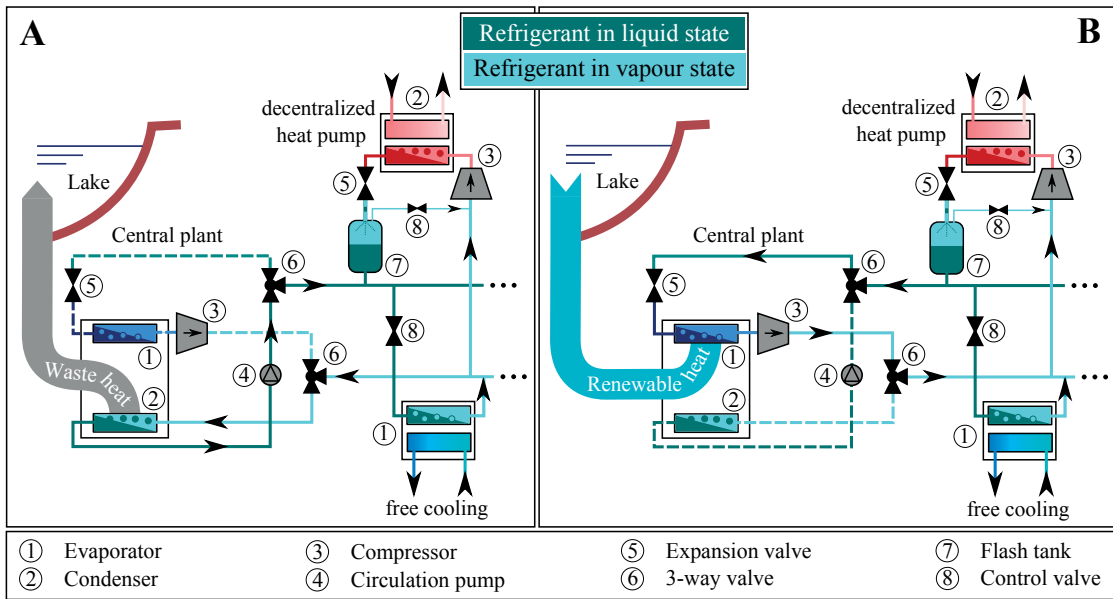


Figure 1.15 – Schematic representation of a refrigerant based district energy network using HFO R1234yf or R1234ze refrigerant. Side A - net cooling operation. Side B - net heating operation. Note: Because of low reduced pressure and provided that oil free operation are feasible, the same refrigerant can be used in open cycle decentralized heat pump and in the network.

### Decentralized heat pumps

The model of decentralized heat pumps used in R1234yf and R1324ze networks are based on computing the thermodynamic cycles for each day, similarly to what was done for the heat pump models used in the CO<sub>2</sub> network. Although the high pressure side of the cycle is almost identical<sup>17</sup> the low pressure side is rather different. First, the suction pressure and temperature correspond to the thermodynamic conditions prevailing in the vapour line of the network, and the expansion valve outlet pressure correspond to the one of the liquid line. As the expansion process causes the fluid to enter the two phase domain, it is required to place a flash tank connecting the expansion valve outlet to the liquid line. Some vapour has to be recirculated from the flash tank to the compressor inlet, as the pressure of the liquid line is around 1 bar above that of the vapour line, a valve must be placed on the recirculation vapour line to control the level of liquid in the flash tank. A representation of the cycle is provided at Fig. 1.16.

The cycle is calculated for every day of the heating season ( $T_a < 12^\circ\text{C}$ ). The temperature supplied to the buildings follows the heating curve described by eq. (1.12). The temperature at the cold source of the heat pump corresponds to the temperature of the network that can vary between the bounds set by eq. (1.10) and (1.11). The minimum approach temperature difference and the temperature differential in the hydronics, are assumed to remain constant. Their value and the relations between these various temperatures are shown at Fig. 1.16.

<sup>17</sup>The temperature at the compressor's discharge are slightly different

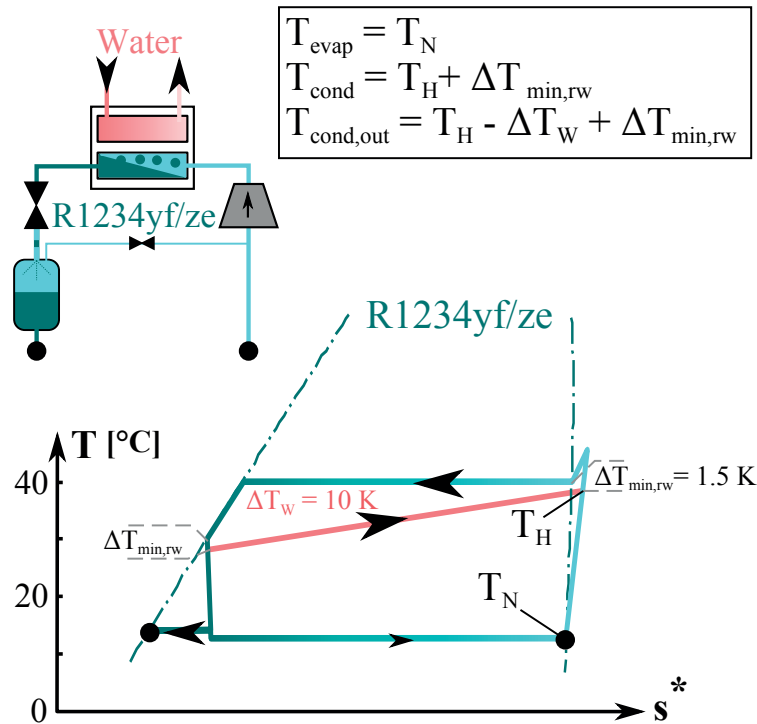


Figure 1.16 – R1234yf/ze network: Representation of the decentralized heat pump cycles and how the relevant temperatures are calculated.

For the R1234yf and R1234ze networks calculations, the model of compressor used in the decentralized heat pumps is the same as was used for the CO<sub>2</sub> network. Note that this particular compressor is not designed for oil free operation, and also that considering the typical capacity required for the buildings in the test case area, it is likely that the right choice would be decentralized heat pumps equipped with variable speed, direct driven, two-stage radial compressors mounted on magnetic bearings [60]. However not enough data on these machines have been gathered to set up a good model. It should be kept in mind that such compressors could also be used for the decentralized heat pumps of the CO<sub>2</sub> network. Keeping the same model of compressors for all the network studied was done assuming that the ranking of the various variants of network regarding their energy performance would not be affected. Nevertheless the shape of the efficiency map of the twin screw compressor chosen (see Fig. 1.10) will affect negatively the performances in cases where the temperature of the network in winter is high.

### Central plant's heat pump

At the central plant, due to the well adapted single stage cycle allowed by both R1234yf and R1234ze, only one variant of cycle was considered. It consist in an open cycle single stage heat pump topologically similar to what was proposed for the CO<sub>2</sub> network variant equipped with a CO<sub>2</sub> heat pump at the central plant. An example of the thermodynamic cycle of the

## 1.4. Conversion technologies: An energy comparison

R1234yf/ze open cycle heat pump is visible at Fig. 1.17, the relevant temperature and how they are computed are also shown.

The performance of the compressors of the central plant for the R1234yf and R1234ze network have been considered identical to the compressors of the R1234yf closed cycle heat pump proposed for the central plant of the CO<sub>2</sub> network. A comparison of the cycles presented at Fig. 1.11 and 1.17 shows clearly the advantage of R1234yf/ze over CO<sub>2</sub>, as the superheat at the compressor discharge is less important and represents a smaller share of the energy transformation [39] provided to the network by the central plant. It is less obvious, but the line of the T-s diagram representing the isenthalpic expansion is steeper in the case of R1234yf/ze which means that less entropy is created.

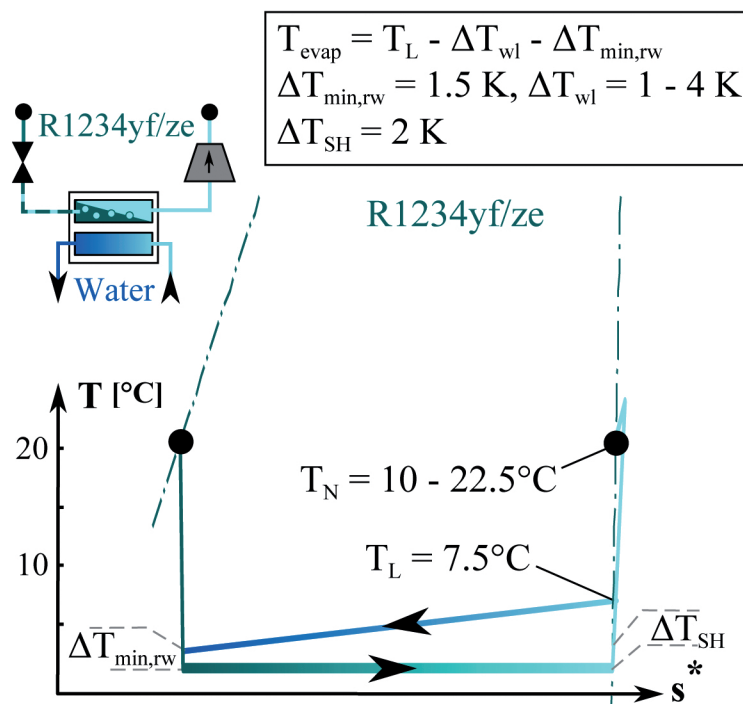


Figure 1.17 – R1234yf/ze network: Representation of the heat pump cycle used at the central plant and of the relevant temperatures.

### R1234yf and R1234ze based networks: Application to the test case area

In this paragraph, both an R1234yf and R1234ze based network are considered as alternatives to the oil fuelled boilers and the air cooled compression chillers currently in place. As for the CO<sub>2</sub> network, the services to be provided remain the same in terms of temperature levels and energy, and the configuration of the proposed network remain the same as the one visible at Fig. 1.12. Again 18 pipe segments were considered and the massflows coming from the groups B1 to B13 (See Fig. 1.1) have been split equally between the two branches of the network. The balancing of the network is done with a central plant that takes heat or releases heat in the nearby lake through heat pumping or direct cooling respectively. A list of the relevant

## Chapter 1. Thermo-economic analysis

Table 1.9 – R1234yf and R1234ze networks: Values of the various numerical parameters.

Description	Parameters	Values	
Refrigerant used		R1234yf	R1234ze
Temperature of the lake water	$T_{lake}$	7.5°C	7.5°C
Temperature of the network in winter	$T_{N,winter}$	20.5°C	20°C
Temperature of the network in summer	$T_{N,summer}$	12°C	12°C
Isentropic efficiency of the central plant's compressors	$\eta_{Cs,CP}$	0.83	0.83
Inside diameter of the liquid lines	$\phi_{liq}$	270 mm	
Inside diameter of the vapour lines	$\phi_{vap}$	700 mm	750 mm
Diameter of the liquid connections	$\phi_{liq,connect}$	105 mm	100 mm
Diameter of the vapour connections	$\phi_{vap,connect}$	270 mm	300 mm
Refrigerant charge	$M_{refr}$	151 tons	154 tons
Central plant: Temperature glide of the water in winter	$\Delta T_{lake,winter}$	4 K	
Central plant: Temperature glide of the water in summer	$\Delta T_{lake,summer}$	3 K	
Length per connection	$l_{connect}$	30 m	
Number of connections	$n_{connect}$	45	
Pressure differential, liquid to vapour line	$\Delta P_{liq-vap}$	1 bar	
Min. approach of temperature, refrigerant - water	$\Delta T_{min,rw}$	1.5 K	
Min. approach of temperature, refrigerant - refrigerant	$\Delta T_{min,rr}$	1 K	
Efficiency of booster compressors	$\eta_{C,booster}$	0.7	
Efficiency of booster pumps	$\eta_{p,booster}$	0.7	
Efficiency of CO <sub>2</sub> condensate pumps	$\eta_{p,condensate}$	0.25	
Pipe roughness	$\kappa_{pipe}$	0.3 mm	

parameters and their value is provided in Table 1.9.

In the case of R1234yf, a diameter of 270 mm for the liquid lines is sufficient to satisfy the maximum velocity criterion, for R1234ze the figure is 250 mm. As was done for the CO<sub>2</sub> network, the diameter of the vapour lines and the temperature of the network in winter and summer have been selected such as to maximize the net present value at the end of the lifetime. It led to an optimal value of 700 mm and 750 mm for R1234yf and R1234ze respectively. This value must be compared to the 330 mm that had been found for CO<sub>2</sub>. The much larger diameter found for both HFOs has its origin mostly in the low pressure at which they operate. As CO<sub>2</sub> can tolerate a pressure drop of around 1 bar to limit the drop in saturation temperature to 1°C, the value is 0.15 bar and 0.12 bar for R1234yf and R1234ze. Note that the preliminary values presented in Table 1.5 exhibit the same tendency, to the exception of the liquid pipe diameter that was not computed using the maximum velocity criterion.

In the case of the R1234yf network, the total annual electricity consumption amounts to 10.09 GWh which is 13.5% lower than that of the CO<sub>2</sub> network<sup>18</sup>. The repartition of the electricity consumption is 64.0% for the decentralized heat pumping at 6.47 GWh, while centralized heat pumping accounts for 28.8% or 2.91 GWh. The electricity consumption for refrigeration and

<sup>18</sup>Equipped with an open cycle CO<sub>2</sub> heat pump at the central plant.

#### 1.4. Conversion technologies: An energy comparison

pumping energy account respectively for 6.65% and 0.55%. The evolution of the electricity consumption around the year is provided at Fig. 1.18.

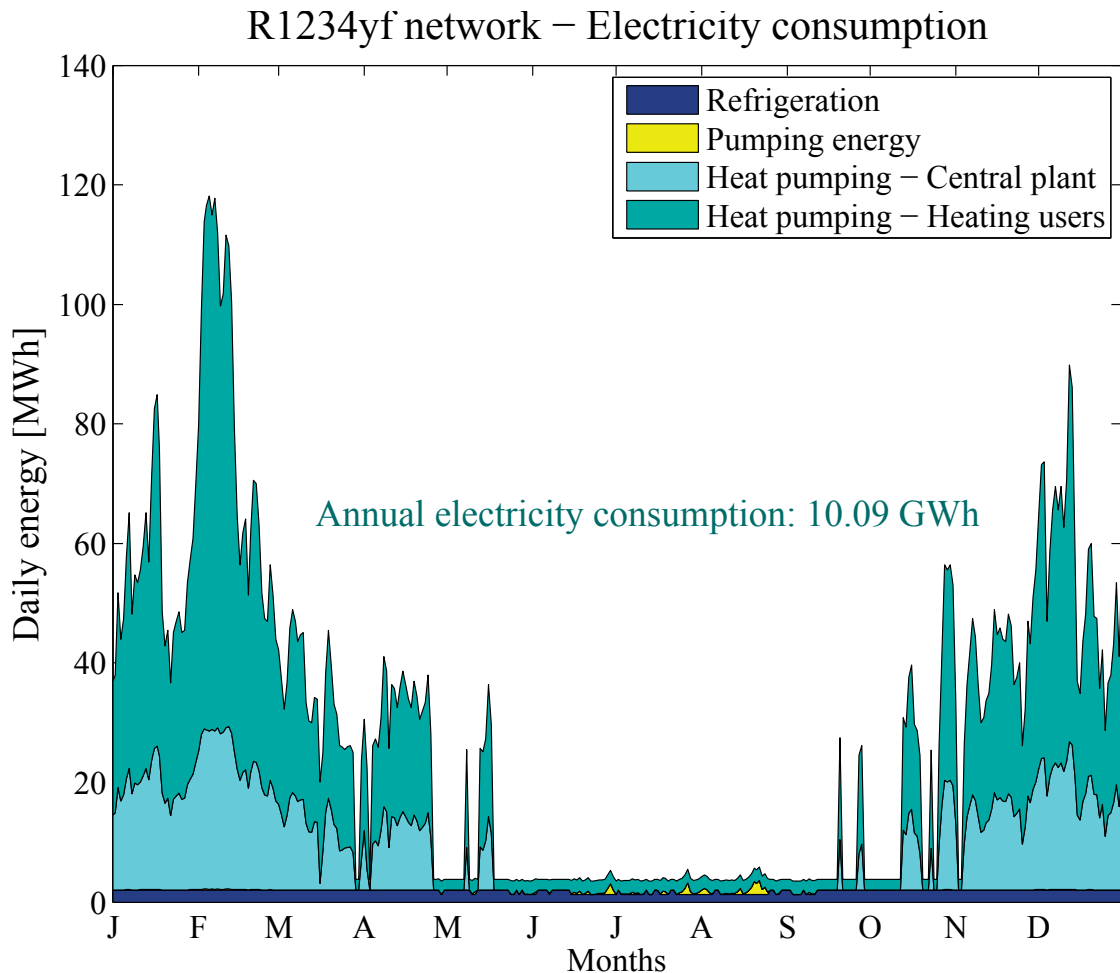


Figure 1.18 – Daily electricity consumption per type of use for a R1234yf network equipped with R1234yf open cycle central and decentralized heat pumps.

The optimal temperature in summer is 12°C and is identical to what was found for the CO<sub>2</sub> based network. The optimal temperature of the network in winter is 20.5°C.

The electric load curve for the R1234yf network is provided at Fig. 1.19. The duration of the summer and winter operation are identical to that of the CO<sub>2</sub> network. During the February peak, the maximum electric load reaches 4.95 MW, which is 11.8% lower than the CO<sub>2</sub> network equipped with an open cycle CO<sub>2</sub> heat pump at the central plant. The minimum electric load also occurs during the interseason at a value of 145 kW which is virtually identical to what was found for the CO<sub>2</sub> variant. The electric load during the peak cooling day is 219 kW, in which 74 kW is used for pumping. A comparison of the electric load curves for CO<sub>2</sub>



and R1234yf (Fig. 1.14 and 1.19) shows very little difference. When comparing the combined heating and cooling coefficients of performance for the two operation modes, it can be seen that the R1234yf is superior mostly in winter. The gain in efficiency mostly comes from the reduction of the centralized heat pumping contribution, which is reduced by 1.09 GWh (-27%) and a slight reduction in decentralized heat pumping (-0.47 GWh) when compared to the CO<sub>2</sub> network with the open cycle CO<sub>2</sub> heat pump. This is due to the absence of evaporators and the associated heat transfer exergy losses at the decentralized heat pumps and the lower exergy loss in the expansion, compression and desuperheating processes of the open cycle R1234yf heat pump at the central plant.

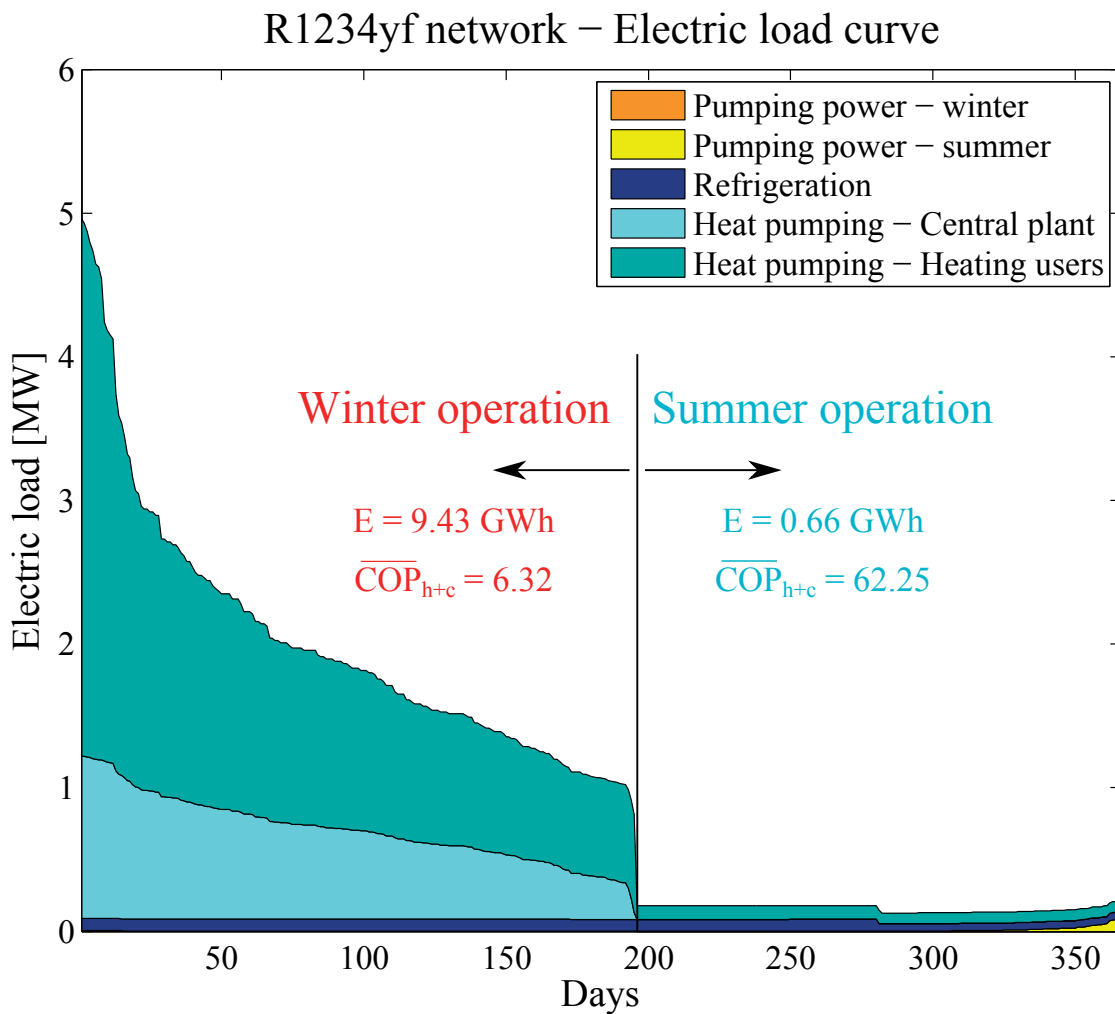


Figure 1.19 – Electricity load curve consumption per type of use for a R1234yf network equipped with open cycle R1234yf centralized and decentralized heat pumps. The winter and summer types of operation are clearly visible. The total electricity consumption and average combined heating and cooling COP are given for the two types of operation respectively.

In the case of the variant using R1234ze, the annual electricity consumption is 9.91 GWh, which is only 1.8% lower than that of the R1234yf network. The optimal temperature of the R1234ze



#### 1.4. Conversion technologies: An energy comparison

network is, similarly to the other variants, of 12°C in summer. For winter operation, the figure is 20°C, which is half a degree lower than was found for the R1234yf and also lower than all the variants of CO<sub>2</sub> network. As a result of the similar winter and summer temperatures there is very little difference among the proposed networks in the repartition between centralized and decentralized heat pumping. The electric load curves for the R1234ze network shown at Fig. 1.20 illustrates clearly this fact. For R1234ze, decentralized heat pumping accounts for 64.8% of the total, the figure is 64.0% in the R1234yf network and around 60% for all the variants of CO<sub>2</sub> network studied. Similarly for centralized heat pumping it represents 28.1% of the total electricity consumption in the R1234ze network, 28.8% for R1234yf, and around one third for the CO<sub>2</sub> networks. The peak electric load for R1234ze is 4.82 MW, which is 2.6% lower than that of the R1234yf network.

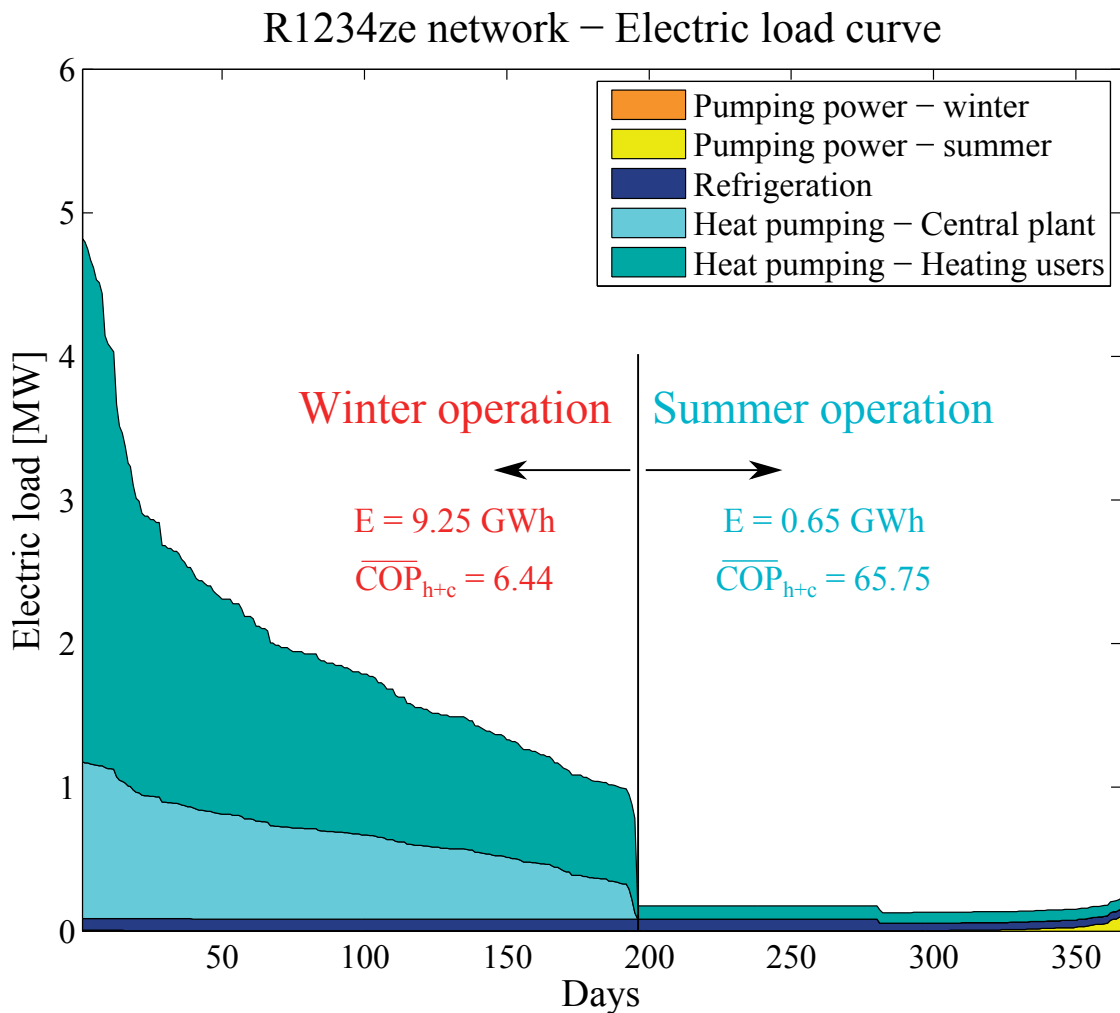


Figure 1.20 – Electricity load curve consumption per type of use for a R1234yf network equipped with open cycle R1234ze centralized and decentralized heat pumps. The winter and summer types of operation are clearly visible. The total electricity consumption and average combined heating and cooling COP are given for the two types of operation respectively.

Overall the two HFO networks exhibit the same sharp peak in the decentralized heat pumps electricity consumption as was observed for the CO<sub>2</sub> networks. Which is logical, as the heating curve is the same for all the variants of network (See eq. (1.12)) and as the working fluid in the decentralized heat pumps is the same for all networks except the R1234ze one. The origin of the differences is then limited to the variation induced by the various temperatures of network in winter and to the fact that the decentralized heat pumps cycles are open or not.

### 1.4.3 Cold water based district energy networks

One can compare the technological evolution of district heating and cooling systems to a thermodynamic evolution. Essentially the path followed is one where the second law of thermodynamics was gradually taken into account, somehow bringing the systems from the energy to the exergy efficiency, by reducing the temperature and introducing ever more efficient conversion technologies at both the central plants and users substations.

Refrigerant based district energy networks are the result of a thought process trying to answer the question: "How to deliver the thermal services needed in urban areas in an exergy efficient way?" And a question worth investigating is whether this high performance is the result of using refrigerants or can it be replicated with liquid water.

Initially, the present study had to focus exclusively on the study of refrigerant based district energy networks. From the start, cold water networks had been identified as the closest competing technology, but it was assumed that refrigerant based networks would be more efficient. However after a discussion with a utility company it appeared necessary to do a proper thermoeconomic comparison of the two technologies.

#### **Cold water network: Description of the models**

It was decided to study a concept of network having the same features as the refrigerant networks discussed in the previous sections. These features are the following:

- Provide heating and cooling services with only one network.
- Use only two-pipes.
- Maximize the use of free cooling.
- Deliver heat at the appropriate temperature for each user.
- Recover some of the waste heat from the cooling services and valorise it for heating purposes.

It appeared eventually that the most straight forward way to reach these requirements was by replacing the refrigerant by liquid water. Basically the network consists of two pipes both

#### 1.4. Conversion technologies: An energy comparison

---

containing water but one with a temperature a few degrees above that of the other one. Any time cooling is required, water is drawn from the cold line, heated and sent back to the hot line. Reversely, when heating is required, water is drawn from the hot line, cooled down and sent back to the cold line. In both cases the flow of water will be controlled such that the water sent back into one of the lines is at the same temperature than that particular line. This process is exactly equivalent to what is proposed in a refrigerant network, the cold water line corresponding to the liquid line of a refrigerant based network, while the hot water line corresponds to its vapour line.

A better denomination would be to call the lines *low enthalpy* and *high enthalpy*, as it is in fact the thermodynamic property that is used. Using that convention renders obvious the analogy between the cold water network and refrigerant based networks, since both cold water and liquid refrigerant lines have a lower enthalpy than hot water and refrigerant vapour lines.

Similarly to the refrigerant network, the temperature of the network<sup>19</sup>(In this study it is defined as the temperature of the hot water line) should be chosen such as to allow the use of free cooling for the air conditioning and the cooling of data centres, thereby setting the upper and lower bounds for temperature in summer:

$$\begin{aligned} T_{N,min,summer} &= T_{lake} + \Delta T_N + \Delta T_{min,ww} = 11.5^\circ\text{C} \\ T_{N,max,summer} &= T_{AC} + \Delta T_{min,ww} = 16^\circ\text{C} \end{aligned} \tag{1.26}$$

and in winter:

$$T_{N,max,winter} = T_{CDC} - \Delta T_{min,ww} = 26^\circ\text{C} \tag{1.27}$$

As the temperature limits defined by eq. (1.26) and (1.27) are lower than the temperature required for the space heating and the service of domestic hot water preparation, the use of decentralized heat pumps is considered for all the heating users. The water drawn from the hot water line of the network being cooled down by the evaporation of the refrigerant at the cold source of the heat pump, exactly in the same way as for groundwater heat pumps. The temperature limits is too high for the supply of commercial refrigeration applications using direct cooling, as a result the use of compression chillers is required, their condenser being cooled by water drawn from the cold water line of the network. There also it is entirely analogous to what is proposed for refrigerant based networks. One important parameter to be chosen is the temperature difference between the hot and cold water lines. In the present study, it was assumed that the temperature difference between the lines is maintained con-

---

<sup>19</sup>(

stant throughout the year. The upper limit is 6.5 K as it is the maximum value that allows a network, with a hot water line at 16°C, to be cooled down in summer by the lake water with a minimum approach of temperature of 2 K. For practical reasons the minimum value for the temperature difference that was considered in this study is 2 K<sup>20</sup>. The minimum temperature of the network in winter is unconstrained but for simplicity reasons it was limited to 11.5°C, the same value as used for summer operation.

A representation of the cold water network proposed here is provided at Fig. 1.21. Except for the use of sensible heat vs. latent heat, the main topological difference between the cold water network proposed here and the CO<sub>2</sub> networks discussed earlier concerns the layout of the pumps used to circulate the fluid.

Instead of imposing a pressure difference between the two lines, as done for the CO<sub>2</sub> networks, suppressing the need for circulation pumps at the cooling users, circulation pumps are considered for each users. Indeed, reducing the number of circulation pumps for the CO<sub>2</sub> network has more to do with the scarcity of suitable models of pumps, than concerns about a more energy efficient solution. Moreover imposing a pressure difference between the lines is rather easy in refrigerant based network as the constraint on the maximum drop in saturation temperature guarantees that variation in pressure along the lines remain small. For liquid water however, as the size of the pipes will necessarily be large due to the low temperature difference between the lines, the possibility to operate the system with the smallest possible pipes and larger pressure drops is advantageous, especially when one consider the very small number of days of peak pumping power observed for the refrigerant networks. Such a decentralized pumping solution makes sense as the variety of water circulation pumps available is virtually infinite and most of them, can be operated with variable speed drives. It results that the flowrate at the central plant is a consequence of the equilibrium between cooling and heating users and depending on the direction of the flow it will pass either through the dissipative heat exchanger or the water cooled condenser of the heat pump. The frequency of rotation of the water pump at users is adapted such that the temperature glide in the heat exchanger is equal to the temperature difference desired between the lines of the network. Similarly, the flowrate of water from the lake and the flowrate of refrigerant in the centralized heat pump is adapted such that the cold water line in summer and the hot water line in winter are maintained at the desired temperature. As the network changes from a net heating mode to a net cooling mode over the course of the seasons, it will probably be necessary to install, flow control valves anti-parallel to the pumps, so that when the pressure differential between the lines is in the right direction, pump are switched off and the flow through the heat exchangers is controlled by the valves. In order not to overload Fig. 1.21 these valves have not been represented.

Overall, the approach followed to model the proposed cold water network is similar to what was done for the variants of CO<sub>2</sub> network using a closed cycle R1234yf heat pump at the central plant. For a more detailed description the reader is advised to refer to section 1.4.2. Regarding the diameter of the lines, as both contain liquid water, the maximum velocity

---

<sup>20</sup>2 K corresponds to the the amount of superheat considered at the decentralized heat pumps in this study, meaning that below this value the electricity consumption becomes constrained by the value of the superheat and not any more the temperature glide of the water.

## 1.4. Conversion technologies: An energy comparison

criterion is applicable (see Table 1.7). Moreover, the change in density between the hot and cold water from the network is negligible and logically the same diameter can be chosen for both the hot and cold water lines. Note that one of the parameters left as a decision variable in refrigerant based networks - the vapour line diameter - cannot be chosen any more in the cold water network. However, the enthalpy difference between the vapour and liquid in refrigerant based networks, that is fixed for obvious thermodynamic reasons, becomes a parameter to be optimized in a cold water network as the temperature differential between the hot and cold water line can be chosen within a certain range - up to 6.5 K in the present study. The T-s diagram of both the centralized and decentralized heat pumps are presented at Fig. 1.22. There are some differences compared to refrigerant based networks with respect to the relevant temperatures. Both centralized and decentralized machines are considered to use R1234yf as a working fluid. The isentropic efficiency for compressors at the decentralized heat pumps is computed the same way as for the other networks (see Fig. 1.10). As the temperatures are constant throughout the period of operation of the heat pump at the central plant and as was done for the other centralized HFO based heat pumps, the efficiency of the compressors at the central plant is assumed constant at 83%.

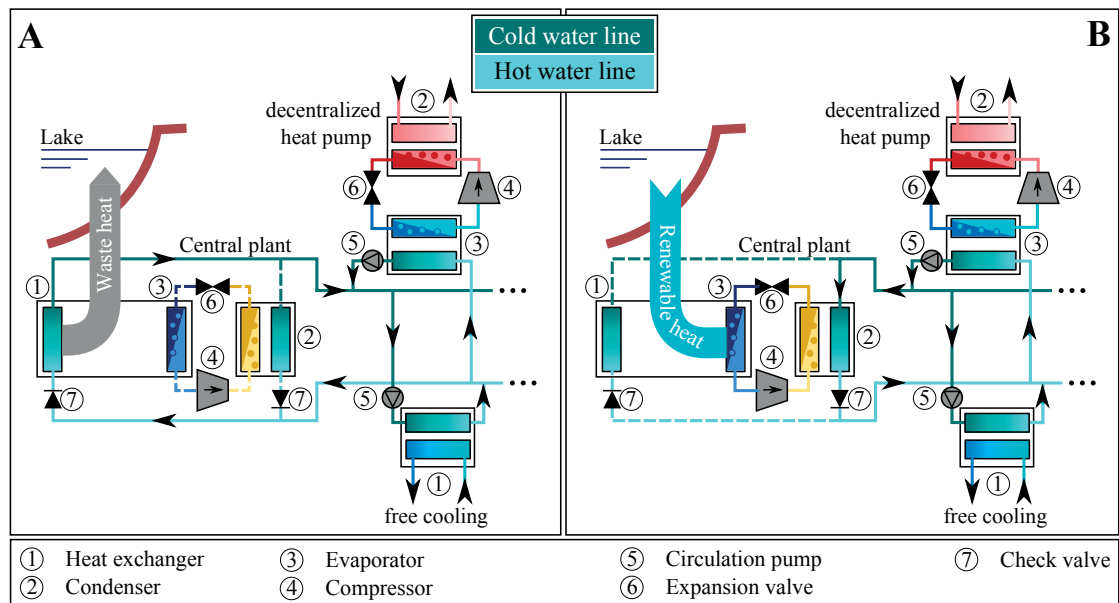


Figure 1.21 – Schematic representation of a water based district energy network also known as an energy network. Side A - net cooling operation. Side B - net heating operation. Note: In this system the pumps for circulating the water are fully decentralized.

### Model of the decentralized pumping scheme

The procedure used to model the decentralized pumping scheme, starts by evaluating the mass flow of water for each of the 32 zones considered in the test case area using eq. 1.18 but with the values of enthalpy for water at  $T_N$  and  $T_N - \Delta T_W$ . The reference pressure for the computation is 1 bar. Afterwards the massflow in each segment of pipe is computed and the

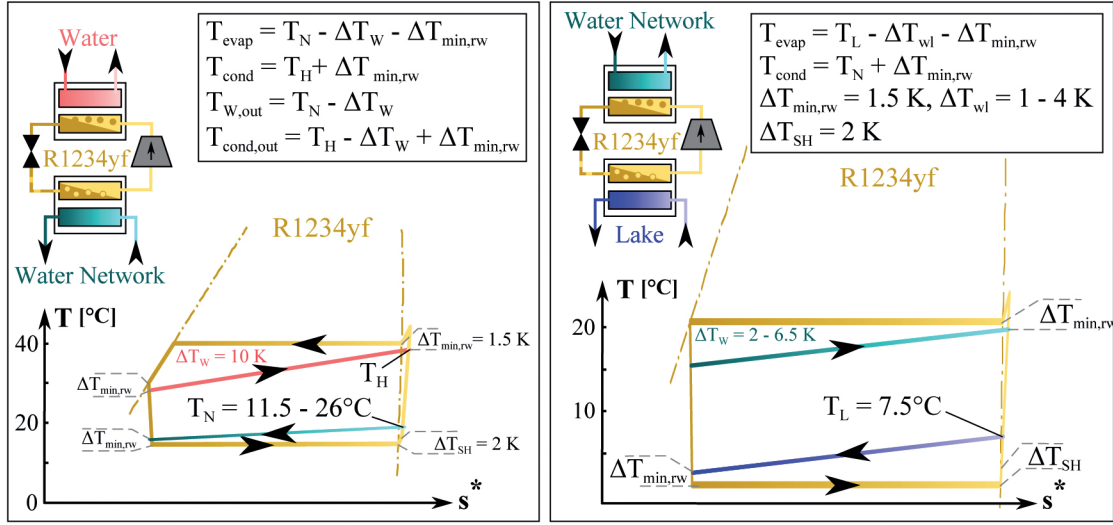


Figure 1.22 – Cold water network: Representation of the T-s diagrams of the heat pump cycles used, together with the relevant temperatures. - Left: decentralized heat pumps - Right: Central plant's heat pump.

pressure drops and their cumulated value are evaluated. The pressure at the central plant is assumed to be the atmospheric pressure. The pressure differential between the hot and cold water line differs for each of the 32 zones on a daily basis. The pumping power required for the heating users of the  $i^{\text{th}}$  zone is computed as follows:

$$\dot{E}_{p,H,i} = \frac{1}{\eta_p(\dot{m}_{H,i}, \dot{m}_{n,H,i})} \frac{\max(P_{N,h,i} - P_{N,c,i}, 0)}{\bar{\rho}_w} |\dot{m}_{H,i}|$$

$$\text{where } \eta_p(\dot{m}_{H,i}, \dot{m}_{n,H,i}) = C_1 \left( \frac{\dot{m}_{H,i}}{\dot{m}_{n,H,i}} \right)^2 + C_2 \left( \frac{\dot{m}_{H,i}}{\dot{m}_{n,H,i}} \right) + C_3 \quad (1.28)$$

where  $P_{N,h,i}$  and  $P_{N,c,i}$  are the pressure of the hot water and cold water line respectively and at the location of the  $i^{\text{th}}$  zone.  $\bar{\rho}_w$  is the density of the water from the network.  $\dot{m}_{H,i}$  is the massflow of water required at the cold source of the decentralized heat pumps of the zone and  $\dot{m}_{n,H,i}$  is the nominal massflow required by the  $i^{\text{th}}$  zone for heating, evaluated for the heating sizing condition ( $T_a = -7^\circ\text{C}$ ). Note that when  $P_{N,c,i}$  is greater than  $P_{N,h,i}$  the pumping power evaluated with eq. (1.28) becomes null representing the fact that when the pressure differential is in the right direction the pump is switched off and the flow is controlled by a

## 1.4. Conversion technologies: An energy comparison

---

valve. Note that as it was initially envisaged that the pumping energy could represent a larger share of the electricity consumption than was obtained for the refrigerant networks, it was decided to assume a quadratic relationship for the pump efficiency, with the hypothesis that the value only depends on the massflow relative to the nominal massflow of the pump. Using the sizing calculators of two pump manufacturers [61, 62] the approximation showed to be in good agreement with their efficiency values. Normally, as variable speed drive are considered, one would have to compute for each day the frequency of rotation, based on the flowrate, pressure differential and the fan's affinity law [63] and then compute the efficiency. However, it was not done as the increase in accuracy did not worth the extra complexity. Furthermore the model of pump efficiency proposed underestimates the value. The value of the coefficients  $C_1$ ,  $C_2$  and  $C_3$  have been fitted from a pump in the average of what is needed for the 32 zones of Rues Basses [62].

For the cooling users the efficiency is computed in a similar way through:

$$\dot{E}_{p,C,i} = \frac{1}{\eta_p(\dot{m}_{C,i}, \dot{m}_{n,C,i})} \frac{\max(P_{N,c,i} - P_{N,h,i}, 0)}{\bar{\rho}_w} |\dot{m}_{C,i}|$$

$$\text{where } \eta_p(\dot{m}_{C,i}, \dot{m}_{n,C,i}) = C_1 \left( \frac{\dot{m}_{C,i}}{\dot{m}_{n,C,i}} \right)^2 + C_2 \left( \frac{\dot{m}_{C,i}}{\dot{m}_{n,C,i}} \right) + C_3 \quad (1.29)$$

where the pressure difference is taken in the opposite direction than for the heating users, and where  $\dot{m}_{C,i}$  is the massflow of water required at the free cooling heat exchangers and at the condenser of the refrigeration chillers in the  $i^{th}$  zone.  $\dot{m}_{n,C,i}$  is the nominal massflow required, evaluated for the cooling sizing condition ( $T_a = 30^\circ\text{C}$ ).

### Cold water network: Application to the test case area

As was done for the other networks, a cold water network is considered for the test case area of "Rues Basses". The energy services, their temperature and the layout of the network are the same as were considered for the refrigerant based networks. For a more detailed description the reader should refer to section 1.4.2. The optimal values for the temperature of the hot water line in winter is  $26^\circ\text{C}$ , its optimal summer value is  $16^\circ\text{C}$ , both correspond to the limits defined in eq. (1.27) and eq.(1.26). The optimal temperature difference between the hot and cold water lines is 6 K. The diameter of the pipes is 625 mm, it was selected using the maximum velocity criterion of Table 1.7. The numerical value of the parameters used for the proposed cold water network are listed in Table. 1.10.

The total annual electricity consumption amounts to 11.49 GWh. It is 1.5% lower than that of the  $\text{CO}_2$  network equipped with an open cycle  $\text{CO}_2$  central heat pump. The R1234yf and R1234ze networks, as well as the variants of  $\text{CO}_2$  network equipped  $\text{NH}_3$  and R1234yf central



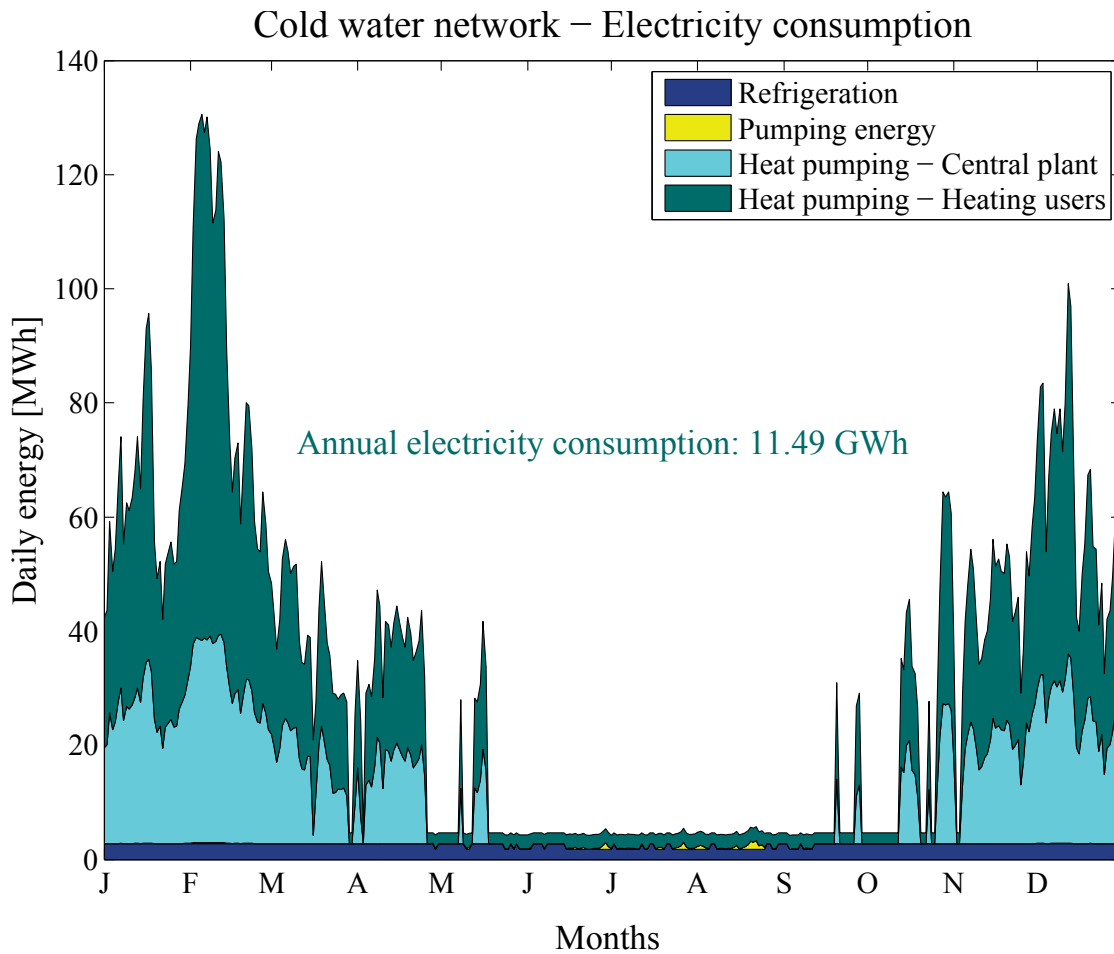


Figure 1.23 – Daily electricity consumption per type of use for a cold water network equipped with R1234yf heat pumps at the central plant and at the heating users.

heat pump have lower electricity consumptions.

The repartition of the electricity consumption is 57.65% for decentralized heat pumping at 6.62 GWh, while centralized heat pumping accounts for 34.02% or 3.91 GWh. The electricity consumption for refrigeration and pumping energy account respectively for 8.05% and 0.28%. The share of electricity used for refrigeration is larger than in the refrigerant networks mostly because the water network impose the condensers of the refrigeration chillers to operate at a higher temperature. The evolution of the electricity consumption around the year is provided at Fig. 1.23. The electric load curve is visible at Fig. 1.24.

The duration of the summer and winter operations are identical to that of the CO<sub>2</sub> network. During the February peak, the maximum electric load reaches 5.44 MW, 3% lower than the CO<sub>2</sub> network equipped with an open cycle CO<sub>2</sub> heat pump at the central plant, but above the HFO based networks and the two variant of CO<sub>2</sub> network using NH<sub>3</sub> and R1234yf heat pumps at the central plant. The minimum electric load also occurs during the interseason at a value of 175 kW which is slightly higher than was found for the other networks. The electric load during the peak cooling day is 241 kW, 65 kW of which are used for pumping. At 33% the share



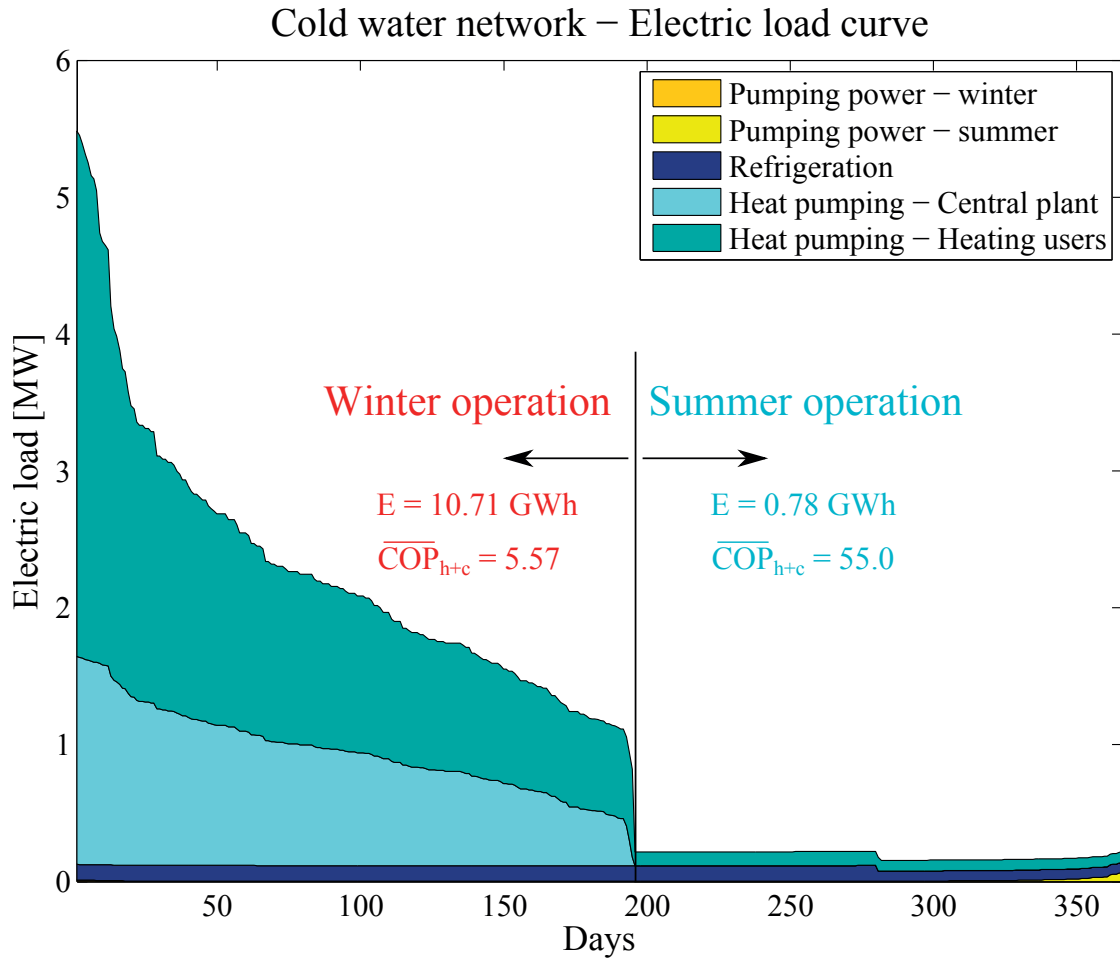


Figure 1.24 – Electricity load curve consumption per type of use for a cold water network equipped with R1234yf centralized and decentralized heat pumps. The winter and summer types of operation are clearly visible. The total electricity consumption and average combined heating and cooling COP are given for the two types of operation respectively.

of centralized heat pumping in the total electricity consumption is higher for the cold water network than for the other networks. It is due essentially to the higher temperature at which the network operates in winter. The CO<sub>2</sub> network equipped with the open cycle CO<sub>2</sub> central heat pump also has a share of centralized heat pumping of around one third, this variant of network is penalized by the lower efficiency of the CO<sub>2</sub> open cycle heat pump in spite of the network being only at 20.5°C in winter.

#### 1.4.4 Exergy loss and efficiency

For all the system studied, the exergy loss and exergy efficiency have been calculated using a control volume analysis [39]. A detailed computation of the exergy losses for every component of the systems would be valuable to rigorously assess the origin of the inefficiencies, however

Table 1.10 – Cold water network: Values of the various numerical parameters.

Description	Parameters	Values
Temperature of the lake water	$T_{lake}$	7.5°C
Temperature of the hot water line in winter	$T_{N,winter}$	26°C
Temperature of the hot water line in summer	$T_{N,summer}$	16°C
Temperature diff, between hot and cold water line	$\Delta T_N$	6 K
Isentropic efficiency of the central plant's compressors	$\eta_{Cs,CP}$	0.83
Inside diameter of the lines	$\phi$	625 mm
Diameter of the connections	$\phi_{connect}$	220 mm
Length per connection	$l_{connect}$	30 m
Number of connections	$n_{connect}$	45
Central plant: Temperature glide of the water in winter	$\Delta T_{lake,winter}$	4 K
Central plant: Temperature glide of the water in summer	$\Delta T_{lake,summer}$	3 K
Min. approach of temperature, refrigerant - water	$\Delta T_{min,rw}$	1.5 K
Min. approach of temperature, water - water	$\Delta T_{min,ww}$	2 K
Efficiency of water pumps - Quadratic coefficient.	$C_1$	-1.63
Efficiency of water pumps - Linear coefficient.	$C_2$	1.94
Efficiency of water pumps - Constant coefficient.	$C_3$	0.03
Pipe roughness	$\kappa_{pipe}$	0.3 mm

because of lack of time only the control volume approach could be completed. The systems studied cogenerate heating and cooling services, and the waste heat emitted by the cooling users is recovered by the heating users, provided that there is a heat demand and otherwise is discharged to the ambient. Intuitively, it appears that the users requirements are energy *assets* or *liabilities* depending on the conditions. Exergywise the same energy service represents an exergy demand or an exergy supply depending on the ambient temperature. In some cases the same energy stream, splits in an exergy demand and an exergy supply. For example, in the production of domestic hot water with cold water entering the the system at 10°C and leaving it at 55°C, every time the ambient temperature value  $T_a$  is between 10 and 55°C, the water heated from 10°C to  $T_a$  supplies exergy to the system, while from  $T_a$  to 55°C it demands exergy.

In order to grasp conveniently these variations with respect to  $T_a$ , the exergy analysis is done on a daily basis using a control volume defined as in Fig. 1.25. On that figure the service of space heating and domestic hot water preparation are on the left, those of air conditioning, cooling of data centres and refrigeration on the right. For all the services, the energy flows crossing the boundary of the control volume are transformation energy flows [39] - namely energy flows associated to mass flows, in the present case hot/chilled water. The boundary is also crossed by two flows of water from the lake, one delivering energy to the control volume and the other one removing energy from it. Electric energy and transformation energy from the combustion of heating oil are also provided to conversion technologies inside the control volume. Finally a heat flow -  $\dot{Q}_a$  - is also defined, from the conversion technologies into the

## 1.4. Conversion technologies: An energy comparison

ambient air<sup>21</sup>.

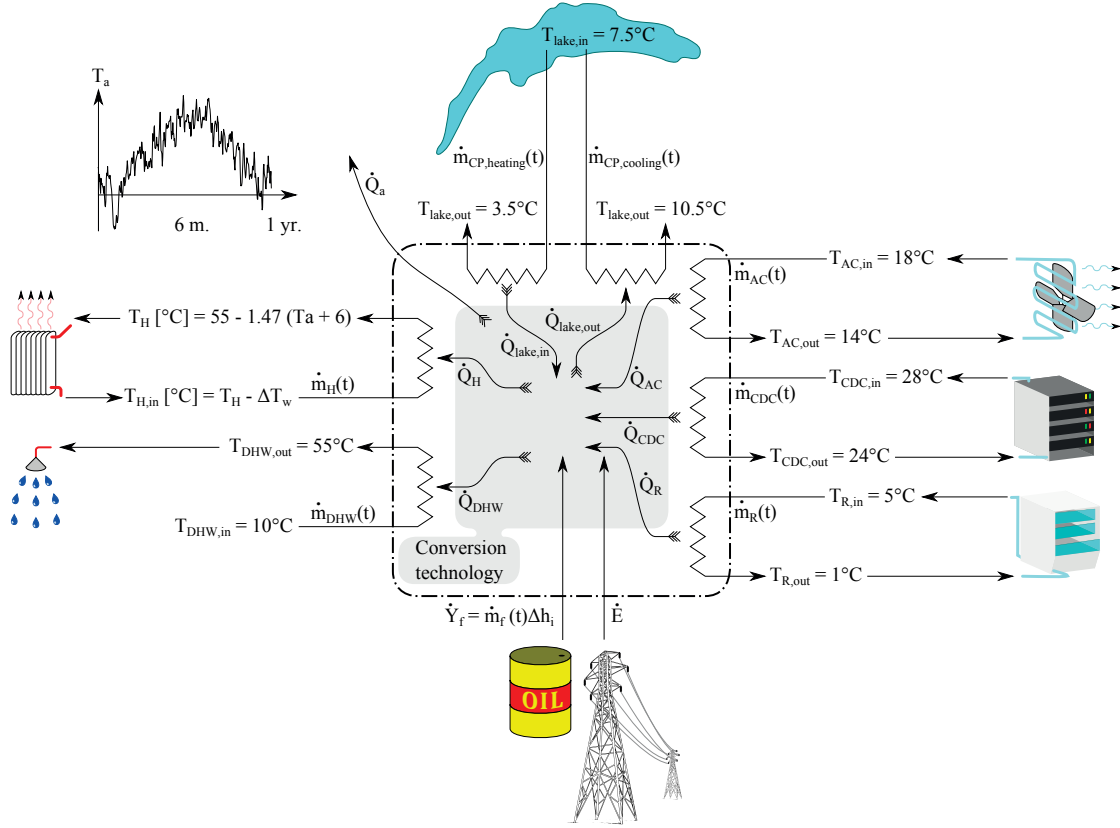


Figure 1.25 – Representation of the control volume, of the energy flows and of the relevant temperature used to compute the exergy loss and exergy efficiency for the various energy conversion technologies discussed in this study.

This schematic is generic and applies to all the conversion technologies discussed in the present study. Obviously, depending on the technology, some of the flows may be null. For instance the heat emitted to the ambient, or the transformation energy originating from the combustion of heating oil in the case of refrigerant and water based networks. For All these energy flows, the associated exergy flows can be computed. Obviously the exergy flow associated to electricity is equal to its energy. The transformation exergy coming from the combustion of heating oil is defined as:

$$\dot{E}_{yf}^+ = \dot{m}_f \Delta k = \dot{Y}_f \frac{\Delta k}{\Delta h_i} \quad (1.30)$$

Where  $\Delta k$  is the exergy value of heating oil and  $\Delta h_i$  its lower heating value.

<sup>21</sup>Typically the heat discharged by the air-cooled chillers.

In the case of the heat flow  $\dot{Q}_a$  towards the ambient, it corresponds to the heat discharged into the air by the air cooled compression chiller of the currently used mix of technologies. In that particular case the hot air leaving the air cooled condensers is assumed to have no exergy, as it is not reused before reaching thermal equilibrium with the ambient through turbulent mixing and diffusion. For the other flows defined in Fig. 1.25, although the energy flows are always in the same direction, their associated exergy will change direction depending on the temperature of the energy flow relative to the ambient temperature. In fact, if the flow "crosses" the ambient temperature, part of the energy flow will have an associated exergy flow directed in one direction and the remainder will have an associated exergy in the opposite direction.

The general expression of the transformation exergy in steady state and with negligible variations in gravitational potential energy and kinetic energy is defined as follows:

$$\dot{E}_y^+ = \sum_j \left[ \dot{m}_j^+ (h_j - T_a s_j) \right] \quad (1.31)$$

In the present study the only fluid involved is liquid water within a narrow temperature range<sup>22</sup>, hence its density and specific heat capacity can both be considered constant. Furthermore all the cases shown in Fig. 1.25 have only one inlet and one outlet. As a result for a stream "i" at time "t", changing from a state "1" to a state "2" the expression in eq. (1.31) becomes:

$$\dot{E}_{yi}^+(t) = \dot{m}_i(t) \left[ \bar{c} (T_{2,i}(t) - T_{1,i}(t)) - T_a(t) \ln \left( \frac{T_{2,i}(t)}{T_{1,i}(t)} \right) \right] \quad (1.32)$$

Depending on whether the water is colder, hotter, or crosses the ambient temperature and on whether it is being heated up or cooled down, the transformation exergy needs to be computed in six different ways. Those six cases are visible at Fig. 1.26. Note that the index denoting the number of the stream and the time have been omitted for readability reasons. The cases depicted at Fig. 1.26 are general and if the fluid cannot be treated as incompressible with a constant specific heat, then the general expression of eq. (1.31) should be used instead [39]. The exergy loss and exergy efficiency expressed in power are computed as follow, for readability reasons the time was omitted:

$$\begin{aligned} \dot{L} = \dot{E}^+ + \dot{E}_{yf}^+ + \dot{E}_{CP,HP}^+ + \dot{E}_{CP,dissip}^+ + \dot{E}_H^+ + \dot{E}_{DHW}^+ + \dot{E}_{AC}^+ + \dot{E}_{CDC}^+ + \dot{E}_R^+ \\ - \dot{E}_H^- - \dot{E}_{DHW}^- - \dot{E}_{AC}^- - \dot{E}_{CDC}^- - \dot{E}_R^- \end{aligned} \quad (1.33)$$

---

<sup>22</sup>Except heating oil that has already been treated in eq.(1.30)

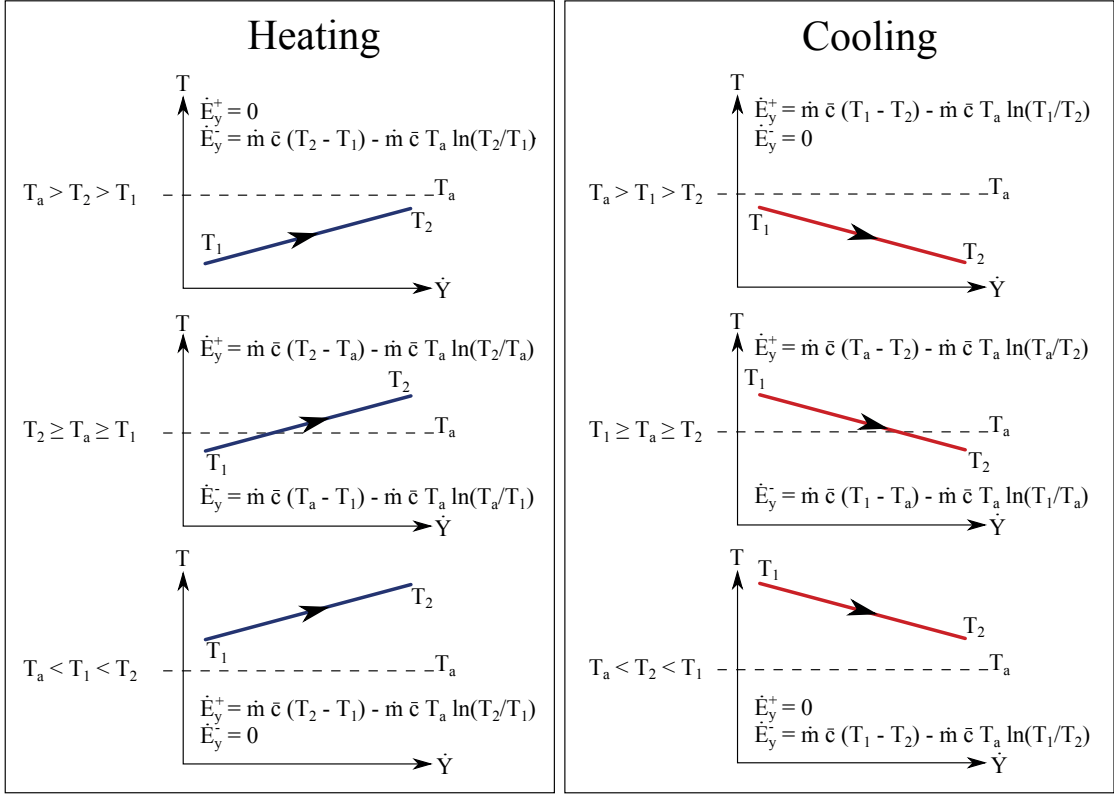


Figure 1.26 – Computation of the transformation exergy for an incompressible fluid with constant specific heat depending on its temperature relative to the ambient and on whether it is being heated up or cooled down.

$$\eta = \frac{\dot{E}_H^- + \dot{E}_{DHW}^- + \dot{E}_{AC}^- + \dot{E}_{CDC}^- + \dot{E}_R^-}{\dot{E}^+ + \dot{E}_{yf}^+ + \dot{E}_{CRHP}^+ + \dot{E}_{CRdissip}^+ + \dot{E}_H^+ + \dot{E}_{DHW}^+ + \dot{E}_{AC}^+ + \dot{E}_{CDC}^+ + \dot{E}_R^+} \quad (1.34)$$

Note that in eq.(1.33) and (1.34) and because the transformation exergy is computed according to the six cases of Fig. 1.26 the terms are all positive definite or zero.

For all the conversion technologies applied to the test case area, the daily exergy demand and supply expressed in power terms were computed. The demand is the sum of the right terms at the numerator of eq. (1.34). The supply was separated in four different contributions, consisting of the electricity supplied by the grid, and the exergy supplied by the lake water, the combustion of heating oil and the users themselves, four instance the waste heat discharged by cooling users in winter has a certain exergy content. A representation of the results is provided for some of the technologies studied at Fig. 1.27 to 1.30. In these figures the exergy demand has been assigned a negative value, and the different contributions to the exergy supply stacked one on top of another. This representation has the advantage that the supply composition

can be easily read, and by comparison with the demand the magnitude of the exergy loss and exergy efficiency at a certain time of the year can be grasped mentally. The value of the total annual exergy loss and of the average annual exergy efficiency is also provided in Fig. 1.28 to 1.30.

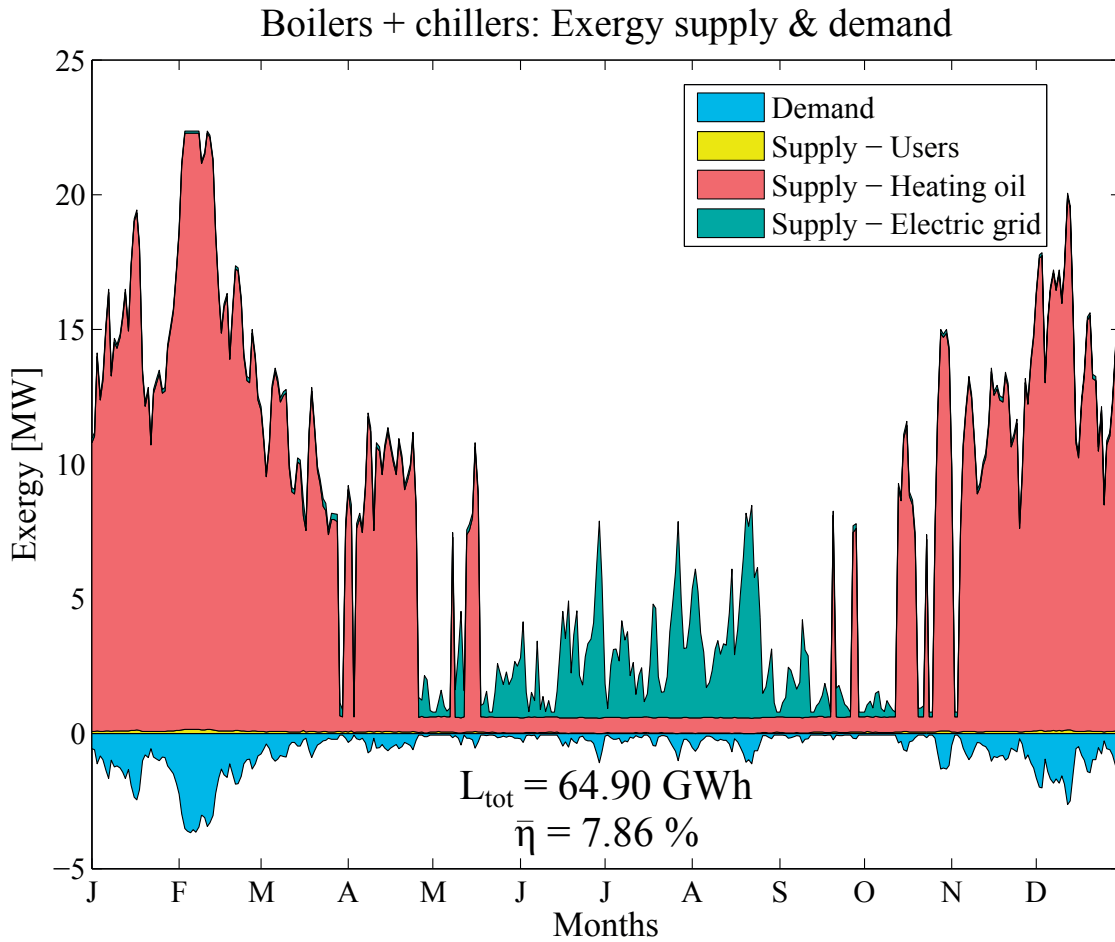


Figure 1.27 – Evolution of the exergy supply & demand for the currently used technology in the test case area.

The exergy demand is the same for all the technologies, as the energy services, their temperature and the evolution of the atmospheric temperature are identical. The peak of exergy demand occurs during the coldest day at 3.67 MW, meaning that the peak demand is driven by space heating. It is worth noticing that the energy demand, visible at Fig. 1.2, is driven by the air conditioning in summer instead. It is easily explained by the greater temperature difference in winter between the atmospheric and the space heating temperature, than it is in summer with the air conditioning temperature.

The lowest exergy demand is around 50 kW and the demand stays below 100 kW for a total of 87 days. These days are mostly during the spring in May - June and at the beginning of autumn in September - October. However, the earliest day with an exergy demand below 100 kW is on

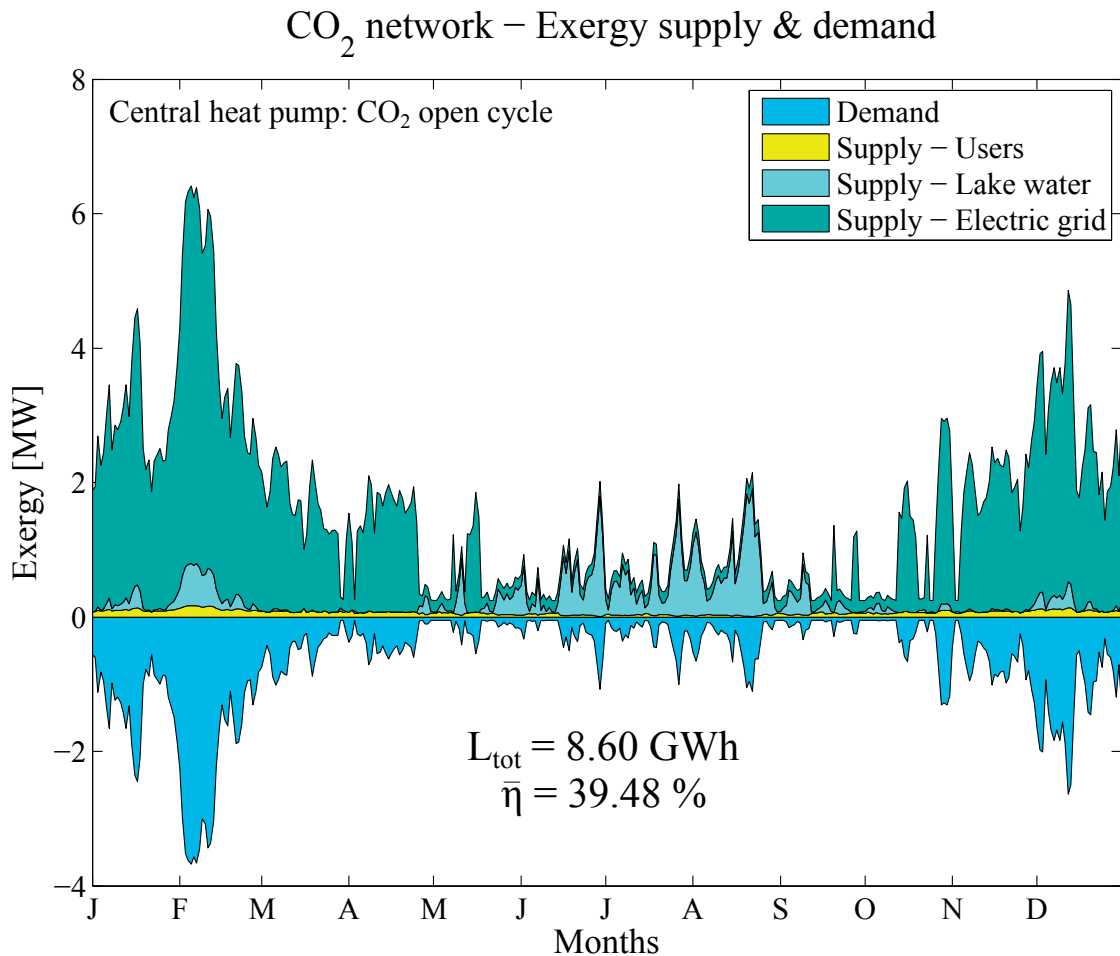


Figure 1.28 – Evolution of the exergy supply & demand in the test case area for a CO<sub>2</sub> network equipped with an open cycle central heat pump.

March the 29<sup>th</sup> and the last day on November the 2<sup>nd</sup>.

The present analysis has the advantage of showing the real thermodynamic value of the energy services required, since exergy takes into account the first and second law of thermodynamics and because the effects on it imposed by the variations in atmospheric temperature are treated rigorously. It is worth noticing that mainly three measures can be taken to reduce the exergy demand. First, the thermal losses through the buildings envelope should be reduced by better insulating them. Second, the air renewal should be done using a heat recovery controlled ventilation and finally the temperature of distribution should be reduced for the heating services and increased for the cooling ones. Although the last measure can be taken automatically after the first two are realized<sup>23</sup>, a full retrofit should include the modification of the hydronics, for instance by replacing radiators by larger ones or even through the installation of an underfloor heating.

<sup>23</sup>A smaller amount of heat needs to be delivered, with a heat transfer area that remained the same.

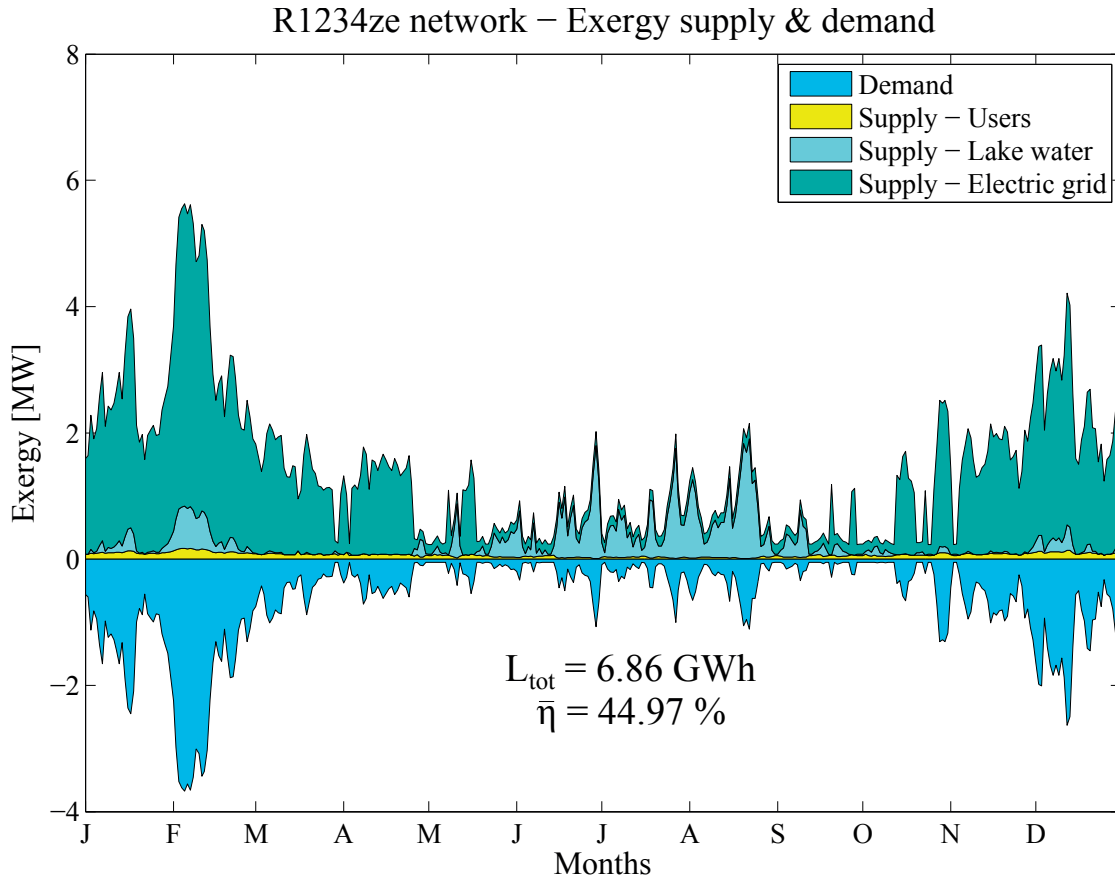


Figure 1.29 – Evolution of the exergy supply & demand in the test case area for an R1234ze network.

For the currently used technologies of boilers and electrically driven compression chillers, by examining Fig. 1.27 it appears, that the majority of the exergy supplied is from the heating oil and corresponds to 87.3% of the total supply. The exergy taken from the electric grid for the chillers corresponds to 11.9%. The rest is the exergy supplied by the users, with a contribution of less than 1%. The large exergy loss is obvious, at its highest it reaches 18.9 MW and at its lowest, during the interseason, it is still around 800 kW. It clearly appears that the biggest loss comes from the conversion of the heating oil high exergy content into low exergy heat. The use of air cooled chillers, although less important in terms of total exergy loss, leads to a somewhat similar peak exergy efficiency for the days with high cooling demand, than boilers do during days with a high heating demand. Typically the figures are 13% and 16% respectively. During the days with the lowest exergy demand, the efficiency drops to around 2%. The average annual efficiency for the currently used technologies is 7.86%.

The refrigerant networks exhibit a much better behaviour, as Fig. 1.28 and 1.29 show for the CO<sub>2</sub> network equipped with an open cycle heat pump at the central plant and for the R1234ze network respectively. Only these two variants are shown as they are respectively the least and most efficient ones, and because the evolution of the exergy supplied for all the refrigerant



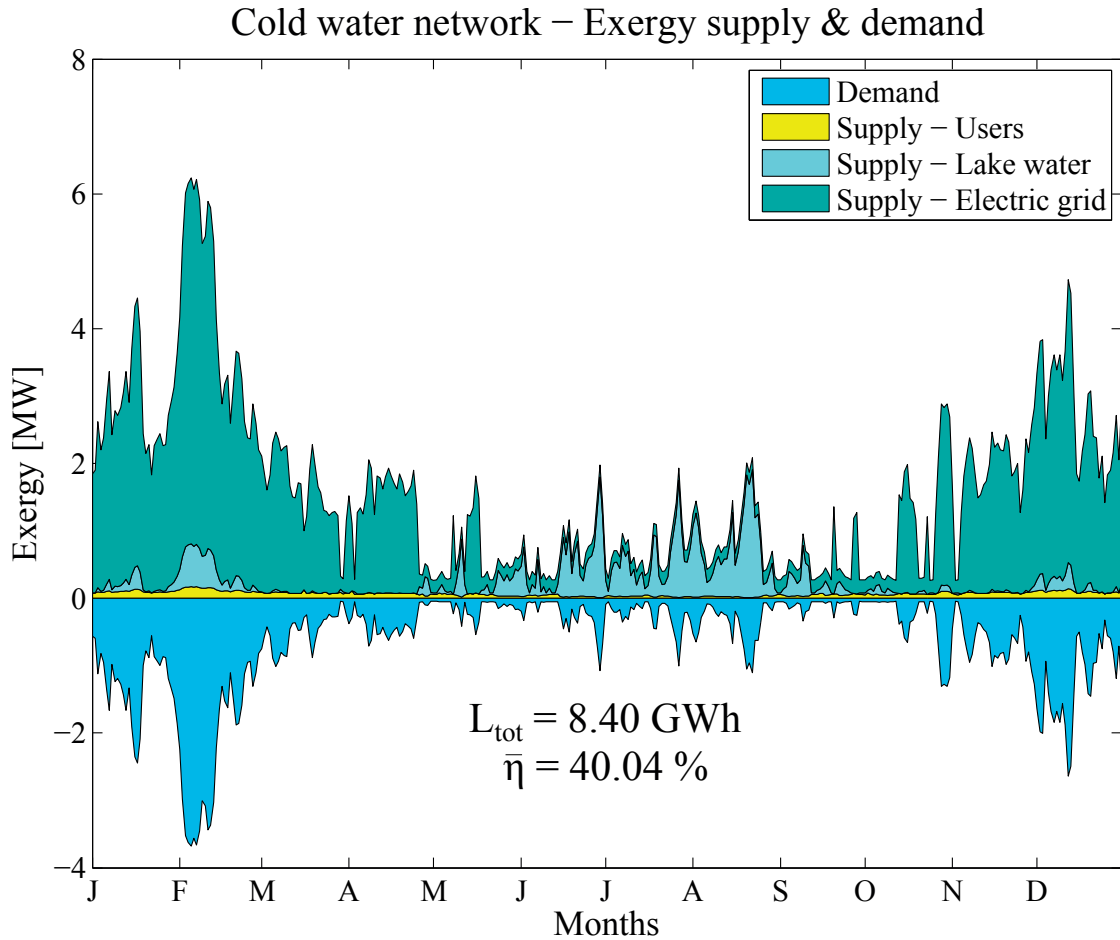


Figure 1.30 – Evolution of the exergy supply & demand in the test case area for a cold water network.

based networks is very similar. The annual exergy loss, when compared to the boilers and chillers case, is very significantly reduced, of a factor between 7 and 9.5.

For the CO<sub>2</sub> network, the exergy supplied annually consists of 82.1 % of electricity from the grid, 13.8% of exergy from the lake water, and 4.1 % of exergy from the users. At the peak load, during the heating season, the total exergy supplied is 6.41 MW, which by comparison with the peak demand of 3.68 MW, yields a peak efficiency of 57.3%. By examining Fig. 1.28 the repartition of the exergy supply during the winter season shows that although the vast majority of it is still provided by the electric grid, the heat pumped from the lake provides also a fair amount of exergy, up to around 10% during the peak of demand. This is explained by the fact that both the amount of heat pumped by the central plant, and the exergy content per unit of heat pumped increase as the days get colder, which show the interest to have an environmental heat source at 7.5°C which in mid winter is significantly hotter than the ambient air. On average, during the heating season<sup>24</sup>, the exergy is supplied at 93.1% by electricity from the grid, 3.3% by the water from the lake and 3.6% by the users, mostly through

<sup>24</sup>Defined here as the period during which the central plant operates as a heat pump.

waste heat emitted by data centres. For the summer peak, the situation is quite different as 88.4% of the supply comes from the lake water, that this time is significantly colder than  $T_a$ , 11.3% comes from the electric grid, and only 0.3% from the users. Over the cooling season the repartition is 65.1% of exergy supplied by lake water, 28.5% from electricity and 6.4% from the users. Note both during the heating and the cooling season the largest contribution to the exergy supply from the users is waste heat from data centres. Though obvious for the heating season, during the cooling season it would not be expected that a cooling load provides exergy, however for the data centres it is explained by the temperature profile considered for the service that stays entirely above the atmospheric temperature all the year except for the 7 hottest day, effectively corresponding to an almost exclusive exergy supply as described by the last graph on the right hand side of Fig. 1.26. As clearly shown by the evolution of the exergy supply and demand curves provided for two of the refrigerant based networks at Fig. 1.28 and 1.29, the structure of the exergy supply are very similar. This matter of fact also apply to the cold water network, as Fig. 1.30 demonstrates. For instance, Over the entire heating season 92.9% of the exergy supplied is provided by the electric grid, 3.4% by the lake water and the remainder 3.7% by the users. For the summer season the figures are 30.4%, 63.4% and 6.2% respectively. The main difference between these three networks is the better COP<sub>h</sub> of the R1234ze in winter (See Fig. 1.14, 1.20 and 1.24) meaning that a larger part of the heating services are supplied with heat energy from the lake instead of electricity from the grid. Because heat from the lake has a reduced exergy content compared to electricity (in the present case at most  $1/20^{th}$ ), as a result the exergy supplied by the lake water increases only little in comparison with the decrease in electricity from the grid. Ultimately it leads to a net diminution of the total exergy loss and an improved efficiency for the R1234ze network.

To clearly illustrate the improvement brought by refrigerant based networks and the cold water network over the currently technologies of boilers and electrically driven air cooled chillers, the efficiency duration curves for all the technologies discussed in this study are given at Fig. 1.31. It is obvious that the various variants of district energy network proposed perform better than the currently used boilers and chillers. Furthermore it is the case under all conditions. The performance of the various networks when compared to one another exhibit little differences. The HFO networks perform better mostly thanks to the use of open heat pump cycles throughout the network. It avoids the heat transfer exergy loss at the evaporator of the decentralized heat pumps and at the condenser of the central heat pump. They also do not need condensate pumps at the heating users. The CO<sub>2</sub> networks with either the R1234yf or the NH<sub>3</sub> heat pump at the central plant perform virtually identically. The CO<sub>2</sub> network network equipped with an open cycle CO<sub>2</sub> heat pump at its central plant has comparable performance to the cold water network. Note that in this study the open cycle CO<sub>2</sub> heat pump is single stage, if a two-stage open cycle CO<sub>2</sub> heat pump with flash economizer is considered instead, the annual exergy efficiency would gain roughly one percentage point and reach 40.51%.

The similarities between the refrigerant networks and the cold water network discussed in this

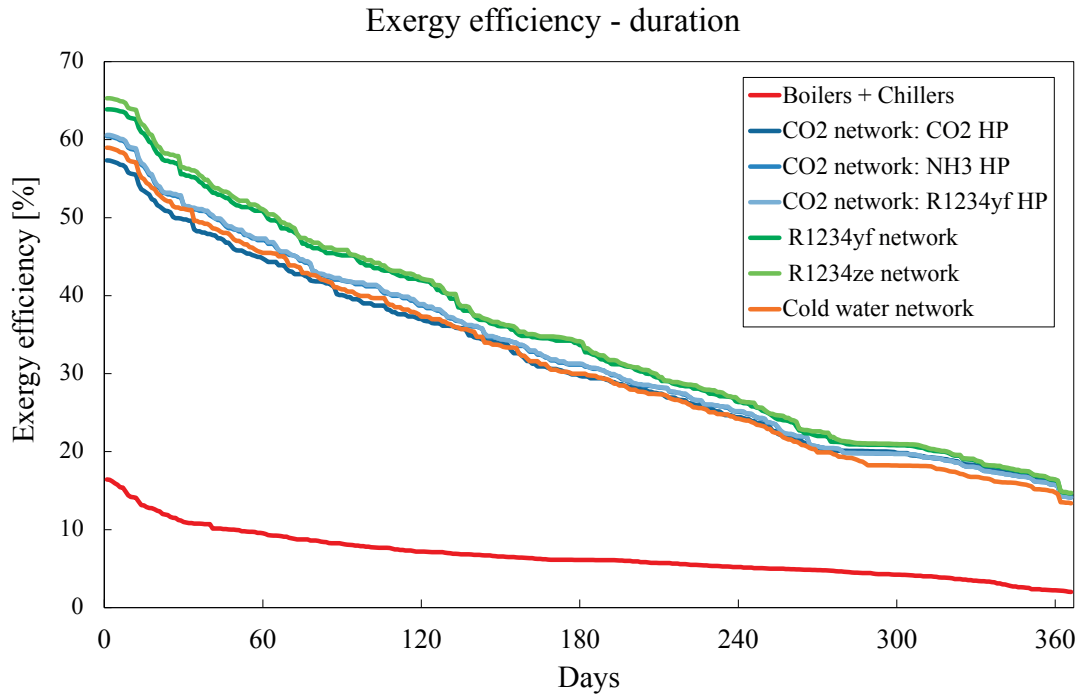


Figure 1.31 – Exergy efficiency vs. duration curve, for all the technologies discussed in this study in the test case area of "Rues Basses"

study were already apparent in the results of the previous sections. The exergy analysis not only confirms these similarities, but provides also a clue that both the refrigerant based networks and the cold water network are slightly different implementations of the same concept. Based on the present exergy analysis it is possible to have a good view over the various contributions that leads refrigerant and cold water networks to have a much higher efficiency than the currently used technologies. To better illustrate this Fig. 1.32 provides the exergy supply and demand for the CO<sub>2</sub> network equipped with an open cycle central heat pump, superimposed to the exergy supply for the boilers and chillers case. From that figure it is clear that the reduction in exergy loss has by order of importance the following origins:

**Generalized used of heat pumping:** The largest share of the exergy demand is driven by space heating. As a result, the use of a combination of centralized and decentralized heat pumps instead of heating oil fuelled boilers is the element that contribute the most in reducing the exergy loss.

**Extensive use of free cooling:** The second important demand for exergy is driven by air conditioning. All the variants of network studied rely as much as possible on free cooling that shifts the use of electricity for the air cooled compression chillers to exergy from the lake. However the reduction in electricity consumed far outweighs the increase in exergy use from the lake water. Ultimately it results in a reduced exergy loss during

summer operation.

**Waste heat recovery:** Technically all the waste heat emitted by the cooling services is collected by the proposed networks. However, only a small share of that waste heat is effectively reused for heating, the rest being discharged into the lake. It is mostly due to the non simultaneity of the dominant services - space heating and air conditioning. If some sort of thermal storage were used to increase the recovery of waste heat, it would essentially reduce the exergy supplied by the lake water and the electricity needed to drive the compressors of the heat pump at the central plant.

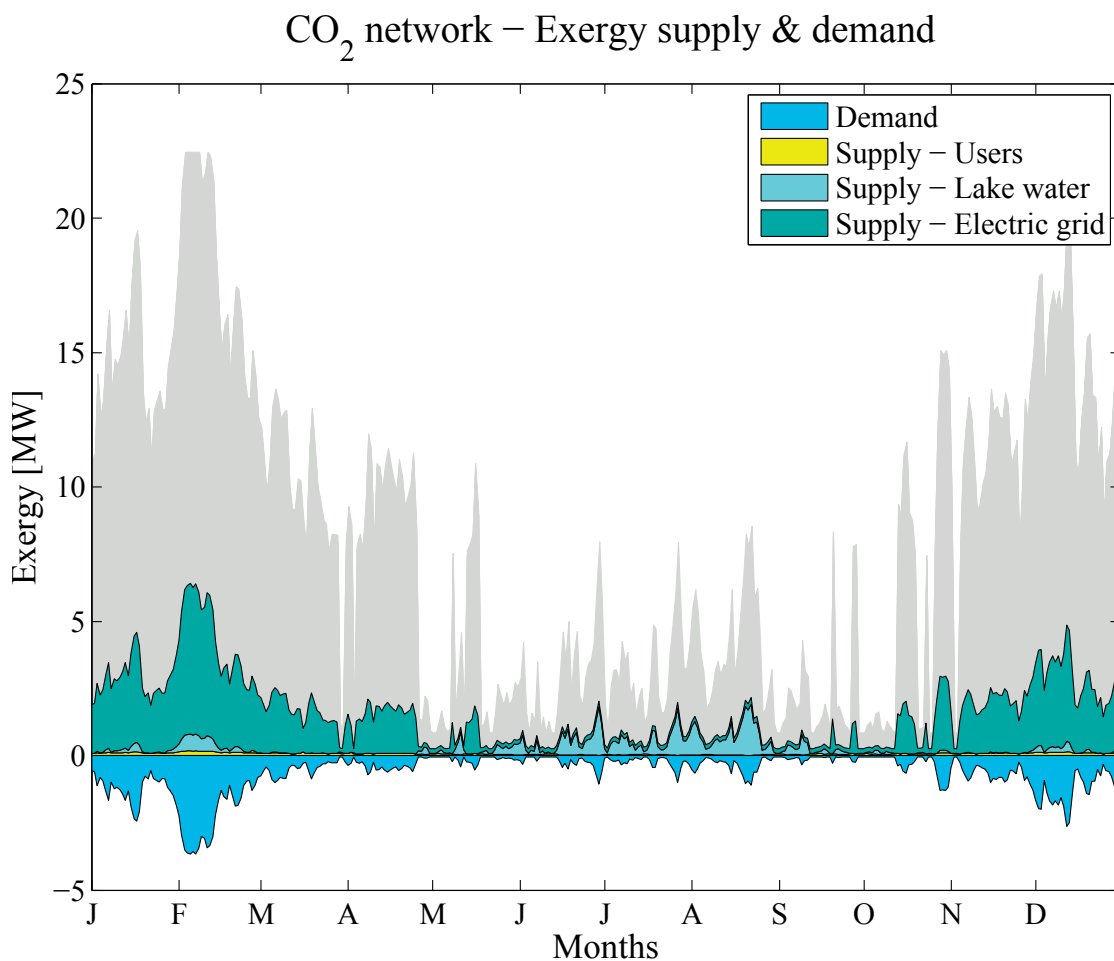


Figure 1.32 – Exergy loss reduction for the CO<sub>2</sub> network with the CO<sub>2</sub> open cycle heat pump, compared to the exergy supply for the currently used technology (in grey).

#### 1.4.5 Comparison and intermediate conclusion

Several energy conversion technologies have been defined and modelled in order to evaluate their energy performance. All these technology have been considered for the test case area

#### 1.4. Conversion technologies: An energy comparison

---

defined earlier at sections 1.2 and 1.3, in order to compare them on the same ground. A particular emphasis was put on modelling the key components, based on their expected importance in the total energy consumption. These components have been selected on the basis of their applicability within the context of the test area, in particular on their characteristic range of application. Care was taken in modelling these components to have a realistic evaluation of the primary energy consumption. It was aimed at representing each technology with the same degree of precision and avoid as much as possible bias in favour of one technology or another. The energy consumption of all the variants of network is very significantly reduced as compared to the currently used technologies. Various energy indicators are presented at Table. 1.11 for all the technology described in the previous sections.

If any of the proposed networks were used instead of the current combination of boilers and chillers, the final energy consumption would be reduced from a total of 66.42 GWh of heating oil and electricity, to less than 12 GWh of electricity only. In fact the figure is comprised between 9.91 and 11.66 GWh or in relative terms between 82.4% and 85.1% of reduction, depending on the type of network. Refrigerant based networks and their cold water counterpart can all be compared, for the winter mode of operation, to a two-stage electrically driven water-to-water heat pump with its first stage centralized and the second decentralized. In summer they can all be compared to district free cooling networks. This is obvious when looking at the combined heating & cooling COP for winter and summer. The greenhouse gas emissions considered for the heating oil boilers are direct emissions, those emitted on site by the boilers exhaust stack. The total emissions for the lifecycle of the fuel are obviously higher. However, the most recent values from the Swiss Federal Office for Environment are for direct emissions. The value for light heating oil is 73.7 tons  $\text{TJ}^{-1}$  or 265.3 g  $\text{kWh}^{-1}$  based on the lower heating value. For electricity from the grid, the carbon intensity used is 526.3 g  $\text{kWh}^{-1}$ , assuming that the cheapest, most carbon intensive, electricity available in Geneva is used. Refrigerant leaks have not been taken into account.

However, in the cases of  $\text{CO}_2$ , R1234yf and R1234ze network, if the annual leakage rate from these networks<sup>25</sup> is assumed to be similar to what is reported for large industrial refrigeration plants or large industrial chillers, then it would be comprised between 3% and 8% of the charge [64]. Which would lead to between 3.9 and 10.4 tons of  $\text{CO}_2$  leaked into the atmosphere per year for the  $\text{CO}_2$  network. For the R1234yf network the emissions of  $\text{CO}_2$  equivalent<sup>26</sup> would range between 10.4 and 48.3 tons  $\text{yr}^{-1}$  and for R1234ze between 27.8 and 74.1 tons  $\text{yr}^{-1}$ . It results that the refrigerant leaks represent at most 1.5% of the emissions of  $\text{CO}_2$  equivalent linked to the the electricity imported from the grid.

Note that the same study [64] mentions annual leakage rates of 20 - 30% in supermarket refrigeration systems, stressing the importance of proper monitoring and maintenance. Supermarket direct expansions refrigeration systems is probably the technology the most topologically close to the refrigerant district energy network. Since the environment in supermarkets is fully enclosed and well controlled which will not be the case for the refrigerant based networks, it is therefore likely that leaks will pose at least similar if not greater challenges in refrigerant

---

<sup>25</sup>Accounting for only the refrigerant contained in the liquid lines, the vapour lines and the connection lines.

<sup>26</sup>Global warming potential (GWP): R1234yf: GWP = 4, R1234ze: GWP = 6

based district energy networks. The exergy analysis, based on the control volume defined at Fig.1.25 showed consistent results in term of reduction of exergy loss and increased efficiency for all the variants of networks compared to what was found from the energy analysis. It also gave a good insight on what are the major contributors to the improved performances over the currently used boilers and chillers. It results that the general use of heat pumping for the heating services is the main source of improvement. It is followed by the replacement of compression chillers by free cooling systems. Finally, the recovery of waste heat, for the mix of services studied, contributes only to a limited extent in improving the performances. However, in an area with a greater share of base load cooling, the situation would change. Thermal storage could also be a way to increase the recovery of waste heat, enabling storing the waste heat emitted mostly in summer to use it later when space heating is needed.

In conclusion, the proposed refrigerant based networks and the cold water counterpart all present much better performances than the current mix of technologies used in the test case area; be it in terms of final energy consumption, exergy efficiency or emissions of greenhouse gases. The relative differences in the performances of the different types of network studied were shown to be narrow, and as a result, the economic profitability, the robustness to changes in economic conditions, the regulatory constraints and technological considerations will become the determining factors in identifying the best systems.

Table 1.11 – Comparison of various energy performance indicators for all the energy conversion technologies studied in the test case area.

Network's fluid	Conventional tech.		Refrigerant based networks				Cold water network	
	-	CO <sub>2</sub>	CO <sub>2</sub>	CO <sub>2</sub>	CO <sub>2</sub>	R1234yf	R1234ze	Liquid water
Central plant: heating mode	-	CO <sub>2</sub> open HP	NH <sub>3</sub> HP	R1234yf HP	R1234yf open HP	R1234ze open HP	R1234yf HP	
Annual final energy consumption	66.42 100%	11.66 17.6%	11.02 16.6%	10.97 16.5%	10.09 15.2%	9.91 14.9%	11.49 17.3%	
Annual combined heating& cooling COP	1.54	8.79	9.30	9.34	10.17	10.35	8.92	
Winter period heating & cooling COP	1.05	5.43	5.78	5.80	6.32	6.44	5.57	
Summer period heating & cooling COP	4.34	62.25	61.55	61.55	62.25	65.75	55.00	
Direct greenhouse gas emissions	19810 100%	6137 31.0%	5800 29.3%	5774 29.1%	5310 26.8%	5216 26.3%	6047 30.5%	
Annual exergy loss	64.90	8.60	7.96	7.92	7.04	6.86	8.40	
Annual exergy efficiency	7.86%	39.48%	41.33%	41.47%	44.33%	44.97%	40.04%	

### 1.5 Conversion technologies: Evaluation of the investment

The present section describes the method used to evaluate the investment cost linked to the various conversion technologies discussed in this study.

A realistic evaluation of the investment cost is a *sine qua non* condition for a proper assessment of the profitability of energy systems. In particular for systems that have large upfront costs, which in general is the case for district heating/cooling networks and heat pumps. In the present study the focus is on existing, commercially available, equipments. Whenever possible, the size of the pieces of equipment and their number are computed in a way that is consistent with the cost information available from commercial sources. Typically these sources encompass catalogue prices from various suppliers and sometimes also budgetary offers. Note that in this study, all the costs were converted from CHF to € using the average exchange rate for the year 2012.

#### 1.5.1 Currently used technologies - Boilers and chillers

The investment cost for the conversion technologies currently in use in the test case area consists of the installed cost for the heating oil fuelled boilers and that of the air cooled compression chillers. As a hypothesis, for each of the 32 zones that have been defined in Section 1.2, only one heating and one cooling installation were considered. This hypothesis leads to slightly underestimating the number of installations since in reality most of these buildings/groups of buildings operate several independent heating and cooling systems that provide the same services.

##### Oil fuelled boilers

Every heating installation is considered to have the following components:

- At least one boiler used for the supply of space heating and domestic hot water
- One set of exhaust gas piping per boiler
- One fuel tank, large enough to contain the amount of heating oil necessary for one year of operation

The total installed capacity of an installation is evaluated at the design atmospheric temperature of  $-7^{\circ}\text{C}$ . The number of required boilers is evaluated considering that the maximum size of a boiler is 2 MW. This limit was chosen because prices could not easily be obtained for bigger boilers. When several boilers are required for space heating, it is assumed that as many maximum size boilers as possible are used, and one additional smaller boiler is added to reach the required sizing load. The cost functions used for computing the cost of the various pieces of equipment involved in heating installations are detailed in Table 1.12. The values obtained



## 1.5. Conversion technologies: Evaluation of the investment

---

with the present costing method were compared to quotes from an industrial partner - the engineering firm Amstein & Walthert. The comparison showed that a multiplication factor of 2 was required to reach an installed cost comparable to that of the quotes.

### Air cooled compression chillers

The cooling installations are assumed to include the following two elements:

- At least one brine-water heat pump per type of cooling service used in the zone considered.
- One mechanical draught air cooler

Air cooled compression chillers exhibit a great variety of topologies and thus are difficult to represent by a single cost function. The present choice is justified by the tendency from the authorities to favour this type of system over direct air-condensing or split units, as it reduces the inventory of fluid and thus diminishes the risk of leak of refrigerant in the environment. The same cost function was used for the chillers as for the decentralized heat pumps in the refrigerant and cold water networks. Similarly to the boilers, when several brine-water heat pumps are required it is considered that as many maximum size units as possible are bought and the complement to the required sizing load is done by a smaller unit. The cost of the mechanical draught air cooler (MDAC) is assumed to be the same as was used by Henchoz et al. [42] Its evaluation requires the heat transfer area of the tube bundle obtained for an overall heat transfer coefficient of  $500 \text{ W m}^{-2}\text{K}$  and with a LMTD evaluated as follows:

$$LMTD_{MDAC} = \frac{\Delta T_{air}}{\ln((\Delta T_{air} + \Delta T_{min}) / \Delta T_{min})} \quad (1.35)$$

It is assumed that there is no maximum size for the MDAC as more or less all the sizes are available. Note that the sizing of both the brine-water heat pumps and the MDAC was done for an atmospheric temperature of  $30^\circ\text{C}$ . The cost functions used to compute the costs of air cooled compression chillers are detailed in Table 1.12. A multiplication factor of 2.65 is applied to the price of the equipment to obtain the cost of the delivered and installed system. The value of this factor was computed using comparisons with budgetary offers and is within the range mentioned by Peters et al. [65]. Details about the investment required for the technologies of boilers and chillers in the test case area are shown at Table 1.13.

### 1.5.2 CO<sub>2</sub> based networks

The evaluation of the investment required for the implementation of a CO<sub>2</sub> network was considered as the sum of the costs for implementing the pipelines and the costs for purchasing

## Chapter 1. Thermo-economic analysis

Table 1.12 – List of the costs/cost functions used to evaluate the investments required for the energy conversion technologies discussed.

Description	Cost function [€ 2012]	X [unit]	Max. unit size
Boiler	$1140 X^{0.5}$	$\dot{Y}_{comb}$ [kW]	2'000 kW
Fuel tank	$1.16 X$	$V_{tank}$ [l]	-
Exhaust piping	$730 X^{0.42}$	$\dot{Y}_{comb}$ [kW]	2'000 kW
MDAC	$1210 X^{0.8}$	$A$ [m <sup>2</sup> ]	2'000 m <sup>2</sup>
Network	$5.67 X + 613$	$\phi$ [mm]	-
Heat pump (domestic hot water)	$1540 X + 7830$	$\dot{E}$ [kW]	15.5 kW
Heat exchanger at central plant	$430 X^{0.82} + 4750$	$A$ [m <sup>2</sup> ]	10'000 m <sup>2</sup>
Pump at central plant / booster pump	$41800 X^{0.9} + 29450$	$\dot{V}_{pump}$ [m <sup>3</sup> s <sup>-1</sup> ]	-
Programmable logic controller	2500	-	-
Control valve	1250	-	-
Condensate refrigerant pump	5000	-	-
Variable speed drive (for water pump)	$750 X^{0.62}$	$\dot{E}$ [kW]	220
Heat pump (space heating) / chiller		See Appendix A, Fig. B.1	
Compressor at central plant / booster compressors		See Appendix A, Fig. B.2	
Heat exchanger at users substations		See Appendix A, Fig. B.3	
Water pump		See Appendix A, Fig. B.4	

and installing all the equipment required at the users and at the central plant. The pipeline implementation costs are based on a correlation from Curti [66], it was actualized to 2012 economic conditions using the index for construction prices for civil engineering works in the lake Geneva area [67]. The cost function is defined per meter of network (or trench) length. It was developed for water based networks and thus for networks where the supply and return lines have the same diameter. Since it is generally not the case for refrigerant based networks it was decided to use the average of the diameters of the liquid and vapour lines. The same cost function as used for the main pipelines, was used to evaluate the cost of 45 connection lines, each considered to have a 30 meter trench length. The values obtained with the cost function from Curti have been confronted to those used by one of the industrial partner - SIG (Geneva's utility company) - and proved to be relatively similar. The exact district heating pipeline costs from SIG could not be used for confidentiality reasons.

The different elements considered for the investment costs related to the equipment are:

- The decentralized heat pumps.
- The central plant, with the various heat-exchangers and the compressor.
- The network regulations, including booster pumps and compressors, CO<sub>2</sub> condensate pumps at the heating users and central plant, control valves and programmable logic controllers (PLC).
- The plate heat exchangers at the free cooling users.
- The compressors and evaporators used for commercial refrigeration.

The various cost functions used are presented in Table 1.12.

### Decentralized heat pumps

The decentralized heat pumps cost function was fitted from data of different manufacturers totalling 95 brine-water heat pumps. For the heat pumps dedicated to hot water preparation the additional cost of a hot water buffer tank was taken into account. In order not to risk an extrapolation of heat pump costs, it has been assumed that the maximum unit size available is 133 kW electrical, which corresponds to the most powerful machine in the survey.

### Central plant

The cost of the central plant is assumed to be the sum of the cost of all the compressors and heat exchangers required to which a multiplication factor of 2.2 is applied to reach the *assembled system* cost. The value of the multiplication factor was chosen to reach in average the prices quoted in several budgetary offers for heat pumps ranging between 1.5 MW and 15 MW of heating capacity. The cost function for the heat exchanger at the central plant is taken from Ref. [42]. Regarding the central plant one has to make a distinction between the variant of CO<sub>2</sub> network equipped with an open cycle CO<sub>2</sub> heat pump and those equipped with a NH<sub>3</sub> or an R1234yf heat pump.

For the CO<sub>2</sub> open cycle version, it is assumed that the heat exchanger of the central plant can operate indistinctly as an evaporator or a condenser. the area chosen to compute the cost being the largest one. The overall heat transfer coefficient assumed is 2'500 Wm<sup>-2</sup>K<sup>-1</sup>. In the present case the sizing load is 46.24 MW and corresponds to the cooling requirements at 30°C of atmospheric temperature, and assuming that there is no heat demand, or in other words, all the waste heat has to be discharged by the central plant. It is significantly higher than the 33 MW of cooling load required on the hottest day of the reference year, which translates directly into an oversized heat exchanger. For consistency reasons with respect to the approach used for the conventional technology, and because oversized HVAC systems is a common practice, it was chosen to keep the design load at its original value. Eventually, when considering a network temperature in summer of 12°C, the heat transfer area required for the heat exchanger at the central plant is 6'715 m<sup>2</sup>.

In the case of the network variants equipped with a NH<sub>3</sub> or an R1234yf heat pump at the central plant, it is not possible to use the same heat exchanger. Moreover these heat pumps need a condenser that is not required in the CO<sub>2</sub> open cycle. Hence, the central plant comprises a total of three heat exchangers:

- A **CO<sub>2</sub> condenser** for the summer operation
- An **evaporator**, that uses heat from the lake water to evaporate the refrigerant in the heat pump.

- A **condenser-evaporator**, that transfer heat from the heat pump's condensing refrigerant, to evaporate CO<sub>2</sub> drawn from the network's liquid line and send it back to the vapour line.

The sizing method and conditions for the CO<sub>2</sub> condenser are identical to that of the variant using the CO<sub>2</sub> open cycle heat pump. The evaporator and condenser-evaporator of the heat pump are both sized for the winter condition -  $T_a = -7^\circ\text{C}$ . For a temperature of the network in winter at  $22.5^\circ\text{C}$ , the sizing load for the condenser-evaporator is 14.01 MW and for the evaporator it is 12.63 MW. The average overall heat transfer coefficient is assumed to be  $2'500 \text{ Wm}^{-2}\text{K}^{-1}$ . For both heat exchangers the area is computed separately for the evaporation/condensation and superheating/desuperheating part of the process. The sum of these two areas is used to compute the cost based on the correlation from [42].

For the three variants of central plant, the cost of the compressors was computed using a cost function obtained from catalogue prices. The cost function and data points can be seen at Fig. B.2 in the appendix. Similarly to other pieces of equipment in this study, the size required exceeds that of the largest of the compressors from which the cost function was derived from. As a consequence, and in order to avoid extrapolating the costs, it was decided to consider as many *maximum volume flowrate* units as necessary and one smaller unit to reach the desired capacity. Obviously the compressors in the survey were generally not CO<sub>2</sub>, NH<sub>3</sub> or R1234yf compressors, nor of the centrifugal type. However, it still was decided to consider the cost function valid because of a lack of more accurate information.<sup>27</sup>

### Cooling users substations

The correlation used to compute the cost of the decentralized heat exchangers used for cooling services, was fitted from data gathered for 206 different heat exchangers. The cost function and data points can be seen at Fig. B.2 in the appendix. These heat exchangers were generally not capable of withstanding the pressure of up to 61 bar that a CO<sub>2</sub> network would require, however, many of them are certified for 45 bar, and budgetary offers for 4 different, 90 bars certified, CO<sub>2</sub> plate heat exchangers have shown that there is no premium associated to the higher pressure. The maximum area for one heat exchanger at the cooling users is  $70 \text{ m}^2$ , which corresponds to the size of the largest of the 206 heat exchangers surveyed. The sizing of these heat exchangers was done using an assumed overall heat transfer coefficient of  $2'500 \text{ Wm}^{-2}\text{K}^{-1}$ . The cost of the refrigeration substations is considered as the sum of the cost for a CO<sub>2</sub> evaporator and a CO<sub>2</sub> compressor. The cost of the heat exchangers is computed with the same cost function as for the cooling substations and the compressor cost is computed with the same cost function as for the compressors in the central plant and the booster compressors.

---

<sup>27</sup>Above suction volume flowrates around  $350 \text{ m}^3\text{h}^{-1}$  both twin-screw and centrifugal compressors are available [60]. It is very likely that the second technology is priced higher, because of its higher efficiency and less complicated integration in the refrigerant circuit serve as a justification for it.

### Circulation and control systems

The same cost function was applied to the booster compressors installed along the vapour lines. The cost function used for the booster pumps was taken from the literature [42]. A fixed unit cost was assumed for the pumps that are used to extract the condensed CO<sub>2</sub> from the decentralized heat pumps and send it into the liquid lines. The value was based on a budgetary offer and includes the cost of the variable speed drive. Fixed costs were also assumed for the regulation valves and PLCs. It is assumed that every heat pump is equipped with one PLC and one CO<sub>2</sub> condensate pump. For each cooling service, one PLC is required, so a maximum of three per zone. However every heat exchanger is equipped with an individual control valve. In order to get an understanding of the costs linked to the control of the network, it was decided to aggregate the cost for the CO<sub>2</sub> condensate pumps, PLCs, control valves and booster pumps/compressors under the label - Control equipment.

Details about the investment required for the three variants of CO<sub>2</sub> networks in the test case area are shown at Table 1.13. The networks parameters correspond to those described at Table 1.8.

### 1.5.3 R1234yf and R1234ze based networks

Exception made of the decentralized heat pumps, the method used to evaluate the investment required for the R1234yf and R1234ze network is identical to that used for the CO<sub>2</sub> based network equipped with a CO<sub>2</sub> open cycle heat pump at the central plant.

In both the R1234yf and the R1234ze network, the decentralized heat pumps are of the open cycle type (See Fig. 1.16, because of that difference with the CO<sub>2</sub> based networks, it was decided not to use the cost function of Fig. B.1, but follow the same methodology used for the central plants instead. Thus, the cost of decentralized heat pumps is considered to be the sum of the cost of a compressor - Fig. B.2 - and of a condenser - Fig.B.3, to which is applied the same 2.2 *assembled system* factor as used in the case of the heat pump at the central plant.

### 1.5.4 Cold water network

The evaluation of the investment cost for the cold water network is almost identical to that of the variants of CO<sub>2</sub> network equipped with the R1234yf heat pump at its central plant. The only difference lies in the system used to circulate the fluid in the network. For the cold water network every zone needs one water pump to feed the evaporators of the decentralized heat pumps and one to feed the cooling services heat exchangers. In order to have a realistic evaluation of the cost for these machines, a cost function was derived based on data for 157 centrifugal pumps. The function and the data points are shown at Fig. B.4 in the appendix. As the flow required and the pressure differential vary throughout the year over a wide range, one variable speed drive was considered for each pump. The cost function used for the variable

speed drive was also derived from catalogue prices.

In all the variants of network and for all the pieces of equipment except the pipelines, a 2.65 multiplication factor was applied to the purchasing cost in order to compute the installed cost. The value is consistent with the one used for the compression chillers of the current energy conversion technologies. An engineering overhead of 18% is also added to the total initial investment for all the variants of network, since careful planning is required for these technologies. No engineering overhead was considered for the currently used technology as it is fully decentralized and hence does not require supervision at the full system level.

Details about the investment required for the R1234yf, R1234ze and cold water networks, in the test case area, are provided at Table 1.13. The networks parameters correspond to those described at Table 1.9 and 1.10.

### 1.5.5 Comparison of the required investment

At this point of the discussion it is worth commenting some of the results presented at Table 1.13 and 1.14. First, in spite of the maximum unit size for the various technologies, mostly defined on the basis of the largest piece of equipment for which pricing information was found, the number of units required is in general not much bigger than the number of zones. It means that, in general, the maximum capacity of the equipment considered available in this study match rather well the required capacity in the 32 zones of the test case area. There are some exceptions though, for instance the 152 chillers required to provide the cooling services in the "currently used technologies" case, could have been reduced to 96, had larger unit been considered. In all the variants of network the user-end heat exchangers also appear to be constrained by the max unit size of 70 m<sup>2</sup>. It is especially visible for the heat exchangers delivering the service of air conditioning and to a lesser extent the condensers of the heat pumps used for space heating in the R1234yf/ze network. A priori, to have just the right number of units maximizes the economy of scale. However, a number larger than necessary of identical systems, would likely allow economies through standardization and would also provide redundancy. The question whether the proposed types of network should be built with a small variety of standardized components or from a collection of tailor made systems could not be investigated in this work but it would be worth investigate this matter as part of future studies.

Regarding the decentralized heat pumps, it has to be mentioned that the cost of open cycle heat pumps of the R1234yf and R1234ze networks once the *assembled system* factor is taken into account, show costs comparable to that of the decentralized heat pumps used in the CO<sub>2</sub> and cold water networks. Although one could expect the open cycle decentralized heat pumps to be slightly less expensive thanks to the absence of evaporator, the difference in the optimal network temperature in winter leads to an increased cost for the compressors that cancels the saving made on the evaporator.

The most striking result however, is that the current technology comprising boilers and chillers

## 1.6. Conversion technologies: An economic profitability analysis

---

is significantly more expensive in term of investment than all the proposed variants of network. The major saving linked to the networks is the change from air cooled chillers to free cooling systems. Part of the difference is offset by the cost for constructing the pipelines, central plant and the users' heating substations.

It is worth mentioning the high investment cost for the heating oil tanks. The cost function might overestimate the cost of fuel tanks themselves, but as already mentioned an installation cost factor was used and its value chosen such as to match the quotes obtained from one of the industrial partners. Hence, one can still have a certain confidence in the evaluation of the investment cost for the heating systems of the currently used technologies.

In the present study, it is assumed that the currently used heating and cooling systems are approaching their end of life and have to be replaced. Obviously it is a simplifying hypothesis, and the author is conscious that in reality the existing pieces of equipment would not all have to be replaced nor would it necessarily take place over a period less than an accounting year. Comparing the investment required for the different types of network it appears that the CO<sub>2</sub> network equipped with the open cycle CO<sub>2</sub> heat pump at the central plant is the least expensive, followed by the R1234yf/ze networks and the version of the CO<sub>2</sub> network equipped with an NH<sub>3</sub> and R1234yf central heat pumps. The cold water network is the last.

From the investment point of view, the costs that cause the proposed networks to be more or less expensive are the cost of the central plant and the cost for constructing the pipelines. These two factors are generally both at play, for instance the pipelines cost for the R1234yf/ze though higher than that of their CO<sub>2</sub> counterparts is compensated by a less expensive central plants than that of the CO<sub>2</sub> networks equipped with the NH<sub>3</sub> and R1234yf central heat pumps. The cold water network is plagued by a combination of the two factors, since it requires the largest pipes of all the proposed networks and it also requires three heat exchangers and more compressors at the central plant.

Finally it is worth mentioning that in this study, at identical average diameters, pipelines cost the same regardless of the fluid carried. It represents a major assumption, as the fluid carried will influence many features, such as pipe material, thickness, associated monitoring and safety equipments, depth of burial, etc...

## 1.6 Conversion technologies: An economic profitability analysis

In this section a comparative profitability analysis is presented. It was assumed that the current boilers and compression chillers used in the test case area are approaching their end of life and that they will be replaced all at once by either new boilers and compression chillers or one of the six variants of network discussed previously.

The performance indicator chosen is the Net Present Value (NPV), which translates the different future cash flows with a fixed interest rate so as to be able to compare these future amounts of money with today's investment. In this study the NPV for every year of operation is computed taking into account:



## Chapter 1. Thermo-economic analysis

Table 1.13 – Detail of the investment required for the currently used technologies and the 3 variants of CO<sub>2</sub> network proposed. The number of units as well as the min, average and max characteristic size encountered are provided.

Conversion Technology	Quantity	Size [min, mean, max]	Equipment [mio € 2012]	Installed cost [mio € 2012]
<b>Boilers + Air cooled Chillers</b>				
Boilers + Exhaust pipes	32	[190 kW, 652 kW, 1996 kW]	1.24	
Fuel tanks	32	[51 m <sup>3</sup> , 181 m <sup>3</sup> , 559 m <sup>3</sup> ]	6.74	
Chillers	152	[1 kW <sub>e</sub> , 68 kW <sub>e</sub> , 133 kW <sub>e</sub> ]	8.76	
MDAC	32	[87 m <sup>2</sup> , 541 m <sup>2</sup> , 1505 m <sup>2</sup> ]	5.77	
Heating systems (installed)				15.96
Cooling systems (installed)				38.50
<b>Total initial investment</b>				<b>54.46</b>
<b>CO<sub>2</sub> network variant 1</b>				
Space heating - HP decentr.	72	[13 kW <sub>e</sub> , 87 kW <sub>e</sub> , 133 kW <sub>e</sub> ]	3.06	
DHW - HP decentr.	32	[1 kW <sub>e</sub> , 3kW <sub>e</sub> , 12 kW <sub>e</sub> ]	0.41	
Air cond. - HEX	92	[3 m <sup>2</sup> , 60 m <sup>2</sup> , 70 m <sup>2</sup> ]	1.15	
Cooling of data centres - HEX	32	[1 m <sup>2</sup> , 4 m <sup>2</sup> , 15 m <sup>2</sup> ]	0.05	
Refrigeration - HEX + comp.	32	[1 m <sup>2</sup> , 2 m <sup>2</sup> , 16 m <sup>2</sup> ]	0.09	
Central plant - CO <sub>2</sub> comp.	2	[35 m <sup>3</sup> h <sup>-1</sup> , 1120 m <sup>3</sup> h <sup>-1</sup> ]	0.14	
Central plant - HEX	1	6715 m <sup>2</sup>	0.59	
Control equipment			1.60	
Pipeline - Main lines	1843 m (trench)		4.30	
Pipeline- Connection lines	1350 m (trench)		1.73	
Installed equipment				27.14
Engineering overhead				4.89
<b>Total initial investment</b>				<b>32.03</b>
<b>CO<sub>2</sub> network variant 2</b>				
Space heating - HP decentr.	39	[6 kW <sub>e</sub> , 85 kW <sub>e</sub> , 133 kW <sub>e</sub> ]	2.95	
DHW - HP decentr.	32	[1 kW <sub>e</sub> , 3 kW <sub>e</sub> , 12 kW <sub>e</sub> ]	0.41	
Air cond. - HEX	92	[3 m <sup>2</sup> , 60 m <sup>2</sup> , 70 m <sup>2</sup> ]	1.15	
Cooling of data centres - HEX	32	[1 m <sup>2</sup> , 4 m <sup>2</sup> , 15 m <sup>2</sup> ]	0.06	
Refrigeration - HEX + comp.	32	[1 m <sup>2</sup> , 2 m <sup>2</sup> , 16 m <sup>2</sup> ]	0.09	
Central plant - NH <sub>3</sub> comp.	5	[446 m <sup>3</sup> h <sup>-1</sup> , 1120 m <sup>3</sup> h <sup>-1</sup> ]	0.18	
Central plant - NH <sub>3</sub> evap. / cond.		1744 m <sup>2</sup> / 6011 m <sup>2</sup>	0.20 / 0.54	
Central plant - Dissipative HEX		6715 m <sup>2</sup>	0.59	
Control equipment			1.59	
Pipeline - Main lines	1843 m (trench)		4.30	
Pipeline - Connection lines	1350 m (trench)		1.73	
Installed equipment				31.43
Engineering overhead				5.65
<b>Total initial investment</b>				<b>37.08</b>
<b>CO<sub>2</sub> network variant 3</b>				
Space heating - HP decentr.	39	[6 kW <sub>e</sub> , 85 kW <sub>e</sub> , 133 kW <sub>e</sub> ]	2.95	
DHW - HP decentr.	32	[1 kW <sub>e</sub> , 3 kW <sub>e</sub> , 12 kW <sub>e</sub> ]	0.41	
Air cond. - HEX	92	[3 m <sup>2</sup> , 60 m <sup>2</sup> , 70 m <sup>2</sup> ]	1.15	
Cooling of data centres - HEX	32	[1 m <sup>2</sup> , 4 m <sup>2</sup> , 15 m <sup>2</sup> ]	0.06	
Refrigeration - HEX + comp.	32	[1 m <sup>2</sup> , 2 m <sup>2</sup> , 16 m <sup>2</sup> ]	0.09	
Central plant - R1234yf comp.	8	[505 m <sup>3</sup> h <sup>-1</sup> , 1120 m <sup>3</sup> h <sup>-1</sup> ]	0.25	
Central plant - R1234yf evap. / cond.		1744 m <sup>2</sup> / 6011 m <sup>2</sup>	0.20 / 0.54	
Central plant - Dissipative HEX		6715 m <sup>2</sup>	0.59	
Control equipment			1.59	
Pipeline - Main lines	1843 m (trench)		4.30	
Pipeline - Connection lines	1350 m (trench)		1.73	
Installed equipment				32.14
Engineering overhead				5.78
<b>Total initial investment</b>				<b>37.92</b>



## 1.6. Conversion technologies: An economic profitability analysis

Table 1.14 – Detail of the investment required for the R1234yf, R1234ze and cold water networks proposed. The number of units as well as the min, average and max characteristic size encountered are provided.

Conversion Technology	Quantity	Size [min, mean, max]	Equipment [mio € 2012]	Installed cost [mio € 2012]
<b>R1234yf network</b>				
Space heating - comp.	35	[173 m <sup>3</sup> h <sup>-1</sup> , 550 m <sup>3</sup> h <sup>-1</sup> , 1120 m <sup>3</sup> h <sup>-1</sup> ]	0.94	
Space heating - cond.	48	[1 m <sup>2</sup> , 49 m <sup>2</sup> , 70 m <sup>2</sup> ]	0.51	
Space heating - HP assembled.			3.19	
DHW - comp.	32	[1 m <sup>3</sup> h <sup>-1</sup> , 12 m <sup>3</sup> h <sup>-1</sup> , 42 m <sup>3</sup> h <sup>-1</sup> ]	0.04	
DHW - cond.	32	[0.1 m <sup>3</sup> h <sup>-1</sup> , 1 m <sup>3</sup> h <sup>-1</sup> , 3.7 m <sup>3</sup> h <sup>-1</sup> ]	0.02	
Air cond. - HEX	92	[3 m <sup>2</sup> , 60 m <sup>2</sup> , 70 m <sup>2</sup> ]	1.15	
Cooling of data centres - HEX	32	[1 m <sup>2</sup> , 4 m <sup>2</sup> , 15 m <sup>2</sup> ]	0.05	
Refrigeration - HEX + comp.	32	[1 m <sup>2</sup> , 2 m <sup>2</sup> , 16 m <sup>2</sup> ]	0.07	
Central plant - R1234yf comp.	7	[1056 m <sup>3</sup> h <sup>-1</sup> , 1120 m <sup>3</sup> h <sup>-1</sup> ]	0.20	
Central plant - R1234yf HEX	1	6714 m <sup>2</sup>	0.59	
Control equipment			1.94	
Pipeline - Main lines	1843 m (trench)		6.18	
Pipeline- Connection lines	1350 m (trench)		2.25	
Installed equipment				30.34
Engineering overhead				5.46
<b>Total initial investment</b>				<b>35.80</b>
<b>R1234ze network</b>				
Space heating - comp.	35	[189 m <sup>3</sup> h <sup>-1</sup> , 601 m <sup>3</sup> h <sup>-1</sup> , 1120 m <sup>3</sup> h <sup>-1</sup> ]	0.88	
Space heating - cond.	46	[3 m <sup>2</sup> , 48 m <sup>2</sup> , 70 m <sup>2</sup> ]	0.48	
Space heating - HP assembled.			2.99	
DHW - comp.	32	[1 m <sup>3</sup> h <sup>-1</sup> , 13 m <sup>3</sup> h <sup>-1</sup> , 49 m <sup>3</sup> h <sup>-1</sup> ]	0.04	
DHW - cond.	32	[0.1 m <sup>3</sup> h <sup>-1</sup> , 0.9 m <sup>3</sup> h <sup>-1</sup> , 3.4 m <sup>3</sup> h <sup>-1</sup> ]	0.02	
Air cond. - HEX	92	[3 m <sup>2</sup> , 60 m <sup>2</sup> , 70 m <sup>2</sup> ]	1.15	
Cooling of data centres - HEX	32	[1 m <sup>2</sup> , 4 m <sup>2</sup> , 15 m <sup>2</sup> ]	0.06	
Refrigeration - HEX + comp.	32	[1 m <sup>2</sup> , 2 m <sup>2</sup> , 16 m <sup>2</sup> ]	0.09	
Central plant - R1234ze comp.	10	[436 m <sup>3</sup> h <sup>-1</sup> , 1120 m <sup>3</sup> h <sup>-1</sup> ]	0.23	
Central plant - R1234ze HEX	1	6714 m <sup>2</sup>	0.59	
Control equipment			2.02	
Pipeline - Main lines	1843 m (trench)		6.35	
Pipeline - Connection lines	1350 m (trench)		2.37	
Installed equipment				30.58
Engineering overhead				5.38
<b>Total initial investment</b>				<b>35.96</b>
<b>Cold water network</b>				
Space heating - HP decentr.	40	[4 kW <sub>e</sub> , 84 kW <sub>e</sub> , 133 kW <sub>e</sub> ]	2.99	
DHW - HP decentr.	32	[1 kW <sub>e</sub> , 3 kW <sub>e</sub> , 12 kW <sub>e</sub> ]	0.41	
Air cond. - HEX	92	[1 m <sup>2</sup> , 59 m <sup>2</sup> , 70 m <sup>2</sup> ]	1.29	
Cooling of data centres - HEX	32	[1 m <sup>2</sup> , 5 m <sup>2</sup> , 19 m <sup>2</sup> ]	0.06	
Refrigeration - Water cooled chiller	33	[1 kW <sub>e</sub> , 3 kW <sub>e</sub> , 26 kW <sub>e</sub> ]	0.33	
Central plant - R1234yf comp.	15	[446 m <sup>3</sup> h <sup>-1</sup> , 1120 m <sup>3</sup> h <sup>-1</sup> ]	0.52	
Central plant - R1234yf evap. / cond.		1611 m <sup>2</sup> / 1493 m <sup>2</sup>	0.19 / 0.18	
Central plant - Dissipative HEX		8188 m <sup>2</sup>	0.70	
Control equipment			0.77	
Pipeline - Main lines	1843 m (trench)		7.67	
Pipeline - Connection lines	1350 m (trench)		2.51	
Installed equipment				34.95
Engineering overhead				6.25
<b>Total initial investment</b>				<b>41.20</b>

## Chapter 1. Thermo-economic analysis

---

- The initial investment
- The revenues raised from the sales of the energy services
- The cost of buying electricity from the grid
- The cost of buying heating oil for the boilers of the current technology
- The cost of replacing the equipment
- The cost of operation
- The cost of maintenance

Purchasing cost and installed cost were discussed in the previous section. Also an engineering overhead of 18% of the total installed cost was considered for the networks; accordingly, and as can be seen at Table 1.13 and 1.14, the total initial investment ranges from 32.03 mio € for the variant of CO<sub>2</sub> network with an open cycle CO<sub>2</sub> heat pump at the central plant, to 41.20 mio € for a cold water network. The total initial investment for pursuing with the current technologies is 54.46 mio €, with no engineering costs.

The price of the kWh of heating respectively cooling supplied to the users is set at 0.108 € kWh<sup>-1</sup>, which is lower than the prices generally mentioned for some new district energy networks in Switzerland. The price of electricity from the grid is 0.15 € kWh<sup>-1</sup>. According to the Swiss Federal Office for Statistics [68] the electricity price for final consumers rose in average of 1.2% per year, between 1980 and 2010. For all the variants of network discussed in this study, a similar rate of increase was taken into account for both the electricity bought from the grid and the thermal energy billed to the customers. Such an indexation on the electricity price is justified by the fact that the proposed networks are exclusively electrically driven.

For what concerns the boilers of the currently used conversion technology, the price of heating oil was selected according to the prices given by the Swiss Federal Office for Statistics [69]. This price depends on the amount bought and on the fact that each heating installation is assumed to buy the quantity of oil equivalent to its annual consumption, once a year. Typically, for 2'000 l. the price is 0.090 € kWh<sup>-1</sup> and over 20'000 l. it is 0.083 € kWh<sup>-1</sup>. Between 1977 and 2015, the average rate of increase of the price of heating was 3.5% per year, and as a result this rate was applied to the heating oil purchased every year. For consistency reason, the price billed to the customers for services provided via heating oil is indexed using the same 3.5% annual rate.

For the current analysis, it was decided to consider an overall lifetime of 40 years, which corresponds to a conservative estimate of the lifetime of the pipes [70]. Nevertheless the lifespan considered for all the pieces of equipment except the pipelines is only 15 years, as advised by the project partner Amstein & Walthert. As a result, two replacements of these pieces of

## 1.6. Conversion technologies: An economic profitability analysis

equipment were taken into account in the NPV computation. The engineering overhead of 18% was also included in the equipment replacement cost in all the network variants. A 3.5% annual increase of the equipment purchasing cost is considered. It corresponds roughly to the average rate of increase of the Chemical Engineering Plant Cost Index (CEPCI) [71] between 1957 and 2010.

The cost of operation is assumed to consist mainly of manpower. It has been assumed that three equivalent full time jobs are required for operating the networks. The manpower rate is  $54.3 \text{ € h}^{-1}$  and increases of 1.2% per year which, according to the Swiss Federal Office for Statistics [72]. Every full time job is considered equal to  $1927 \text{ yr}^{-1}$  [73]. The annual maintenance cost considered was 4% of the installed cost for the decentralized heat pumps, the chillers and the boilers and 1.5% for the pipelines. A 1.2% annual increase of the maintenance cost was considered, assuming that the maintenance cost is mainly driven by the related manpower. Finally the interest rate used in the actualization of all the future cash flows was set at 6%.

### 1.6.1 Maximisation of the net present value

As already mentioned in the description of the models of the refrigerant and cold water networks, many of the parameters are constrained for technical reasons or as a result of the assumptions made. However, a few parameters can be chosen within certain bounds and thus can be used as a set of decision variables in an optimization problem. The parameters left as decision variables for all the refrigerant networks are:

$\phi_{vap}$ : The diameter of the vapour pipes.

$T_{N,winter}$ : The temperature of the network during winter operation

$T_{N,summer}$ : The temperature of the network during summer operation

The two temperatures can be chosen inside the bounds defined by eq. (1.10) and eq. (1.11). No constraint limits the choice of  $\phi_{vap}$ .

In the case of the cold water network the decision variables are the following:

$T_{N,winter}$ : The temperature of the hot water line during winter operation

$T_{N,summer}$ : The temperature of the hot water line during summer operation

$\Delta T_N$ : The temperature differential between hot and cold water lines

The two temperatures can be chosen inside the bounds defined by eq. (1.26) and eq. (1.27). For  $\Delta T_N$ , the upper limit is 6.5 K as it is the maximum value that allows a network, with a hot water

line at  $16^{\circ}\text{C}$ <sup>28</sup>, to be cooled down in summer by the lake water with a minimum approach of temperature of 2 K. For practical reasons the minimum value for the temperature difference that was considered in this study is 2 K and corresponds to the amount of superheat considered at the decentralized heat pumps, below this value the electricity consumption becomes constrained by the value of the superheat instead of the temperature glide in the water.

With respect to the oil fuelled boilers and air cooled compression chillers, with the modelling approach followed in this study there are no parameters left as possible decision variables. As a result no optimization was carried out for that variant.

Obviously as the number of decision variables and their range are limited there is no need to use an optimization procedure, exploring the search space systematically can be done quickly enough and will provide results that are accurate enough, as in practice there is no reason to explore the search space using very small intervals. In the present study, steps of 10 mm were used for the diameter of the vapour lines and  $0.5^{\circ}\text{C}$  steps were used to explore both the temperature of the network in summer and in winter. In the case of the cold water network the temperature difference between hot and cold water lines was explored using 0.5 K steps. Exploring systematically the search space around the optimum is interesting as it can then be used to get a good grasp on the shape of the objective function - the NPV after 40 years - and show graphically the effect of the decision variables on the optimality of the various technologies. The objective function are shown at Fig. 1.33 to Fig. 1.38 for all the networks studied. The effect of the temperature of the network in summer is not shown as it is proven to have virtually no effect on the NPV. At Fig. 1.33 to Fig. 1.38, the surfaces drawn are for the optimal value of  $T_{N,summer}$ , which, for all the refrigerant network happens to be  $12^{\circ}\text{C}$  and for the water network<sup>29</sup>,  $16^{\circ}\text{C}$ .

For the refrigerant networks, the two distinct effects of the temperature of the network in winter and of the diameter of the vapour lines can be discussed independently.

Indeed, the temperature that maximizes the NPV after 40 years is roughly the same for all the diameters of vapour lines, which indicates an absence of coupling between  $T_{N,winter}$  and  $\phi_{vap}$ . A comparison of the NPV after 40 years for all the refrigerant based network shows that under the range of temperature and diameter explored the value of the NPV remains positive, meaning that all variants are profitable under the hypotheses made in this study. It also appears that the worst performing combination of  $T_{N,winter}$  and  $\phi_{vap}$  lead at most to 15% less profit than the optimum combination. It is also worth mentioning the relatively flat character of the NPV around the optimum with respect to  $T_{N,winter}$ , it results that selecting the most appropriate temperature in winter, though advantageous, is not absolutely vital to the economic profitability of the refrigerant networks discussed in this study.

At Fig. 1.39 and Fig. 1.40 are shown the total actualized costs linked to investment and opera-

---

<sup>28</sup>upper bound of eq. (1.10)

<sup>29</sup>Temperature of the hot water line

## 1.6. Conversion technologies: An economic profitability analysis

tion as functions of  $T_{N,winter}$  and  $\phi_{vap}$  for the both the R1234yf network and CO<sub>2</sub> network equipped with a CO<sub>2</sub> heat pump at the central plant. Only these two variants of networks are shown but similar conclusions apply to all the other refrigerant networks discussed here. Investment related costs comprise the initial investment, the two replacements of equipment after 15 and 30 years of operation and the maintenance costs. Maintenance costs are in general considered in the operating costs but in the present work they are computed as fractions of the equipment purchasing cost, thus they are investment related. Operation related costs comprise the electricity purchased from the grid and the cost of manpower for operating the network. The separation done at Fig. 1.39 and 1.40 clearly shows that the non-continuous behaviour of NPV with respect to  $\phi_{vap}$  is in fact linked to investment. It appears that the number of booster compressors are at the origin of this non-continuous behaviour. Indeed, when the diameter of the vapour lines increases, the length of pipeline between two booster compressors also increases<sup>30</sup> As a result, at certain threshold values of  $\phi_{vap}$  the number of booster compressors is reduced causing a step reduction in the investment costs. Fig. 1.39 and 1.40 also show that the operation related costs are almost independent of  $\phi_{vap}$ , which is logical since the only varying part in the operation related costs is the electricity purchased and pumping energy represents only a few percent of the total consumption.

Comparing investment and operation related costs, it appears that investment related costs are dominant by around a factor 2 in magnitude. In general, the rate of increase of operation costs with respect to  $T_{N,winter}$ , exclusively driven by the electricity cost, is smaller than the rate at which the investment related costs decrease. Toward higher values of  $T_{N,winter}$  however, the rate of increase of operation costs accelerates while the decrease rate for investment costs decelerates. The minimum total cost is reached when the rate of increase of operation costs is exactly compensated by that of the decrease in investment related cost. For the CO<sub>2</sub> network equipped with a CO<sub>2</sub> centralized open cycle heat pump, and also in the cases of the R1234yf and R1234ze networks, the optimum occurs before the maximum bound for  $T_{N,winter}$  is reached. For the two other variants of CO<sub>2</sub> network the optimum corresponds to the upper bound at 22.5°C.

For what concerns the cold water network, the maximum of NPV, as visible at Fig. 1.38, occurs for a temperature in winter that corresponds to the upper bound of 26°C in the hot water pipe and a for temperature difference between the hot and cold water lines of 6 K, also close to the maximum bound. Similarly to the refrigerant based networks, the investment related costs are much higher than operation related costs. The relative importance of investment related costs is even stronger in cold water network than in the refrigerant networks. As already said the operation related costs are mostly due to the purchase of electricity, and since all the networks discussed in this study deliver the same services and have been shown to have comparable electricity consumption, these costs are very close together. The lower maximum NPV achieved by the cold water network is explained by the higher investment related costs, mostly the higher initial investment. It is caused by the larger diameter of the pipes and a central plant that needs a large water-water heat exchanger for cooling and an R1234yf heat pump with costlier compressors. Notice that the cost penalty for larger pipes is only felt once,

<sup>30</sup>The maximum tolerable pressure drop having been fixed and the sizing flowrate being equal.

## Chapter 1. Thermo-economic analysis

while the central plant affects the balance three times as it is replaced after 15 and 30 years of operation.

In all the proposed networks, refrigerant or water based, the dominant factor in terms of economics is the investment. Such systems are often described as having a high *upfront cost* or of being *front loaded*. The first disadvantage of such systems is the necessity to raise capitals in relatively large amounts before operations can start. The second disadvantage is the effect on the optimum configuration of the networks that tend to minimize the investment at the expense of the energy efficiency. However, in the present case the variations between lowest and highest annual  $COP_{h+c}$  are comprised between 7.8% for the water network and 11.9% for the  $CO_2$  network with the  $CO_2$  open cycle heat pump at the central plant. It is also worth remembering that in the section describing the energy and exergy performance of the network, the configuration corresponds to that of the maximum of NPV after forty years of operation, and although for all networks it is the configurations with the lowest efficiency that have the highest NPV, the final energy consumption obtained is still between 82% and 86% lower than that of the current combination of boilers and air cooled chillers.

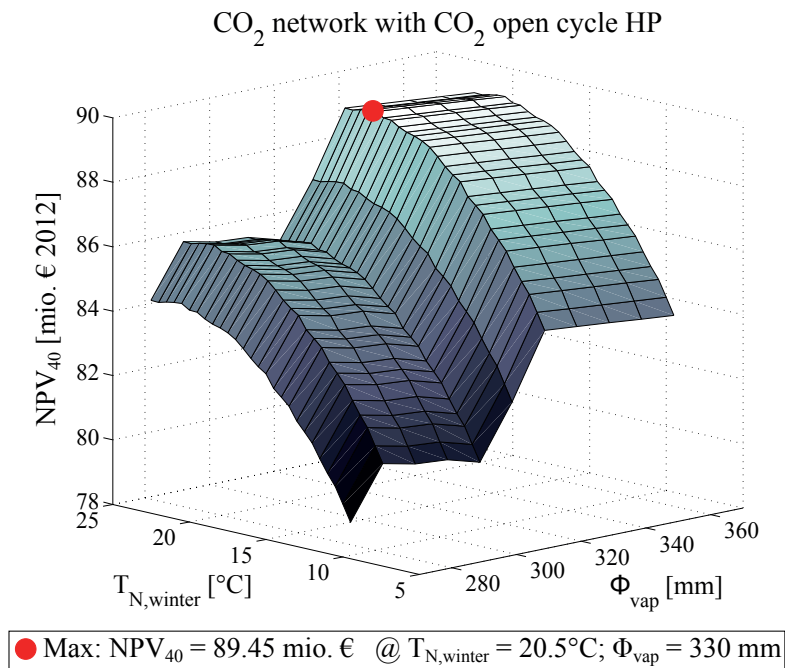


Figure 1.33 –  $CO_2$  network equipped with an open cycle  $CO_2$  heat pump at the central plant: NPV after 40 years as a function of the temperature of the network in winter and of the diameter of the vapour lines. The surface is drawn for the optimal temperature in summer of  $12^\circ C$ .

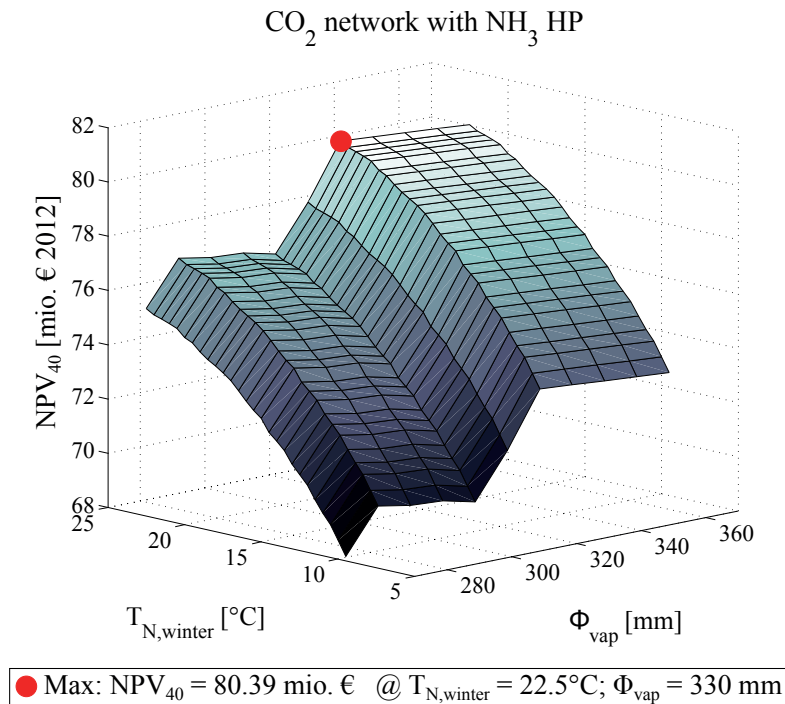


Figure 1.34 – CO<sub>2</sub> network equipped with a NH<sub>3</sub> heat pump at the central plant: NPV after 40 years as a function of the temperature of the network in winter and of the diameter of the vapour lines. The surface is drawn for the optimal temperature in summer of 12°C.

### 1.6.2 Evolution of the NPV for the different technologies

The evolution of the NPV along the lifetime considered, for the currently used technologies and the six different networks, is provided at Fig. 1.42. Obviously it starts with a negative net present value at year zero. The value corresponds to the total initial investment listed in Table. 1.13 and 1.14. After, the NPV increases, provided that the annual revenues from the sales of energy services are larger than the costs. The rate of increase of the NPV depends on the difference between the annual revenues and costs. Hopefully after less than the lifetime considered the NPV reaches zero, the time taken to reach this value is the payback time, before the system did not generate sufficient revenues to cover the initial investment. It should also be noticed that rate of increase of the NPV diminishes with the year, it represents the fact that a same amount of money in nominal value, if earned in the future as less value than if earned in the present day, hence the concept of present value. A simple way to view it is to imagine that the same future amount of money could have been obtained by investing a lesser amount of present money at a certain interest rate. The downward jumps in the NPV after 15 and 30 years of operation correspond to the re-investment in equipment, assuming that everything has to be replaced except the pipelines.

Fig. 1.42 shows clearly the economic benefits of the proposed network based technologies over the fully decentralized combination of boilers and air cooled chillers. The boilers and air cooled chillers have the highest initial investment and high operating costs, which lead to a



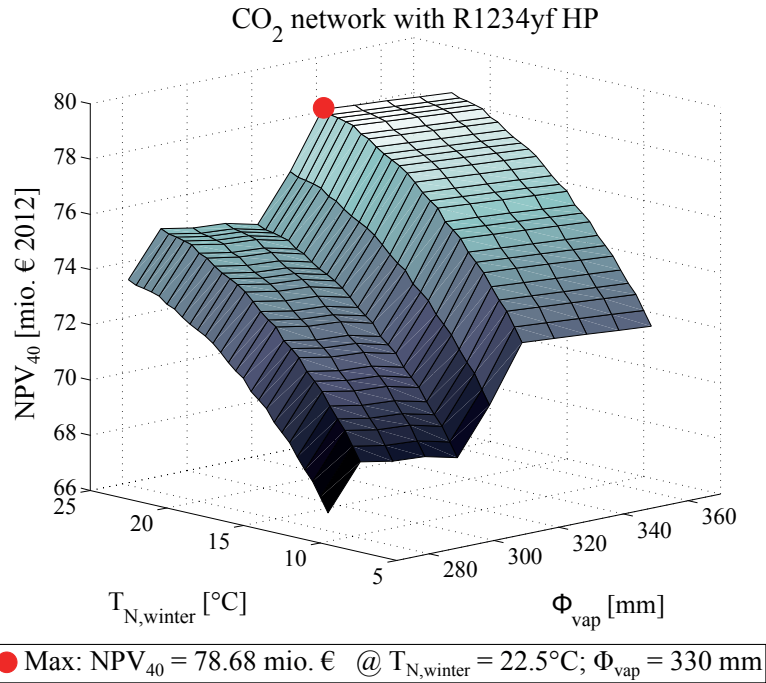


Figure 1.35 – CO<sub>2</sub> network equipped with an R1234yf heat pump at the central plant: NPV after 40 years as a function of the temperature of the network in winter and of the diameter of the vapour lines. The surface is drawn for the optimal temperature in summer of 12°C.

payback time of 14 years, just a year before investment for replacing the equipment makes the NPV return to a negative value, before the NPV raises back in the positive at year 25 and falls down again at the second replacement of equipment. This sawtooth profile that oscillates around NPV = 0 is a sign that at the sale price for heating and cooling services of 0.108 € kWh<sup>-1</sup><sup>31</sup> the combination of boilers and chillers is only marginally profitable at a value of 9.1 mio € after 40 years.

In comparison, all the networks exhibit much better economic performances, since they require a lower initial investment than the conventional technologies<sup>32</sup>, mostly thanks to the savings made possible by the use of free cooling substations instead of air cooled compression chillers. In term of NPV, the various networks can be grouped in three clusters. The three networks with an open cycle heat pump at the central plant, the two CO<sub>2</sub> based networks equipped with an NH<sub>3</sub>/R1234yf heat pump at the central plant and the cold water network. The three networks equipped with an open cycle heat pump at the central plant are the least expensive in term of initial investment and as a direct consequence in terms of cost of replacement of the equipment. After 40 years these three networks lead to very similar profits (89.5 and 90.9 mio €). It is due to the higher energy performance of the R1234yf and R1234ze networks compared to their CO<sub>2</sub> counterpart, that compensates for the higher initial cost. Of

<sup>31</sup>At the start of operation, as said earlier the sale price is considered to increase annually of 3.5% for the boilers and chillers and 1.2% per year for the networks.

<sup>32</sup>Keeping in mind that in this study all the chillers and boilers are considered to be purchased and installed at year 0, which in reality would very likely not be the case.



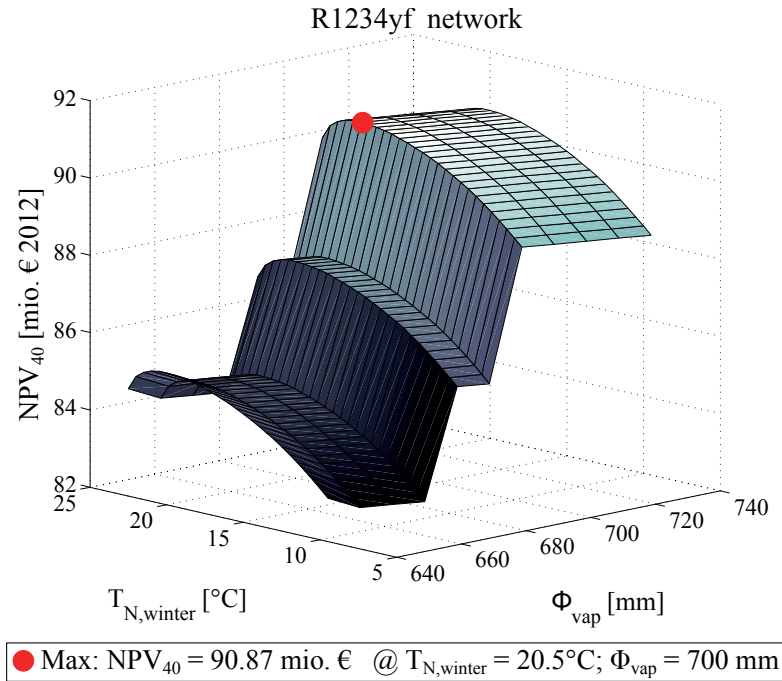


Figure 1.36 – R1234yf network: NPV after 40 years as a function of the temperature of the network in winter and of the diameter of the vapour lines. The surface is drawn for the optimal temperature in summer of 12°C.

all networks the CO<sub>2</sub> version with the open cycle heat pump is the least expensive and has the shortest payback time - slightly more than 4 years - but all the refrigerant based networks have payback times ranging between 4.5 and 5 years, for the cold water network the value is a bit more than 5.5 years. In spite of the similar sawtooth NPV profile than observed with the boilers and chillers, for all the networks the re-investment required for the replacement of equipment at year 15 and 30 does not cause the NPV to become negative again. The two others clusters of networks, i.e. the two CO<sub>2</sub> networks with the NH<sub>3</sub>/R1234yf heat pump at the central plant and the cold water network, lead to lower profit after 40 years of 80.4, 78.7 and 74.7 mio € respectively.

The cost of production of the delivered energy services, i.e. the value of the sale price that lead to NPV = 0 after forty years of operation is for the boilers and chillers of 0.105 € kWh<sup>-1</sup>, while for the networks it is comprised between 0.059 € kWh<sup>-1</sup> for the cluster of networks with an open cycle heat pump at the central plant and 0.068 € kWh<sup>-1</sup> for the cold water network.

### 1.6.3 Safety and its impact on the profitability

In the profitability analysis presented here, the cost of safety measures has not been taken directly into account. In general, the safety related cost can be considered as part of the 2.65 multiplication factor used to compute the installed cost from the purchasing cost of the various pieces of equipment. However, no difference were considered with respect to this

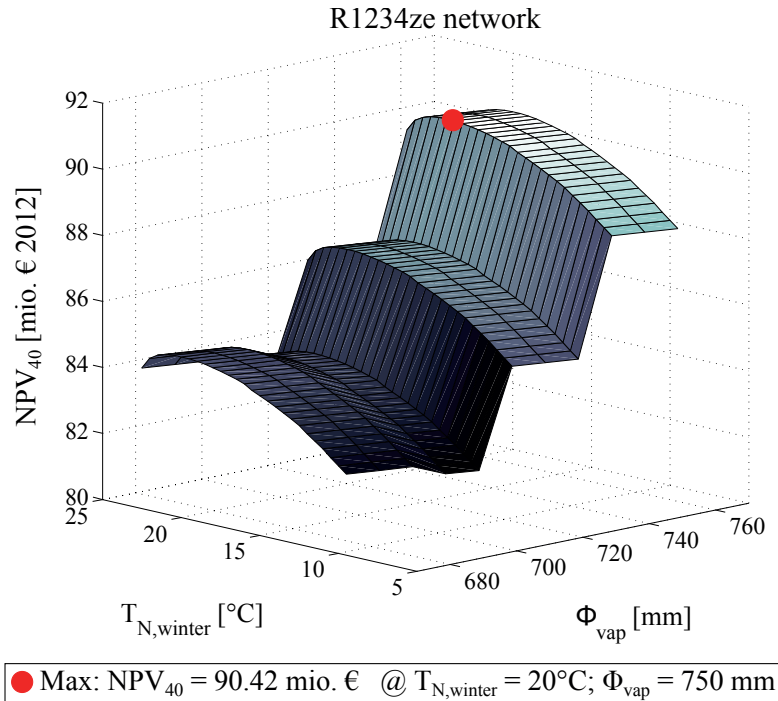


Figure 1.37 – R1234ze network: NPV after 40 years as a function of the temperature of the network in winter and of the diameter of the vapour lines. The surface is drawn for the optimal temperature in summer of 12°C.

multiplication factor that would mark the difference between the cold water network and the various refrigerant networks proposed. The reason is that at the present stage, without a comprehensive safety concept, including proposals for its implementation and maintenance throughout the lifetime of the networks, it is absolutely impossible to evaluate the safety related costs in a meaningful way. However, this question should not be overlooked, since the difference in terms of energy and economic performances between the various refrigerant networks proposed and their cold water counterpart are probably not conclusive making other "second order" considerations become determining factors in assessing which of these technologies are the most promising. In this paragraph however, some preliminary considerations with respect to safety will be provided, in order to give an idea of the tasks ahead should a district energy network using a refrigerant be constructed.

The safety of a technology is a very important factor regarding its potential of development. A technology can be considered safe as long as it does not threaten unacceptably the human population and/or the environment during its construction, use and dismantling/disposal. The threat is associated to the concept of risk, generally defined by the multiplication of a probability of occurrence of a given event with the severity of the damage caused by this particular event. Since the beginning of the industrial era, the introduction of safety measures has been done through various mechanisms, like new laws and regulations, technical standards, and risk insurances [74]. In the context of the proposed networks, one has to make a distinction

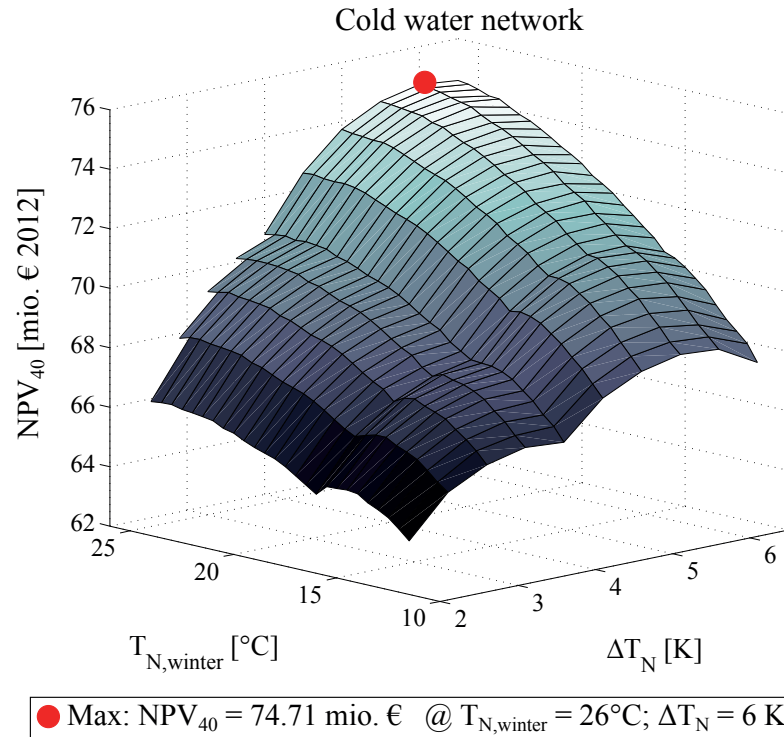


Figure 1.38 – R1234ze network: NPV after 40 years as a function of the temperature of the network in winter and of the temperature difference between the hot and cold water lines. The surface is drawn for an optimal hot water line temperature in summer of 16°C.

between the variant using water as a heat transfer fluid, and those using refrigerants. For the water variant, it is fairly obvious that no uncertainty exists with respect to the safety of the network. Indeed, the central plant is similar to “standard” central plants equipped with large heat pumps and the heating/refrigeration substations at the users are submitted to the technical standards that apply to refrigeration and heat pumping equipments [75, 76, 77]. Regarding the refrigerant based networks, the rules and technical standards for refrigeration and heat pumping equipments also apply to the central plant and to all substations at the users in spite of their novelty. For all these equipments, the foundation of the safety analysis is given by European union’s pressure equipment directive [78]. It defines safety categories for the pressure equipments according to the fluid they are using (toxic and/or flammable vs. others), the product of the maximum operating pressure times the volume for each component that can be assimilated to a vessel, and the product of the maximum operating pressure times the nominal diameter for each component that can be assimilated to piping. The safety category of the equipment is defined by the category of its “worst” component. The higher the category, the more stringent the certification procedure becomes. It is very important to carry a risk analysis that will focus first on identifying all the risks, and then propose a set of measures such that all the residual risks remain under a tolerance threshold. Such an analysis is required in the directive 2006/42/CE "machines". The results of this risk analysis will also affect the choice of the control devices. Indeed for control devices constituting a part of a control chain

### CO<sub>2</sub> network with CO<sub>2</sub> open cycle heat pump

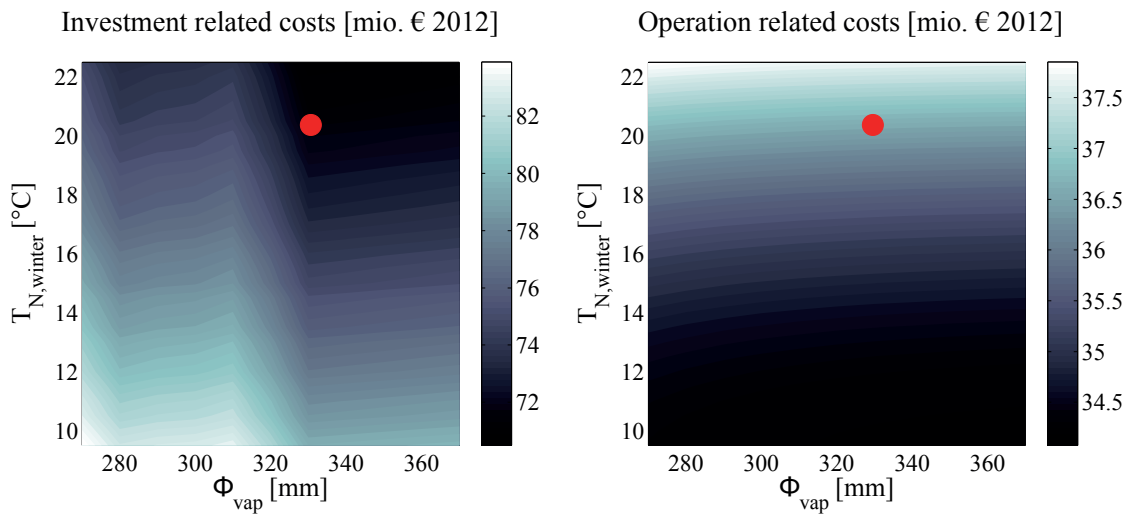


Figure 1.39 – CO<sub>2</sub> network equipped with an open cycle CO<sub>2</sub> heat pump at the central plant: Cumulated investment and operation related cost after 40 years of operation as a function of the temperature of the network in winter and of the diameter of the vapour lines. The surface is drawn for the optimal temperature in summer of 12°C.

### R1234yf network

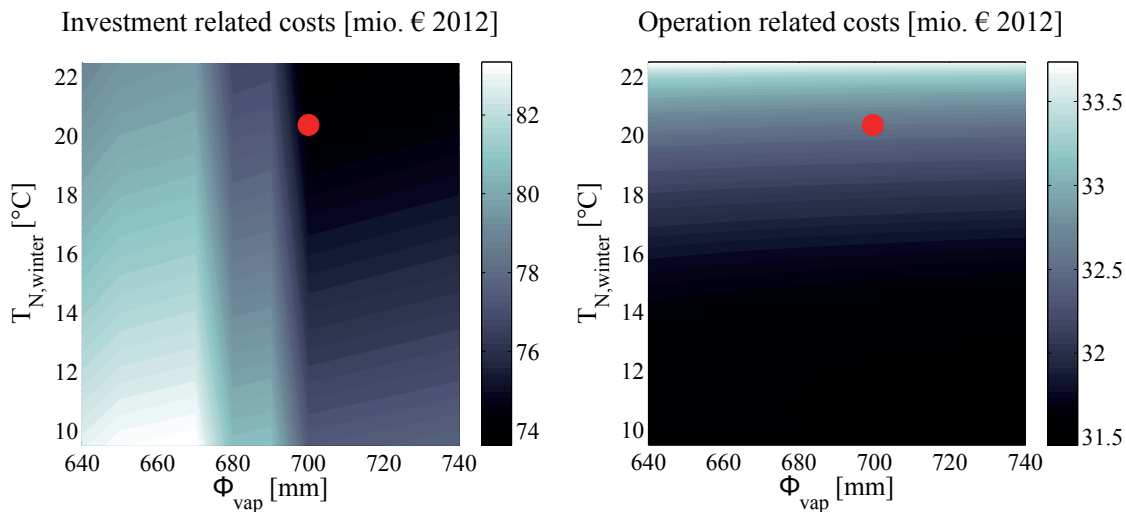


Figure 1.40 – R1234yf network: Cumulated investment and operation related cost after 40 years of operation as a function of the temperature of the network in winter and of the diameter of the vapour lines. The surface is drawn for the optimal temperature in summer of 12°C.

ensuring a safety functionality, the required performance level is a function of the severity of the potential injury, the frequency of exposition to the risk and whether there is a possibility of avoiding the hazard/harm [79, 80]. The European standard for refrigeration and heat pumping

### Cold water network

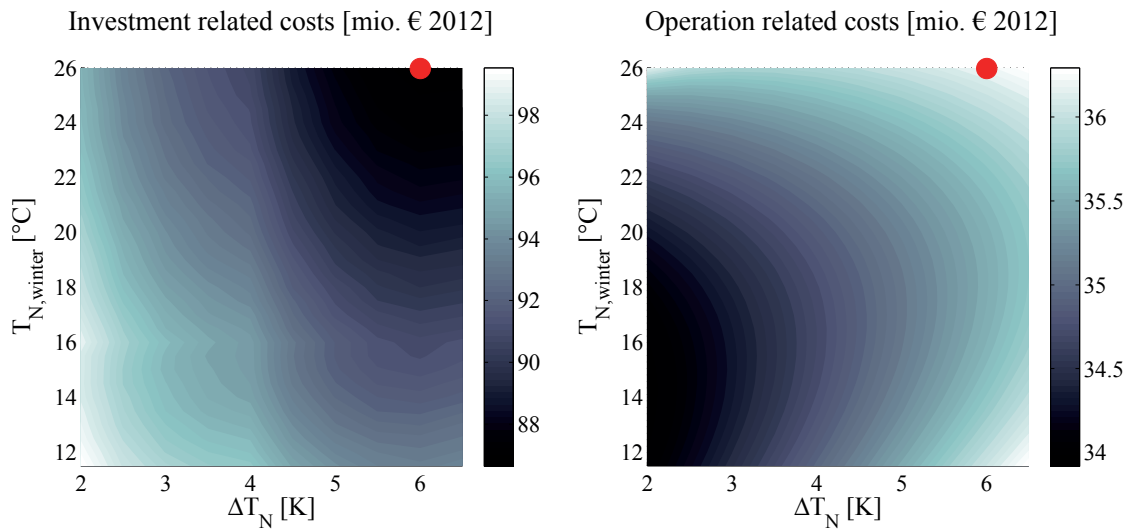


Figure 1.41 – Cold water network: Cumulated investment and operation related cost after 40 years of operation as a function of the temperature of the network’s hot water line in winter and of the temperature difference between hot and cold water lines. The surface is drawn for the optimal temperature in summer of 16°C.

equipments [75, 76, 77] also applies. It considers differently equipments with compressors and tanks installed in unoccupied machinery rooms than those that aren’t and if they use a secondary loop (indirect system) for the distribution or not (direct system). The latter cases require more safety measures to be taken.

In the case of the CO<sub>2</sub>, R1234yf and R1234ze based networks, the safety requirements at the user-end substations are very likely going to be more demanding than for the water variant. Indeed, the system would likely fall into the “direct system” category since a large amount of refrigerant is contained in pipes located outside the machinery room. In the case of the water network, the same installation could be made an “indirect system” by keeping the entire refrigerant circuit enclosed in the machinery room. In the case of the direct system it is most likely that, to meet the standard, it would be necessary to install a dedicated ventilation system controlled by a gas detection.

The major uncertainty regarding safety is linked to the presence of pipelines in a densely populated area. On the one hand, for the water network, the pipeline system is in all points similar to already existing district cooling networks, consequently one can argue that no supplementary risk is involved and the same sets of safety regulations, technical standards, and good practice rules apply. On the other hand, in the case of refrigerant based networks the requirements for the pipelines themselves are not clear as the idea was not put into practice yet. Pipeline specific regulations do not apply to CO<sub>2</sub>, R1234yf or R1234ze as they only focus on fuel dedicated facilities [81]. The European pressure equipment directive remains applicable

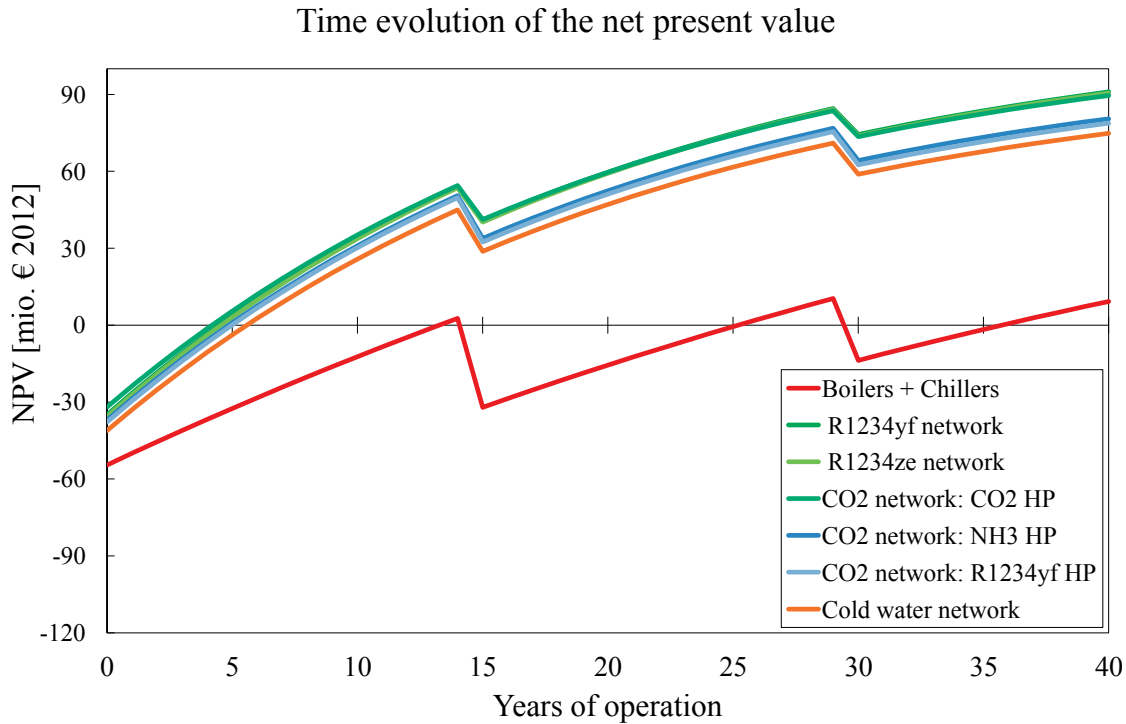


Figure 1.42 – Time evolution of the NPV over the 40 years lifetime for all the variants of energy conversion technologies discussed in this study. The curves for refrigerant and cold water networks correspond to the configuration that maximize the NPV (See Fig. 1.33 - 1.38)

[78] while the European standard on refrigeration and heat pumping equipments does not [75, 76, 77]. Eventually, in the case of Switzerland, and after a discussion with local authorities from the city and state (canton) of Geneva, it appeared that the art. 10 on disaster prevention of the environment protection act [82] would apply, leading to a procedure described in the Ordinance on Protection against Major Accident (MAO) [83]. The MAO procedure follows two steps. The first one – the summary report – consists in identifying the various possible disaster scenarios and then evaluates the damage caused by the worst case scenario identified. The state (cantonal) authorities decide if the second step has to be carried out based on the gravity of the damage identified in step 1. In Step 2 – the risk report – a quantitative evaluation of the damage and probability of occurrence of all the envisaged disaster scenarios is done. A cumulative risk curve is generated on which the authorities decide whether the risk is acceptable or not and in the latter case, will ask for more safety measures and if necessary will limit or forbid the operation.

Though the tediousness of the MAO procedure and its seemingly uncertain outcome can appear discouraging, it has to be kept in mind that it is a common procedure that many industrial facilities are required to fulfil, like natural gas and petroleum products transportation pipelines, railways potentially carrying hazardous materials, sites with a total storage capacity of chemical substances exceeding the MAO threshold quantity (for instance 20 tons of LPG, 2 tons of Ammonia or 500 tons of diesel/heating oil.) Facilities like these continued to exist and

## 1.6. Conversion technologies: An economic profitability analysis

---

operate in Switzerland, after the introduction of the MAO in 1991. The main objective of the approach is for the authorities to know about the potential industrial hazards present on their territory and for the companies operating potentially hazardous facilities to be aware of the risks and to act on reducing both probability of occurrence of disastrous events and the extent of the damages they would cause.

In the case of very common facilities requiring MAO procedures, such as fuel and LPG storages, or natural gas transportation pipelines, examples have been made available by the Swiss Federal Office for the Environment [84, 85, 86, 87, 88, 89, 90], thus drastically reducing the amount of work necessary to do the study. However, in the case of a refrigerant based network the MAO procedure, required prior to the construction of at least the first pilot plant, can be expected to be more cumbersome, as the accident scenarios analysis will likely require some modelling effort. For instance, to be able to simulate realistically the propagation of a plume of refrigerant in an urban area after an uncontrolled release. The MAO procedure, to be done during the design stage of the first refrigerant network, will help defining a set of design rules and construction principles that will ensure safe operations of such a network. These rules and principles could then be reused for new networks. Depending on the result of the first MAO procedure and on the experience gained over the construction/operation of the early networks, it might as well be that the MAO procedure will or will not be required for subsequent networks. The damages that the proposed refrigerant networks can cause are listed in Table 5. It also specifies whether a particular damage applies to a CO<sub>2</sub>, R1234yf or R1234ze network respectively and provides example of events that could cause them. It also proposes technical measures that can be envisaged to prevent the occurrence of such events and/or reduce the magnitude of the ensuing damage.

Obviously other kind of prevention and protection measures should be taken. It includes avoiding unauthorized persons to be in direct contact with sensitive and/or potentially hazardous parts of the network, using a properly equipped and trained staff to operate and maintain the system. Regular training should also be organised for the staff to rehearse the procedure in case of a catastrophic event in coordination with the authorities. Finally, adequate personal protection equipments should be made available to the staff. A last point on the safety concerns the refrigerant R1234yf. This fluid was developed as a replacement of the R134a in automotive air conditioning applications in order to meet the new greenhouse gas emissions standards set by the European Union. Over the last 4 years a controversy raged among the automotive industry regarding the potential hazard that the new refrigerant could cause in a fire. Indeed, on the one hand some manufacturers claim that during such a fire the R1234yf degrades into a dangerous chemical compound and used this argument not to operate the transition to the new fluid waiting for what they perceive as a safer alternative to be available, namely CO<sub>2</sub> based air conditioning equipments. On the other hand, a report from the society of automotive engineers [91] stresses the low risk for an individual to be exposed in a car to an open flame or to an excessive concentration of hydrogen fluoride. In Switzerland, the Federal office for environment considers R1234yf to be of safety group A2, that is non-flammable and



non-toxic. However, it also says that it is not a definitive decision [27]. Overall, looking at the evolution of the controversy, it seems that R1234yf will eventually be widely adopted as a refrigerant.

As said earlier, at the current stage it is not possible to determine safety related costs for a refrigerant district energy network. However, it is fairly easy to give a value that the extra investment for safety should not exceed, if a refrigerant network is to reach at least the same profitability than an equivalent cold water network.

If one considers that the safety equipment must be replaced at year 15 and 30 and, similarly to other equipment, that the cost increases annually of 3.5% then the extra initial investment that can be spent on safety is around 8 - 9 mio €, for the CO<sub>2</sub> network with an open cycle CO<sub>2</sub> heat pump at the central plant, as well as for the R1234yf and R1234ze networks. In relative value it corresponds to around 24 - 26% of the total initial investment. For the two other variants of CO<sub>2</sub> networks the maximum amount that can be spent on safety is 2.5 - 3 mio € or 6 - 8% of the original initial investment. In present value the cost for the replacement of safety equipment at year 15 and 30 amounts respectively to 70% and 49% of the cost at year 0.

### 1.6.4 Cost of the fluid and its impact on the profitability

In the present profitability analysis the cost of the fluids have not been taken into account. Initially the work focussed on CO<sub>2</sub> exclusively for which the cost was known to be very low. The International Institute of Refrigeration [92] mentions, in its guide on CO<sub>2</sub> refrigeration, prices for bulk delivery in tanker of 0.3 £ kg<sup>-1</sup> in 2010 which translates into around 0.4 € kg<sup>-1</sup> for the year 2012. The amount of CO<sub>2</sub> required for the network being 130 tons, bulk delivery is very likely to be used, the cost of the first charging of the network would be around 52'000 €. If then one considers the same 3-8% annual leakage rate than was considered in the discussion on greenhouse gas emissions (see Section 1.4.5) it represents annually between 3.9 and 10.4 tons of refrigerant to be reinjected in the network. In that case the addition of new refrigerant will be done gradually and hence the use of standard 60 kg refrigerant bottle is more likely. According to [92], the cost for delivery in cylinders reaches up to 6.6 € kg<sup>-1</sup> which yield an annual cost of 25'700 - 40'600 €. When assuming an annual increase of the CO<sub>2</sub> refrigerant price of 3.5% [71] and the actualization rate of 6% previously used, it results in a decrease in the NPV after 40 years of operation comprised between 0.68 and 1.05 mio €, which in relative terms corresponds to a decrease of 0.7 to 1.2% of the total profits.

Regarding the cold water network, since the temperature is comparable to that of fresh water networks or in some open loop district cooling networks [14], it is likely that no particular treatment will be required for the water. However if it appears that water treatment is necessary it would at most be of the same kind as used to reach the water quality required in high temperature district heating networks. Recommended values [93] for the water quality are presented in Table 1.16. The above considerations allow to conclude that it can be reasonably expected for the cost of the water to have a negligible effect on the NPV.

R1234yf and R1234ze networks are more difficult to assess from the point of view of the cost



## 1.6. Conversion technologies: An economic profitability analysis

Table 1.15 – Possible damages that might be caused by a refrigerant network and technical measures preventing them

Damage	CO <sub>2</sub>	R1234yf/ze	Events	Technical measures
Injuries to persons /damage to things caused by projection of debris	Yes	Yes	Equipment failure after an uncontrolled pressure build-up. Act of a third person.	Place pressure release valves in accordance with the EU-PED. Indicate the presence of the pipeline. Use double wall pipes or place pipes in a suitable utility tunnel.
Asphyxia	Yes	Yes	Leak from an equipment due to faulty sealing. Large leak after a pipe/equipment failure or misuse.	Place detectors and alarms. Use ventilation in conjunction with double wall pipes or a suitable utility tunnel. Place network sectioning valves.
Burns	Yes	(Yes)	CO <sub>2</sub> : dry ice projection after a failure/misuse of a piece of equipment. R1234yf/ze: combustion of the fluid during a fire.	Avoid proximity with potential ignition sources. Place network sectioning valves. Apply the appropriate fire safety standards.
Intoxication	No	(Yes)	(R1234yf/ze: combustion of the fluid during a fire leading to emission of noxious chemical compounds.)	Avoid proximity with potential ignition sources. Place network sectioning valves. Apply the appropriate fire safety standards.
Electrocution	Yes	No	Dry ice projection after a failure/misuse of a piece of equipment and submitted to a strong enough electrical field.	Apply appropriate electricity standards.

of these fluids. Very little information was found on the cost of these two fluids, however based on a british website [94] the 2015 price of R1234ze for delivery in 63 kg cylinders was 134 € kg<sup>-1</sup>, assuming that the same ratio between bulk and cylinder delivery as that of the CO<sub>2</sub> applies also to R1234ze<sup>33</sup>, then bulk cost should be around 8.1 € kg<sup>-1</sup>. Again, one can consider the initial charge of the network to be done with bulk delivered refrigerant, the initial charge would cost around 1.13 mio € 2012. Similarly to what was considered for the CO<sub>2</sub> network, the annual amount of R1234ze needed to compensate for the 3-8% leakage rate can be assumed to be delivered in cylinders, leading to an annual cost comprised between 558'000 and 1'489'000 € 2012. When assuming the same annual increase of R1234ze price of 3.5% [71] and the same actualization rate of 6% than used for CO<sub>2</sub>, it results in a decrease in the NPV after 40 years of operation comprised between 14.86 and 37.76 mio €, which in relative terms corresponds to a decrease of 16.4 to 41.8% of the total profits. In that case the profit generated at the end of the lifetime would be at best equivalent to that of the cold water network. The figure can be expected to be at least the same for R1234yf, since its price seems to be higher at around 260 € kg<sup>-1</sup>, but only prices for 5 kg cylinders could be found [95].

It can be concluded that the cost of the fluid has no significant impact for the CO<sub>2</sub> and cold water networks discussed in the present study. In the case of R1234yf and R1234ze refrigerant networks however, the cost of the fluid has a strong negative impact on the profitability of those systems in such a way that these two variants of network are likely to be less economically profitable than the cold water network. Moreover, the tendency towards stricter regulation on refrigerant fluids initiated in the late 1980's is still going on. Fluids considered environmentally friendly alternatives to CFCs and HCFCs twenty years ago are about to be phased out for environmental reasons. As a result, it seems reasonable to consider uncertain the availability of R1234yf and R1234ze at a horizon of 30 to 40 years. The cost burden caused by the use of R1234yf and R1234ze cumulated with the risk on the availability of these fluids in the future, are two sufficient criteria to declare R1234yf and R1234ze networks as impractical solutions.

Table 1.16 – Required water quality in hot water and superheated water district heating network according to [93]

Water quality parameter	Value
Electrical conductivity	10 μΩ <sup>-1</sup> cm <sup>-1</sup>
pH-value	9-10
Hardness	0.1 tH <sup>0</sup>
Appearance	clear and sediment free
O <sub>2</sub> concentration	0.02 mg l <sup>-1</sup>

### 1.6.5 Intermediate conclusion from the profitability analysis

The thermo-economic analysis done in this study, and as far as the author is concerned based on accurate and unbiased models of technologies, was used to compare five different

---

<sup>33</sup>Very optimistic assumption

## 1.6. Conversion technologies: An economic profitability analysis

---

possible implementations of refrigerant based district energy networks and two other energy conversion technologies comprising the currently used system that uses boilers and air cooled compression chillers, as well as the very state of the art in term of combined district heating and cooling network using water as a transfer fluid.

The analysis was separated in two sections. The first one was dedicated to the comparison of the energy and exergy performances of the various systems, that showed that indeed all the variants of network, refrigerant or cold water based perform undoubtedly better from an energy standpoint than the current boilers and chillers. The figure is a reduction in final energy consumption of 82.4 - 85.1%, with the best energy performing variants being the R1234ze and R1234yf network.

The second part of the analysis was aimed at giving a realistic evaluation of the economic performances of the energy conversion technologies studied. It first focussed on determining the magnitude of the investment required to build the various systems. It appeared that the least capital intensive system is the version of network using CO<sub>2</sub> has a transfer fluid and having an open cycle CO<sub>2</sub> heat pump at the central plant. At the other end of the scale, rather surprisingly, the boilers and air cooled chillers proved to be more expensive than the variants based on networks. A profitability analysis based on the net present value as a performance indicator was subsequently carried out and it showed that for the economic framework conditions considered, the conventional technologies of boilers and chillers are only marginally profitable over the 40 years lifespan considered. Conversely, all the networks show good economic performances. All the networks have shown to have payback times comprised between 4 and 6 years and generate profits in present value after 40 years comprised between 75 mio € for the cold water network and 90 mio € for networks using CO<sub>2</sub>, R1234yf or R1234ze as a transfer fluid and having an open cycle heat pump at the central plant. It is interesting to compare these figures to the initial investment required of 41 mio € and 32 mio € for the cold water and the cheapest CO<sub>2</sub> network respectively.

In the economic analysis the costs of the various fluids were not taken into account. However a computation was carried out subsequently and although the cost of the fluid proved to be relatively negligible for the CO<sub>2</sub> networks, it appeared that at the current prices, R1234yf and R1234ze networks suffer a penalty in terms of profitability that renders them unsound from an economic point of view. Moreover, these two fluids being synthetic, there is a degree of risk regarding the availability of these fluids in the future, mostly because in the long run there is a non-zero probability that new regulatory constraints apply to these fluids. As a result, and in spite of their better energy performance, the versions of refrigerant network using R1234yf and R1234ze as transfer fluids can be declared as not interesting from a practical standpoint. Since it was too difficult to compute a realistic cost for the safety measures that will be required for the refrigerant based networks, it was not included in the economic models. However, the value of the maximum investment that can be spent on safety before refrigerant networks become less profitable than a cold water network was computed. It shows that the higher profit generated by the CO<sub>2</sub> network<sup>34</sup> when compared to that of the cold water network, allows for up to 8 mio € extra investment in safety at year 0, 5.59 mio € at year 15 and 3.91

---

<sup>34</sup>The variant with a CO<sub>2</sub> central heat pump

mio € at year 30 (all in present value) and still be more profitable than the cold water option. In comparison to the initial investment originally computed, it corresponds to a relatively comfortable margin of 25% available for absorbing the extra cost of safety.

As a conclusion, of the variants of network using a refrigerant as transfer fluid the best option is the CO<sub>2</sub> network version equipped with an open cycle CO<sub>2</sub> heat pump at the central plant. Its advantage over the cold water network comes from the lower investment required thanks to the smaller diameter of the pipelines and cheaper central plant. Although it has the highest final energy consumption of the network discussed in this work, it still is the most cost effective solution as all the variant of network studied have much higher investment than energy (operation) related costs. Moreover the difference in terms of final energy consumption is only 1.5% more that of the cold water network. Finally, of the variants of network than can be practically envisaged - the CO<sub>2</sub> based ones - the version with a CO<sub>2</sub> open cycle is the one with the biggest economic reserve available for absorbing the extra cost for safety equipment of a CO<sub>2</sub> based network.

### 1.7 Conversion technologies: Economic robustness

So far, in this study, all the computations regarding energy and economics are based on the assumptions that the framework conditions are known. Regarding the energy, it typically assumes:

- A perfectly known energy demand of the buildings.
- No evolution of the energy performance of the buildings along the years.
- Identical years.
- A perfectly known performance of the various pieces of equipment.

And regarding economics, the following assumptions were done:

- A known cost for the various pieces of equipment
- A known multiplication factor to account for the installation cost
- A known evolution of the cost of equipment
- A known evolution of the electricity and heating oil prices<sup>35</sup>
- A known evolution of the cost of manpower, that influences maintenance and operation costs.

---

<sup>35</sup>As well as the sale price of the energy services that are indexed on the electricity price for the networks and the heating oil price for the currently used boilers and air cooled chillers.

Obviously all these assumptions are questionable especially since the period of 40 years considered in this study is very long when it comes to economic questions.

As a consequence, it is attempted in the present section to give a realistic evaluation of the economic robustness of the proposed technologies. The methodology adopted follows a stochastic approach based on probability distribution functions of the parameters mentioned above. The focus is on the economic robustness and as a result, of the energy related assumptions mentioned above, only the year-to-year evolution of the buildings energy demand will be kept in the analysis, since a downward evolution of the demand can be expected to have a significant impact on the economics of district heating and cooling networks [11]. Indeed, in Switzerland it is likely that extensive renovations of the envelopes of buildings will be carried out continuously over the next 35 years [96] as part of the measures at the national level to reach the targets defined in the 2050 energy strategy of the federal council<sup>36</sup>. The probability distribution functions have been derived from statistical data available spanning a significant period for the inflation rates of energy, equipment and manpower costs and a significant amount of machines for the various pieces of equipment.

The goal is to be able to assess, with the help of a quantitative and motivated methodology, the probability of profit of the various conversion technologies envisaged and should lead to answers to the following questions:

- How accurate is the evaluation of the profitability carried previously in this study?
- What are the driving elements in terms of uncertainty?
- How robust are the technologies studied to uncertain economic conditions?
- How the profitability will be affected by the expected reduction in heating and cooling demand over the years?

### 1.7.1 Simulation of the Rues Basses test case using stochastic processes: Modelling

Simulation of complex systems using stochastic processes is typically a branch of operational research. In this subsection, the description will be limited to the elements necessary for the reader to understand the approach followed to assess the economic robustness of the various energy conversion technologies studied. For a more fundamental description the reader is advised to consult the textbook of Ross [97].

The method used is configured as a post processing approach using the results of the thermoeconomic models described previously. The basic underlying idea is to calculate a large number of times - 100'000 - the evolution of the NPV along the lifetime with varying economic parameters. These parameters are randomly selected according to probability distribution functions derived from statistics. Slight differences have been made to distinguish the case of the boilers and air cooled chillers with that of the refrigerant and cold water networks.

---

<sup>36</sup>Executive body of the government

## Chapter 1. Thermo-economic analysis

---

In the case of the combination of boilers and air cooled chillers, each of the 100'000 repetitions follow the steps detailed below:

**Initial investment:** The initial investment is re-evaluated from the one previously obtained at section 1.5. The total purchasing cost of the boilers<sup>37</sup> and mechanical draught air coolers (MDAC) are randomly modified according to the probability distribution of the relative error between the cost function for the heat exchangers and the data points it is based on. (See Fig.B.3). Similarly the total purchasing cost of the compression chillers is modified according to the probability distribution of the relative error between the cost function for the decentralized heat pumps and the data points it is based on. (Fig.B.1). To consider the distribution of prices of brine-to-water heat pumps as representative of the price distribution of liquid cooled chillers was considered a reasonable assumption. It is more questionable to use the price variation of plate heat exchangers as representative of that of the of boilers and MDACs. In the case of the boilers, it would have been possible to obtain a specific price distribution but the time lacked to do it. In the case of the MDACs, no catalogue with prices were found and hence it was is not possible to derive a distribution.

**Years 1 - 5:** The rate of increase of the priced billed to the customers is the same than that of the heating oil purchased for the boilers, the first one being assumed to be indexed on the second one. The five year annual rate is randomly selected following the probability distribution of the relative error between the 3.5% average annual increase used earlier and statistically derived values [69]. Similarly the rate of increase of the electricity purchased for the chillers is selected from the probability distribution of the relative error between the 1.2% average annual increase used earlier and values derived from [68]. The rate of increase of maintenance costs is modified following the distribution of relative error between the 1.2% annual increase of manpower costs used earlier and statistically derived values [72]. The distributions of probability for these rates are done on statistical values computed on a five years basis. The method will be detailed later in this section.

**Years 6 - 10 and 11 - 15:** The rates of increase of electricity and heating oil prices, as well as the heating and cooling services billed to the customers and the rate of increase of maintenance costs are recomputed following the same procedure as for the first 5 years.

**Years 1 - 15:** The energy billed to the customers is reduced linearly each year at a rate selected randomly from a distribution expressing the potential of improvement of the envelopes of buildings in the area considered. Details on that particular distribution will be given later in this section.

**1<sup>st</sup> Replacement of equipment:** The investment for the new boilers, MDACs are recomputed based on the same distributions as was done for the initial investment. The rate of

---

<sup>37</sup>Including the heating oil tank and the exhaust stack

## 1.7. Conversion technologies: Economic robustness

---

increase of the prices of equipment are reselected on a five years basis from a distribution derived from the relative error between statistical values for the 5 years increase rate of the Chemical Engineering Plant Cost Index [71] and the average annual rate of increase of 3.5% used earlier in the study. The cumulated values of the first 15 years of operation is used to compute the new price of the equipment to be replaced.

**Years 16 - 20, 21 - 25 and 25 - 30:** The rates of increase of electricity and heating oil prices, as well as the heating and cooling services billed to the customers and the rate of increase of maintenance costs are recomputed following the same procedure as for the other periods of 5 years.

**Years 16 - 30:** Another rate of the linear decrease of the amount of thermal energy services sold to the customers is selected for that period, in a similar fashion to what was done for the first 15 years of operation.

**2<sup>nd</sup> Replacement of equipment:** The investment for the new boilers, MDACs are recomputed based on the same distributions as was done for the 1<sup>st</sup> replacement of the equipment.

**Years 31 - 35, 36 - 40:** The rates of increase of electricity and heating oil prices, as well as the heating and cooling services billed to the customers and the rate of increase of maintenance costs are recomputed following the same procedure as for the other periods of 5 years.

**Years 31 - 40:** Another rate of the linear decrease of the amount of thermal energy services sold to the customers is selected for that period, in a similar fashion to what was done for the other sets of 15 years.

It follows that each repetition requires 41 random numbers to be drawn, making the total reach 4.1 mio draws.

In the case of the CO<sub>2</sub> or the cold water networks, each of the 100'000 repetitions follow the steps detailed below:

**Initial investment:** The initial investment is re-evaluated from the one previously obtained at section 1.5. The total purchasing cost of the decentralized heat pumps is randomly modified according to the probability distribution of the relative error between the cost function for the heat pumps and the data points it is based on. (See Fig.B.1). Similarly the total purchasing cost of the free cooling heat exchangers, and that of the heat exchangers at the central plant are modified according to the probability distribution of the relative error between the cost function for the plate heat exchangers and the data points it is based on. (Fig.B.3). The price of the compressors at the central plant is recomputed following a similar procedure but with a distribution derived from Fig. B.2. The cost of the pipes of the main and connection lines is recomputed following a probability distribution, that one obtained from the statistical variations of the KBOB index for boiler tubes [98].



**Years 1 - 5:** The rate of increase of the electricity price and that of the price of the energy services billed to the customers are the same, the second one being assumed to be indexed on the first one. The five year annual rate is randomly selected following the probability distribution of the relative error between the 1.2% average annual increase used earlier and statistically derived values for the electricity price [68]. The rate of increase of maintenance costs is modified following the distribution of relative error between the 1.2% annual increase of manpower costs used earlier and statistically derived values [72]. The distributions of probability for these rates of increase are done on statistical values computed on a five years basis, similarly to what was done for the boilers and chillers. Again, it should be pointed out that the same random number is used to select the rate of increase of the thermal services billed to the customers and that of the electricity, as these two rates cannot be assumed to be independent one from another.

**Years 6 - 10 and 11 - 15:** The rates of increase of the electricity price, of the heating and cooling services billed to the customers and of the maintenance costs are recomputed following the same procedure as for the first 5 years.

**Years 1 - 15:** The energy billed to the customers is reduced linearly each year at a rate selected randomly from a distribution expressing the potential of improvement of the envelopes of buildings in the area considered. Details on that particular distribution will be given later in this section.

**1<sup>st</sup> Replacement of equipment:** The investment for the new equipment is recomputed based on the same distributions as was done for the initial investment. The price of the pipes is obviously not recomputed as these are not replaced. The rate of increase of the prices of equipment is reselected on a five years basis from a distribution derived from the relative error between statistical values of the Chemical Engineering Plant Cost Index [71] and the average annual rate of increase of 3.5% used earlier in this study. The cumulated values of the first 15 years of operation is used to compute the new price of the equipment to be replaced.

**Years 16 - 20, 21 - 25 and 25 - 30:** The rates of increase of electricity prices and that of the heating and cooling services billed to the customers and of the maintenance costs are recomputed following the same procedure as for the other periods of 5 years.

**Years 16 - 30:** Another rate of the linear decrease of the amount of thermal energy services sold to the customers is selected for that period, in a similar fashion to what was done for the first 15 years of operation.

**2<sup>nd</sup> Replacement of equipment:** The investment for the equipment to be replaced is recomputed based on the same distributions as was done for the 1<sup>st</sup> replacement of the equipment.



## 1.7. Conversion technologies: Economic robustness

---

**Years 31 - 35, 36 - 40:** The rates of increase of electricity prices and that of the heating and cooling services billed to the customers and of the maintenance costs are recomputed following the same procedure as for the other periods of 5 years.

**Years 31 - 40:** Another rate of linear decrease of the amount of thermal energy services sold to the customers is selected for that period, in a similar fashion to what was done for the other sets of 15 years.

It follows that each repetition requires 37 random numbers to be drawn, making the total reach 3.7 mio draws.

For each repetition and indistinctly for the boilers and chillers case or the CO<sub>2</sub> / cold water networks, the same actualization procedure was followed as that of the rest of the economic analysis. the actualization rate of 6% being conserved. This particular rate represent a choice and not an external constraint, to the contrary of the other rates of increase. Obviously another value might have been used, but it is worth noticing that there is no reason to use the same kind of randomized process for the actualization rate than was used, for instance with the electricity price. It is also worth mentioning that, although it would have been interesting to randomize the installation cost and engineering cost factors, time constraints prevented representative enough statistical data to be gathered and hence these two factors have been dropped out of the present uncertainty analysis.

### **Modelling of stochastic processes: Rates of increase of energy, equipment and manpower costs**

In this paragraph, the methodology used to obtain the distribution of probability necessary to recompute the various inflation rates will be presented. In order to simplify the discussion the electricity price will be used as an example. As the computation was imagined as a post treatment of the result of thermoeconomic models discussed earlier, the aim was to obtain distribution of probability that would be used to generate *probabilistically sound perturbations* around the average inflation rates used earlier, that had been defined using the same data. The process to get a new value of the 5 years inflation rate of the price of electricity follows the 5 steps illustrated at Fig. 1.43:

**A:** Statistical data are available on the electricity prices for different types of consumers in Switzerland. These data span the period 1966 - 2014 [68]. A price function is fitted on the data. It is characterized by an initial value for the price  $P_0$  in 1966 and a constant an annual rate of increase  $\tau_0$ . These two parameters are selected such as to minimize the sum of the squared differences between the real price and the price function. The annual rate of increase that minimizes the error is  $\tau_0 = 1.2\%$ , and was also used where needed in previous parts of this work.

**B:** The 5 years annual inflation rate of the electricity price is computed for each year in the

dataset except the last 5. The equation for the 5 year annual inflation rate of the year "i" being:

$$\tau_i = \left[ \frac{P_{i+5}}{P_i} \right]^{1/5} \quad (1.36)$$

The choice of computing the inflation rate on a five years basis is the result of a compromise between accuracy and computation time. A 5 years rate allows for only eight draws compared to 40 in the case of an annual rate, it also has the advantage of only diminishing the size of the dataset of its five last elements which in that particular case represent a loss of 10% of the samples.

**C:** The vector of relative error  $\epsilon_i$  between the elements  $\tau_i$  of the vector of inflation rate and the average inflation rate found in **A** is computed:

$$\epsilon = \frac{\tau_i - \bar{\tau}}{\bar{\tau}} \quad (1.37)$$

the elements of  $\epsilon$  are sorted in ascending order and plotted against a y-axis spanning linearly the interval [0,1], thus providing a cumulative probability distribution function of  $\epsilon$ .

**D:** The reciprocal function of the cumulative probability distribution found in **C** is taken, thus providing a function that translates a random number taken from the uniform probability distribution  $U(0,1)$  in a value of the relative error  $\epsilon_k$ . The subscript changed as it denotes the  $k^{th}$  draw and not the  $i^{th}$  year of the initial dataset.

**E:** The value of the 5 year inflation rate of the electricity price is finally computed using the value of  $\epsilon_k$  from **D**:

$$\tau_k = \bar{\tau} \cdot (\epsilon_k + 1) \quad (1.38)$$

The process involved is exactly identical, although with different datasets, for the inflation rate of the heating oil price [68], the thermal energy services billed [99], the manpower cost [72] and the equipment costs [71].

### Modelling of stochastic processes: Equipment costs

The stochastic modelling of the equipment costs is similar to that of the inflation rates, but shorter. For instance, in the case of the compressors, the relative error between the catalogue price of the compressor and that given by the cost function can directly be computed (See the histogram at Fig. B.2). Then the vector of relative error can be sorted in ascending order and plotted against a y-axis spanning the interval [0,1], giving the same kind of cumulative probability distribution as was found for the inflation rate (Fig. 1.43), then the process is exactly the same except that at the last step the average inflation rate -  $\bar{\tau}$  - is replaced by the

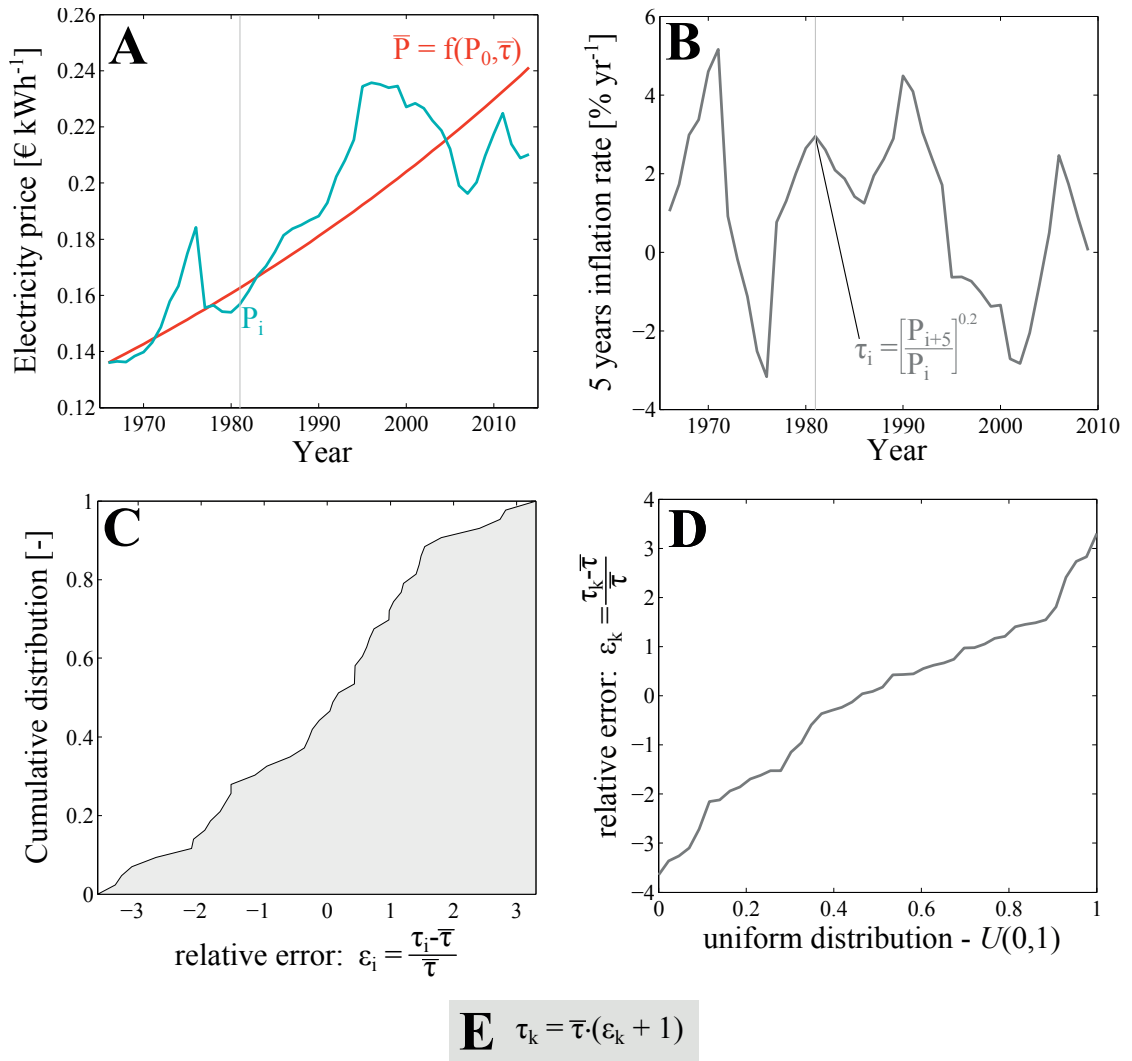


Figure 1.43 – 5 Steps methodology to obtain a stochastic modelling of the rate of increase of the electricity price. **A**: Fitting of a reference price curve with a constant annual rate of increase  $\bar{\tau}$  from statistical data of the electricity price. **B**: Computation of the 5 years rate of increase  $\tau_i$  for every year of the dataset, except the last 5. **C**: Computation of the relative error  $\varepsilon_i$  for every year of the dataset and build of the cumulative distribution of it. **D**: From the reciprocal of the cumulative distribution obtained in **C** and using a random number drawn from the uniform distribution  $U(0,1)$ , computation of the relative error  $\varepsilon_k$ . **E**: Computation of the new rate of increase of the electricity price  $\tau_k$  using the relative error  $\varepsilon_k$  found at the previous step.

cost of compressor obtained with the cost function from Fig. B.2. The process is identical for the other types of equipment. In the case of the cost of pipelines, the distribution is built using the price index for boiler tubes obtained from [98] by computing the relative error between the various data points and the average value.

**Modelling of stochastic processes: Decrease of the amount of thermal services provided as a result of improved envelopes of buildings.**

The heating and cooling demands of the studied area correspond to the year 2012. Since improvement in the building sector is seen as a pillar of the new energy strategy of the federal council, it is very likely that in the future the envelope of the buildings will progressively be improved. As a result, one can assume that the amount of thermal services to be provided by the conversion technologies will decrease over the forty years period considered in this study. Table 1.17 shows the number of residential buildings constructed in the area of Geneva according to their year of construction [100]. The sum of the space heating and hot water yearly requirements is also given for each year of construction [34]. The difference between these values of specific heat demand and that required by the most recent mandatory standard applicable [101] for a renovated building<sup>38</sup> is computed. This difference is taken as the reduction potential of the buildings requirements for space heating and hot water preparation. The data of Table 1.17 are ordered according to this reduction potential.

The distribution of the number of buildings with regard to their reduction potential is then computed. As for the inflation rates and the investment costs, a function that translates a random number drawn from a uniform distribution  $U(0,1)$  is derived. Based on this function, the reduction potential is by choosing a random value between 0 and 1 at year 0, 15 and 30.

Table 1.17 – Potential or reduction of the energy consumption for space heating and domestic hot water in buildings according to their year of construction. [34, 100, 101]

Reduction potential [%]	Years of construction	Specific heat demand (SH + DHW) [kWh m <sup>2</sup> yr <sup>-1</sup> ]	Number of buildings
58	2006-2012	106.6	2'648
63	2001-2005	120.7	2'274
64	1991-2000	125.8	4'857
69	1981-1990	144.5	5'245
70	Before 1919	149.9	7'636
71	1971-1980	154.9	5'299
72	1946-1960	162.8	4'694
74	1919-1945	170.0	4'749
75	1961-1970	177.3	4'938

Renovated buildings with reduced heating requirements would also require lower supply temperature  $T_H$ . This temperature depends on the outside temperature and in this study it varies between 22 and 55°C. According to the heating curve described by eq. 1.12. Considering an ambient temperature of 20°C in the buildings, the heat rate emitted by their radiators can

---

<sup>38</sup>Approximately 45 kWh m<sup>-2</sup> yr<sup>-1</sup>

be described by the following equation:

$$\dot{Q} = U_{rad} A_{rad} (T_H - 20) \quad (1.39)$$

The heat rate of the same building with a renovated envelope but equipped with the same surface of radiators becomes:

$$\dot{Q}_{ren} = U_{rad} A_{rad} (T_{H,ren} - 20) \quad (1.40)$$

The reduction potential of the annual heating requirements is equal to the ratio of the two heat rates. The supply temperature after renovation can therefore be expressed as a function of the reduction potential.

$$T_{H,ren} = \frac{\dot{Q}_{ren}}{\dot{Q}} (T_H - 20) + 20 \quad (1.41)$$

Although for a boiler a reduction of the supply temperature has a very limited effect on its first law efficiency, it is not the case for a heat pump.

As in winter, refrigerant and cold water networks can be assimilated to large electrical heat pumps that take heat from a cold source at a temperature  $T_{lake}$  (7.5°C) and provide heat at hot source at the temperature  $T_H$ , it seems reasonable to account for both the changes in heat and temperature delivered. However, in order not to have to re-run the full models of the networks, which would have been too time consuming, the following simplified approach was used:

Assuming a renovation of some buildings connected to a refrigerant/cold water network, it follows that both the energy supplied and the temperature in the hydronics are reduced from  $Q$  to  $Q_{ren}$  and  $T_H$  to  $T_{H,ren}$  respectively. The effect on the electricity consumption is twofold, since the heat to be provided by the decentralized heat pumps is reduced and their  $COP_h$  is increased.

The annual electricity consumption of the network can therefore be expressed as a function of the heat provided to the buildings by using a Carnot heat pump corrected of a constant exergy

efficiency  $\eta$ . Before the renovation the annual electricity consumption is given by:

$$E = Q \frac{1}{\eta} \left( 1 - \frac{T_{lake}}{\bar{T}_H} \right) \quad (1.42)$$

and after it becomes:

$$E_{ren} = Q_{ren} \frac{1}{\eta} \left( 1 - \frac{T_{lake}}{\bar{T}_{H,ren}} \right) \quad (1.43)$$

Based on, eq. 1.42 and eq. 1.43, the reduction of the electrical consumption corresponding to a given reduction of the heat demand is obtained (eq. 1.44). The supply temperature before and after renovation  $\bar{T}_H$  and  $\bar{T}_{H,ren}$  used are mean annual supply temperatures.  $\bar{T}_H$  is equal to the mean value of the daily supply temperatures weighted by the daily heat demand. In the present case  $\bar{T}_H$  is equal to 37.0°C. The exergy efficiency of the conversion technology is assumed to be the same before and after the renovation and as a consequence it cancels out in eq.1.44.

$$\frac{E_{ren}}{E} = \frac{Q_{ren}}{Q} \frac{\bar{T}_H}{\bar{T}_{H,ren}} \frac{\bar{T}_{H,ren} - T_{lake}}{\bar{T}_H - T_{lake}} \quad (1.44)$$

As the supply temperature for the renovated case -  $T_{H,ren}$  - solely depends on the ratio  $Q_{ren}/Q$  and on the initial average supply temperature  $\bar{T}_H$ , it results that eq. 1.44 depends de facto only on these two quantities.

For  $\bar{T}_H = 37^\circ\text{C}$ , the maximum coupled effect of a reduced heat demand and of the resulting lower supply temperature occurs for a value of  $Q_{ren}/Q = 42\%$  and in that case the value of  $E_{ren}/E$  is 38.1%.

In spite of being a relatively crude approximation, this method has the merit of capturing a key feature of heat pumps at a low computational cost. Moreover the coupled effect of the reduced amount of heat and of a higher  $\text{COP}_h$  is still relatively small and as a consequence it would not justify much more effort from the modelling point of view.

Several other assumptions had to be made regarding the improvement of the buildings, and its subsequent effect on the profitability of the conversion technologies studied here:

- Renovated buildings see also their air conditioning needs reduced. The reduction is supposed to be equal to the heating reduction potential.
- The heating and cooling demand reduction is equally divided over the years. For in-

stance, a reduction potential of 58% corresponds to subtract every year 1.45% of the initial demand. Obviously the revenue linked to the sale of energy to the users is reduced proportionally to the reduction of energy delivered.

- All the equipment, except the pipes, being replaced every fifteen years. The energy requirements reduction has also an impact on the replacement cost of the equipment. As a consequence it is assumed that the reduction in cost for the heat pumps and the compressors at the central plant follows the electrical consumption reduction predicted by eq. 1.44, while the reduction of the cost for all the rest of the equipment replaced is assumed to follow the heat reduction.
- The yearly reduction of the electrical consumption is applied to the maintenance cost of the decentralized heat pumps. It was assumed to be realistic as they will clock less hours of equivalent full load than they were initially intended to.

### 1.7.2 Simulation of the Rues Basses test case using stochastic processes: Results

The simulation models based on stochastic processes have been applied to the following variants of energy conversion technologies:

1. Current technologies of boilers and air cooled electric chillers.
2. CO<sub>2</sub> network with an open cycle CO<sub>2</sub> heat pump at the central plant.
3. Cold water network.

The other versions of refrigerant network are not included in the analysis, the two other CO<sub>2</sub> variants being less promising economically than that already included in the analysis and the R1234yf and R1234ze networks having been discarded on the basis of the excessive price of these two fluids and because of the risk of them becoming unavailable in the long run.

The possible evolutions of the NPV, according the stochastic modelling done in this study, is represented for the boilers and chillers at Fig. 1.44. On that figure, the x-axis represents the number of year of operation of the system, the y-axis the NPV, and the gray-shade the probability of obtaining a certain NPV during a given year. This representation is a convenient way to highlight the most probable path (darker zones), but also gives an idea of the extent of the possible fluctuations. For the case of the boilers and chillers, it appears that the marginal profitability of the base case (See Fig. 1.42) was slightly optimistic, as the stochastic simulation show a trend towards a negative NPV after 40 years. In fact, when compared to the base case of the NPV evolution at Fig. 1.42 the marginal profitability of 9.1 mio € turns into a net loss of -28.2 mio € in present value at the peak of probability (see the insert at Fig. 1.44).

The spread in NPV, which increases with the years, is due to the cumulating effect of the various fluctuations. The single biggest contribution to the spread is the rate of increase of the price of heating oil. It is rather intuitive since it is more volatile than the other rates of increase and the

purchase of heating oil represents an important share of the total costs, for the base case at Fig. 1.42 the value is around 45%. A high share in total costs tends to transfer more directly the effect of the volatility on the profitability in general. Overall, of the 100'000 repetitions, 64.4% led to a net loss after 40 years (See the insert at Fig. 1.44). The lower profitability obtained with the stochastic simulation when compared to the base case is mainly due to the effect of the volatility of the price of heating oil, if that particular contribution is removed from the stochastic simulation, the most probable NPV after 40 years rises from -28.2 mio € to around +2 mio €.

The continuous decrease in the amount of energy services delivered to the buildings has a slight negative effect on the profitability. If no renovation is assumed, hence no reduction in the thermal energy services provided, then the NPV at year 40 rises from -28.2 mio € to -25.5 mio €. The relatively small negative effect on profitability when the fleet of buildings is improved has to do with the relatively high importance of operation related costs (dominated by the purchase of oil and electricity) over investment related ones. As a result, although the boilers and chillers are almost always oversized<sup>39</sup>, the effect on the total cost is not very important.

It appears that a combination of boilers and chillers to supply the thermal energy needs in the are studied is likely not to be profitable at the initial retail price of the energy service of 0.108 € kWh<sup>-1</sup>. The stochastic process based simulation used, allowed to highlight the poor ability of that combination of technologies to cope effectively with the uncertain character of the economic conditions. The high dependence to the heating oil prices for the supply of space heating and domestic hot water through boilers is the weakest point of the system in terms of risk for the profitability. The probability of facing a net loss at the end of the period considered is 64.4%, while the probability of generating a profit higher than that of the cold water network from the base case - 74 mio € in present value - is only of 8% and the probability of generating a profit higher than that of the CO<sub>2</sub> network with an open cycle CO<sub>2</sub> heat pump at the central plant is 5.4%.

The evolution of the NPV, according to the stochastic simulation and for the version of the CO<sub>2</sub> network equipped with a CO<sub>2</sub> heat pump at the central plant, is shown at Fig. 1.45. It appears that profitability of that technology within the context of the test case area is guaranteed in spite of the uncertainties on the economic parameters, as shown by the histogram for the year 40 at in the insert of Fig. 1.45. Although there is also a tendency towards a larger spread of the NPV with the years, the extent of it is much more reduced than what was observed for the boilers and chillers. It also appears that the uncertainty regarding the initial investment is smaller in the case of the CO<sub>2</sub> network than for the boilers and chillers. The combined result of the rather small uncertainty on the initial total investment and the low impact of the cumulated uncertainty on the rate of increase of electricity prices is that the payback time<sup>40</sup> is rather stable with a probability greater than 95% for the break-even time to be comprised between 4 and 6 years.

---

<sup>39</sup>Actually all years except year 0, 15 and 30, when they are replaced

<sup>40</sup>The number of years required for the NPV to cross zero.



## Oil fuelled boilers + air cooled chillers

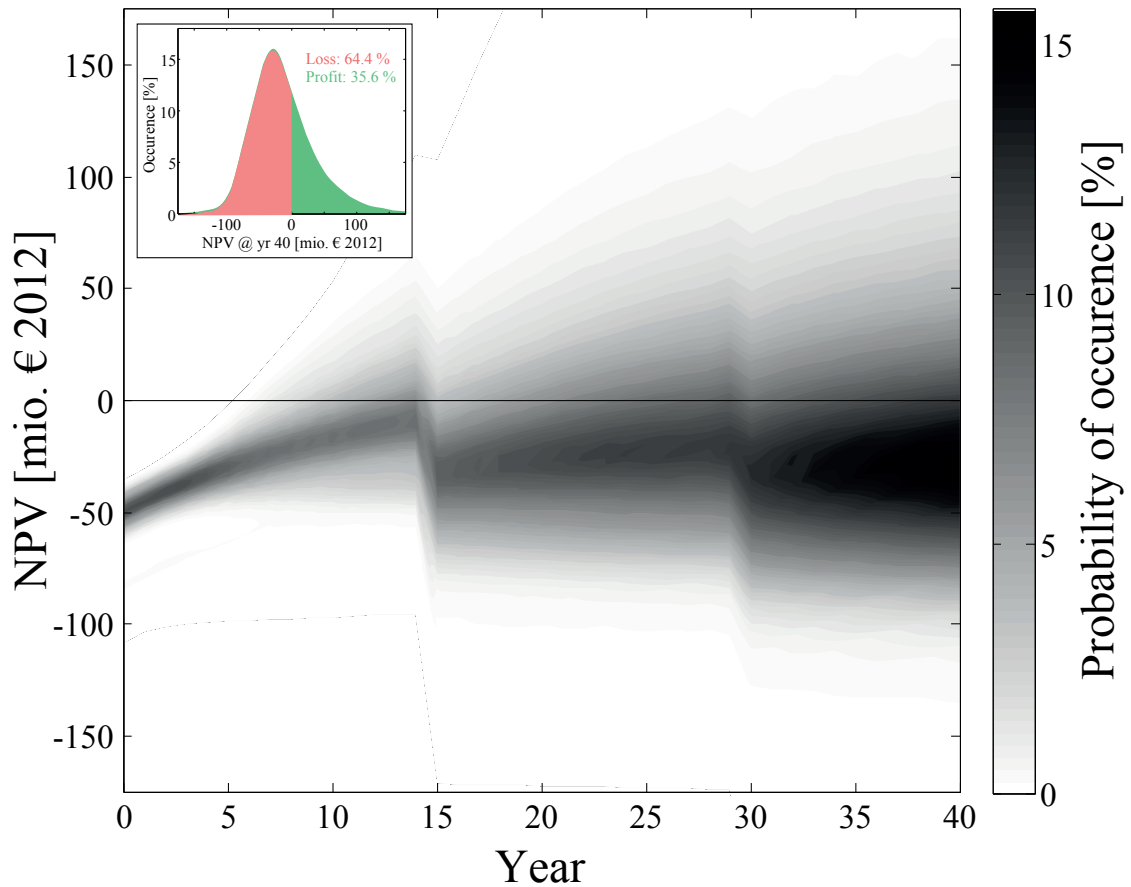


Figure 1.44 – Results of the stochastic processes based simulation when applied to the case of the boilers and air cooled chillers. It shows the distribution of the evolution of the NPV along the lifetime of 40 years. The grey-shade represents the probability of occurrence of a particular value of the NPV (y-axis) during a given year (y-axis). The insert gives the histogram of the NPV after 40 years of operation, the share of the repetitions that lead to a loss are in red, while the share of those generating a profit are in green.

The effect of the replacement of the equipment at year 15 is a large increase of the spread of the possible NPV. Indeed it is possible to have cases with a low NPV at year 14 that also have high investment costs needed for the replacement of equipment at the year 15 and conversely to have cases with a high NPV at year 14 with a low investment required at year 15. These extreme cases are rendered possible by the fact that the rate of increase of the electricity price, that of the equipment price and the uncertainty on the prices of the various pieces of equipment are all decided by independently drawn random numbers. In reality however, these parameters are very likely not independent. For instance, one could expect the rate of increase of the equipment and electricity prices to exhibit some sort of coupling, but accounting for it would have required effort beyond the scope of the present study. Note that the second replacement of equipment at year 30 also increases the spread in NPV but with a lesser impact.

To determine which of the uncertain parameters used in the present analysis contributes the most to the total uncertainty on the profitability, simulations were reconducted with the stochastic behaviour removed for one parameter at a time. It results that for the CO<sub>2</sub> network the variations in the inflation rate of the electricity price<sup>41</sup> has the strongest spreading effect on the NPV, followed by the uncertainty on the purchase price of the various pieces of equipment and the uncertainty on the rate of increase of those prices.

Although not really contributing to the spread in NPV, the reduction in the amount of energy services provided to the customers has a very significant effect on the profit. Indeed, considering the base case NPV for the CO<sub>2</sub> network at Fig. 1.42 as well as the result of the stochastic simulation without the decrease in the amount of energy services delivered, the NPV at year 40 should be around 90 mio €, by comparison the case with the reduction in sales of energy services shows a most probable NPV after 40 years of only 56.6 mio €, or in relative terms a 37.1% diminution in profit. This loss of economic performance is explained by the high share of investment related costs in a CO<sub>2</sub> network. These investments become more difficult to amortize as the sales of energy decrease over the years. However, it must still be kept in mind that more energy efficient buildings cause a drop in profit and not an economic loss.

Similar results are obtained from the stochastic simulation of the cold water network. It is unsurprising, since the technologies have been shown to be very similar. The higher investment for the cold water network, due to its larger pipes and more expensive central plant, shows a larger spread than the CO<sub>2</sub> network. Logically, the larger uncertainty regarding the initial investment tends to amplify the spread in NPV over the years which result in slightly more uncertain payback time, comprised between 5 and 9 years with a probability greater than 95%. The probability of generating a profit at the end of the 40 years is greater than 99.6% which, although slightly lower than for the CO<sub>2</sub> network is still an excellent figure. The effect of the improvement of the envelope of buildings is also very similar to that observed with the CO<sub>2</sub> network. From a most probable profit of 74 mio € after 40 years when no reduction of the energy supplied to the buildings is considered, it goes down to 44.4 mio €. In absolute terms the reduction in profit is slightly smaller than for the CO<sub>2</sub> network - 29.6 vs. 33.4 mio €, however the net result is still in favour of the CO<sub>2</sub> network.

The approach used to assess the economic robustness of the boilers and air cooled chillers, CO<sub>2</sub> network with an open cycle CO<sub>2</sub> heat pump at the central plant and the cold water network, confirmed the economic benefit of the network based technologies. Indeed, under the assumptions of the current stochastic models, a combination of boilers and air cooled chillers has a 64% probability of being not profitable after 40 years, at the proposed initial price of 0.108 € kWh<sup>-1</sup> for the energy services delivered. In comparison, when put in the same economic conditions, the soundness of the two network based technologies is not questionable. Indeed, only 14, respectively 375, of the 100'000 scenarios generated by the simulation have led to a net loss after 40 years for the CO<sub>2</sub> and cold water network respectively. Moreover, these

---

<sup>41</sup>As well as the inflation rate of the sale price of the energy services since it is indexed on that of the electricity.

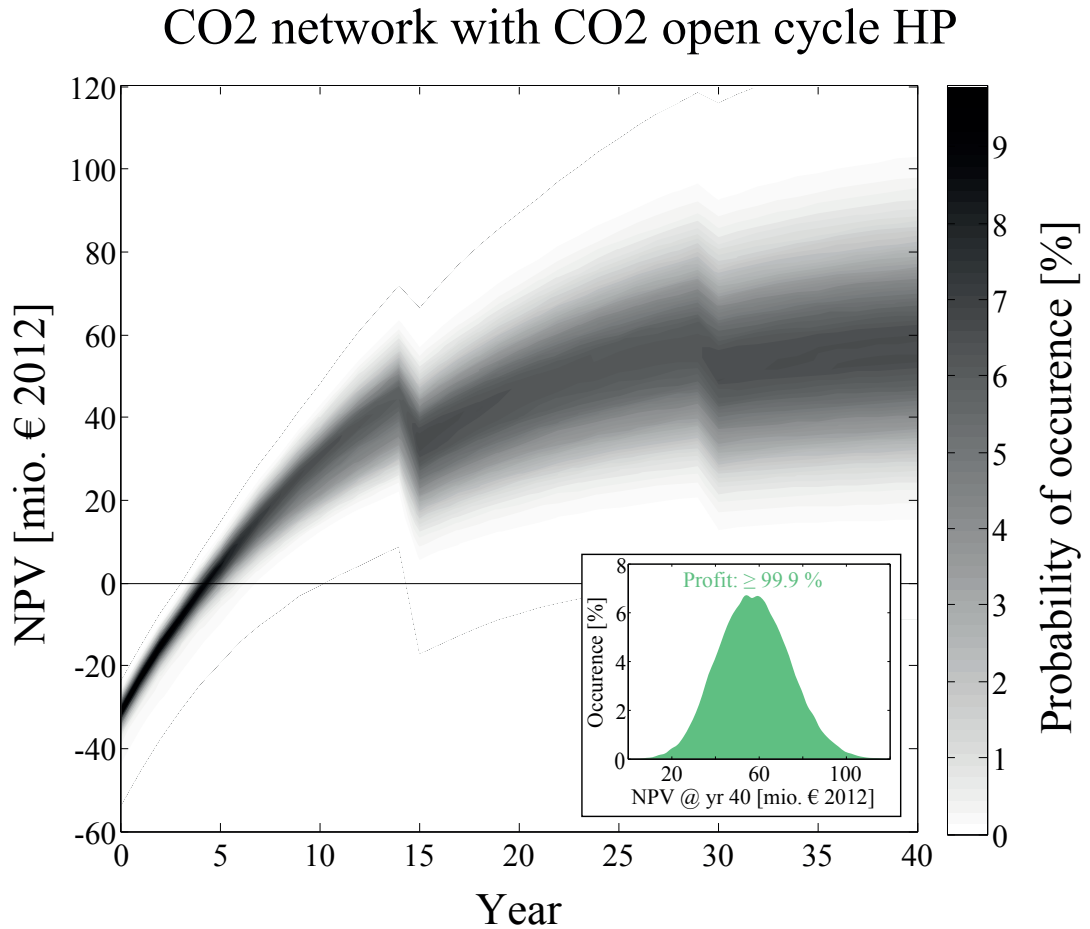


Figure 1.45 – Results of the stochastic processes based simulation when applied to the CO<sub>2</sub> network equipped with an open cycle CO<sub>2</sub> heat pump at the central plant. It shows the distribution of the evolution of the NPV along the lifetime of 40 years. The grey-shade represents the probability of occurrence of a particular value of the NPV (y-axis) during a given year (y-axis)

probabilities of economic benefit are reached in spite of the reduction in the energy services delivered over the years. a reduction caused by the future energy retrofit of the buildings connected.

On can conclude from the present assessment that the proposed CO<sub>2</sub> and cold water network are economically robust technologies for the supply of thermal energy services in dense urban areas, and that they make much more sense economically than the currently used boilers and air cooled chillers.

According to the current analysis, the cold water network still performs a little lower in economical terms than the CO<sub>2</sub> network, essentially due to the expected lower investment costs for the latter one. It is important to recall that uncertainty regarding the cost of the additional safety measures that will necessarily apply to the CO<sub>2</sub> network was not included in the present analysis, and whether the CO<sub>2</sub> network will economically outperform the cold water network,

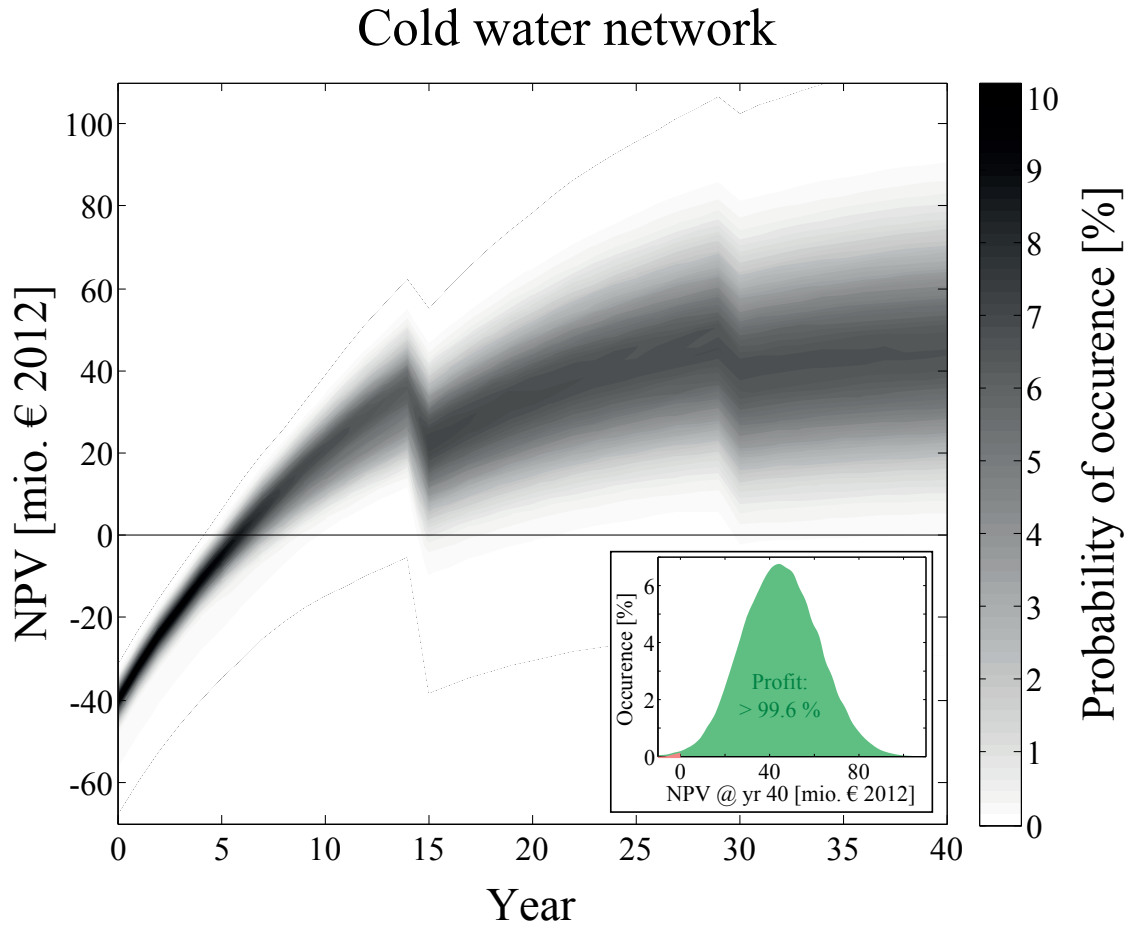


Figure 1.46 – Results of the stochastic processes based simulation when applied to cold water network. It shows the distribution of the evolution of the NPV along the lifetime of 40 years. The grey-shade represents the probability of occurrence of a particular value of the NPV (y-axis) during a given year (y-axis)

remains an open question.

On the one hand, the difference in economic performance of the cold water network and the CO<sub>2</sub> network will tend to be reduced (maybe even reversed) as a consequence of the safety related costs. On the other hand however, the use of CO<sub>2</sub> might allow some innovations in the layout of the pipelines which could lead to savings. The balance of these two elements cannot be determined at the time these line are being written. A glimpse of these innovations will be provided in the next section.

## 1.8 CO<sub>2</sub> vs. cold water: On technical issues.

The result of the energy, profitability and economic robustness analyses have demonstrated the benefits of advanced energy networks over the currently used technologies and showed

that the designs of these networks should focus on reducing the investment cost rather than improve further their energy efficiency. Additional considerations allowed to rule out the use of HFO refrigerants as transfer fluids, leaving only water and CO<sub>2</sub> as potential candidates. However, the relatively small difference between these two types of network in term of energy performance and to a lesser extent in term of profitability, are insufficient to determine which of two technologies is the most promising.

Moreover, safety considerations that have already been discussed as part of the profitability analysis (1.6.3), showed that extra safety measures, that will be required for the CO<sub>2</sub> network, will reduce even more the economic advantage of the CO<sub>2</sub> over the cold water based network. As a consequence of these relatively equivalent performances, other decision factors are going to play a defining role on the future of both the CO<sub>2</sub> and cold water networks.

### 1.8.1 Compactness

It is a known fact that district heating and cooling should be placed preferentially in areas with high energy density. However, as high energy density is generally correlated with a high population density, many reasons can impede the realization of a district heating/cooling network in a given area, such as:

- A congested underground, due to the presence of other infrastructures such as fresh water pipes, sewers, natural gas pipelines, underground power or telecommunication lines.
- The presence in the area of important public transportation facilities that would be too difficult/costly to re-route or interrupt during the construction of the network.
- A re-routing of the road traffic during the construction that would be too difficult.

All these constraints could be released, if a more compact form of network could be built. Smaller cross sections would give more freedom to lay the network between the other underground infrastructures. It would also reduce the footprint and the time duration of the construction, which translates into smaller perturbations of the road and public transportation traffic as well as reduced costs. Among the proposed networks, the water variant is the least favourable from the point of view of the compactness. The primary reason is the low energy density that results from the small enthalpy difference between the two lines. The resulting large mass flowrate of water to be transferred in the network combined with the restriction on the maximum velocity in the pipes leads to large pipe diameters. The second reason is the necessity to bury the pipe deep enough to prevent the water inside them from freezing, should a section of the network be disabled for long enough in winter time. Note that thanks to the low temperature differential between the water and the ground surrounding the network, the amount of insulation required is small in comparison to the one used in more conventional networks operating at higher temperatures. Typically for Geneva, the minimum freeze safe depth is 90 cm above the top of the pipes. For pipes directly buried in the ground, as

opposed to those put into utility tunnel, a minimum depth is also required to avoid excessive loading on the pipes for instance from heavy vehicles. Minimum depth of 1.2 m above the top of the pipes is required to withstand the mechanical load imposed by bridge-class SLW60 vehicles for DN600 - DN1000 pre-insulated pipes. [102, 103]. Hence, in the present case, the depth of the trench is constrained by the necessity to withstand the design load caused by the road traffic. At Fig. 1.47 - part B, is represented the cross section for the cold water network discussed in this study, for a network branch directly buried in a road used by heavy vehicles. The shaded area shows the minimum size of the excavation according to [103].

In the present study the temperature of the cold water network and the temperature difference between the hot and cold water lines have been selected in order to maximize the profit after 40 years of operation. The result from that process was that the optimum temperature difference between the lines was almost at its maximum bound (See Fig. 1.38), therefore there isn't much room to increase the compactness as long as free cooling is considered for air conditioning and the cooling of data centres. However, if vapour compression chillers were used instead, the temperature difference between the lines could be further increased. Obviously, the penalty in term of exergy efficiency would be costly and a significant extra investment for the cooling substations would have to be borne, because of the switching from free cooling systems to water cooled chillers.

In the case of refrigerant networks buried under roads, either using CO<sub>2</sub>, R1234yf and R1234ze, one can expect a greater compactness thanks to the smaller diameter of both lines for CO<sub>2</sub>, but only the liquid line for the HFO based networks. Furthermore, the problem of the depth of burial with refrigerant networks is not constrained by the necessity to avoid freezing but only by the mechanical design load, assumed to be SLW 60 vehicles [102]. If it is assumed that double wall pipes are required for refrigerant networks a minimum depth on top of the pipes of 0.9 m is required [104]. At Fig. 1.47 - part A, are represented the cross sections for the three types of refrigerant discussed in this study and for a network branch directly buried in a road used by heavy vehicles. The shaded area show the minimum size of the excavations according to [104]. Although the R1234yf and R1234ze networks have already been declared impractical, they are nevertheless represented for didactic reasons, as it clearly shows the advantage in term of compactness of using a fluid at a high reduced pressure (CO<sub>2</sub>), in order to profit from its high density in vapour phase and its ability to tolerate larger pressure drops. Note that on Fig. 1.47 all the cross-sections are represented at the same scale. The greater compactness of the refrigerant based variants is obvious. When compared to the cold water network, in term of excavation work, the volume of material to be processed is smaller of 42%, 48% and 63% for the R1234ze, R1234yf and CO<sub>2</sub> network respectively. Such reductions have several advantages, such as reduced costs, easier logistic, shorter duration and reduced impact on the direct environment. Compared to the water network, the trench's width is also significantly reduced by 39%, 43% and 50% for the R1234ze, R1234yf and CO<sub>2</sub> network respectively. Widths of less than 2 m are especially advantageous in large roads since only one lane will be disabled during the construction, thus preventing a total disruption in the traffic.

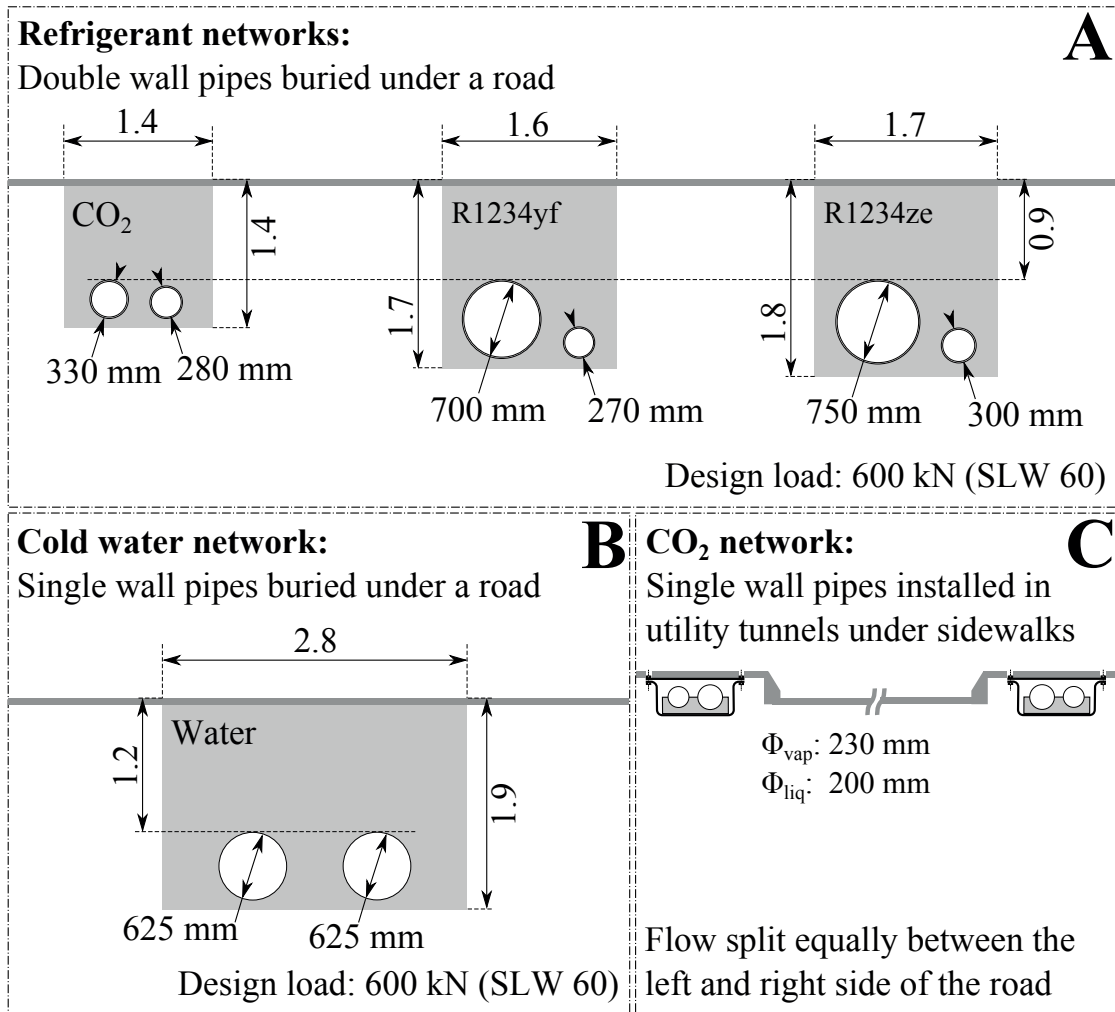


Figure 1.47 – Scale representation of the cross-section of the different networks discussed in this study. Part A: CO<sub>2</sub>, R1234yf and R1234ze networks using double wall pipes that are buried under a heavy traffic road. Part B: Cold water network using single wall pipes that are buried under a heavy traffic road. Part C: CO<sub>2</sub> network using single wall pipes, installed in utility tunnels under the pavement on both sides of a road. In Part A and B, the light gray rectangles show the approximate size of the excavation required, for part C the excavation required is assumed to correspond to the space required by the two utility tunnels.

A further leap in compactness could come from installing the pipes on both side of a road inside small utility tunnels buried right under the pavement, as it is shown at Fig. 1.47 - part C. In this concept, the design load could be reduced, as only in exceptional circumstances high external loading would apply. It also has the advantage of allowing easier inspection and maintenance work, with a possibility of continuing operation on the leg located the other side of the road. The tunnels would have to be designed such as to include the necessary safety measures defined through the MAO procedure (See description at 1.6.3) and those required by standards and regulations. The comparison of the cross sections of the trenches is



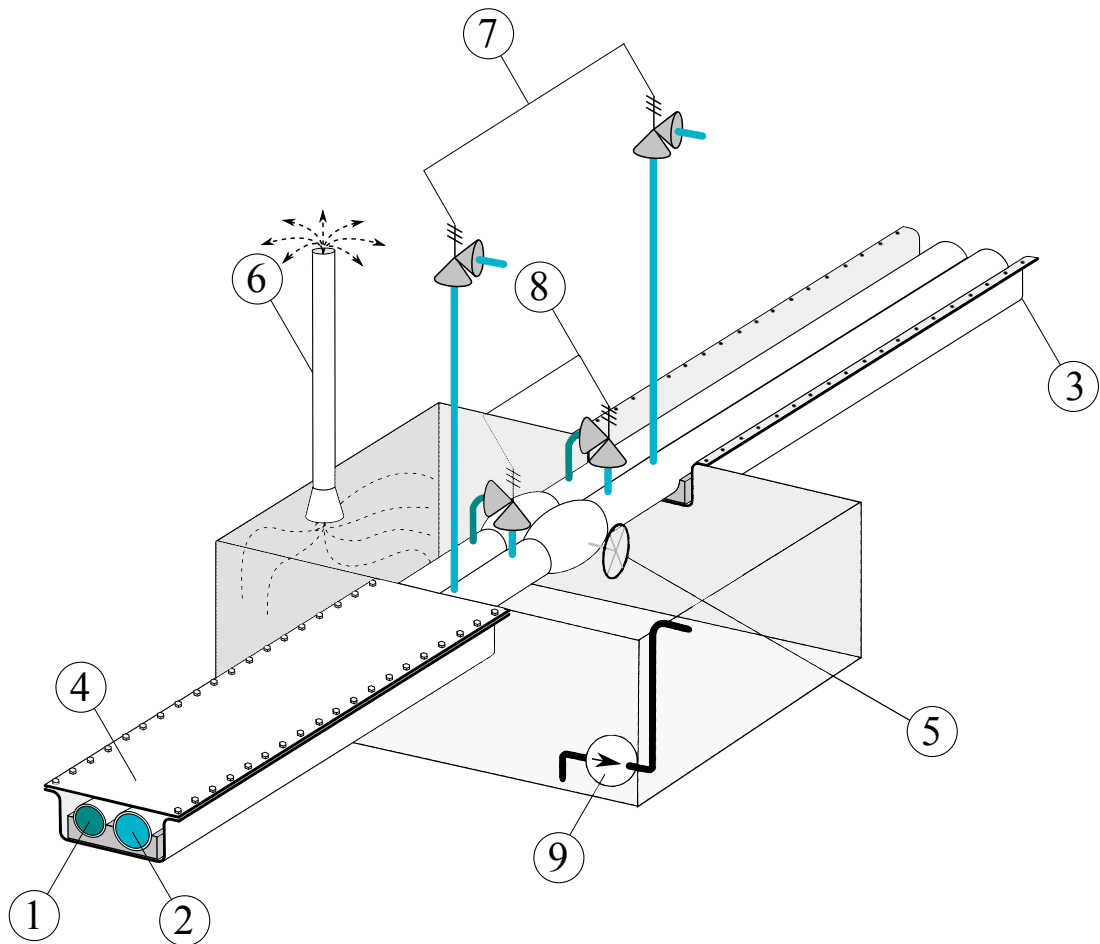
meaningful but some additional aspects need to be discussed. For all the refrigerant networks some elements will have to be installed along the network in technical rooms that typically will take more space than the cross sections presented at Fig. 1.47. These rooms will serve as accommodation for the sectioning valves and safety valves. They could also include extractor fans, possibly controlled by a gas detector, to ensure that small leaks of refrigerant would be collected and discharged in a controlled fashion. Water pumps might also be needed to ensure that rain water leaked in the tunnels and ending into the rooms would be evacuated to the outside. The technical rooms required along both proposed refrigerant networks decrease their gain in compactness compared to cold water network. However, this gain is still significant, and the location of the technical rooms will be flexible (within a certain limit) allowing them to be placed where their size matters less. Fig. 1.48 provides a representation of a possible implementation of refrigerant network. It is a configuration with both pipes installed in “surface” utility tunnels. As discussed earlier, other configurations can be imagined, like networks with single/double wall pipes directly buried under a road or networks with liquid and vapour pipes installed in separate utility tunnels. With the current state of knowledge, it is still impossible to determine which configuration is to be preferred. The question of the choice of the proper configuration should however be addressed with a cost-benefit analysis under the constraints imposed by applicable regulations and standards, especially regarding safety. Some site dependency effects are likely to play a role too, as for example the amount of available space in the roads or local laws and regulations as for example the EPA and MAO in Switzerland.

However, it can already be stated that a clever design of the pipelines and substations of the network will ultimately be the key to the future development of CO<sub>2</sub> based district energy networks. For instance, to try to adapt a pipeline layout from a standard district heating network and figure out the safety question afterwards would likely be the least intelligent and most failure prone way to proceed. It would be much more productive to include safety requirements from the beginning in the design process, to fulfil them in the simplest possible way, with adequate safety margins and avoiding as much as possible single points of failure. Finally the design should focus on exploiting the key advantages of a CO<sub>2</sub> based network, that are: its compactness and its potential to be routed where there is no other underground network.

### 1.8.2 Availability of the equipment

The various pieces of equipment required for a successful implementation are in general commercially available for both the CO<sub>2</sub> and the cold water network. In terms of availability of components, the CO<sub>2</sub> network is more critical as the number of pieces of equipment compatible with this fluid is relatively small, mostly because of the high operating pressure. However, as CO<sub>2</sub> becomes a more widely used refrigerant, mostly for commercial refrigeration plant [105, 106, 107], the number of components on the market tends to increase. Mainly two components remain problematic, the condenser-evaporator at the cold source of the decentralized heat pumps and the CO<sub>2</sub> condensate pump connected to it. At the time of





- |   |                   |   |                           |
|---|-------------------|---|---------------------------|
| ① | Liquid pipe       | ⑥ | Extractor fan             |
| ② | Vapour pipe       | ⑦ | Vapour pipe safety valves |
| ③ | Utility tunnel    | ⑧ | Liquid pipe safety valve  |
| ④ | Bolted lid        | ⑨ | Water extraction pump     |
| ⑤ | Sectioning valves |   |                           |

Figure 1.48 – Possible implementation of a refrigerant network in a “surface” utility tunnel and with a typical technical room accommodating network’s sectioning valves and other safety devices.

writing, commercially available heat pumps do not have heat exchangers strong enough to withstand the pressure on the CO<sub>2</sub> side. However the modification required is relatively minute and should not prove too cumbersome. A second possibility would be to use an intermediate water loop connecting an off-the-shelf water-water heat pump to a CO<sub>2</sub> condenser on the network. Though in principle very simple, this solution causes a significant penalty in term of energy efficiency, the COP<sub>h</sub> of the heat pump being degraded by the lower temperature of

evaporation imposed by the intermediate water loop. Moreover it involves purchasing and putting together a CO<sub>2</sub> condenser, a condensate pump, a water circulation pump and the necessary water pipes which renders this solution likely to be at least as expensive as fitting the heat pump directly with a condenser-evaporator. Regarding CO<sub>2</sub> condensate pumps, their availability is limited, at the time of writing, one manufacturer proposes a range of CO<sub>2</sub> compatible, multi-stage centrifugal canned pumps that could be used for heat pumps with a capacity at the cold source of up to 200 kW<sub>th</sub> [108]. A higher cooling capacity would require either a custom built pump, or installing several existing models in parallel. Other manufacturers [109, 110] propose CO<sub>2</sub> compatible triplex pumps, but these are not hermetic<sup>42</sup> and they are far from being maintenance free [111].

In the present study, heat pumps used for domestic hot water production have been assumed to use another working fluid than CO<sub>2</sub>. From an energy performance point of view, the use of a transcritical CO<sub>2</sub> heat pump would be beneficial, because of the lower exergy loss in the heat transfer between the supercritical cooling of CO<sub>2</sub> and domestic hot water. The evaporator could also be removed, the vapour being directly taken by the compressor from the vapour line, and the liquid directly sent to the liquid line after the expansion valve. Considering the area used as a test case in this study, the gain in performance would be minute as domestic hot water represents only a small fraction of the energy demand. However in some particular cases such as hotels, hospitals or elderly homes, the development of such "open cycle" transcritical heat pumps should be considered. Domestic hot water heater using transcritical CO<sub>2</sub> cycles have been used in Japan for more than a decade, and over 3 mio units had been delivered in 2011. It would also be possible to change the heat exchanger at the cold source, such that it can accommodate CO<sub>2</sub> from the network on one side and CO<sub>2</sub> from the heat pump on the other. This solution has the advantage of preventing the migration of the compressor's lubricating oil into the network. However, in the same time it is likely to cause a slight drop in efficiency. Regarding the cold water network, there is no issue regarding the availability of components, all of them being already off-the-shelf pieces of equipment. The availability of a very large number of similar equipment is a significant advantage of the cold water over the CO<sub>2</sub> network, as it avoids being exposed to suppliers benefiting from a monopolistic situation.

### 1.9 Conclusion from the thermo-economic analysis

In this chapter, a thermo-economic analysis was carried out in order to compare thoroughly different energy conversion technologies for the supply of heating and cooling services to an urban area in Geneva, Switzerland.

The urban area considered - known as "Rues Basses", roughly 1 km long and 200 m wide is located on the shore of lake Geneva, at its junction point with the Rhône river. The affectation of the buildings is mixed with roughly 23% of the heated floor being commercial, 60% office and 17% residential buildings. Initially chosen for the availability of data on it, the area chosen is nevertheless relatively characteristic of urban centres in Switzerland as well as of cities in other

---

<sup>42</sup>They are driven externally by an electric motor, therefore there is a shaft seal where leaks occur.

## 1.9. Conclusion from the thermoeconomic analysis

---

north-western european countries. Five thermal energy services were considered as being used in this area, space heating, domestic hot water preparation, air conditioning, commercial refrigeration and the cooling of data centres. The area was separated in 32 building blocks, using the energy reference area and the affectation, the energy demand for each service in each block was computed based on an energy signature model.

A verification of the prediction of the model was done for the services of space heating and hot water preparation. It showed that, although slightly underestimating the energy demand, the model had a sufficient accuracy for the purpose of this study. The total annual heat demand predicted by the model for the entire area is 53.1 GWh, and the cooling demand is 49.4 GWh. The peak of heating occurs in February, when the design load of 19.2 MW is reached due to a cold snap in the year 2012 used as a reference in this study. The cooling peak occurs in august at a load of 33.0 MW, which is significantly lower than the design cooling load of 44.0 MW.

A thermoeconomic analysis was then carried out on seven different energy conversion technologies considered as options for the supply of the thermal energy services in the test case area. One, consisting in a combination of oil fired boilers and air cooled electrically driven chillers was considered representative of the conversion technologies currently used in that area. Five were refrigerant based networks in which the evaporation/condensing of fluid is used to transfer heat across the network. The first three were based on CO<sub>2</sub>, one relied on HFO R1234yf and the last one on HFO R1234ze. Finally, a concept of network similar to the refrigerant based ones but using liquid water instead was added to the comparison.

The comparison of the systems consisted in five steps:

- An energy/exergy analysis
- An evaluation of the investment
- A profitability analysis
- An evaluation of the economic robustness to changing economic conditions
- A qualitative assessment of safety and technical issues

In the energy comparison, several energy conversion technologies have been defined and modelled in order to evaluate their energy performance. A particular emphasis was put on modelling the key components, based on their expected importance in the total energy consumption of the technologies. These components have been selected on the basis of their applicability within the context of the test area, in particular on their characteristic range of application. Care was taken in modelling these components to have a realistic evaluation of the primary energy consumption. It was aimed at representing each technology with the same degree of precision and avoid as much as possible bias in favour of one technology or another. The energy consumption of all the variants of network is very significantly reduced

as compared to the currently used technologies. If any of the proposed networks were used instead of the current combination of boilers and chillers, the final energy consumption would be reduced from a total of 66.42 GWh of heating oil and electricity, to less than 12 GWh of electricity only. In fact the figure is comprised between 9.91 and 11.66 GWh or in relative terms between 82.4% and 85.1% of reduction, depending on the type of network. However, as these numbers show, the difference in electricity consumption between the networks is not large enough to determine the most promising candidates.

Likewise, the emissions of greenhouse gases would be reduced significantly, even considering CO<sub>2</sub> emissions from the generation of the electricity from the grid. The figure is a reduction comprised between 69.0% and 73.7% depending on the type of network.

An exergy analysis, based on a control volume method showed consistent results in term of reduction of exergy loss and increased efficiency for all the variants of networks. The results were also consistent when compared to those of the energy analysis. It also gave a good insight on what are the major contributors to the improved performances over the currently used boilers and chillers. It results that the general use of heat pumping for the heating services is the main source of improvement. It is followed by the replacement of compression chillers by free cooling systems. Finally, the recovery of waste heat, for the mix of services studied, contributes only to a limited extent in improving the exergy performance.

The evaluation of the investment required to purchase the various pieces of equipment was done, whenever possible, on the basis of cost functions derived from catalogue prices. For the equipment for which catalogue prices were not available, cost functions from the literature have been used. Care was also taken not to extrapolate from cost functions, and as a result several equipment put in parallel were considered whenever the total size required exceeded the largest piece in the dataset from which the cost function was derived. It appeared from that evaluation that had all the currently used boilers and chillers to be replaced at once. The investment required to pursue with the same technologies would be 54.4 mio € while if one of the proposed networks was used instead, the investment to build it would range between 32.0 and 41.2 mio €. The major saving linked to the networks is the change from air cooled chillers to free cooling systems. Part of the difference is offset by the cost for constructing the pipelines, central plant and heating substations at the users. In terms of investment, the cheapest network is the CO<sub>2</sub> network with an open cycle CO<sub>2</sub> heat pump at the central plant, while the most expensive is the cold water network, that needs bigger pipes and a more expensive central plant.

Subsequently, a profitability analysis based on the net present value as a performance indicator was carried out and showed that, for the economic framework conditions used, the conventional technologies of boilers and chillers are only marginally profitable over the 40 years lifespan considered. Conversely, all the proposed networks show good economic performances. The payback times were shown to be comprised between 4 and 6 years and the profit generated after 40 years are comprised between 75 mio € for the cold water network and 90

## 1.9. Conclusion from the thermoeconomic analysis

---

mio € for networks using CO<sub>2</sub>, R1234yf or R1234ze as a transfer fluid and having an open cycle heat pump at the central plant. All these values are expressed in present value. It is interesting to compare these figures to the initial investment required of 41 mio € and 32 mio € for the cold water and the cheapest CO<sub>2</sub> network respectively.

In the economic analysis the cost of the various fluids were not taken into account. However a computation was carried out subsequently and although the cost of the fluid proved to be relatively negligible for the CO<sub>2</sub> networks, it appeared that at the current prices R1234yf and R1234ze networks suffer a penalty in term of profitability that renders them unsound from an economic point of view. Moreover, these two fluids being synthetic, there is a degree of risk regarding the availability of these fluids in the future, mostly because in the long run there is a non-zero probability of regulatory ratcheting towards these fluids. As a result, and in spite of their better energy performance, the versions of refrigerant network using R1234yf and R1234ze as transfer fluids can be declared as not interesting from a practical standpoint.

Regarding the three types of CO<sub>2</sub> network and based on the analysis of the repartition between investment related and operation related costs it appears that the most promising variant is the one equipped with a CO<sub>2</sub> open cycle heat pump at the central plant, indeed the lower electricity consumption of the two other CO<sub>2</sub> networks equipped with an ammonia and a R1234yf heat pump respectively, cannot compensate for the extra investment required. Since it was too difficult to compute a realistic cost for the safety measures that will be required for the refrigerant based networks, it was not included in their economic models. However, the value of the maximum investment that can be spent on safety before refrigerant networks become less profitable than their cold water counterpart was computed. It resulted that the margin in term of profit of the cheapest version of the CO<sub>2</sub> network over the cold water network, would allow up to 8 mio € investment in safety at year 0, 5.59 mio € at year 15 and 3.91 mio € at year 30, all in present value, before becoming less profitable than the cold water option. In comparison to the initial investment originally computed, it corresponds to a relatively comfortable margin of 25% available for absorbing the extra cost of safety.

As a result of the profitability analysis, and having considered the question of the cost and the availability of the fluid in the future. It appears that the most promising candidates are the cold water network, essentially because its simplicity and ruggedness compensate for the slightly lower economic performance and, for its economic potential, the CO<sub>2</sub> network equipped with an open cycle CO<sub>2</sub> heat pump at the central plant. Note that both networks present very similar annual electricity consumption at 11.49 and 11.66 GWh respectively.

The economic robustness of the boilers and chillers, the remaining CO<sub>2</sub> network and the cold water network was evaluated based on a stochastic process based simulation. The principle was to vary economic parameters using probability distribution function derived from historic statistical data. Those parameters included inflation rates (electricity, heating oil, equipment and manpower), the cost of the various pieces of equipment and the reduction of the energy services delivered. The latter one being an attempt to account for the effect of an improvement of the envelope of buildings over the years. For each technology, the simulation was repeated

100'000 times in order to draw a probabilistic evolution of the NPV for the three technologies over a period 40 years long. The result confirmed the economic benefit of the network based technologies. Indeed, under the assumptions of the current stochastic models, a combination of boilers and air cooled chillers has a 64% probability of being not profitable after 40 years, at the proposed initial price of  $0.108 \text{ € kWh}^{-1}$  for the energy services delivered. In comparison, when put in the same economic conditions, the soundness of the two network based technologies is not questionable. Indeed, only 14, respectively 375, of the 100'000 repetitions have led to a net loss after 40 years for the CO<sub>2</sub> and cold water network respectively. Moreover, these probabilities of economic benefit are reached in spite of the reduction in the energy services delivered over the years. One can conclude from the robustness analysis that both the CO<sub>2</sub> network equipped with an open cycle CO<sub>2</sub> heat pump at the central plant, and the cold water network are economically robust technologies for the supply of thermal energy services in dense urban areas, and that they make much more sense economically than the currently used boilers and air cooled chillers.

The last part of the comparison dealt with technical particularities of the CO<sub>2</sub> and cold water network, mostly in terms of potential for a higher compactness of the CO<sub>2</sub> network but also regarding the issue in terms of equipment readily available, where CO<sub>2</sub> is plagued by a scarce offer when compared to what is available for the cold water network.

Eventually it can be concluded that the two advanced networks discussed in this study that present the greatest potential are a CO<sub>2</sub> network equipped with an open cycle CO<sub>2</sub> heat pump at the central plant and a cold water network, sometimes referred to as an anergy network. Both will reach very similar efficiencies, around 40% annual exergy efficiency, as they've been conceived with the same thermodynamic objective in mind. This value should be compared to the 8% exergy efficiency of the currently used boilers and air cooled chillers. Both systems are very likely to be successful economic enterprises, as they've shown to be economically robust, both in absolute terms and relatively to the boilers and chillers. The CO<sub>2</sub> network appears however to have more potential in term of economic profit over its lifetime, provided that the extra cost for safety measures stay below 20 - 25% of the initial investment. It also appears that there is some potential to exploit the higher compactness of the CO<sub>2</sub> network in an innovative layout, that could prove valuable if properly developed, and would definitely render the CO<sub>2</sub> an interesting candidate in energy dense urban areas. Ultimately it appears that choosing between cold water and CO<sub>2</sub> boils down to balancing risks and opportunities.

## 2 Experimental facility and test campaign

### 2.1 Design process

The need to provide a proof of concept of CO<sub>2</sub> based district energy networks was identified as early as December 2010 and the design process of an experimental facility capable of providing such a demonstration really started in September 2011. Regarding the timeline, it is worth mentioning that, the definition of the configuration of the test facility was done prior to the thermoeconomic analysis presented in the previous chapter had been carried out. Luckily however, this analysis pointed out that, if a refrigerant network were to be built in the near future, it should use CO<sub>2</sub> as a transfer fluid, and that in comparison to a cold water network, there is a potential for a more compact network exhibiting better economic performances with a similar energy efficiency.

The initial statement of the objectives that the experimental demonstration was to fulfil is the following:

*"The working principles of a CO<sub>2</sub> district energy network should be demonstrated using a lab scale experimental facility."*

In order to provide a proof of concept, several requirements emerged:

- 1: Practical feasibility** The feasibility of the concept will be demonstrated by designing and building the facility using only existing and commercially available components.
- 2: Scalable results** The scalability of the results will be taken care of by selecting the size of the components maximum one order of magnitude smaller than what they would be in a real life pilot network.
- 3: Representative components** The transferability of the results will be ensured by selecting as much as possible technologies for the components comparable to what they would be in a real life pilot network.



## Chapter 2. Experimental facility and test campaign

---

- 4: Automation level** The transferability of the results will be ensured by relying on a comparable level of automation to what they would be in a real life pilot network.
- 5: Control schemes** The feasibility of the control will be demonstrated using standard control schemes representative of the HVAC industry.
- 6: Operating envelope** The envelope within which the network is practically controllable will be surveyed. It involves operating the system over the entire range of pressure, heating load, cooling load and superheat in the vapour line.
- 7: Hydro-acoustic effects** The extent of hydro-acoustic phenomena will be demonstrated through tests. Particularly the possible occurrence of liquid hammer in normal and abnormal operating conditions will be looked after. Ultimately it should answer the question about liquid hammers and whether they pose a threat to the reliable and safe operation of a CO<sub>2</sub> network.
- 8: Automated mode switch** The central plant of the test facility will be designed such as to switch from net cooling (summer) to net heating operation (winter) and reversely in a fully automated fashion, in order to demonstrate one of the key functionalities needed in a CO<sub>2</sub> network.
- 9: Safety standard** The level of safety and the type of safety measures implemented will be representative of what is required in HVAC systems of similar size and type.
- 10: Network sectioning** Automated sectioning valves will be installed on the pipelines, as these are very likely to be required in a real life pilot network.
- 11: Instrumentation** The instrumentation of the test facility should allow for a sufficient monitoring and data extraction from the test facility, with the aim of capturing the necessary trends. Accurate performance monitoring is not the prime focus.

For reasons external to the author's competence<sup>1</sup> the experimental facility had to be installed at one of the industrial partners. It had the advantage of allowing to use directly the building's heating and cooling hydronics, with no restriction on the capacity. Another consequence was that the test bench had to be fully certified (obtain the CE marking). It is also important to note that from the beginning it was not considered to build a CO<sub>2</sub> heat pump at the central plant, first because no suitable, commercially available, CO<sub>2</sub> compressors could be found and second the technology (semi-hermetic pistons) would anyway have been unlike what is envisaged for a real life network.

After iteration the following design specifications were issued:

---

<sup>1</sup>The building at EPFL that could have housed the facility was being reconstructed.



Table 2.1 – Design specifications for the cooling users, heating users and central plant of the lab scale experimental CO<sub>2</sub> network.

<b>General Specifications</b>	
Total number of users	4
- of which are far from the central plant	2
- of which are close to the central plant	2
Network length (central plant - "far end" users)	100 m
Supply temperature from the hot source	40 °C
Supply temperature from the cold source	8 °C
CO <sub>2</sub> saturation temperature	13 °C
	2 heating / 2 cooling
	1 heating / 1 cooling
	1 heating / 1 cooling
	Requirement N° 2
	sizing value, below the lowest temperature of the building's heating system
	sizing value, average value for the building's cooling water
	sizing value
<b>Safety limits</b>	
Minimum operating pressure	40.6 bar
Maximum operating pressure in the liquid line	64 bar
Setpoint of vapour line's safety valves	60.5 bar
Setpoint of pressure switches	40.6 bar
CO <sub>2</sub> concentration triggering the alarm	5000 ppm
	Saturation of CO <sub>2</sub> at 6°C, the coldest value for the cooling water
	Limit imposed by the casing of the CO <sub>2</sub> pump [108]
	liquid line limit minus the liquid line safety valves opening $\Delta P$
	Below the electricity is cut off, triggering the closure of sectioning valves
	Also ventilation "on" and closure of sectioning valves triggered
<b>Cooling user substation (CO<sub>2</sub> evaporation)</b>	
Minimum approach of temperature	3 K
Evaporator superheat	3 K
Design heat rate	13 kW
Design CO <sub>2</sub> mass flow	67 g s <sup>-1</sup>
Design hot source massflow	130 g s <sup>-1</sup>
	sizing value
	sizing value
	smallest plate HEX for CO <sub>2</sub> from AlfaLaval [112]
<b>Heating user substation (CO<sub>2</sub> condensation)</b>	
Minimum approach of temperature	2 K
CO <sub>2</sub> superheat at condenser inlet	3 K
Design cooling rate	13 kW
Design CO <sub>2</sub> mass flow	67 g s <sup>-1</sup>
Design cold source massflow	1037 g s <sup>-1</sup>
	sizing value
	sizing value
	same capacity as for cooling users
<b>Central plant (CO<sub>2</sub> evaporation and condensation)</b>	
Sizing condition	Cooling mode
Sizing capacity	26 kW
Minimum approach of temperature	2 K
CO <sub>2</sub> superheat at condenser inlet	3 K
Design CO <sub>2</sub> mass flow	134 g s <sup>-1</sup>
Design cold source massflow	2074 g s <sup>-1</sup>
Sizing pressure differential between liq. and vap. lines	2 bar
	LMTD in cooling mode is lower than in heating mode.
	Two cooling users operating at design capacity
	sizing value
	sizing value
	Value compatible with the CO <sub>2</sub> pump from [108]

## Chapter 2. Experimental facility and test campaign

---

From the beginning the system was designed with modularity in mind. The experiment was to be carried out in two phases. Using a two steps approach leaves the possibility to modify the design of the systems of the second phase to take into account the experience gained with the first phase of the experimental campaign. It is a way to limit the risk and improve the research outcome and cost effectiveness.

The first phase implied constructing, a central plant already equipped to work in both cooling and heating mode, 100 m of network "squeezed" in a 4 X 2 X 2 m volume<sup>2</sup>, and a cooling user installed at the other end of the network. With this primary phase, requirements 1-5, 7, 9, 10 and 11 could be fulfilled, requirement 6 could be partially fulfilled, as the envelope in net heating mode cannot be surveyed. Requirement 8 could not be fulfilled, as the switching from net heating to the cooling mode and reversely cannot be tested as no heating user's substation is connected yet.

Phase two, would have consisted in building and connecting one more cooling users and two heating users substation, possibly consisting of water-water heat pumps with the evaporator replaced by condenser-evaporator. It would have allowed completion of requirements 6 and 8, and the implementation of real heat pumps would have added credit to the demonstration. For time, financial and project management reasons however, this second phase could not be realized.

The process flow diagram of the test bench in its current form is provided at Fig. 2.1. It represents the system in its state of april 2015, when the test campaign with the "phase-one" layout was over. The main CO<sub>2</sub> loop is clearly visible. The vapour and liquid side are represented with two different color. Thinner lines of the same colour than the CO<sub>2</sub> main lines represent pipe sections that are filled with CO<sub>2</sub> liquid, respectively vapour, having auxiliary roles. In normal operation there is no flow through these sections. They comprise bypass lines for the CO<sub>2</sub> pumps, connecting lines for potential future heating and cooling users, servicing lines used to fill/empty the system and safety lines, that connect the liquid lines to the vapour line and are fitted with a safety pressure release valve (150XX). The supply and return lines of the heating water are shown in two different tones of red, while those of the cooling water are shown in two different tones of blue. The colour orange is used to highlight equipment with a safety functionality and green is reserved for sensors, the letter  $P$ ,  $T$ , and  $\dot{V}$ , denote the type of measurement. For readability reasons, the wiring is not shown.

It can still be mentioned that three types of current are used for the power supply (230 V 1 phase 50 Hz, 400 V 3 phases 50 Hz, 24 V DC) and that the data acquisition and experiment control is done using a National Instruments cRIO system for the hardware, and the LabVIEW suite (2013) for the software part. The use of a cRIO was dictated by the necessity to have a system equipped with its own on-board computer that continues to control and monitor the system in a standby mode when no experiment is being carried out and no operator is present. In particular the automatic start-up functionality was interesting to guarantee that the control will resume after a power outage. Three photographs of the real implementation of the test bench are provided at Fig. 2.2 - 2.4

---

<sup>2</sup>Necessary to make it pass the door of the room it was to be installed in.

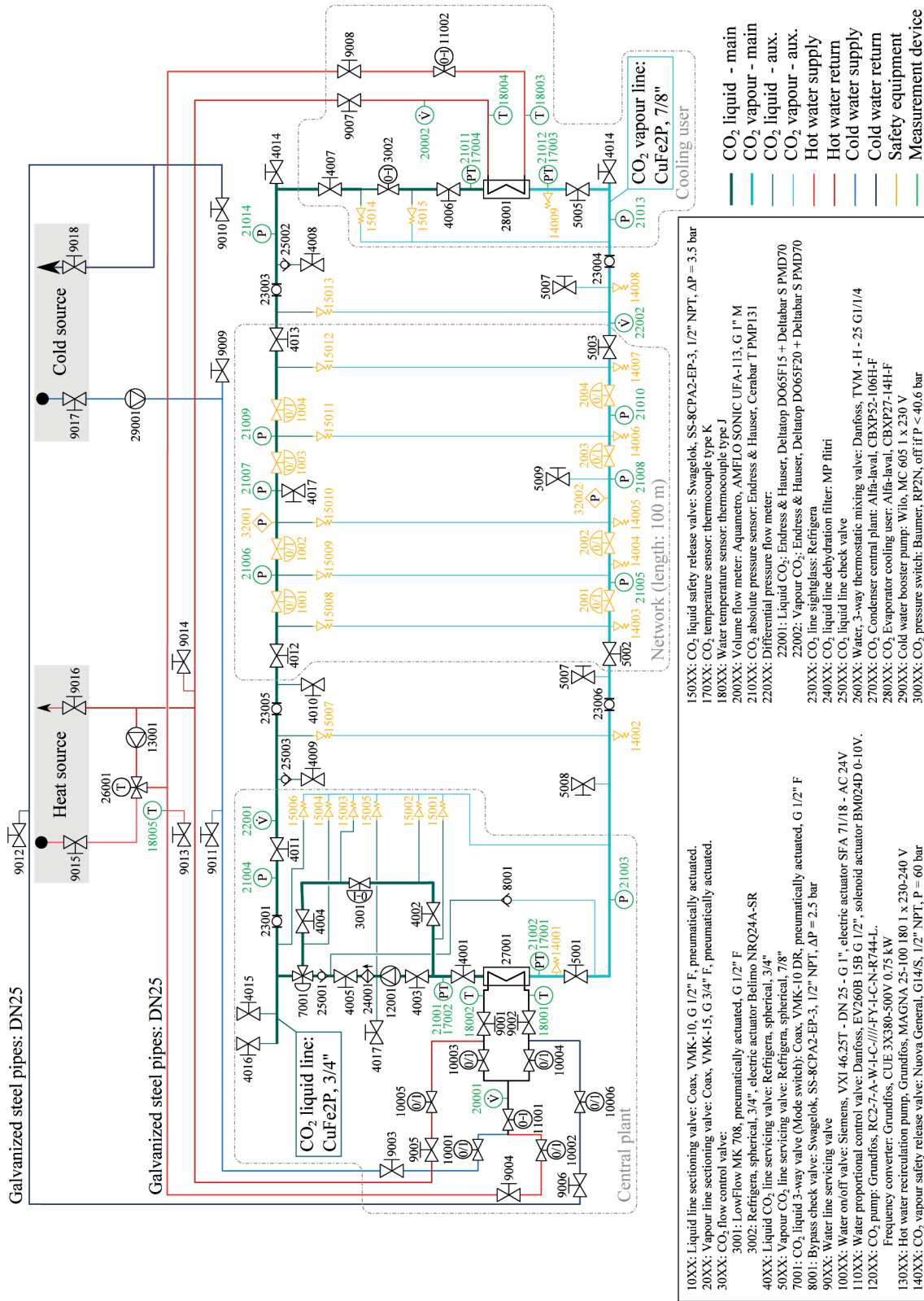


Figure 2.1 – Process flow diagram of the CO<sub>2</sub> network's demonstration experimental facility, the various components are numbered, a list of the components and an explanation of the colour code is provided below the diagram. State: april 2015



Figure 2.2 – View of the test facility on the central plant side.





Figure 2.3 – View of the test facility on the cooling user side.

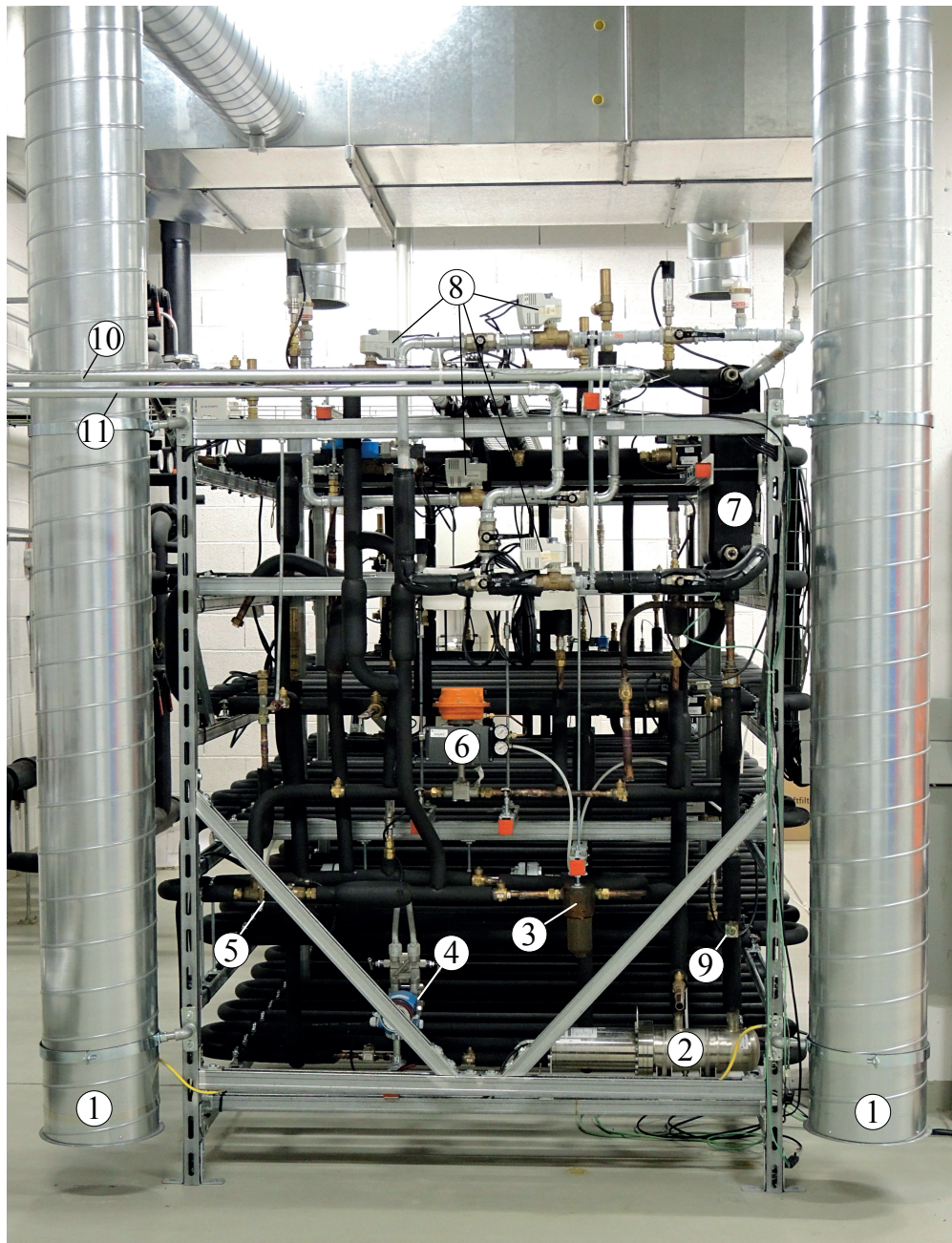
### 2.2 Description of the normal operation

The central plant is connected to both the building's heating and chilled water hydronics, which constitute the heat and cold source of the network. To operate in cooling mode (the only mode for "phase-one") the normally closed valves 10001, 10003 and 10006 are energised, allowing chilled water to flow through the proportional control valve 11001, the ultrasonic flow meter 20001 and the heat exchanger 27001 that in this case works as a condenser. In heating mode the process is the same except that valves 10002, 10004 and 10005 are open and the exchanger works as a CO<sub>2</sub> evaporator, but as said earlier, this mode could not be used. In both cases the opening of the water flow control valve is adjusted automatically in order to stabilize the pressure of the CO<sub>2</sub> vapour at the central plant around a setpoint selected by the operator (based on the reading of sensor 21002).

To accommodate fluctuations in supply temperature from the heat source, which was observed to vary between 55 and 65°C, it was decided to mix water from the return line with that of the supply using the circulation pump 13001 and the thermostatic mixing valve 26001. The temperature sensor 18005 is located just after the mixing valves and helps the operator adjust manually the thermostat to reach the desired heat source temperature. The supply temperature of the chilled water from the cold source varies between 8 and 11°C, which doesn't leave enough "room" to control the supply temperature with a thermostatic mixing valve. It means that the stability of the cold water supply temperature was not as good as that of the heat source. Initially, a pressure differential of 1 bar was thought to be available between the cold source supply and return. It has been estimated to be large enough to feed properly the condenser 27001. It has proven to be wrong as the pressure difference available was only of 0.3 bar and the pressure drops through valve 10001, 11001, 10003 and 10006 had been miscalculated. As a result a booster pump - 29001 - had to be installed just after the cold source supply, it needed to be able to generate a substantial pressure differential estimated to 3 bar at a flowrate of 1.55 kg s<sup>-1</sup> (5.6 m<sup>3</sup> h<sup>-1</sup>) hence the choice of the pump [113]. Although it has proven a sufficient fix to reach all the operating points of the "phase-one" tests, the flow rate obtained are not as high as desired. Consequently additional measures will be needed if future tests are to be conducted at the design load of 26 kW for CO<sub>2</sub> vapour at 50 bar. The best option would be to replace valves 10001, 10003, 10006 and possibly 11001 as well, with ball valves equipped with fast actuators, similar to that of the CO<sub>2</sub> flow control valve 3002 [114]. To characterize cooling/heating water at the central plant, the temperature in and out of the exchanger as well as the volume flow are measured (18001, 18002 and 20001).

The cooling user is also connected to the heat source and receive water at a controlled temperature, typically around 40°C. The flow is controlled by a valve 11002, identical to the one controlling the flow of water at the central plant. The opening of the valve is set by the operator. The flow of water in the evaporator (28001) acts as an external perturbation, much like the flow in the hydronics of a building does on its heating/cooling generator. In fact, to demonstrate one of the features of a CO<sub>2</sub> network, it is important to show that flowrate in the evaporator can be adapted automatically in order to guarantee the complete evaporation and the desired





1: Ventilation (extraction) duct	7: Heat exchanger (27001)
2: CO <sub>2</sub> pump (12001)	8: Water on/off valves (100XX)
3: CO <sub>2</sub> dehydration filter (24001)	9: CO <sub>2</sub> sightglass (23006)
4: Pressure diff. flowmeter (22001)	10: Heat source: supply
5: 3-way valve (7001)	11: Heat source: return
6: CO <sub>2</sub> flow control valve (3001)	

Figure 2.4 – Detailed view of the central with some of the components highlighted. For readability reasons only the most obvious ones are shown.

## Chapter 2. Experimental facility and test campaign

---

amount of superheat, regardless of the flow on the water side. This explains why no closed loop control acts upon valve 11002.

The heat exchange between water and CO<sub>2</sub> causes the latter to evaporate, as mentioned above the flowrate of CO<sub>2</sub> must be adapted to guarantee the full evaporation. The method used to control the evaporation relies on a closed loop control of the superheat at the evaporator outlet. The reading of the pressure sensor 21012 is used to compute the saturation temperature which is then subtracted to the temperature measured by 17003 to obtain a value of the superheat. This value is then fed to a standard implementation of PID controller that generates the signal controlling the opening of the CO<sub>2</sub> valve 3002. Note that it was decided to add the signal generated by the PID controller to a *feed forward* control set by the operator, as for a given opening of the water valve an approximate opening for valve 3002 can be guessed fairly easily. Note that it is a crude way of implementing a *feed forward* in a control loop and although it proved satisfactory for the purpose of the experiment, in a real life application a more sophisticated method should be used to avoid relying on an operator.

To ensure that enough CO<sub>2</sub> is fed to the evaporator (28001) a sufficient pressure differential is needed at the valve 3002. It is achieved by controlling the pressure difference between liquid and vapour lines at the central plant (21004, 21003) via a PI controller acting on the frequency output of the converter that feeds the CO<sub>2</sub> pump 12001. It has been found that a setpoint at 0.7 bar worked adequately. For a few tests at the highest load, the value had to be increased to 0.9 bar in order to have a sufficient CO<sub>2</sub> flowrate to allow reaching the desired superheat.

Almost directly downstream of the evaporator, the CO<sub>2</sub> passes through a volume flowmeter of the pressure differential type (22002). Using the value of the temperature and pressure sensors (17003, 21012) the data acquisition and control system computes the density of the CO<sub>2</sub> vapour, and therefore the mass flowrate of vapour can be computed. Similarly the volume flowrate of liquid leaving the central plant is measured downstream of the CO<sub>2</sub> pump also by a differential pressure flowmeter (22001), the density of the liquid phase is evaluated using the value of the closest temperature and pressure sensors (17002, 21004), and eventually the mass flowrate of liquid CO<sub>2</sub> is computed. This arrangement of two pressure differential flow sensors was designed to track the way the refrigerant was moving and particularly how it accumulated during transients. Once the liquid and vapour flows have passed through the flowmeters, they both travel in the part of the test bench that simulates a section of network 100 m long. As already said, the arrangement of the pipelines needed to be such that the system could be brought in the room. The result can be seen at Fig. 2.3 with both the CO<sub>2</sub> vapour and liquid lines squeezed in three layers, each constituted of approximately 20 u-bends. The three top layers constitute the vapour main line and the three from the bottom the liquid main line. These lines are each equipped with normally closed pneumatically actuated valves (1001-1004, 2001-2004). These valves are part of the safety concept of the test facility. During normal operation they are energized and remain open.

To sum up, for the phase-one experiment, during normal operation, the process is the following:



## 2.2. Description of the normal operation

---

- 1 - Setting the external perturbation to be tested:** The flow and temperature of the hot water supplied to the user are chosen by the operator. These two parameters act as perturbations of the evaporation process occurring in the heat exchanger 28001.
- 2 - Automatic control of the evaporator superheat:** The opening of the CO<sub>2</sub> flow control valve 3002 is automatically adjusted with the help of a PID controller to stabilize the superheat at the evaporator outlet. The setpoint for the superheat is decided upon by the operator<sup>3</sup>. Typically if the measured superheat is smaller than the setpoint, too much CO<sub>2</sub> flows through the evaporator and the controller commands the valve to close. Reversely, when the measured superheat exceeds the setpoint, the controller commands the valve to open wider.
- 3 - Automatic control of the vapour pressure (21002):** The evaporation of CO<sub>2</sub> at the cooling users causes the pressure to rise within the system, since it is almost isochoric and the density of CO<sub>2</sub> in vapour phase is 3.5 - 7.5 times lower than that in liquid phase.<sup>4</sup> To compensate the central plant must condense the same mass of CO<sub>2</sub> vapour than the users produce. If the vapour line pressure rises above the setpoint, it means that more vapour needs to be condensed, hence the PI controller commands valve 11001 to open more. Reversely when the pressure is below the setpoint, the controller commands the valve to close.
- 4 - Automatic control of the pressure differential between liquid and vapour lines:** The evacuation of the condensed CO<sub>2</sub> is done by the CO<sub>2</sub> pump 12001. When the pressure difference between 21004 and 21001 is below the setpoint, a PI controller commands the output frequency of the variable speed drive to increase. Reversely, when the pressure difference decreases the controller commands the frequency to decrease.

The program implemented in LabVIEW, exploits its real-time feature. It has the advantage to guarantee that high priority tasks are carried out at a predefined rate. In the present application the values from the sensors are read and the output signals are generated at a rate defined by the operator, usually 1 s. but possibly down to 200 ms. This rate is guaranteed, which means the time interval between does not fluctuates depending on the computational load on the data acquisition and experiment control computer (cRIO). Non prioritized tasks are for instance, filling the results in a file (for post processing), displaying data on the host computer or reading input changes from that computer. The host computer is a standard laptop on which the operator monitors the systems and from which he can change the various setpoints and parameters. The PI controllers, used to control the vapour line pressure and the pressure differential between liquid and vapour lines are standards blocks available in LabVIEW. They are part of the prioritized tasks. The proportional gain and integral constant

---

<sup>3</sup>The feed-forward value of the valve opening is also entered by the operator, but this element is less crucial.

<sup>4</sup>For the lowest operating pressure of 40.6 bar ( $T_{sat} = 5.9^{\circ}\text{C}$ ) the ratio of the saturated phase densities is 7.55. For the highest operating pressure of 60.5 bar ( $T_{sat} = 22.3^{\circ}\text{C}$ ) the ratio is 3.49. The drastic decrease is linked to the proximity of the critical point. (73.8 bar, 30.98°C)

(reset time) could be found easily by try-and-error. Regarding the PID controller controlling the superheat at the cooling user's evaporator outlet, try-and-error did not lead to satisfactory results. Fortunately a spectral analysis had been performed earlier using a dynamic model of the cooling user's substation. Both the proportional gain and the integral constant predicted appeared to work perfectly. Later during the test campaign the controller type had to be changed from a PI to a PID type. Indeed, at the start of the experimental campaign, the valve 3002 that controls the flow of CO<sub>2</sub> was a solenoid operated valve, controlled by custom made pulse width modulation, the period of modulation could be chosen by the operator. Pulse modulating expansion valves are becoming common in commercial refrigeration, and so it was considered a good idea to apply the same principle. It worked reasonably well until, the solenoid broke down on December 1, 2014. Since the broken coil could not be replaced without disconnecting the valve from the refrigerant network, it had to be done by approved refrigeration personnel. In order to avoid a second breakdown, and especially one that could not be fixed by the operator, it was decided to change for a motorised ball valve, with the motor outside of the pressured loop. Due to some delays, the valve could only be replaced on January 21 and a hysteresis in its operation, combined with the long reaction time of the actuator made the control of the superheat difficult. Eventually, it was decided to change the motor for a 10 times faster one and the situation went back to normal on February 12. The fix did not suppress the hysteresis, but increasing its frequency 10 times reduced sufficiently its influence. However, the initially used PI controller had still some difficulty controlling the superheat. A PID controller was tried and showed better performance. A similar spectral analysis was carried out, this time directly on signals from the test bench instead of a dynamic simulation model and showed that in a relatively narrow frequency band, the derivative term helped.

Finally, a description of the certification procedure and of the resulting safety concept, is provided in the appendix.

### **2.3 Test campaign: Stationary tests and fitting of a heat transfer correlation**

Once operational, the first series of experiment consisted in exploring the test envelope and seeing how the control coped with the different operating conditions. The second goal was to be able to obtain parameters for a simplified correlation for the heat transfer coefficient on the CO<sub>2</sub> side of the heat exchangers. The correlation was to be used in a dynamic simulation model that would replicate the test bench. The existing correlations that could be found for CO<sub>2</sub> in evaporation were not really practical for this kind of simulation [115, 116] and no correlation were found for condensation. The method assumes that the same correlation can be used for evaporation and condensation and has to be simple enough for the parameters to be obtained using the instrumentation available. It also assumes that the heat transfer coefficient on the water side is exactly that predicted by Focke et al. [117] for plate heat exchangers with a corrugation angle of 45°. Obviously as only the temperature, pressure and volume flowrate

### 2.3. Test campaign: Stationary tests and fitting of a heat transfer correlation

in and out of the heat exchangers (27001, 28001) are measured, the resulting heat transfer coefficient for CO<sub>2</sub> is an average value.

A total of 118 stationary points were exploitable and could be used to fit the 5 parameters of the correlation. It is visible at eq. 2.1. The pressure ranged from 48 to 57 bar and the mass velocity<sup>5</sup> from 1.6 to 30.5 kg s<sup>-1</sup> m<sup>-2</sup>. Unfortunately the quality of the fit is not very good as it can be seen at Fig. 2.5 where the histogram of the relative error between the observed coefficient and the one predicted by eq.2.1 is represented. Although this tentative of obtaining a simple correlation for CO<sub>2</sub> in evaporation and condensation was not particularly successful, it was still used in the models because considering the time line there was no better option. The fitting of the correlation however, did highlight an interesting phenomenon occurring with the test bench.

Indeed, on the histogram shown at Fig. 2.5, close to 12% of the data points show a measured heat transfer coefficient around -100% of that predicted by the correlation, meaning essentially that a very low effective heat transfer coefficient is measured.

By examining the dataset the various heat transfer coefficients measured for CO<sub>2</sub> vs. the mass velocity are represented at Fig. 2.6. It appears that all the datapoints with very low measured heat transfer coefficient are related to the condenser. The condenser is much larger than the evaporator, 5.3 m<sup>2</sup> of heat transfer area, 4.95 l of volume on the CO<sub>2</sub> side and an active length of 0.41 m, versus 0.3 m<sup>2</sup>, 0.35 l and 0.19 m. for the evaporator. It results that at low heat rate and/or when the system operates at high pressure, the condenser can be flooded without causing too much problem to the control of the pressure in the network, the cooling water being cold enough and its flowrate high enough to reach the necessary cooling load with only a fraction of the heat transfer area normally available for condensation.

$$\begin{aligned} \alpha_{CO_2} &= \alpha_{ref} \left( \frac{P}{P_{ref}} \right)^\psi \left( \frac{\dot{G}}{\dot{G}_{ref}} \right)^\zeta \quad \forall h < h'' = 1605 \cdot \left( \frac{P}{50.86} \right)^{4.61} \left( \frac{\dot{G}}{3.27} \right)^{0.91} \\ \alpha_{CO_2} &= \kappa \alpha_{ref} \left( \frac{P}{P_{ref}} \right)^\psi \left( \frac{\dot{G}}{\dot{G}_{ref}} \right)^\zeta \quad \forall h \geq h'' = 0.05 \cdot 1605 \cdot \left( \frac{P}{50.86} \right)^{4.61} \left( \frac{\dot{G}}{3.27} \right)^{0.91} \end{aligned} \quad (2.1)$$

To have an idea of the cause of the flooding it is worth discussing the distribution between liquid and vapour volume in the test bench for different operating pressure and at steady state. The installation can be viewed as a closed volume, part of it filled with saturated liquid and the rest with saturated vapour both at the same saturation temperature:

<sup>5</sup>Mass flowrate of the fluid divided by the cross sectional area of the channel it passes through.

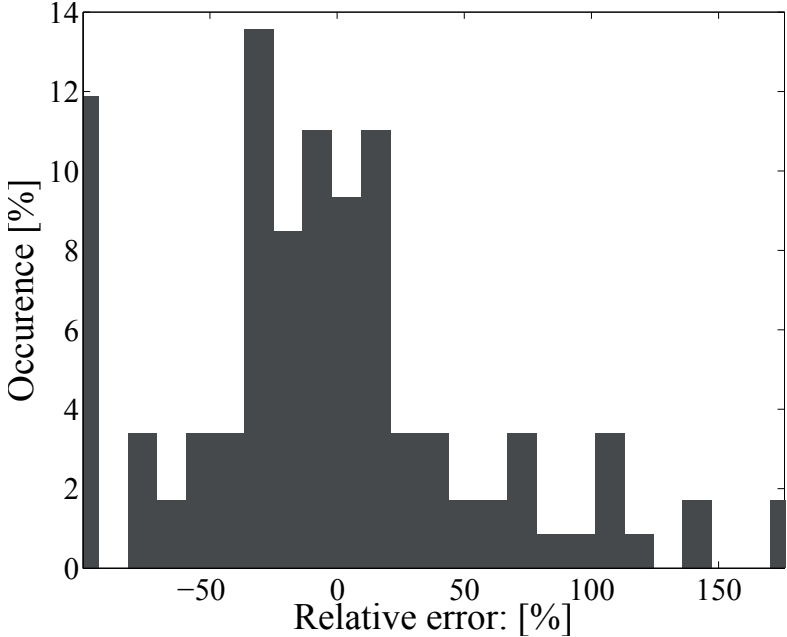


Figure 2.5 – Histogram of the relative error between the observed heat transfer coefficient in CO<sub>2</sub> for evaporation and condensation and the value predicted by the correlation of eq. 2.1.

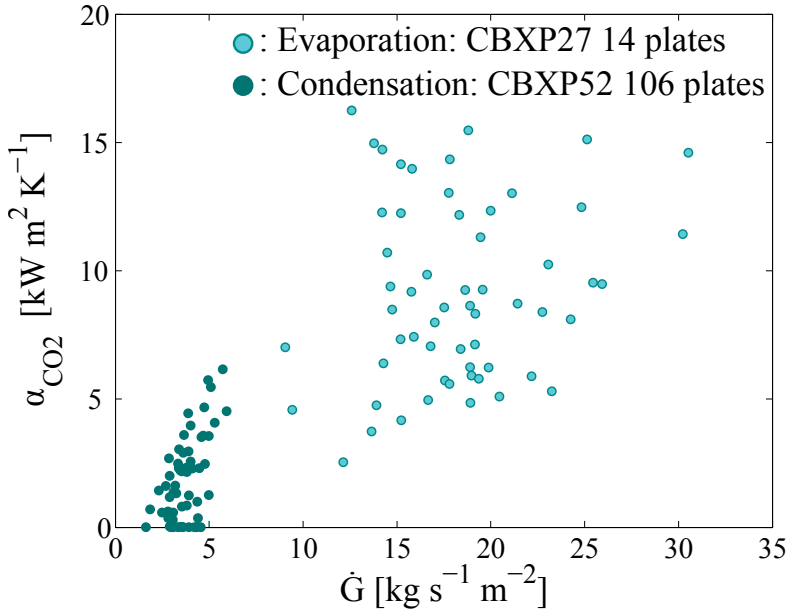


Figure 2.6 – Data point of the measured heat transfer coefficient in the CO<sub>2</sub> as a function of the mass velocity and whether they've been measured at the condenser or the evaporator.

### 2.3. Test campaign: Stationary tests and fitting of a heat transfer correlation

The total mass of CO<sub>2</sub> in the volume is expressed by:

$$M_{CO_2} = (1 - \epsilon(T_{sat})) V \rho_l(T_{sat}) + \epsilon(T_{sat}) V \rho_v(T_{sat}) \quad (2.2)$$

Where  $\epsilon$  is the void fraction<sup>6</sup>,  $\rho_l$  the saturated liquid density and  $\rho_v$  the saturated vapour density. These three parameters depend on the saturation temperature, however, the mass of CO<sub>2</sub> is obviously constant since the system is closed. For the test bench which has a volume of 70 l. if one considers a void fraction of 0.5 at the design saturation temperature of 15°C, the mass of CO<sub>2</sub> contained in the system is 34.4 kg.

Once the mass of CO<sub>2</sub> is known, the void fraction for different saturation temperatures can be calculated as follows:

$$\epsilon(T_{sat}) = \frac{(M_{CO_2}/V) - \rho_l(T_{sat})}{\rho_v(T_{sat}) - \rho_l(T_{sat})} \quad (2.3)$$

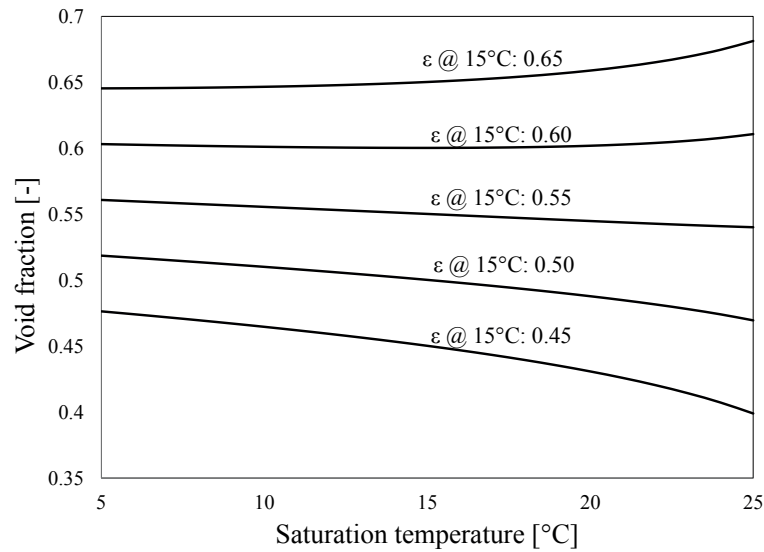


Figure 2.7 – CO<sub>2</sub> average void fraction in the test bench as function of the saturation temperature (network's temperature) and for 5 different void fractions at the design temperature of 15°C.

The result is shown at Fig. 2.7 for CO<sub>2</sub> at  $T_{sat}$  ranging between 5 and 25°C and void fractions at design conditions ( $T_{sat} = 15^\circ\text{C}$ ) comprised between 0.45 and 0.65. It is interesting to notice that for small "design void fractions", the void fraction in the system decreases with increasing saturation temperature, while for the larger "design void fractions" it increases. Normally, since the volume of the vapour line is larger than that of the liquid and based on an average void fraction in the heat exchangers of 0.7, the design void fraction should be 0.59, Which is

<sup>6</sup>Volume filled with vapour divided by total volume

just in the area where the void fraction is almost independent to the saturation temperature. In other words, in this test bench, the distribution of the volume between heat exchangers, liquid and vapour lines more or less minimizes the changes in the respective volume of the liquid and vapour phases, which is very favorable<sup>7</sup> (0.4 l). Therefore it can be concluded that the slight variation in the volume of liquid (around 10% of the CO<sub>2</sub> channels in the condenser), cannot explain the poor performance in terms of heat transfer coefficient observed for certain stationary points. The flooding of the condenser observed is probably linked to dynamic phenomena. Typically, the operators have observed some very slow dynamic phenomena (10 - 20 min). In some of these cases it could be traced back to slow changes in the supply temperature of the chilled water, but not always. In general, it is probable that the operator did not notice them while he was recording measurements. In fact, it is only after the campaign of stationary that the data files were analysed and that the extent of slow fluctuations was really grasped.

Initially the risk of flooding the condenser was to be dealt with by using a refrigerant receiver. A vessel had to be installed at the outlet of the condenser to absorb changes in density of the liquid. However, the consultant in charge of helping with the certification did not recommend it as it would be cumbersome. In the end it appeared to be a misunderstanding between EPFL's team and him and when this was realized, the system was being pressure tested and thus it was too late to modify it.

### **2.4 Test campaign: Assessment of dynamic behaviour and controllability.**

An important part of the tests were dedicated to assess the dynamic behaviour of the test bench, first to determine whether the concept of automatic control used was reliable and second to verify the absence of strange dynamic phenomena that could occur and be a threat to the reliability of a refrigerant based network.

#### **2.4.1 Stationary tests and example of a heat load step reduction.**

Overall, the control scheme allowed an adequate control of the system for most of the stationary points tested. Maintaining the pressure in the network at the desire setpoints being straightforward. An example is provided at Fig. 2.8, where the pressure oscillates around the setpoint with a magnitude of around 0.5 bar. In that case a step change in the opening of the water flow control valve - 11002 was done by the operator at time 3.1 min. It corresponds to a load reduction on the evaporator of roughly 45%. The effect of the load reduction on the control of the pressure is very limited and the only noticeable change is the amplitude of the fluctuations that increases slightly. The only difficulties with control of the pressure appeared for points in the low pressure range (48-50 bar) as sometimes the cold source supply

---

<sup>7</sup>At this stage it is worth mentioning that it happened completely by chance.

## 2.4. Test campaign: Assessment of dynamic behaviour and controllability.

---

temperature was not cold enough, leading to a saturation of the control with valve 11001 fully open. However, the only effect was that the pressure stabilized at a higher than desired level, in fact the lowest possible pressure achievable with the cold source temperature and its flowrate. The control of the superheat at the cooling user was more difficult, but in the majority of cases, stable superheat between 2 and 8°C could be achieved. Problematic fluctuations in superheat occurred mostly at low load, typically for opening of the valve 11002 below 30%. These fluctuations are linked to the hysteresis of valve 3002, that causes the CO<sub>2</sub> to flow through the evaporator intermittently and the relative fluctuations in flowrate increase in intensity at low load. An example of the kind of control achieved for the superheat is shown at Fig. 2.8. In that case the superheat is controlled within 1 K around the setpoint which is satisfactory. Similarly to the control of the pressure, the step change in heat load does not cause a superheat excursion. The evolution of the mass flowrate of CO<sub>2</sub> in the vapour and liquid line are represented at Fig. 2.9 for the same test than Fig. 2.8. The importance of the fluctuations in flowrate are obvious. They are also in phase. An offset between the two signals can be observed, particularly after the load was reduced, and is only the result of measurement errors. For the liquid, the magnitude of the fluctuations increases after the load was reduced and it can be observed that the maxima of the liquid flowrate remain more or less identical at around 85 g s<sup>-1</sup>. This is typical of the hysteresis observed for the CO<sub>2</sub> valve (3002). The hysteresis can be seen at Fig. 2.10 where the PID output signal commanding valve 3002 and the mass flowrates of liquid and vapour are shown for the last 2.5 minutes of the test of Fig. 2.8 and Fig. 2.9. The min. and max. bounds for the output of the PID controller have been limited respectively to 0.17 and 0.6, since in a ball valve an opening of 0.6 leads to almost the same flow coefficient than when fully open and it was observed that an opening below 0.17 would lead to a complete stopping of the flow, leading to large disturbances that proved too much for the controllers implemented to cope with.

The control of the pressure differential between liquid and vapour lines by varying the CO<sub>2</sub> pump frequency gave satisfactory results and an example of the kind of control achieved can be seen on Fig 2.9. Regarding this last control, some improvement needs to be made regarding its starting behaviour, since the ramp up time is very long if the operator does not control the frequency manually when the system is started for the first time of the day. Finally, it is worth noticing that the hysteresis of valve 3002 affects the entire system, as fluctuations with the same period of around 23 s. are observed in all signals.

### 2.4.2 Example of pressure setpoint step change (50-52 bar)

In this subsection the effects of a step change in the setpoint of the pressure PI controller is discussed. In a real CO<sub>2</sub> based district heating and cooling network such sharp changes in pressure setpoint would not be used, but in the context of the experiment step changes allow for a clear view of the effects and they also have the advantage of putting at test the control more intensely. The results of the test are shown at Fig. 2.11, 2.12 and 2.13. First, it can be seen at Fig. 2.11 that the pressure takes 40 seconds to reach the new setpoint. For the rest of the duration of the test, the pressure is maintained at the 52 bar setpoint (within the usual



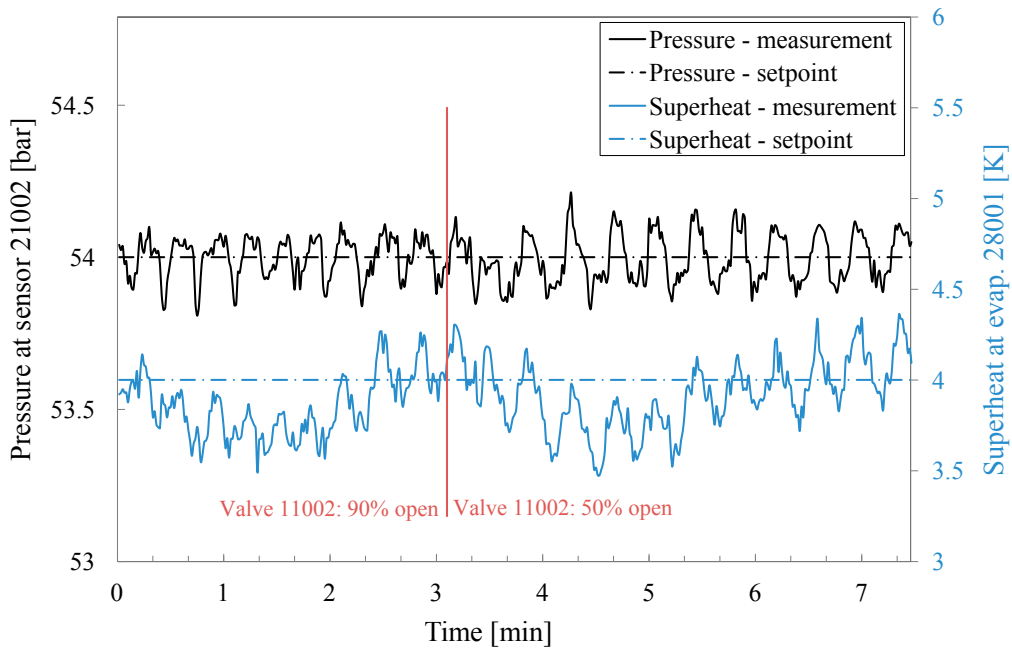


Figure 2.8 – Example of the control achieved on the pressure by acting on the cooling water flow in the condenser (27001) and the control of the superheat at the outlet of the evaporator (28001) by acting on the opening of valve 3002 at the user.

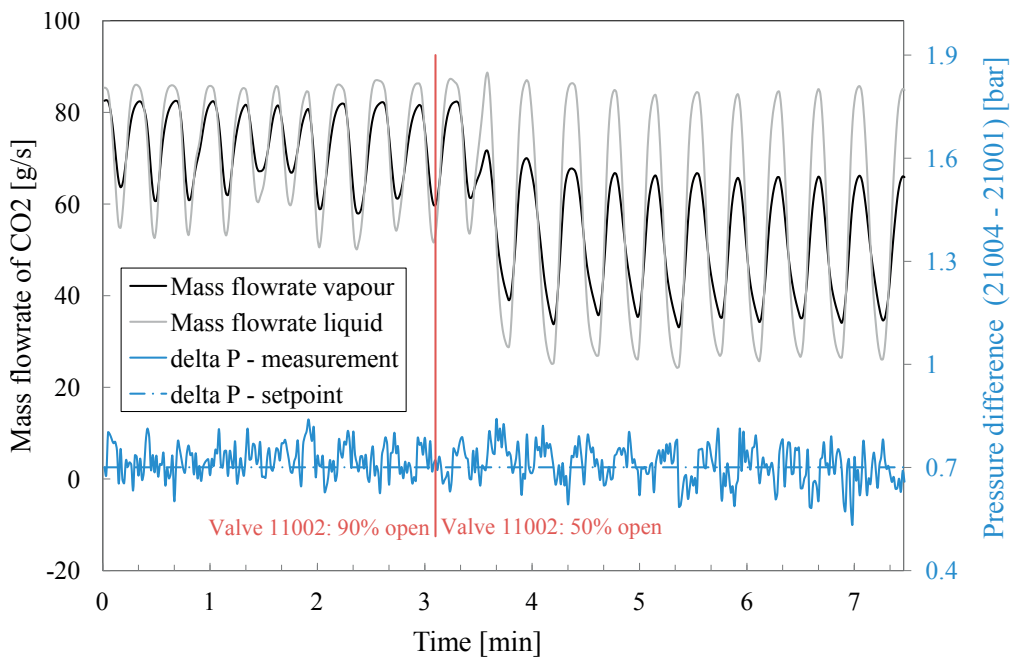


Figure 2.9 – Example of the control achieved on the pressure difference between liquid and vapour lines. The mass flowrates of CO<sub>2</sub>, vapour and liquid, are also shown to highlight their large fluctuations. The results are for the same test than plotted at Fig. 2.8.

## **2.4. Test campaign: Assessment of dynamic behaviour and controllability.**

---

fluctuations). The superheat is much more strongly affected by the the step change, since a large excursion occurs from 45 s. after the step change and lasts for more than 4 min. The excursion in superheat seems to start around when the pressure reaches its new setpoint. Fig. 2.12 shows the control of superheat and that of the pressure difference. Directly after the step change, an excursion of the pressure difference starts. The pressure difference diminishes for around 45 s. which corresponds to the time needed for the pressure to reach its new setpoint. The pressure difference then takes around 4 min to recover the setpoint. The step change in pressure setpoint causes the cooling water valve 11001 to close, as can be seen at Fig. 2.14, which in turn stops the condensation at the central plant. However, the cooling user continues to draw more or less the same amount of fluid from the liquid line than prior to the step change and the CO<sub>2</sub> pump continues pumping condensate into the liquid line to maintain the pressure difference. It results that the condensed CO<sub>2</sub> pumped by 12001 out of 27001 is not replaced since there is no cooling water flow to condense the vapour entering the condenser. Very quickly vapour forms at the pump inlet and the pump becomes unable to generate the required pressure difference. Note that the pump 12001 tended to make more noise and that vapour could be observed through the sightglass installed on the suction line at inlet during the pressure difference excursion. The pump accelerates as shown at Fig. 2.13, attempting to reach back the pressure difference setpoint. However during all the time the pressure difference is below a certain threshold since not enough CO<sub>2</sub> flows through the evaporator, in spite of the CO<sub>2</sub> valve being fully open (Fig. 2.14), which leads to an excursion in superheat.

### **2.4.3 Example of pressure setpoint change, 3 min ramp (50-52 bar)**

As said earlier, a step change in setpoint is probably not going to be used in a real network. Moreover, the step change for the pressure setpoint discussed previously showed that it led to a cascade of perturbation in the control. Although the control architecture has shown that it could ultimately recover and reach the desired operating point in a few minutes, it is still desirable to avoid such situations with large excursion of the controlled variables. A simple way to avoid problems is to use ramps for the setpoint changes. To illustrate the difference, the same change of the pressure setpoint was done (50-52 bar) but following a 3 min. ramp. The results are shown at Fig. 2.15 - 2.18. From Fig. 2.15 it is clear that the pressure remains under control during the ramp an evidence of that is the valve 11001 controlling the cooling water flow that does not fully close (Fig. 2.18). The excursion in superheat is also much reduced compared to what was observed for the step change. At Fig. 2.16 it can be seen that the excursion in pressure difference is also still present and reduced. During all the ramp it can be seen at Fig.2.17 that the mass flowrates fluctuate, indicating that the CO<sub>2</sub> valve (3002) is not fully open hence that the controller is not saturated, as shown at Fig. 2.18. At Fig. 2.17 it can also be seen that the maximum pump frequency reached is not very different to that observed in 2.13, its acceleration at the start of the ramp however is not as fast.

It can be concluded that the use of ramps for setpoint changes are more adapted and should be preferred in a real life application. Moreover, there is no real practical reason for changing the pressure in a real network over periods of less than a few hours, it is likely then that a ramp

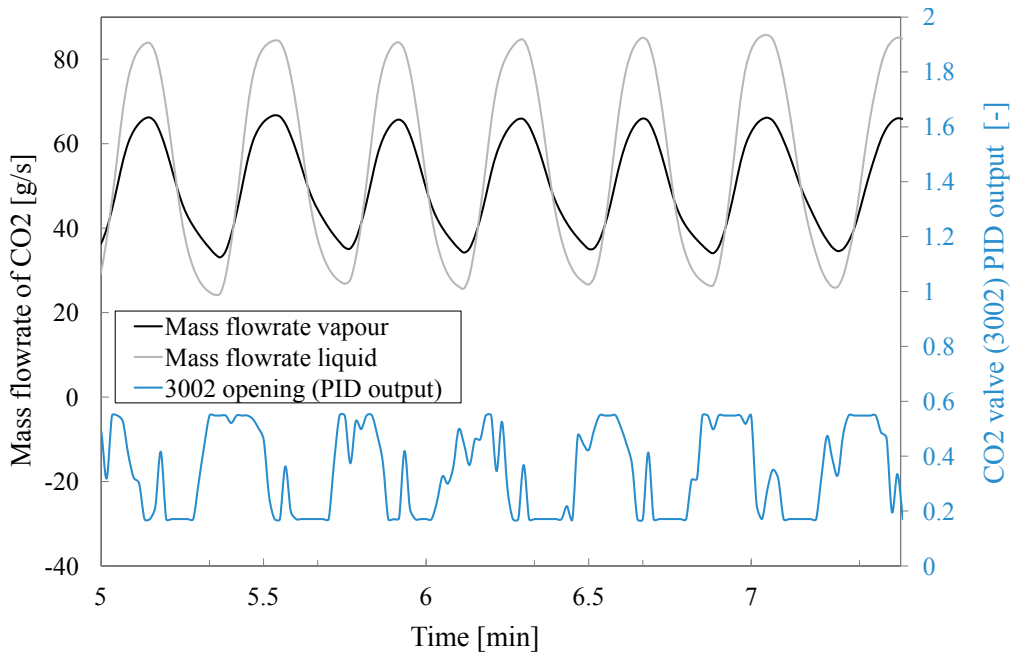


Figure 2.10 – Example of the control output sent by the PID controller to the CO<sub>2</sub> valve 3002 at the user, the mass flowrates of CO<sub>2</sub>, vapour and liquid, are also shown in an attempt to illustrate the hysteresis of valve 3002. The time frame is the last 2.5 minutes of the results plotted at Fig. 2.8 and Fig. 2.9.

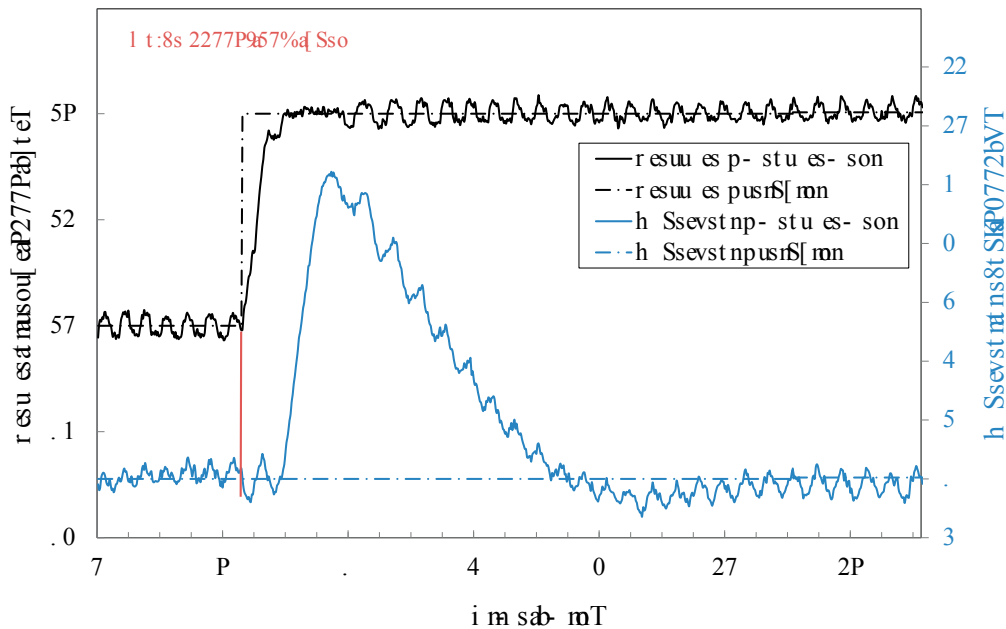


Figure 2.11 – Control achieved on the pressure (21002) and on the superheat at the outlet of the evaporator, after a step change of the pressure setpoint from 50 to 52 bar. The quality of the control of the pressure is obvious, the new setpoint is reached after around 40 s. The control of the superheat is not satisfactory, as a large excursion is observed for a period of almost 5 min. after the step change.

## 2.4. Test campaign: Assessment of dynamic behaviour and controllability.

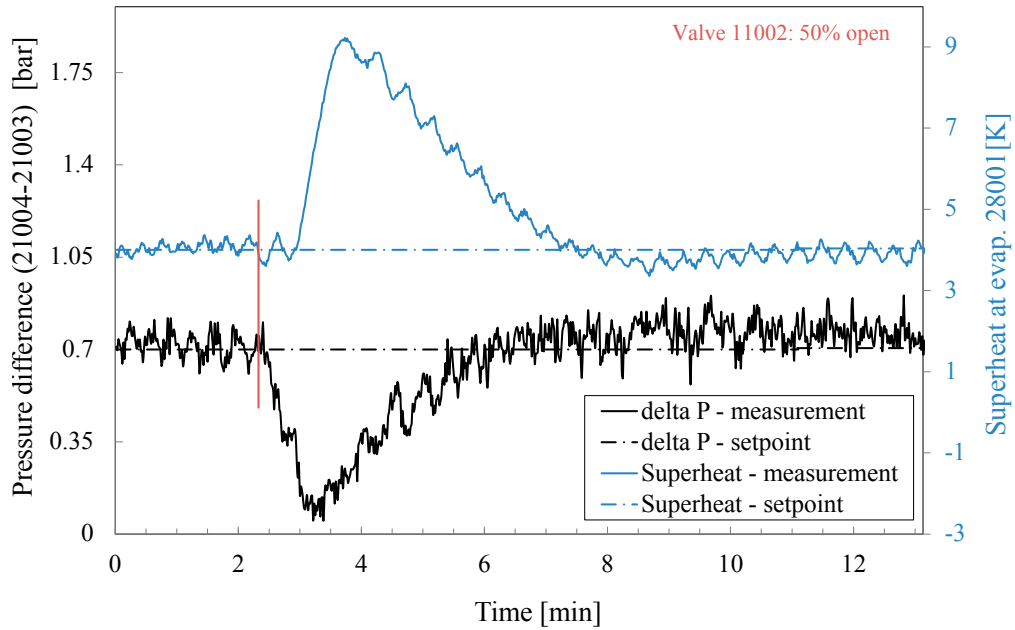


Figure 2.12 – Control achieved on the pressure difference between liquid and vapour line and on the superheat at the outlet of the evaporator, after a step change of the pressure setpoint from 50 to 52 bar. The excursion in superheat is caused by the lack of a sufficient pressure differential between the line starting around when the new pressure setpoint is reached (Fig. 2.11) and it takes from that point around 4 min 10 s, to reach back the desired pressure difference.

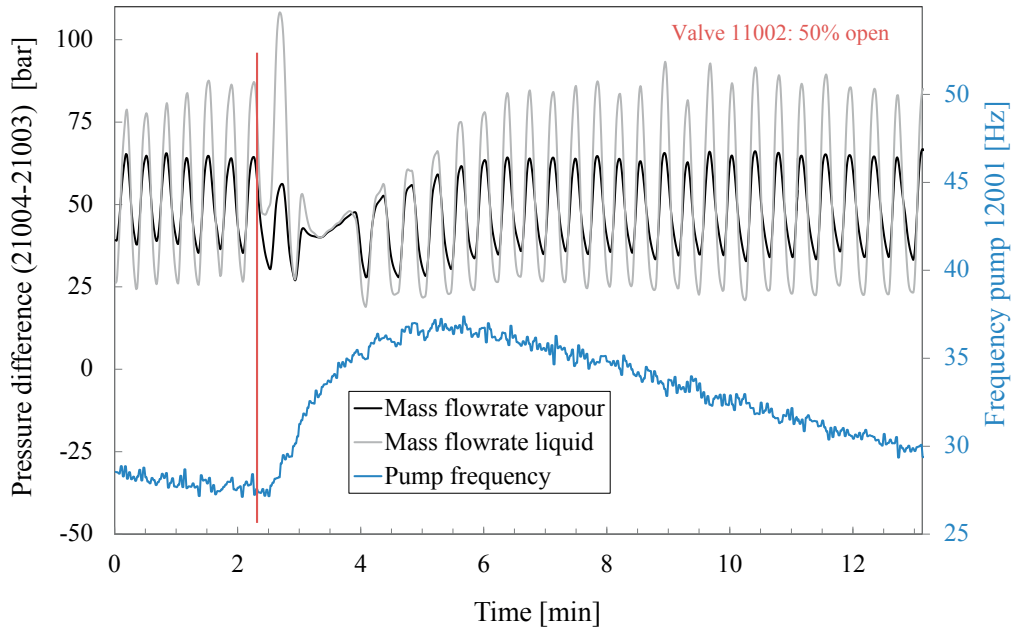


Figure 2.13 – Evolution of CO<sub>2</sub> liquid and vapour line’s mass flowrate and of the rotational frequency of the CO<sub>2</sub> pump 12001, after a step change of the pressure setpoint from 50 to 52 bar. The loss of pressure difference between the lines causes the pump to accelerate until the desired pressure differential is reached back (Fig. 2.12). It then gradually decelerates for the rest of the duration showed. During this deceleration, pressure difference, superheat and pressure all remain at their setpoint value. The liquid mass flowrate shows a spike right after the step change, both liquid and vapour mass flowrates are perturbed for a duration corresponding to the superheat excursion (Fig. 2.11 and Fig. 2.12).

## 2.4. Test campaign: Assessment of dynamic behaviour and controllability.

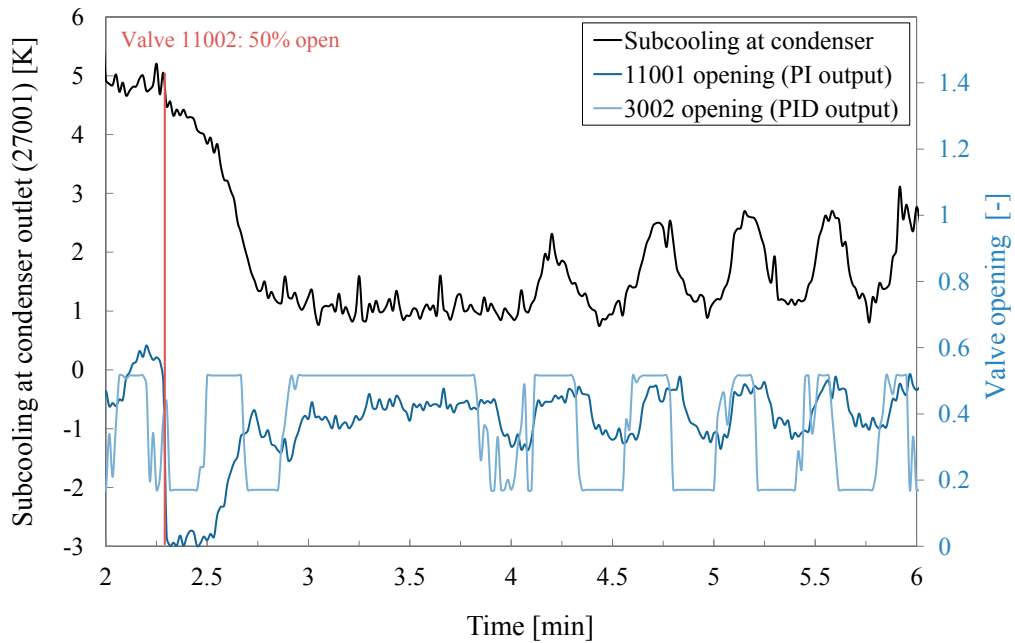


Figure 2.14 – Evolution of the subcooling at the condenser (27001) outlet and evolution of the cooling water valve opening (11001) and CO<sub>2</sub> valve opening (3002), after a step change of the pressure setpoint from 50 to 52 bar. The time period plotted corresponds to that during which the superheat excursion occurs (Fig. 2.11). The diminution of the subcooling is symptomatic of the cooling water flow to the condenser being stopped by valve 11001 in order to induce the pressure increase. A lower subcooling ultimately leads the CO<sub>2</sub> pump (12001) to lose its capacity to generate a sufficient pressure difference (Fig. 2.12) which in turn leads to the flow in the evaporator (28001) to be too low in spite of the CO<sub>2</sub> valve (3002) being fully open, causing ultimately the superheat excursion observed (Fig. 2.11).

this long would be a seamless experience.

### 2.4.4 Example of pressure setpoint downward change, 2 min ramp (58-54 bar)

The upward change in pressure setpoint caused the condenser to empty, which led, by a cascading effect, to a loss in pressure difference between the lines, causing not enough CO<sub>2</sub> to flow through the user's evaporator, finally leading to an excursion in superheat. The effect of a downward pressure setpoint change leads to a slightly different chain of events. The same set of graphs is presented at Fig. 2.19 - 2.22 for a change in pressure setpoint from 58 to 54 bar by following a 2 min. ramp. The striking difference compared to downward and upward pressure ramps, is the appearance of a pressure excursion at the end of the ramp, as can be seen at Fig. 2.19, while the superheat remains controlled for the duration of the ramp. Note that in Fig. 2.19 - 2.22 the start of the ramp is shown by a solid red line and the period during which the pressure excursion occurs is shown by dotted red lines. At Fig. 2.20 it can be observed that, similarly to the superheat, the pressure difference also remains under full control during the ramp. The inability for the system's pressure to follow the prescribed trajectory is due to the flooding of the condenser. Indeed, one can observe that a mass flowrate imbalance occurs between T = 1 min. and T = 2 min. 30 s. with the liquid mass flowrate being lower. A second mass flowrate imbalance occurs between T = 4 min. 15 s and T = 5 min. 30 s. this time with the mass flowrate of liquid being higher than that of the vapour. Another evidence of the condenser filling up with liquid is visible at Fig. 2.22, with the appearance of a large subcooling at the condenser outlet, which is explained by the fact that the liquid already present in the condenser is being cooled down by the high flowrate of cooling water. In fact, once the condenser is filled with liquid, the pressure cannot continue to decrease, which results in the saturation of the pressure controller and the command of the cooling water valve (11001) to remain fully open. To evaluate the level of filling up of the condenser, the integral of mass flowrates or *mass processed* and the difference between the two integrals are shown at Fig. 2.23. It can be observed that up to 1.5 kg of liquid which, accounting for its average density in the condenser, represents around 1.8 l. or 36% of the refrigerant channel volume. It must also be noted that the duration the mass imbalance is observed (in direction of a filling up of the condenser) and the duration the subcooling stays around its maximum value, both correspond quite well to the duration of the pressure excursion observed. It is also important to see that once the pressure recovers it remains at the setpoint (Fig. 2.19), but the pressure difference and the superheat (Fig. 2.20) seem to have a slow excursion toward the end of the test when in fact there seems to be a mass imbalance in the other direction with a similar magnitude of 1.5 kg (Fig. 2.23). Earlier, it was mentioned that slow transients were observed while the system had been in an *observed* steady state. It is quite plausible that mass oscillations caused some of these slow transients. Unfortunately, the test was not conducted over a period long enough to see whether and how these mass oscillations damp out. Toward the end of the test, from around T = 6 min. 30 s. onward, the low subcooling (Fig. 2.22), the reverse sign of the mass imbalance (Fig. 2.23), the reduced pressure difference between the lines and the superheat higher than desired (Fig. 2.20), are all signs of an empty condenser.



2.4. Test campaign: Assessment of dynamic behaviour and controllability.

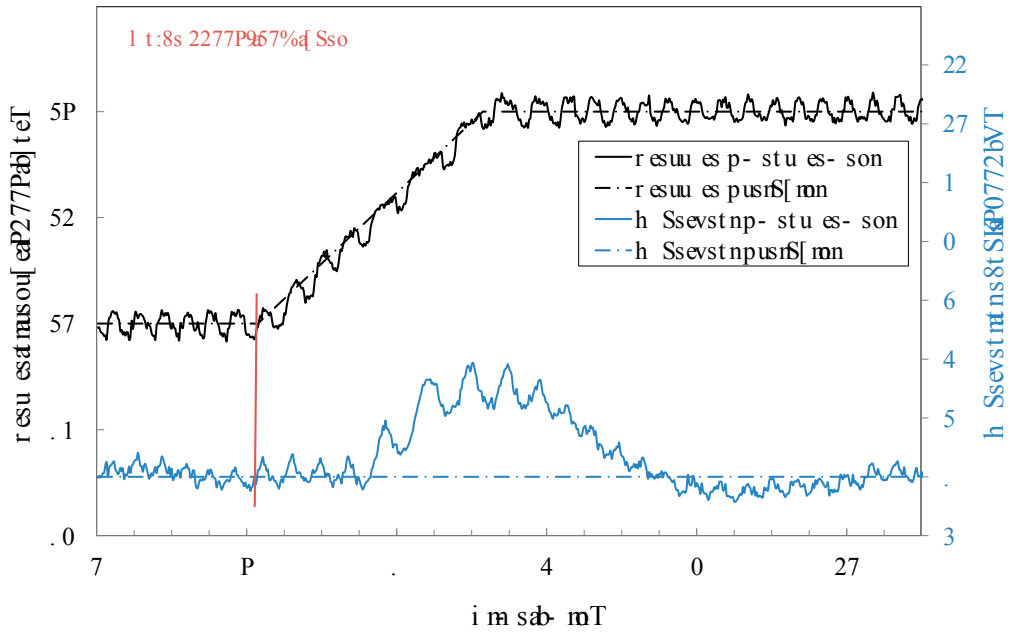


Figure 2.15 – Control achieved on the pressure (21002) and on the superheat at the outlet of the evaporator, after a change of the pressure setpoint from 50 to 52 bar during a 3 min. ramp.

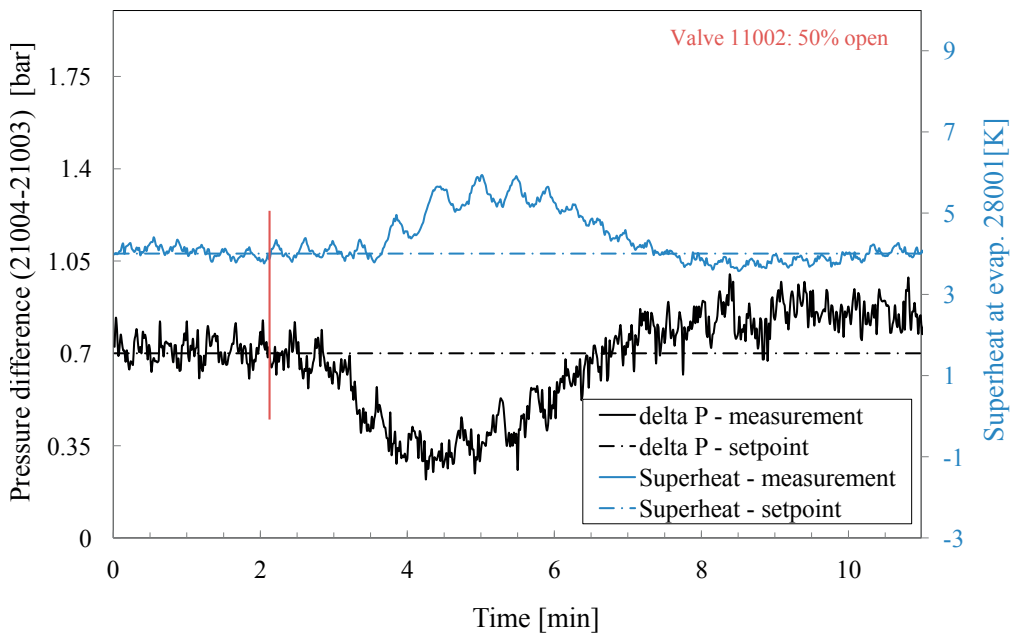


Figure 2.16 – Control achieved on the pressure difference between liquid and vapour line and on the superheat at the outlet of the evaporator, after a change of the pressure setpoint from 50 to 52 bar during a 3 min. ramp.

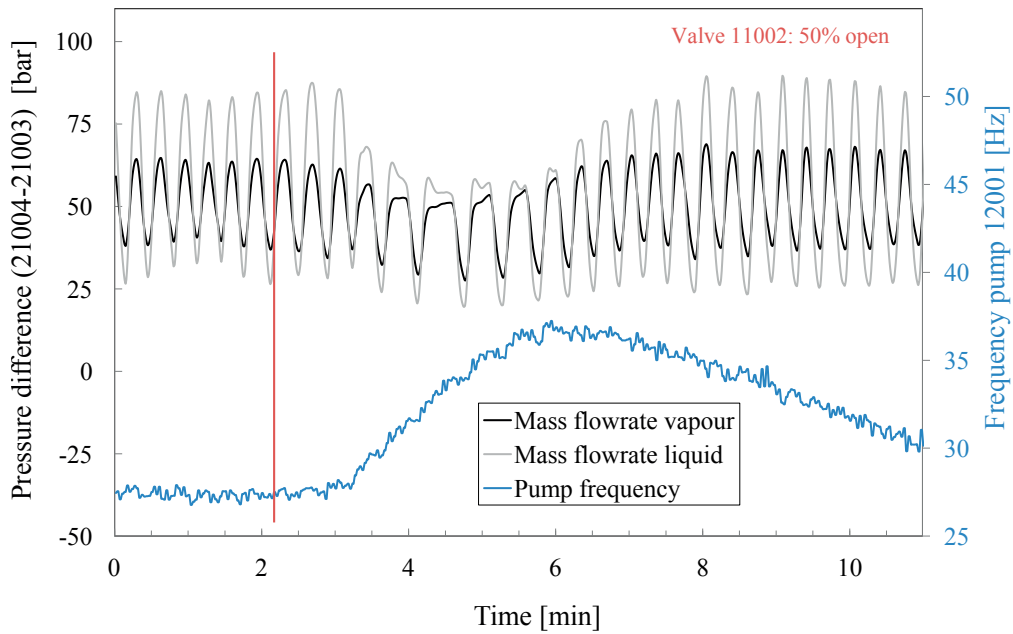


Figure 2.17 – Evolution of CO<sub>2</sub> liquid and vapour line’s mass flowrate and of the rotational frequency of the CO<sub>2</sub> pump 12001, after a change of the pressure setpoint from 50 to 52 bar during a 3 min. ramp.

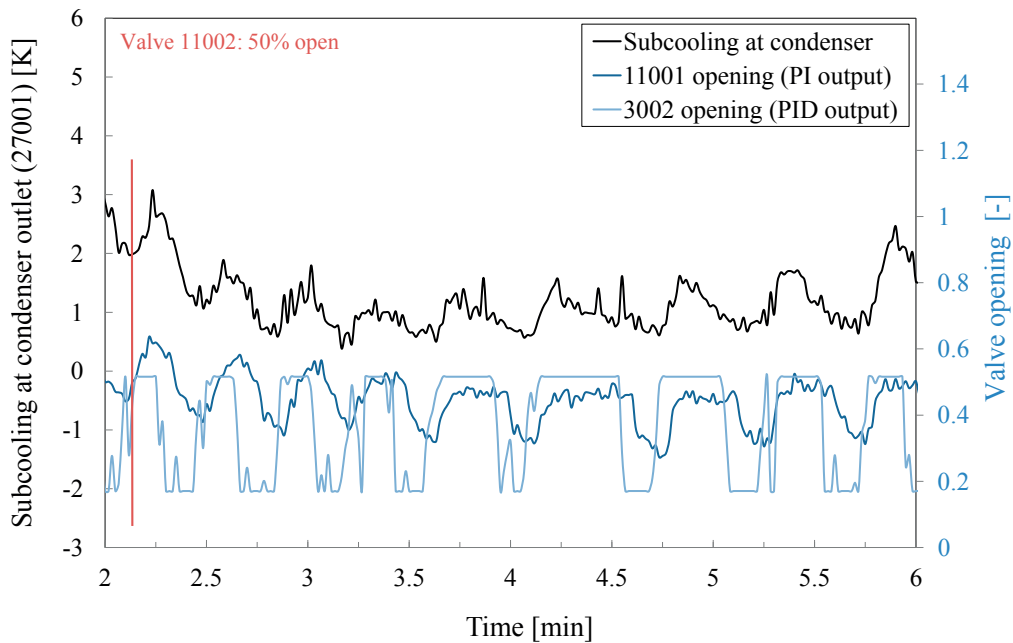


Figure 2.18 – Evolution of the subcooling at the condenser (27001) outlet and evolution of the cooling water valve opening (11001) and CO<sub>2</sub> valve opening (3002), after a change of the pressure setpoint from 50 to 52 bar during a 3 min. ramp.

## 2.4. Test campaign: Assessment of dynamic behaviour and controllability.

Which is further evidence that there is indeed a mass oscillation occurring.

Finally, a remark can be made on the fact when the pressure recovers at around 4 min. 20 s. It first undershoots the setpoint which is typical of a PI controller having been saturated for some time. Note that in that case the saturation causes the integral term to wind up, which was taken care of by applying the standard *Anti Reset Wind-up* [118] measure, but in spite of that the pressure still undershot a bit.

It can be concluded from the dynamic tests that the main source of control inaccuracy is the tendency for the central plant's condenser to flood or dry out. In a full scale system or if the "phase two" of the experiment is realised, adding a receiver tank of a capacity more or less equivalent to the volume of CO<sub>2</sub> in the condenser should be considered. Ideally, in order to have maximum controllability, this receiver tank should be equipped with a liquid level sensor, an auxiliary heating and a piloted valve to discharge excess vapour in the vapour line of the network.

### 2.4.5 On other dynamic tests

One as to mention that during all the test campaign, including the stationary tests, the various operating points have been reached using the control scheme of the installation. Although not necessarily recorded, the list of the transients done to reach these operating points include:

- Step up of the pressure setpoint, that spanned the interval [48 bar, 59 bar].
- Step down of the pressure setpoint, that spanned the interval [59 bar, 48 bar].
- Ramp up of the pressure setpoint, that spanned the interval [48 bar, 59 bar] for variable ramp durations comprised between 1 and 5 min.
- Ramp down of the pressure setpoint, that spanned the interval [59 bar, 48 bar] for variable ramp durations comprised between 1 and 5 min.
- Step up of the opening of the hot water valve at the user (11002), that spanned the interval [0.2, 1].
- Step down of the opening of the hot water valve at the user (11002), that spanned the interval [1, 0.2].
- Ramp up of the opening of the hot water valve at the user (11002), that spanned the interval [0.2, 1] for variable ramp durations comprised between 1 and 5 min.
- Ramp down of the opening of the hot water valve at the user (11002), that spanned the interval [1, 0.2] for variable ramp durations comprised between 1 and 5 min.
- Step up of the superheat setpoint, that spanned the interval [1 K, 8 K].

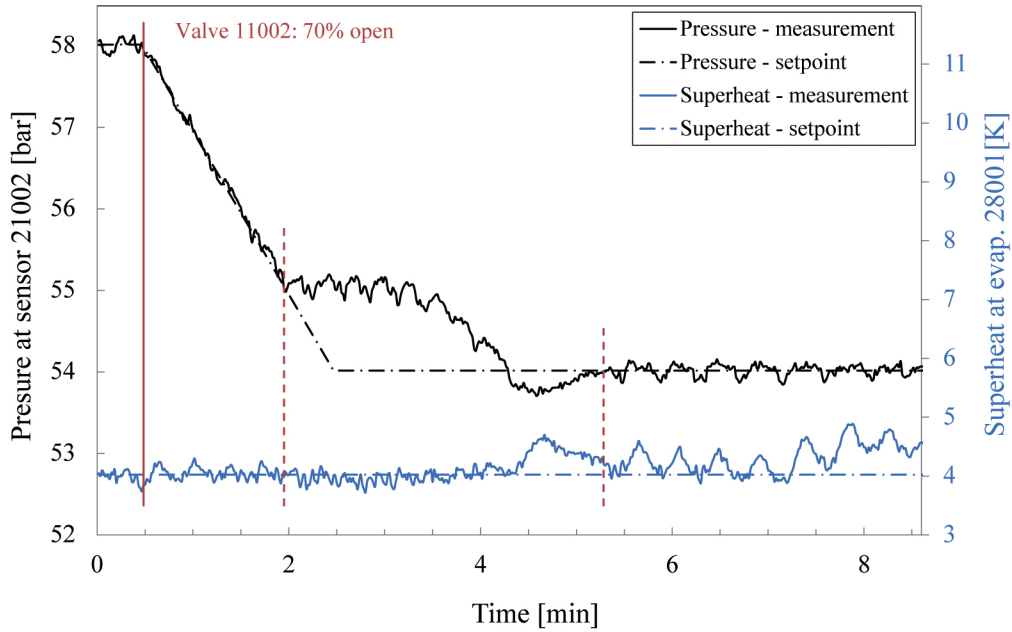


Figure 2.19 – Control achieved on the pressure (21002) and on the superheat at the outlet of the evaporator, after a change of the pressure setpoint from 58 to 54 bar during a 2 min. ramp.

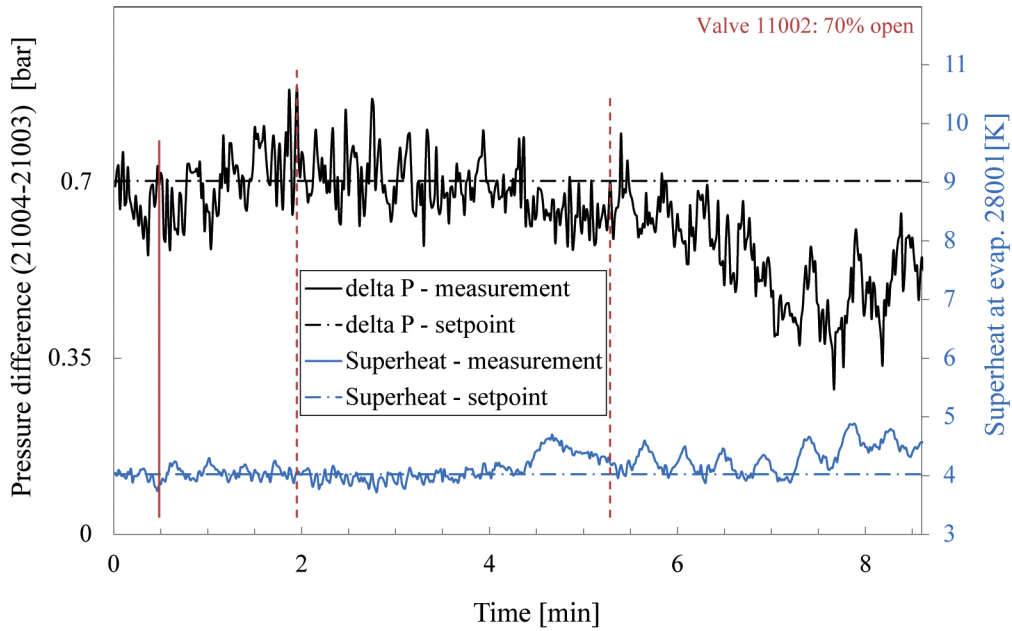


Figure 2.20 – Control achieved on the pressure difference between liquid and vapour line and on the superheat at the outlet of the evaporator, after a change of the pressure setpoint from 58 to 54 bar during a 2 min. ramp.

2.4. Test campaign: Assessment of dynamic behaviour and controllability.

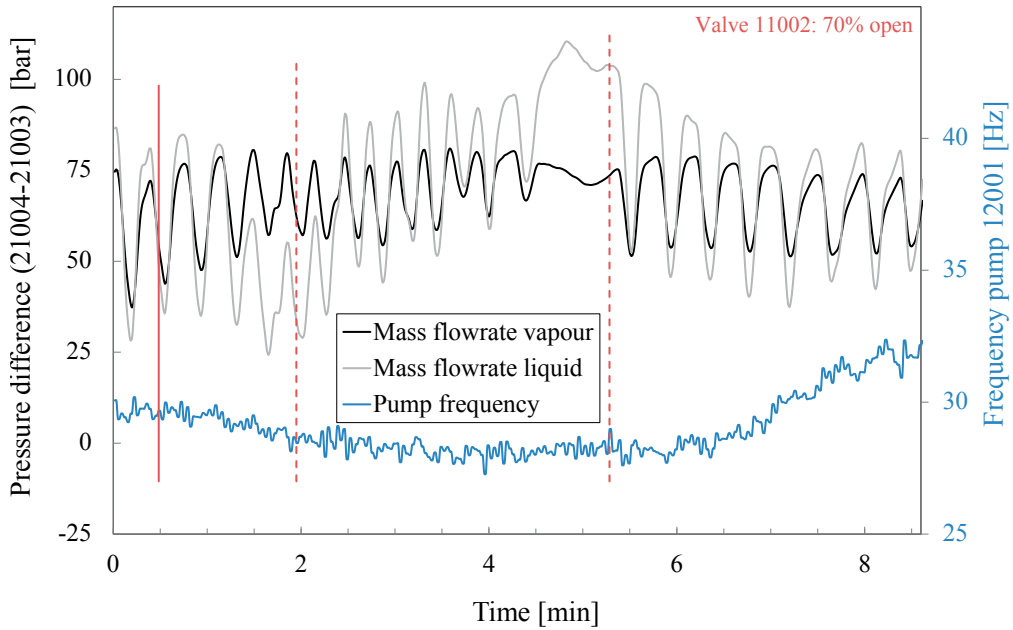


Figure 2.21 – Evolution of CO<sub>2</sub> liquid and vapour line's mass flowrate and of the rotational frequency of the CO<sub>2</sub> pump 12001, after a change of the pressure setpoint from 58 to 54 bar during a 2 min. ramp.

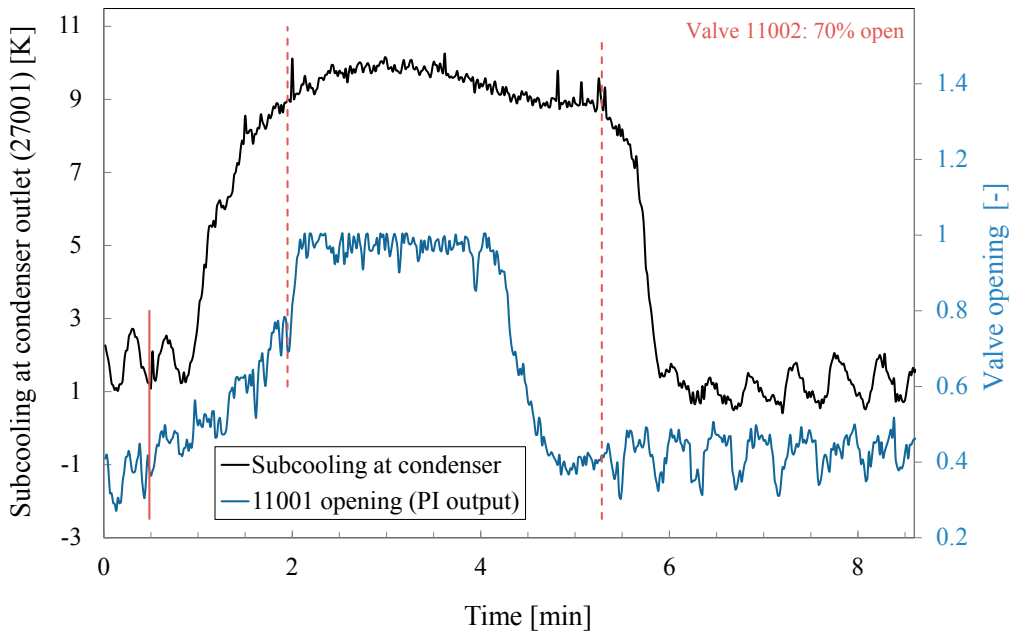


Figure 2.22 – Evolution of the subcooling at the condenser (27001) outlet and evolution of the cooling water valve opening (11001), after a change of the pressure setpoint from 58 to 54 bar during a 2 min. ramp.

- Step down of the superheat setpoint, that spanned the interval [8 K, 1 K].
- Ramp up of the superheat setpoint, that spanned the interval [1 K, 8 K] for variable ramp durations comprised between 1 and 5 min.
- Ramp down of the superheat setpoint, that spanned the interval [8 K, 1 K] for variable ramp durations comprised between 1 and 5 min.

During all these transients the only recurrent action of the operator, was to enter the step/ramp parameters and command the start. In some cases he had to adapt the value of the feed-forward output of the superheat controller and for high load tests, to command a step up of the pressure difference controller from 0.7 to 0.9 bar. The hundreds of transients realized over the 140 hours of tests, carried out in an almost fully automatic way, serve as evidence of the reliability/robustness of the control scheme.

### 2.4.6 Tests assessing the risks linked to hydro-acoustic phenomena

Two tests were conducted to determine whether hydro-acoustic phenomena, essentially under the form of "liquid" and "gas" hammer pose a threat in a CO<sub>2</sub> district network.

The rapid stopping of a fluid in a pipe can cause a series of pressure wave travelling back and forth, in particular when the flow velocity is high and the fluid relatively incompressible. This phenomenon, known as liquid or water hammer, is well known in accumulation hydroelectric schemes, where it puts constraints on the minimum time for the valves to be closed [119] to avoid excessive over and particularly under pressure<sup>8</sup>.

The liquid hammer test consisted in running the test bench at the highest achievable load, by feeding the user with water at the temperature provided by the source (60°C) on the day of the test. It led to a pressure in the network (21002) of 53 bar and a mass flowrate of CO<sub>2</sub> around 140 g s<sup>-1</sup>. The heat rate at the central plant achieved in those conditions was 26.3 kW. After stabilisation, one of the network's sectioning valves (1004) is closed<sup>9</sup>. These conditions were expected to lead to the worst liquid hammer that can be done with the test bench. The result is shown at Fig. 2.24. The positive pressure spike observed is characteristic of a liquid hammer as the start of the pressure spike starts 0.2 s later for 21007 than for 21009, 0.4 s. later 21006 and 0.6 s. for 21004. This is consistent with the fact that 21007, 21006 and 21004 are located around 33 m, 67 m and 100 m upstream of 21009 respectively. It corresponds to a travelling wave velocity of around 170 m s<sup>-1</sup>. Note that this value is highly inaccurate as the time between the recordings corresponds to the sampling frequency<sup>10</sup>. This travelling velocity of 170 m s<sup>-1</sup> corresponds to around half the sound velocity of CO<sub>2</sub> in the same thermodynamic conditions (around 370 m s<sup>-1</sup>). The travelling wave velocity in a pipe is always lower than the sound velocity in an infinite medium due to the flexibility of the pipe material. A modified sound

---

<sup>8</sup>Under pressure in pipes is to be avoided as it can cause their collapse.

<sup>9</sup>These valves close in less than 0.1 s.

<sup>10</sup>The sampling frequency could not be over 5 Hz with the current data acquisition and control of experiment system.

## 2.4. Test campaign: Assessment of dynamic behaviour and controllability.

velocity can be estimated using the isothermal bulk modulus of the fluid, Young's modulus of the pipe material, the diameter and thickness of the pipe [119]:

$$a = \left[ \rho \left( \frac{1}{E} + \frac{\phi}{eY} \right) \right]^{-1/2} \quad (2.4)$$

Where  $a$  is the travelling wave velocity,  $\rho$  the density of the fluid,  $E$  its isothermal bulk modulus,  $Y$  Young's modulus of the pipe material,  $\phi$  and  $e$  its diameter and thickness respectively. The bulk modulus and density of liquid CO<sub>2</sub> in the conditions of the test are 290.5 bar and 800 kg m<sup>-3</sup> respectively. The Young's modulus of the CuFe2P alloy is 115 GPa and liquid pipes have an outside diameter of 19.05 mm and a thickness of 1.3 mm. It results in a wave velocity of 190 m s<sup>-1</sup>, which is in line with the measured 170 m s<sup>-1</sup>.

The maximum pressure rise during a liquid hammer can be computed as [119]:

$$\Delta P = \rho a C_0 \quad (2.5)$$

In which  $C_0$  is the flow velocity prior to the valve closure and can be computed as a function of the mass flowrate, fluid density and pipe cross-section. In the conditions of the test it is equal to 0.82 m s<sup>-1</sup>. It results in a predicted maximum pressure rise of 1.25 bar, which is consistent with the value of 1.12 bar measured. It can be concluded that indeed it is possible to generate a liquid hammer, that in the conditions of the test bench represent an over pressure of around 2% which is low.

In a full scale network however, the maximum flow velocity is going to be higher, even when constrained according to [58] it would reach 2 - 2.5 m s<sup>-1</sup>. If Summer conditions are considered, and steel pipes are used for the liquid pipe of the CO<sub>2</sub> network discussed in the chapter on thermoeconomics ( $\phi = 280$  mm,  $e = 5$  mm,  $Y = 210$  GPa,  $E = 474$  bar,  $\rho = 850$  kg m<sup>-3</sup>) it could lead to a maximum overpressure comprised between 4 and 5 bar, which is less than 10% of the operating pressure during summer.

Finally note that the test showed only one overpressure spike, which is unlike what generally happens in water based scheme, in which a series of over and under pressure are observed and take a relatively long time to damp out. A plausible explanation is that liquid CO<sub>2</sub> is closer to its saturation point, which probably causes vapour to form during the downward pressure change leading to a very fast damping. The same test was done on the vapour line by running the system in the same conditions and closing valve 2001. No noticeable "gas" hammer was observed.

It can be concluded that the hydro-acoustic phenomenon of liquid hammer can indeed occur in a CO<sub>2</sub> based district heating and cooling network. However, the magnitude of the phenomenon should not cause too much of a problem as the overpressure would at most



reach 5 bar or 10% of the operating pressure.

### 2.4.7 Mishaps, or why the full certification was in the end useful

As mentioned in an earlier section, a great deal of effort had to be invested in full certification of the test facility. Although cumbersome and time consuming, it had the merit of allowing identifying the risks associated with the facility and to propose adequate safety measures. One can classify the events causing risks in two categories: Low flowrate leaks and High flowrate leaks. Low flowrate leaks typically occur at faulty seals, bad soldered/welded joints or other small defects. The only risk linked to such leaks is the risk of suffocation. In the installation it is dealt with by the gas detection and alarm. Large leaks are the results of catastrophic rupture of components and of their misuse<sup>11</sup>. The risk associated with these events have been listed in another chapter at Table 1.15. The suffocation risk is also dealt with by the gas detection and alarm, while the mechanical risks are dealt with the use of safety valves, normally closed sectioning valves and pressure switches. It appeared that over the course of the test campaign, these two types of event happened.

First, in December 2014, while the test facility had been in standby mode for three or four weeks, waiting for the replacement of the faulty solenoid valve 3002 a leak developed at one of the bolted flanges of flowmeter 22001. It resulted in a slow venting of CO<sub>2</sub> in the room until that remained undetected until a routine check of the installation was carried out about one week later. The amount of CO<sub>2</sub> vented had caused the pressure to drop below the 40.6 bar threshold of the pressure switches causing the installation to shut down and the sectioning valve to close. However, the gas detection did not sound the alarm, probably because the CO<sub>2</sub> concentration never exceeded 5000 ppm. Note that during all the period the system had a faulty CO<sub>2</sub> valve (3002), the ventilation had been forced on to keep the temperature in the room as low as possible, thus reducing the pressure in the system. It explains why the leak was not detected as the ventilation renews the air in the room several times per hour. Fortunately the leak could be repaired when the new CO<sub>2</sub> valve was installed.

Second, on June 10 2015, as the system had been in standby since the end of the test campaign three weeks earlier, a fitting connecting the discharge port of a liquid line safety valve (15004) did burst. The bolt of the fitting ripped open as can be seen at Fig. 2.25. As no one was in the room at the time, the chain of events had to be reconstructed from the few available data<sup>12</sup>. When the fitting did burst, the pressure in the system was around 50 bar and dropped very quickly (in around 10 s.) to the threshold pressure of 40.6 bar in the vapour lines close to the failure point, triggering the pressure switch (32002) and the subsequent shut-down of the power supply and closure of the sectioning valves. The location of the faulty fitting has caused the draining of the CO<sub>2</sub> contained in the section of vapour line and the liquid sections of the network and central plant connected to it through liquid safety valves. It resulted in a release of CO<sub>2</sub> in the room large enough to exceed 5000 ppm at the detection device, triggering the alarm and alerting the security lodge. Note first that the pipe section where the rupture

---

<sup>11</sup>Like opening the wrong servicing valve.

<sup>12</sup>During standby the data acquisition software plotted only the pressures and at an interval of 7 s.

## 2.5. Conclusion on the experimental facility and test campaign

---

occurred was significantly bent in the event (visible at Fig. 2.4, half way between number 6 and 11) which, considering the stiffness of the copper alloy used, gives an idea of the force of the CO<sub>2</sub> jet and second, that the reason why the fitting failed is not known at the time these lines are being written. Eventually it can be concluded that the certification procedure that was carried out, and the two safety chains that resulted from it have performed as designed and that a thorough accounting of safety considerations in a CO<sub>2</sub> based district energy network is of the utmost importance.

## 2.5 Conclusion on the experimental facility and test campaign

An experimental facility aimed at demonstrating the functionalities of a CO<sub>2</sub> district heating was designed and built. Although a lab scale experiment, some characteristic sizes had to be comparable to those to be encountered in a real life pilot CO<sub>2</sub> network - hence the length of the lab scale network of 100 m - which is around one order of magnitude smaller than a real network would be. The system could be built using exclusively off-the-shelf components which was one of the requirements. The technology of the components was also chosen according to what would likely be used in full scale network.

Over the course of the development, it appeared necessary to obtain the full CE certification of the test facility. Although a cumbersome and extremely time consuming enterprise it has proven valuable in learning the work flow to design and build a safe refrigeration/heat pump system, the applicable standards, and all sort of elements that would have been impossible to grasp without doing it for real. Although not directly applicable to the pipelines of a full scale CO<sub>2</sub> network, the procedure is entirely similar to what will have to be done for the user substations and possibly the central plant.

The design of the control, was focused on demonstrating that standard control schemes were applicable, that a high level of automation could be achieved and that it would lead to a system operating reliably without control inputs from an operator.

Initially the test facility had to be built in two phases. "Phase one" should have provided the demonstration of the basic principles and would have allowed gathering information that could have been used in the design of "phase two". However, for time and financial reasons, only "phase one" could be implemented. Once the test facility had been built, tests were conducted first in stationary conditions in order to obtain information on the heat transfer coefficient in the heat exchangers and also to survey the extent of the operating envelope of the system, mostly in term of ability of the automation to stabilize the system.

The stationary tests showed that the system could be operated reliably between 48 and 59 bar, with superheat at the evaporator outlet stabilized at setpoint values comprised between 1 K and 8 K and for heat rates between 3.6 kW and 16.4 kW at the central plant condenser. Dynamic tests were also carried to study the behaviour of the system and of its control. It led to the conclusion that the controllability of the system was good, that it could cope reasonably well with step changes of setpoint and good for ramp changes. In a full scale system it would be advised to follow ramps for changes in setpoint as they are less demanding in term of control

## Chapter 2. Experimental facility and test campaign

---

and thus give higher guarantee regarding the reliability of operation. It also appeared that the condenser in the current system had tendency to either flood or dry out, and was the main cause of inaccuracy of the control. In a full scale system or if "phase two" is realised, adding a receiver tank of a capacity more or less equivalent to the volume of the CO<sub>2</sub> channel in the condenser should be considered. Tests were also done in order to assess the risks linked with "liquid" and "gas" hammer, consecutive to a rapid stopping of the flow in the network. It resulted that only liquid hammer are possible and the overpressure generated is not incompatible with safe operation of a CO<sub>2</sub> network. Moreover, contrarily to liquid hammer in water networks, there seems not to be a succession of over and under pressure waves but only one positive pressure spike. The test bench clocked over 140 hours of tests and the standby by time during the system was working at just the minimum cooling load to maintain its pressure as low as possible amounted to 4850 h. However, two mishaps happened one causing a two months shut-down in winter 2014-2015, waiting for the replacement of a valve and the second, when a catastrophic rupture of a fitting caused a large leak. The good news about this last mishap is that the safety features designed during the certification did function as required, but the bad news is that there are over 50 similar fittings on the facility and, at the time these lines are being written, the reason of the failure is unknown. If in the future the second phase of the experiment is to be conducted, an investigation should be carried out in order to determine whether or not the remaining fittings pose a threat.

Overall and considering that only the first of the two steps of the experiment was realized, it can be concluded that the requirements for the building and testing of a lab scale CO<sub>2</sub> network fulfilled the requirements. Potentially helping pave the way towards a practical implementation of a reliable and safe CO<sub>2</sub> based district heating and cooling network.

## 2.5. Conclusion on the experimental facility and test campaign

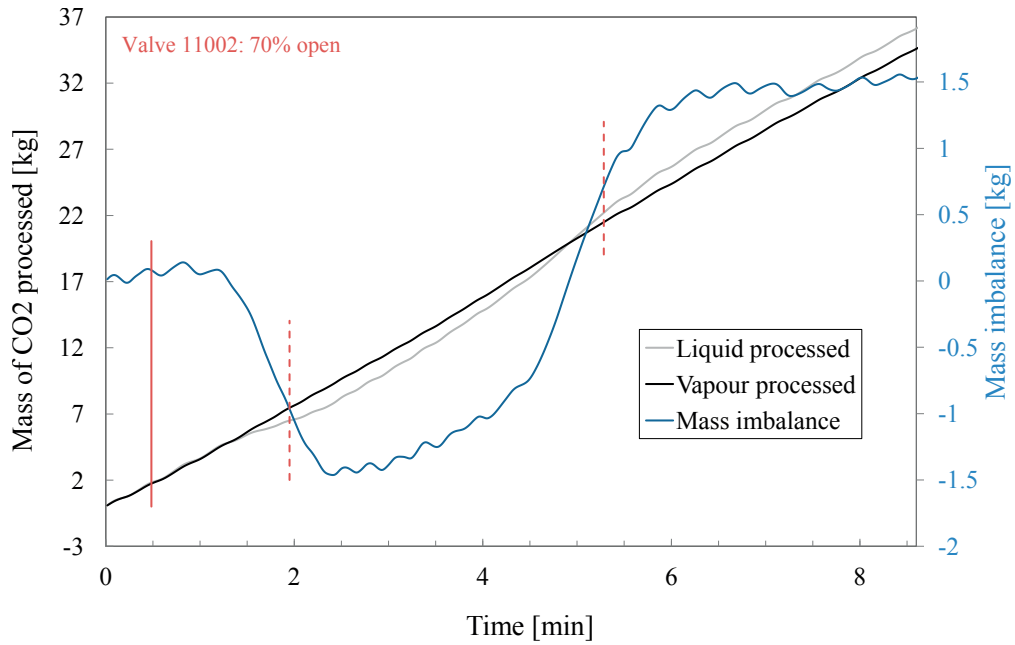


Figure 2.23 – Evolution of the mass of liquid CO<sub>2</sub> processed by the flowmeter 22001, the mass of CO<sub>2</sub> vapour processed by the flowmeter 22002 and the mass imbalance between liquid and vapour flows, after a change of the pressure setpoint from 58 to 54 bar during a 2 min. ramp.

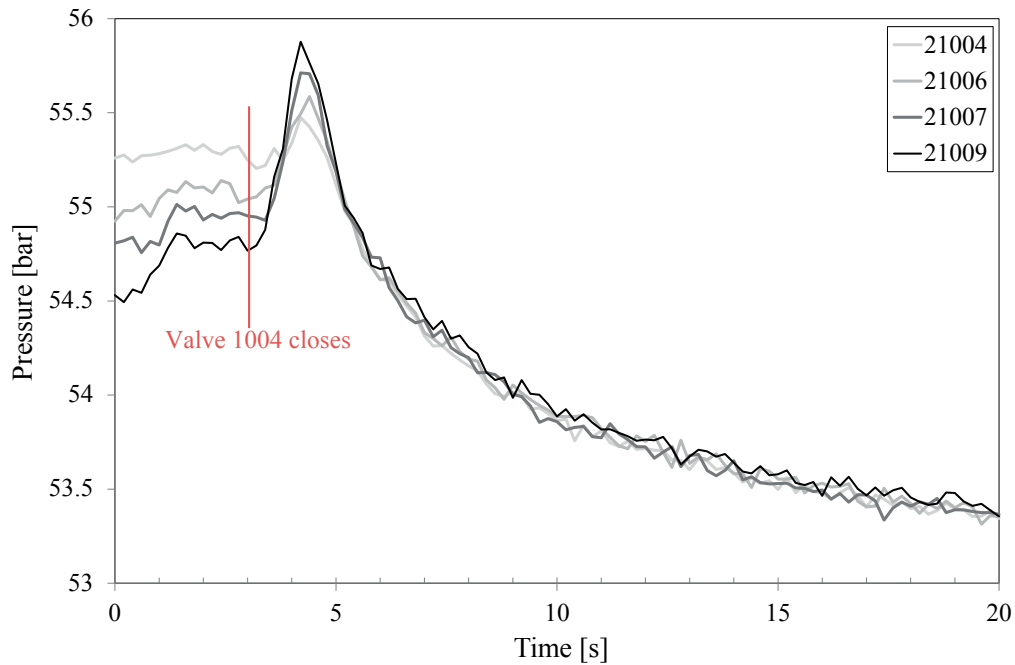


Figure 2.24 – Liquid hammer triggered by the closure of one of the network's sectioning valve (1004) when the system was operated at high load (26.3 kW).



Figure 2.25 – Close view of the bolt of the fitting that burst, causing a large leak of CO<sub>2</sub> that triggered both the gas detection and the pressure switch safety chains.

# 3 Dynamic Modelling and Simulation

## 3.1 Introduction

As part of the development process of a CO<sub>2</sub> district heating and cooling network, dynamic simulation was perceived as a helpful tool for the assessment of the technical feasibility of the system. In particular, it was aimed at providing helpful insight for designing the control of the experimental facility described previously. By first comparing the behaviour of the test facility with that predicted by the simulation, which would give confidence in the understanding of the physics at play, and then by simulating a full scale network, or at least its constituting parts, would ultimately help demonstrating the scalability of the technology.

As a result dynamic models for all the relevant pieces of equipment of the test bench were developed.

It includes:

- a dynamic model of plate evaporator
- a dynamic model of plate condenser
- a dynamic model of pipe
- a quasi steady model of pump
- a quasi steady model of valve

In this chapter these models will be presented.

## 3.2 State of the art

The dynamic simulation of systems including two phase heat exchangers is relatively well documented in the literature. Two different modeling trends can be distinguished; the first

### Chapter 3. Dynamic Modelling and Simulation

---

one uses a one dimensional finite difference formulation of the equation of conservation of mass and energy, and sometimes of the linear momentum. The second trend is based on multizone models in which the mass and energy conservations are written for the subcooled, two-phase and superheated zones. The length of these zones is variable and, depending on the conditions, one or two of them might be nonexistent.

Among the papers using the finite difference formulation, [120] studied an ORC and compared several control methods to maximize the efficiency of the ORC when connected to a hot source with varying temperature. Haberschill et al. [121] proposed a model of a transcritical  $CO_2$  heat pump with internal heat exchanger. The model was validated with experimental data. It showed that the prediction of the steady state is very accurate, but the duration of transients is too short. It is argued that these imprecisions are due to a poor accuracy of the compressor model. Shi et al. [122] published a dynamic modeling of a  $CO_2$  Supermarket Refrigeration System. It focuses essentially on the modeling of the air cooled gas cooler (apparently working both in subcritical and supercritical conditions) using a 1D and 2D discretization. The model was validated with field data, and proved to be sufficiently accurate for control purposes. Jia et al. [123] proposed a dynamic model of a dry expansion evaporator. It takes into account the conservation of linear momentum, and was tested with various drift flux models computing the velocity ratio between vapour and liquid phases.

Among the studies based on a multizone approach, a dynamic model of vapor compression cycle operating in start-up/shut-down mode is presented by Li and Alleyne [124]. It relies on an enhanced moving boundary model for the condenser and the evaporator switching between 1, 2 and 3 zones. Hence it is capable of dealing with extreme variations due to the "on/off" operations, experimental validation of the model was done, and proved a sufficient accuracy, at least for control applications. Liang et al. [125] proposed a model of a variable capacity refrigeration system working under abnormal conditions. It is intended for this model to be validated with a future experiment. Finally, Wei et al. [126] presented a dynamic model of an ORC for waste heat recovery. It includes a comparison between the finite difference and multizones methods. Both methods were validated by experimental data and it is shown that they predict the experimental points with an accuracy of 4%. It also shows that the multizone method is slightly less accurate than the finite difference method, however its computational speed makes it more suited for real time applications such as model based control.

The model of pipe is quite similar in the development than that of the channels in the 1D finite difference model of the heat exchangers. However some refinement was included in order to account for the radial expansion of the pipe caused by pressure transients [119].

The models of the valve and pump are straightforward and very common.



### 3.3 Condenser and evaporator: Modelling approach

The equation solver chosen for the present study is gPROMS [127]. It uses its own programming language to model virtually any kind of system that can be described through a set of partial differential and algebraic equations. The equations are expressed in their symbolic form, and in the case of spatially dependant problem, the discretization domain and scheme are specified by the user but it is the solver that takes care of its application.

Because of the automatic discretization features offered by the software, and since real time applications are not considered, it has been decided to use a finite difference approach in spite of being more computationally intensive. Moreover it is expected to reach a better accuracy with this method. The heat exchangers considered here are of the single pass brazed plate type. The geometrical parameters and the properties of the construction material used in the current model are visible at Fig. 3.1. Note that the number of channels is considered equal for both the heating and cooling side.

Finally, the discussion will focus on the evaporator case as both models of the plate evaporator and condenser are entirely similar. Hence in this discussion the subscript "c" denoting the cold fluid, refers to the refrigerant and the subscript "h" denoting the hot fluid refers to the water.

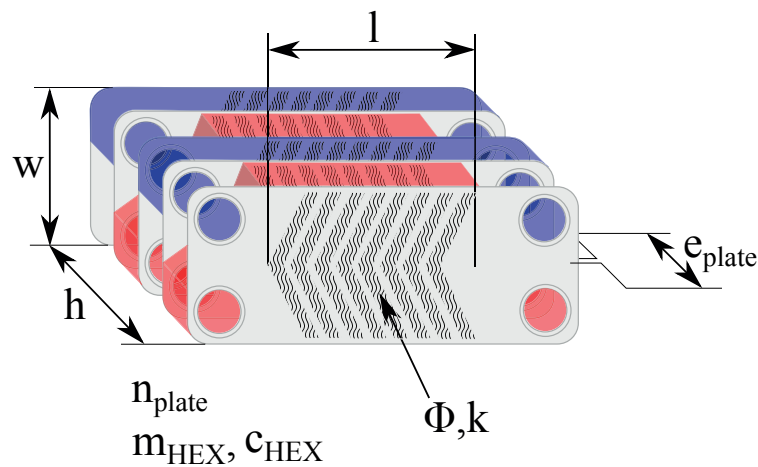


Figure 3.1 – Geometrical parameters considered in the dynamic modelling of plate evaporator and condenser.

An area enhancement factor  $\phi$  was used to account for the effect of corrugation. The empty mass  $m_{HEX}$  and the mass specific heat capacity of the construction material  $c_{HEX}$  are needed since the resulting thermal mass can significantly affect the dynamics. The pipe roughness  $k$  is needed to compute the friction factor on the water side.

For the completeness of the discussion it is useful to give the equations of the three main geometrical parameters that are used throughout this document.

### Chapter 3. Dynamic Modelling and Simulation

The perimeter of one channel (water or refrigerant side) given by:

$$\Pi = \left[ 2w + \frac{2(h - n_{plate}e_{plate})}{n_{plate} - 1} \right] \Phi \frac{n_{plate}}{2} \quad (3.1)$$

The cross sectional area of one channel is given by:

$$A = w \frac{(h - n_{plate}e_{plate}) n_{plate}}{n_{plate} - 1} \frac{1}{2} \quad (3.2)$$

The hydraulic diameter of one channel is by definition:

$$D_H = \frac{4A}{\Pi} \quad (3.3)$$

The current dynamic model of heat exchanger comprises several sub-models, a block representation showing the sub-models and the fluxes of information is provided at Fig. 3.2. In this study it has been decided to use a homogeneous approach, in which the specific volume and the velocity of the fluid are averaged values of the liquid and vapour phase, hence the flow is treated as a compressible flow.

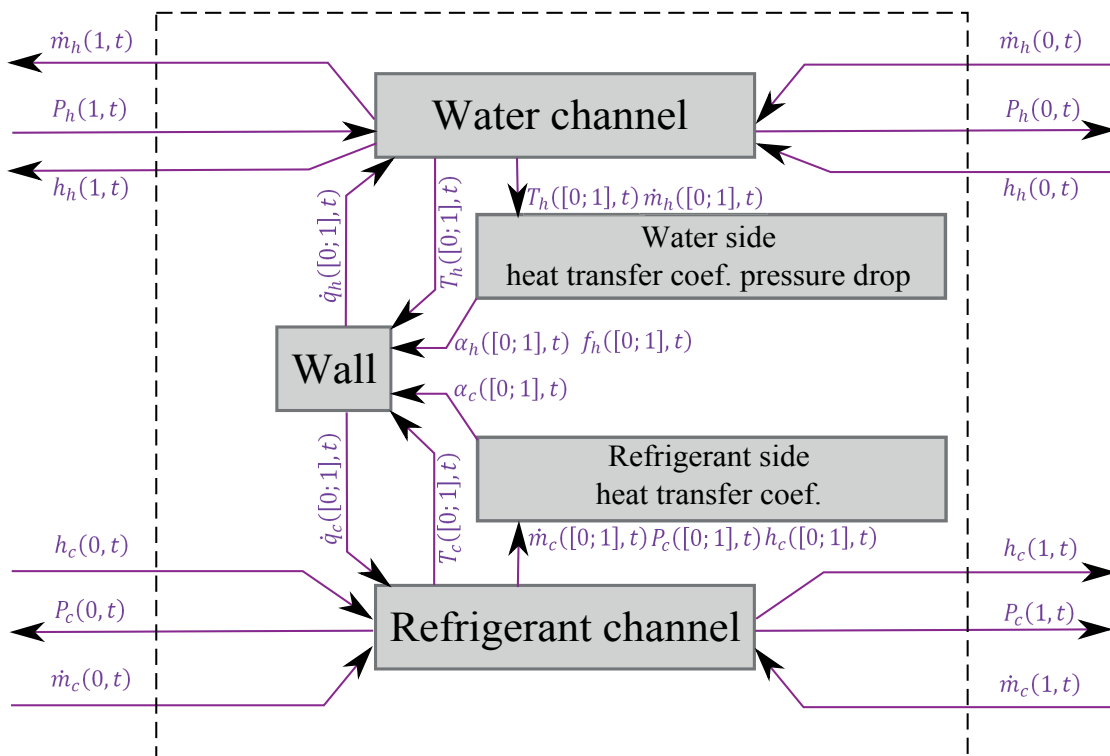


Figure 3.2 – Block diagram of the heat exchanger dynamic model. The flux of information through the boundary of the system, as well as between the sub-models are shown.

3.3.1 Refrigerant channel

In this sub-section the main equations used to model the refrigerant channel are presented, leading to the system of partial differential and algebraic equations to be implemented. Notice that for easier of reading the subscript  $c$  has been omitted.

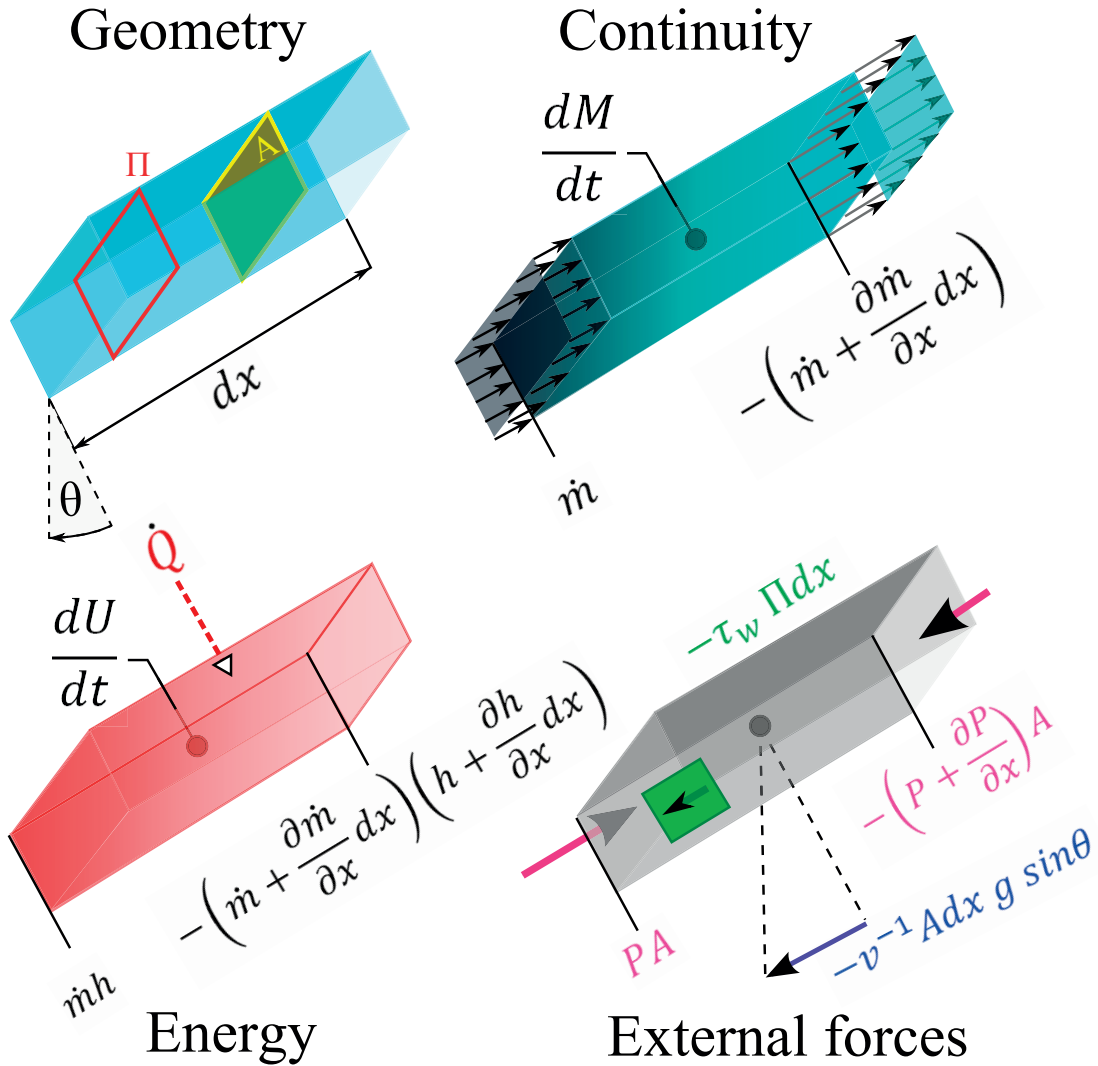


Figure 3.3 – Schematic representation of the control volume of infinitesimal length, used to derived mass, energy and linear momentum conservation equations for the refrigerant and water channels.

**Continuity equation** A control volume of infinitesimal length is considered, a representation of which is visible at Fig. 3.3. This representation includes the geometry and its parameters, the continuity and energy equation formulation used, as well as the balance of external forces. The expression of the continuity equation on the control volume

considered is

$$\frac{dM}{dt} = \dot{m} - \left( \dot{m} + \frac{\partial \dot{m}}{\partial x} dx \right) \quad (3.4)$$

Where M is the mass of fluid and  $\dot{m}$  its mass flow rate. Taking the mass balance (3.4) and introducing the specific volume  $v^1$ , the velocity C, and the cross-sectional area A, and using the fact that A remains constant throughout the length, it can be rewritten as:

$$A dx \frac{\partial}{\partial t} v^{-1} = - \left( C + \frac{\partial C}{\partial x} dx \right) \left( v^{-1} + \frac{\partial}{\partial x} (v^{-1}) dx \right) A \quad (3.5)$$

By simplifying (3.5) and neglecting the infinitesimal terms of order higher than 1. One gets the following expression for the continuity equation for a one dimensional compressible flow in a pipe of constant cross-section:

$$v^{-1} \left( \frac{\partial v}{\partial t} + C \frac{\partial v}{\partial x} \right) - \frac{\partial C}{\partial x} = 0 \quad (3.6)$$

**Energy conservation equation** According to [39] the equation of the first Law of thermodynamics for a system only submitted to a heat rate  $\dot{Q}$ , to an advection of mass through its boundary and where the variation in kinetic and potential gravitational energy have been neglected reduces to:

$$\frac{dU}{dt} = \dot{m}h - \left( \dot{m} + \frac{\partial \dot{m}}{\partial x} dx \right) \left( h + \frac{\partial h}{\partial x} dx \right) + \dot{Q} \quad (3.7)$$

By introducing into (3.7) the definition of enthalpy, recalling that A remains constant throughout the length, and by introducing the velocity C and specific volume v, the left hand side of (3.7) becomes:

$$\frac{dU}{dt} = \frac{d}{dt} (H - PV) = \frac{d}{dt} (v^{-1}h - P) A dx = \left( v^{-1} \frac{\partial h}{\partial t} - h v^{-2} \frac{\partial v}{\partial t} - \frac{\partial P}{\partial t} \right) A dx \quad (3.8)$$

while on the right hand side, once the high order terms have been removed, it becomes:

$$\dot{m}h - \left( \dot{m} + \frac{\partial \dot{m}}{\partial x} dx \right) \left( h + \frac{\partial h}{\partial x} dx \right) + \dot{Q} = - \left( v^{-1} C \frac{\partial h}{\partial x} + v^{-1} h \frac{\partial C}{\partial x} - h C v^{-2} \frac{\partial v}{\partial x} \right) A dx + \dot{Q} \quad (3.9)$$

---

<sup>1</sup>Specific volume was chosen instead of density because of its less non linear evolution with respect to mass specific enthalpy.

Reorganizing the terms of (3.8) and (3.9) one gets:

$$h \left( v^{-1} \left[ \frac{\partial v}{\partial t} + C \frac{\partial v}{\partial x} \right] - \frac{\partial C}{\partial x} \right) + \left( \frac{\partial h}{\partial t} + C \frac{\partial h}{\partial x} \right) = \frac{\dot{Q}}{dx} \frac{v}{A} + v \frac{dP}{dt} \quad (3.10)$$

The first parenthesis is identically equal to (3.6) hence its value is 0, thus the energy equation becomes:

$$\frac{\partial h}{\partial t} + C \frac{\partial h}{\partial x} = \frac{\dot{Q}_c}{dx} \frac{v}{A} + v \frac{dP}{dt} \quad (3.11)$$

**Conservation of linear momentum** The change in linear momentum is equal to the resulting external force, hence it can be written as follows:

$$\frac{d}{dt} (MC) = \dot{m}C - \left( \dot{m} + \frac{\partial \dot{m}}{\partial x} dx \right) \left( C + \frac{\partial C}{\partial x} dx \right) + \sum F_{ext} \quad (3.12)$$

Introducing into (3.12) the specific volume  $v$  and the cross-sectional area  $A$ , it becomes:

$$\frac{d}{dt} (v^{-1}C) A dx = v^{-1}C A dx - \left[ v^{-1} + \frac{\partial}{\partial x} (v^{-1}) dx \right] \left( C + \frac{\partial C}{\partial x} dx \right)^2 A + \sum F_{ext} \quad (3.13)$$

Through derivation, simplification and neglecting the high order terms, (3.13) can be rewritten as:

$$C \left( v^{-1} \left[ \frac{\partial v}{\partial t} + C \frac{\partial v}{\partial x} \right] - \frac{\partial C}{\partial x} \right) + \left( \frac{\partial C}{\partial t} + C \frac{\partial C}{\partial x} \right) = \frac{v}{A dx} \sum F_{ext} \quad (3.14)$$

The first parenthesis in (3.14) is identically equal to (3.6), thus its value is 0, and the conservation of linear momentum for a one dimensional flow in a pipe of constant cross-section becomes:

$$\frac{\partial C}{\partial t} + C \frac{\partial C}{\partial x} = \frac{v}{A dx} \sum F_{ext} \quad (3.15)$$

The right hand side of (3.15) includes the contribution of the various forces considered. In the present study it has been decided to include the forces that derive from pressure and gravity potentials, as well as from the friction of the fluid against the wall. The resulting force can be written as

$$\sum F_{ext} = PA - v^{-1} g \sin \theta A dx - \tau_{wall} \pi dx - \left( P + \frac{\partial P}{\partial x} dx \right) A \quad (3.16)$$

### Chapter 3. Dynamic Modelling and Simulation

---

Where  $\pi$  is the channel perimeter and  $\tau_{wall}$  the wall shear stress. It has been decided to use a friction factor model of the frictional pressure drop, that is,

$$\frac{\partial P_f}{\partial x} = -\tau_{wall} \frac{\pi}{A} = f \frac{C^2}{2\nu} \frac{1}{D_H} = f \frac{C^2}{2\nu} \frac{\pi}{4A'} \quad (3.17)$$

where  $f$  is the friction factor and  $D_H$  the hydraulic diameter. The expression of the shear stress  $\tau_{wall}$  can be found from (3.17), which allows (3.16) to be rewritten as

$$\sum F_{ext} = -\nu^{-1} g \sin \theta A dx - f \nu^{-1} \frac{C^2}{8} \pi dx - \frac{\partial P}{\partial x} A dx \quad (3.18)$$

Finally (3.18) and (3.15) can be combined to obtain the equation of conservation of the linear momentum for a fluid flowing in a pipe of constant cross-section, submitted to pressure, gravity and friction forces.

$$\frac{\partial C}{\partial t} + C \frac{\partial C}{\partial x} = -g \sin \theta - f \frac{C^2}{8} \frac{\pi}{A} - \nu \frac{\partial P}{\partial x} \quad (3.19)$$

**System of equations** The system of partial differential equations is constituted of (3.6), (3.11) and (3.19). A priori it requires four initial conditions, one for each of the variable having a time differential, namely  $\nu$ ,  $P$ ,  $h$ , and  $C$ . However the three thermodynamic variables are linked by an equation of state, typically in this study,  $\nu = g_1(P, h)$ . This implies that only two initial conditions need to be specified for these three variables. In the present case it was chosen to specify the following initial values:

$$\begin{cases} P([0, 1], 0) = P_{ini} \\ h([0, 1], 0) = h_{ini} \end{cases} \quad (3.20)$$

the equation of state  $g_1$  specifies  $\nu$ . Specifying the boundary conditions finishes closing the system (including at  $t = 0$ ). The boundary conditions chosen consist in specifying the following values:

$$\begin{cases} \dot{m}(0, t) = \dot{m}_{in} \\ \dot{m}(1, t) = \dot{m}_{out} \\ h(0, t) = h_{in} \end{cases} \quad (3.21)$$

Finally the system of partial differential and algebraic equations characterizing a diabatic compressible fluid submitted to pressure, gravity, friction forces, and which is flowing in

a pipe of constant cross-section can be written as:

$$\begin{cases} v^{-1} \left( \frac{\partial v}{\partial t} + C \frac{\partial v}{\partial x} \right) - \frac{\partial C}{\partial x} = 0 \\ \frac{\partial h}{\partial t} + C \frac{\partial h}{\partial x} = \frac{\dot{Q}_c}{dx} \frac{v}{A} + v \frac{dP}{dt} \\ \frac{\partial C}{\partial t} + C \frac{\partial C}{\partial x} = -g \sin \theta - f \frac{C^2}{8} \frac{\pi}{A} - v \frac{\partial P}{\partial x} \\ v = g_1(P, h) \end{cases} \quad (3.22)$$

**Simplified system of equations** The derivation that led to (3.22) was voluntarily kept as general as possible, such as to keep a clear starting point for all the simplifications that might be undertaken afterwards. The first underlying assumption that must be mentioned is that the model of refrigerant channel described here is an homogeneous model, as the two phases travel at the same velocity. According to the nature of the problem studied, it was decided to implement a simplified version of (3.22) using only two other assumptions than that of the homogeneous model. First, the unsteady term in the conservation of linear momentum has been neglected. It is based on the assumption that the characteristic time for any change in velocity at one location, is much shorter than the time for some mass or energy to accumulate at the same location. Typically, the pressure waves will travel along the heat exchanger several hundreds of time per second, while the time scale for the mass to accumulate in an evaporator/condenser is generally in the order of seconds or tens of seconds. As a second assumption the time derivative of the pressure can be neglected. It is a more questionable assumption than the first one; however, it leads to a very much simpler set of equations. Furthermore, the pressure in an evaporator/condenser is mostly driven by the temperature of the source/sink to which it is connected. In domestic heating and cooling applications such as ours, it does not change quickly. Under these simplifications, the system of partial differential and algebraic equations becomes:

$$\begin{cases} v^{-1} \left( \frac{\partial v}{\partial t} + C \frac{\partial v}{\partial x} \right) - \frac{\partial C}{\partial x} = 0 \\ \frac{\partial h}{\partial t} + C \frac{\partial h}{\partial x} = \frac{\dot{Q}_c}{dx} \frac{v}{A} \\ C \frac{\partial C}{\partial x} = -g \sin \theta - f \frac{C^2}{8} \frac{\pi}{A} - v \frac{\partial P}{\partial x} \\ v = g_1(P, h) \end{cases} \quad (3.23)$$

#### 3.3.2 Water channel

The system of equations of the water channel model derives from the same principles that led to (3.23) but adding a condition of incompressibility of the fluid. Notice that for an easier



reading the subscript  $h$  has been omitted. The system of equations that has been implemented is:

$$\begin{cases} \dot{m} = v^{-1} C A dx \\ \frac{\partial h}{\partial t} + C \frac{\partial h}{\partial x} = \frac{\dot{Q}_h v}{dx A} \\ C \frac{\partial C}{\partial x} = -g \sin \theta - f \frac{C^2 \Pi}{8 A} - v \frac{\partial P}{\partial x} \\ v = g_1(h) \end{cases} \quad (3.24)$$

### 3.3.3 Wall

The wall is treated as a thermal mass submitted to two heat flows, one from/towards the water channel and the other from/towards the refrigerant channel. The transverse heat conduction is considered as perfect while the axial heat conduction is neglected. The system of equation reduces to only one differential equation, the energy balance, and two algebraic heat transfer equations:

$$\begin{cases} \frac{m_{HEX}}{l} c_{HEX} \frac{dT_{wall}}{dt} = -\frac{\dot{Q}_h}{dx} - \frac{\dot{Q}_c}{dx} \\ \frac{\dot{Q}_h}{dx} = \alpha_h \Pi (T_{wall} - T_h) \\ \frac{\dot{Q}_c}{dx} = \alpha_c \Pi (T_{wall} - T_c) \end{cases} \quad (3.25)$$

It has to be noticed that all heat flows are expressed per unit length, hence the same is required that for the mass of construction material. The negative signs are required to remain consistent with the positive entering convention used in the water and refrigerant channels.

### 3.3.4 Water side heat transfer coefficient and friction factor

On the water side the heat transfer coefficient  $\alpha_h$  is computed using Focke's correlation [117], the friction factor  $f$  is computed using Churchill's formula [59].

### 3.3.5 Refrigerant side heat transfer coefficient

The amount of literature on  $CO_2$  heat transfer coefficient in evaporation is somewhat limited. A correlation using flow pattern maps was published in [116], though very convincing, the mass flux validity range is slightly too high for our application and the degree of complexity would have made it difficult to integrate in the model presented here. At the time of writing, no correlation developed especially for  $CO_2$  condensation was found. Because of these difficulties,

### 3.3. Condenser and evaporator: Modelling approach

it was decided to implement the following simple heat transfer model for the  $CO_2$  side. The parameters of which have been calibrated *a posteriori* based on the stationary tests. Although calibrating the parameters for both the condenser and the evaporator was done in (2.1) of the previous chapter it was found later to be rather inaccurate when used in the dynamic simulation. As a result the parameters have been modified as follows for the evaporator:

$$\begin{cases} \alpha_c = \alpha_{ref} \left( \frac{P}{P_{ref}} \right)^\psi \left( \frac{\dot{G}}{\dot{G}_{ref}} \right)^\zeta \quad \forall h < h'' = 2000 \cdot \left( \frac{P}{50.86} \right)^{4.61} \left( \frac{\dot{G}}{21.1} \right)^{0.91} \\ \alpha_c = \kappa \alpha_{ref} \left( \frac{P}{P_{ref}} \right)^\psi \left( \frac{\dot{G}}{\dot{G}_{ref}} \right)^\zeta \quad \forall h \geq h'' = 0.05 \cdot 2000 \cdot \left( \frac{P}{50.86} \right)^{4.61} \left( \frac{\dot{G}}{21.1} \right)^{0.91} \end{cases} \quad (3.26)$$

For the condenser it was modified as follows:

$$\begin{cases} \alpha_h = \alpha_{ref} \left( \frac{P}{P_{ref}} \right)^\psi \left( \frac{\dot{G}}{\dot{G}_{ref}} \right)^\zeta \quad \forall h < h'' = 1000 \cdot \left( \frac{P}{50.86} \right)^{4.61} \left( \frac{\dot{G}}{4.67} \right)^{0.91} \\ \alpha_h = \kappa \alpha_{ref} \left( \frac{P}{P_{ref}} \right)^\psi \left( \frac{\dot{G}}{\dot{G}_{ref}} \right)^\zeta \quad \forall h \geq h'' = 0.05 \cdot 1000 \cdot \left( \frac{P}{50.86} \right)^{4.61} \left( \frac{\dot{G}}{4.67} \right)^{0.91} \end{cases} \quad (3.27)$$

Where  $G$  is the mass velocity  $\dot{G} = \dot{m}A^{-1}$  and  $\alpha_{ref}$  a measured value of the average heat transfer coefficient at the reference condition  $P_{ref}$  and  $\dot{G}_{ref}$ . The condition on the mass specific enthalpy is used to discriminate the subcooled liquid and two-phase zones of the superheated vapour zone. Explicitly, the heat transfer coefficient is reduced by a factor  $\kappa$  when the fluid is in a superheated vapour state. The exponent  $\psi$  and  $\zeta$  reflects the dependency of the heat transfer coefficient with respect to change in pressure and mass flux. Though correlations for the friction factor have been published for  $CO_2$  in evaporation [115] it has been decided to consider a constant value of the friction factor in the present model. Indeed the mass flux range being low, the frictional component in the momentum equation is expected to have little effect.

#### 3.3.6 Thermodynamic and transport properties

The thermodynamic and transport properties of both the  $CO_2$  and the water are taken from tabulated values computed with refrpop 8.0 from NIST [57]. For the  $CO_2$  a double entry table was used, with a 1 bar discretization step for  $P$ , and a 2 kJ/kg discretization step for  $h$ . The range of the tabulated data extends from 20 to 80 bar for  $P$  and from 120 to 520 kJ/kg for  $h$ . For the water the values have been assumed to depend only on  $P$  and thus have been taken on the 15 bar isobaric curve. A discretization step of 5.64 kJ/kg has been used for  $h$ . The range of the tabulated data extends from 10 to 833 kJ/kg for  $h$ .

### 3.3.7 Discretization scheme

The gPROMS tool automatically takes care of the discretization. It is fully automatic for what concerns the time discretization. However, it is required to define which are the variables to be spatially discretized and the *distribution domain*. Namely the discretization scheme, the order and the number of cells. For the models of the heat exchangers, the scheme is a backward finite difference of first order with 100 discretization cells.

## 3.4 Pipes: Modelling approach

The dynamic models of the pipes have been derived on the basis of the dynamic model of evaporator/condenser. The work was carried out within the framework of a semester project of a master student.

### 3.4.1 Refrigerant pipe

In this subsection, A system of one-dimensional partial differential and algebraic equations will be derived. It describes the flow of a compressible fluid, flowing in a pipe in which the cross-section can change elastically due to the pressure exerted by the fluid on the wall.

#### Continuity equation

Taking the continuity equation (3.6) from the models of the evaporator/condenser but considering that the cross-sectional area of the pipe can change over time and length the equation is modified as follows:

$$v^{-1} \left( \frac{\partial v}{\partial t} + C \frac{\partial v}{\partial x} \right) = \frac{\partial C}{\partial x} + \frac{1}{A} \left( \frac{\partial A}{\partial t} + C \frac{\partial A}{\partial x} \right) \quad (3.28)$$

The change in cross-sectional area can be assumed to be related exclusively to the pressure exerted on the pipe wall by the fluid and the properties of the pipe, i.e., its thickness  $e$  and Young's Modulus  $Y$ .

$$\begin{cases} \frac{dA}{dt} = \frac{1}{A} \left( \frac{\partial A}{\partial t} + C \frac{\partial A}{\partial x} \right) \\ \frac{1}{A} \left( \frac{dA}{dt} \right) = \frac{D_H}{eY} \frac{dP}{dt} = \frac{4A}{\Pi eY} \frac{dP}{dt} \end{cases} \quad (3.29)$$

By inserting (3.29) into (3.28), one obtains an expression of the one-dimensional continuity equation for a compressible fluid flowing through a pipe the wall of which allows

for an elastic deformation in a direction transverse to the flow:

$$v^{-1} \left( \frac{\partial v}{\partial t} + C \frac{\partial v}{\partial x} \right) = \frac{\partial C}{\partial x} + \frac{4A}{\Pi e Y} \frac{dP}{dt} \quad (3.30)$$

**Energy conservation equation** Using the same method than in the model of the evaporator/condenser (3.7 - 3.11), but accounting for the changes in cross-section over time and length, the energy conservation equation becomes:

$$\frac{\partial h}{\partial t} + C \frac{\partial h}{\partial x} = \frac{\dot{Q}}{dx} \frac{v}{A} + v \frac{\partial P}{\partial t} + \frac{vP}{A} \frac{\partial A}{\partial t} \quad (3.31)$$

**Conservation of linear momentum equation** Again using the same kind of derivation than was used for the conservation of linear momentum in the model of evaporator/condenser (3.12 - 3.19), but accounting for the changes in cross-section over time and length the equation becomes:

$$\frac{\partial C}{\partial t} + C \frac{\partial C}{\partial x} = -g \sin \theta - f \frac{C^2}{8} \frac{\Pi}{A} - v \frac{\partial P}{\partial x} - \frac{vP}{A} \frac{\partial A}{\partial x} \quad (3.32)$$

**System of equations** The system of partial differential equations is constituted of (3.30), (3.31) and (3.32). Similarly, to the model of evaporator/condenser, it requires four initial conditions, one for each of the variable having a time differential, namely  $v$ ,  $P$ ,  $h$ , and  $C$ . The three thermodynamic variables are linked by an equation of state. However, to overcome some numerical problems, it was decided to introduce some flexibility in the coupling of (3.30), (3.31), (3.32) and the equation of state by introducing a fictitious first order equation:

$$\tau \frac{dv}{dt} = v' - v \quad (3.33)$$

In which  $v'$  is computed by the equation of state -  $v' = g_1(P, h)$ . The time constant  $\tau$  has a value of 0.01 s, implying that  $v$  tracks  $v'$  very closely. The initial conditions chosen are:

$$\left\{ \begin{array}{l} \frac{dv([0, l], 0)}{dt} = 0 \\ \frac{dP([0, l], 0)}{dt} = 0 \\ P([0, l], 0) = P_{ini} \\ h([0, l], 0) = h_{ini} \end{array} \right. \quad (3.34)$$

The boundary conditions chosen are the following and allow the closure of the system:

$$\left\{ \begin{array}{l} \frac{\partial \dot{m}(0, t)}{\partial x} = \frac{\dot{m}_{out}(t) - \dot{m}_{in}(t)}{l} \\ \frac{\partial \dot{m}(l, t)}{\partial x} = \frac{\dot{m}_{out}(t) - \dot{m}_{in}(t)}{l} \\ h(0, t) = h_{in} \\ \frac{\partial h(l, t)}{\partial x} = 0 \\ P(0, t) = P_{in} \\ P(l, t) = P_{out} \end{array} \right. \quad (3.35)$$

Note that contrarily to the evaporator/condenser in which the length was normalized to 1, for the pipes the length is specified to a value  $l$ . Finally one get the system of partial differential and algebraic equations characterizing a diabatic, compressible, fluid submitted to pressure, gravity and friction forces. The fluid flows in a pipe, the cross section of which changes elastically with the pressure exerted by the fluid:

$$\left\{ \begin{array}{l} v^{-1} \left( \frac{\partial v}{\partial t} + C \frac{\partial v}{\partial x} \right) = \frac{\partial C}{\partial x} + \frac{4A}{\Pi e Y} \frac{dP}{dt} \\ \frac{\partial h}{\partial t} + C \frac{\partial h}{\partial x} = \frac{\dot{Q}}{dx} \frac{v}{A} + v \frac{\partial P}{\partial t} + \frac{vP}{A} \frac{\partial A}{\partial t} \\ \frac{\partial C}{\partial t} + C \frac{\partial C}{\partial x} = -g \sin \theta - f \frac{C^2 \Pi}{8 A} - v \frac{\partial P}{\partial x} - \frac{vP}{A} \frac{\partial A}{\partial x} \\ v' = g_1(P, h) \\ \tau \frac{dv}{dt} = v' - v \end{array} \right. \quad (3.36)$$

### 3.4.2 Refrigerant side heat transfer coefficient and friction factor

To compute the heat flow between the wall of the pipe and the refrigerant flow it was decided to use the very common Dittus-Boelter correlation that can be found in [128]. In a refrigerant based district heating and cooling network, during normal operation, the fluid in the pipes is in a single phase, hence the choice of a single phase correlation. The choice of Dittus-Boelter in particular is related to its simplicity. Potentially the model of pipe proposed here, should be able to deal with two-phase flows. However if such conditions occur, the heat-transfer coefficient is simplistically computed using the average saturated liquid and vapour heat transfer coefficient computed with Dittus-Boelter. The average is based on the vapour mass fraction. The friction factor  $f$  used in the momentum equation of (3.36) is computed through Churchill's correlation [59]. To reduce the computational load during simulations, the friction factors for a large range of Reynolds number and non-dimensional pipe roughness have been

pre-computed and regrouped in a lookup table.

#### Heat flow: environment - pipe wall - refrigerant

The effect of the heat transfer per meter of pipe length between the environment and the pipe wall, as well as between the pipe wall and the refrigerant is treated by the following differential equation:

$$\rho_{pw} \bar{c}_{pw} (De + e^2) \frac{dT_{pw}}{dt} = \alpha_{\infty-pw} (D + 2e) (T_{\infty} - T_{pw}) - \alpha_{pw-c} D (T_{pw} - T_c) \quad (3.37)$$

The pipe has an inside diameter  $D$ , a thickness  $e$ . It is characterized by a constant specific heat  $\bar{c}_{pw}$  and it has a density of  $\rho_{pw}$ . The heat transfer coefficient between the environment and the pipe wall -  $\alpha_{\infty-pw}$  - is constant. Its value should account for the conduction through the insulation material and the convection heat transfer coefficient if the environment is air, or conduction in the ground over a few centimetres or tens of centimetres. As said earlier the heat transfer coefficient between the pipe wall and the refrigerant -  $\alpha_{pw-c}$  - is computed using a Dittus-Boelter correlation. Obviously the temperature of the refrigerant is computed using an equation of state.  $T_c = g_2(P, h)$ .

#### 3.4.3 Thermodynamic and transport properties

The evaluation of the thermodynamic properties are done identically to what was done for the condenser/evaporator

#### 3.4.4 Discretization scheme

For the models of pipe, two different spatial discretization were used. The scheme used for  $h$  is a backward finite difference of first order with 100 discretization cells. The scheme used for  $P, C$  and  $v$  is a centred finite difference of second order with 100 discretization cells.

### 3.5 Pump model

The model of pump is very simple, its only refinement is the use of the volume flowrate vs. pressure difference -  $\dot{V}_{0,in} = g_3(\Delta P_0)$  and efficiency vs. volume flowrate characteristics -  $\eta = g_4(\dot{V}_{0,in})$  - both at nominal rotational frequency. The performance at other frequencies are computed using fans affinity law [63]. It results in the following model, in which,  $\nu$  is the rotational frequency and the subscript 0 denotes the conditions at nominal rotational

frequency:

$$\left\{ \begin{array}{l} \Delta P = P_{out} - P_{in} \\ \Delta P_0 = \Delta P \left( \frac{v}{v_0} \right)^{-2} \\ \dot{V}_{0,in} = g_3(\Delta P_0) \\ \eta = g_4(\dot{V}_{0,in}) \\ \dot{V}_{in} = \dot{V}_{0,in} \left( \frac{v}{v_0} \right) \\ \rho_{in} = g_1(P_{in}, h_{in})^{-1} \\ \dot{m}_{in} = \rho_{in} \dot{V}_{in} \\ \dot{m}_{in} = \dot{m}_{out} \\ \dot{E} = \frac{\Delta P \dot{V}_{in}}{\eta} \\ h_{out} = h_{in} + \frac{\dot{E}}{\dot{m}_{in}} \end{array} \right. \quad (3.38)$$

The values from the characteristics  $\dot{V}_{0,in} = g_3(\Delta P_0)$  and  $\eta = g_4(\dot{V}_{0,in})$  are obtained by interpolation from a lookup table derived from data from the pump manufacturer.

### 3.6 Valve model

The model of valve is very simple and is typical of what is generally done for liquid valves. It assumes an isenthalpic process, a linear relationship between the valve opening and the effective  $Kv$ . It results in the following model, in which,  $U_{valve}$  is the percentage of opening of the valve and  $Kv_0$  the flow factor when the valve is fully open:

$$\left\{ \begin{array}{l} \Delta P = P_{out} - P_{in} \\ h_{in} = h_{out} \\ \rho_{in} = g_1(P_{in}, h_{in})^{-1} \\ \dot{V}_{in} = U_{valve} \frac{Kv_0}{3600} \left( \frac{\Delta P}{100\rho_{in}} \right)^{1/2} \\ \dot{m}_{in} = \rho_{in} \dot{V}_{in} \\ \dot{m}_{out} = \dot{m}_{in} \end{array} \right. \quad (3.39)$$

Finally, the model of PID controller is the one already provided as part of the gPROMS software



[127] and thus it is not described here.

### 3.7 Example of results: Cooling user substation

As mentioned in the previous chapters, CO<sub>2</sub> based district heating and cooling networks can provide both cooling and heating services. In the case of cooling it is intended to rely as much as possible of free cooling systems, in which the service is provided via a CO<sub>2</sub> evaporator used to cool down the secondary loop of the building, for example, water supplying a radiant chilled ceiling system. This section describes a simulation of such a system, a schematic representation of which is provided at Fig. 3.4. The output to control is the degree of superheating at the evaporator outlet -  $\Delta T_{SH}$  - that has to be maintained at the setpoint -  $\Delta T_{SH,setpoint}$ . The input of the dynamic system,  $U_{valve}$ , is the percentage of opening of the control valve. The controller implemented is of the proportional integral type. The goal of this control system is to ensure complete evaporation of the CO<sub>2</sub> before it leaves the heat exchanger, whatever the external perturbation might be. The possible external perturbations are shown in purple at Fig. 5. They consist of the CO<sub>2</sub> liquid line and vapour line pressures, the mass flow rate of water and the specific enthalpy at inlet of both chilled water and CO<sub>2</sub>. In this study the evaporator is a 106 plates Alfa Laval CBXP52-106H-F [129]. The control valve is a LowFlow MK708 [130], with a flow factor  $Kv_0$  of 0.173 and the characteristic of which is proportional to the percentage of opening of the valve. Finally, the proportional gain of the controller is 3 and its reset time is 10 s.

An assessment of the behaviour of the system under abrupt perturbation was made. It consisted in submitting the system of Fig. 3.4 to a change in one of the five possible perturbations, and to evaluate the closed loop response of the system. The changes in the perturbations were all done by following a 6 s duration ramp following a period in which the system was at steady state. Table 3.1 presents the initial conditions used and the final values of the perturbation reached after the ramp.

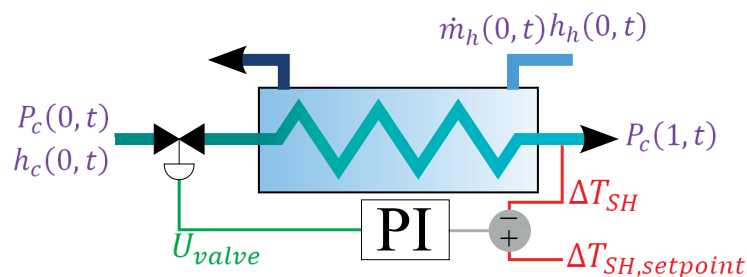


Figure 3.4 – Schematic representation of a free cooling substation - red: output and setpoint. - green: input. – purple: perturbations.

The results of the tests are visible on Fig.3.5 – 3.7. In the case of a downward change in mass flow of water it can be seen that closed loop response of the system is characterized by a stable

### Chapter 3. Dynamic Modelling and Simulation

Table 3.1 – Conditions of the simulation: Initial conditions, and final values of the perturbations

<b>Parameters</b>		
$\Delta T_{SH}$	4 K	
$\Delta T_{SH, setpoint}$	4 K	
PI Controller - Proportional gain	3	
PI Controller – Reset time	10 s.	
$U_{valve}$	92.7% (steady state)	
<b>Perturbations</b>	Initial value	Final value
$\dot{m}_h(0, t)$	0.5 kg s <sup>-1</sup>	0.1 kg s <sup>-1</sup>
$h_h(0, t)$	85 kJ kg <sup>-1</sup> (19.9°C)	83 kJ kg <sup>-1</sup> (19.4°C)
$h_c(0, t)$	220 kJ kg <sup>-1</sup> (8.3°C)	220 kJ kg <sup>-1</sup> (11.8°C)
$P_c(v, t)$	51 bar	52 bar
$P_c(1, t)$	50 bar	49 bar

oscillatory behaviour, especially visible on the evolution of superheat at the evaporator outlet - Fig. 3.5 side B. The period of oscillation is comprised between 85 s. at first and decrease to about 60 s. Oscillations are almost fully damped out after 3 cycles, which corresponds to a duration of around 210 s. The cooling load of the chilled water - Fig. 3.5 side A - decreases a little less than proportionally with the change in water mass flow - from 12.5 kW to 3.0 kW. In a real system the mass flow in the chilled water loop will be determined by the cooling load required for the service. The simulation predicts that the evaporator can cope with such sharp changes in chilled water flowrate. This is inline with what was observed with the test bench (Fig. 2.8). It is worth noticing that the cooling load adapts very swiftly to a change in water mass flow. Indeed the long lasting oscillations only affect the superheat which represents only a few percent of the total load. In the case of perturbations due to change in the enthalpy at inlet of either the water or the CO<sub>2</sub>, the behaviour of the superheat is also a stable oscillatory one. However, their period, amplitude and relative damping are different - Fig 3.6 side B. For the water case, the period of oscillation is around 120 s, the oscillations amplitude decrease of approximately 35% after each cycle, except for the first one. In the case of the CO<sub>2</sub> inlet enthalpy change, the amplitude is much lower, the period is 110 s. and the amplitude decreases by 50% at each cycle. Note that it takes around 120 s before the oscillations begin to damp out. It also appears that an increase of the CO<sub>2</sub> inlet specific enthalpy leads, once the steady state is reached again, to a decrease in the total cooling rate - Fig. 3.6 side A. As expected, a decrease in the inlet enthalpy of water also leads to a decrease in heat transfer. The cooling load oscillates much more in the case of the change in the water enthalpy. Pressure perturbations have only been studied for the CO<sub>2</sub> channel since water is incompressible and thus a change in its pressure does not affect significantly the behaviour of the heat exchanger. Variation of the inlet pressure of CO<sub>2</sub> leads to a stable oscillatory closed loop response of the superheat – Fig 3.7 side B. The period of oscillation is around 70 s, and are damped out after 210 s. A change in inlet pressure does not change significantly the heat load on water – Fig. 3.7

### 3.7. Example of results: Cooling user substation

side A - since steady state inlet and outlet enthalpies, as well as CO<sub>2</sub> mass flow, remain the same. In fact all the pressure change is absorbed in the valve that the PI controller commands to close a bit. It results that the evaporator does not see any change in its operating conditions. In the case of a downward change in outlet pressure, the saturation temperature decreases in the evaporator, leading to a large positive excursion in superheat – Fig. 3.7 side B. During the first oscillation the valve is fully opened (actuator saturated), but from the second oscillation, it starts to operate normally again, the response is stable and oscillatory but looks less like a harmonic oscillator response than with the other perturbations cases. The aforementioned decrease of the saturation temperature, leads to a higher heat transfer – Fig. 3.7 side A. Indeed, as a consequence of the drop in saturation temperature caused by the pressure change, the mean temperature difference between chilled water and CO<sub>2</sub> is increased and so does the cooling rate.

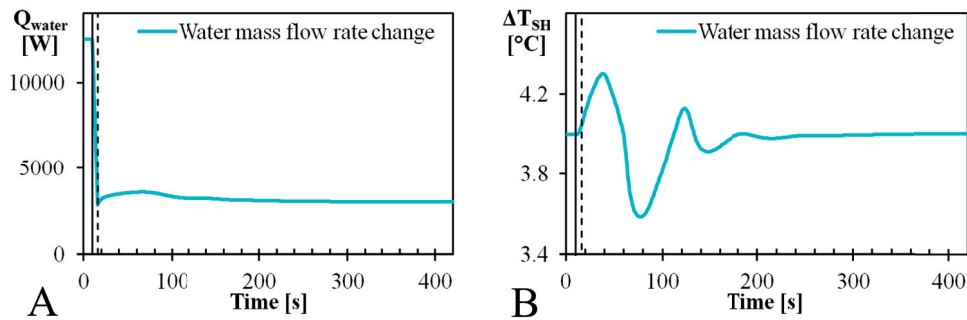


Figure 3.5 – Closed loop response of a free cooling substation to an abrupt change in mass flow of the chilled water: **A** Cooling load on the water side, **B** Superheat at the evaporator outlet.

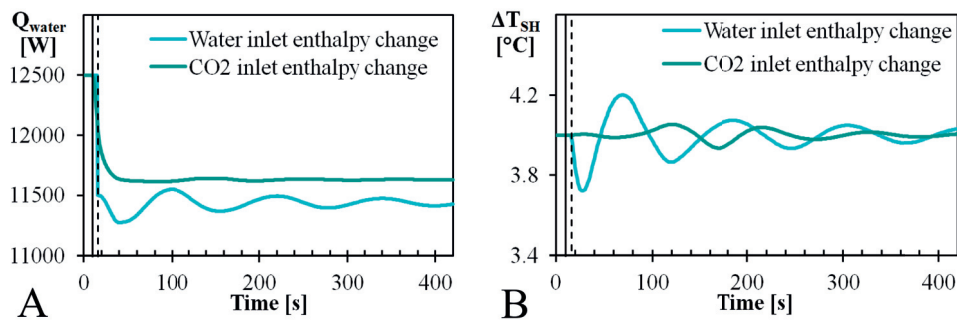


Figure 3.6 – Closed loop response of a free cooling substation to an abrupt change in enthalpy of water/CO<sub>2</sub> at inlet: **A** Cooling load on the water side, **B** Superheat at the evaporator outlet.

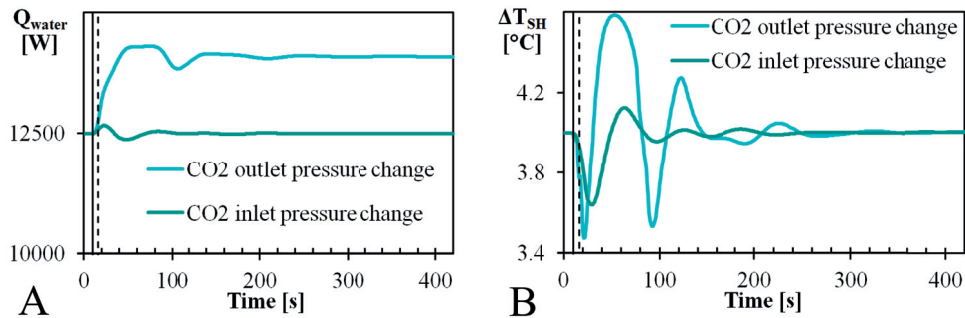


Figure 3.7 – Closed loop response of a free cooling substation to an abrupt change to an abrupt change in the inlet/outlet pressure of CO<sub>2</sub> at inlet and outlet: **A** Cooling load on the water side, **B** Superheat at the evaporator outlet.

### 3.8 Example of results: Comparison of the test bench dynamics and a simulation

In an attempt to validate the models developed a comparison between the test bench and the dynamic simulation was carried out and was based on a spectral analysis. Spectral analysis is a method typically used for the identification of dynamic system. The way it was used in this study is a direct application of what is described by Bonvin and Karimi in [131]:

**1: Test bench - PRBS excitation of valve 11001, recording of pressure (21002)** The first step consists in applying an input signal, known as a Pseudo-Random Binary Signal, to an actuator. The PRBS is a deterministic and periodic approximation of a white noise<sup>2</sup>, and is generated using a shift register that shifts with constant sampling frequency. The sampling frequency will determine the highest frequency visible in the spectral analysis, and should not be selected too low in order to respect the condition for the analysis to be valid [131]. The length of the shift register combined with the sampling frequency will determine the longest period that can be seen in the spectral analysis. This period must be longer than the time required for an impulse response to damp out in order not to lose information on the slow dynamic response. Both the input signal on the actuator and the process variable to be controlled - the output signal - are recorded at the sampling frequency of the PRBS. To reduce the effect of measurement errors, the signal can be repeated several time (as it is periodic). It is important however, that the subsequent computations for the spectral analysis are conducted on entire periods of the PRBS.

For the present discussion, the input signal  $u$  was applied on the water valve used to control the pressure in the network (11002)<sup>3</sup> and the output signal  $y$  was the pressure itself (21002). The sampling frequency used was  $1/3 \text{ s}^{-1}$ , the length of the shift register

<sup>2</sup>A white noise excite all frequencies with the same magnitude

<sup>3</sup>The numbers refer to the PFD of the experimental facility, provided at Fig. 2.1.

### 3.8. Example of results: Comparison of the test bench dynamics and a simulation

was 7 elements which correspond to a duration for one PRBS period of 381 s. To reduce measurement errors the signal was repeated 9 times. Thus, for each test it was required to excite valve 11001, record pressure 21001 and have the rest of the test bench automatically running for a duration of 3429 s. Note that the excitation signal was not causing the valve to switch on and off completely. Instead it was implemented as a perturbation of a few valve opening percentage points around the steady state value required to maintain the pressure. Thus the pressure was guaranteed to remain more or less at the level desired for the test.

**2: Test bench - Spectral analysis** First the signals  $u$  and  $y$  are cut in 9 signals of 127 elements each, corresponding to every repetition of the PRBS. Then for each of these 9 signals, the autocorrelation function of  $u$  - ( $R_{uu}$ ) and the inter-correlation function of  $u$  with  $y$  - ( $R_{uy}$ ) are computed. The fast Fourier transform for each of the 9 autocorrelation functions are taken and then their average is computed -  $\bar{\Phi}_{uu}$ . The same process is carried out for the 9 inter-correlation functions leading to -  $\bar{\Phi}_{uy}$ . An estimation of the transfer function  $G(j\omega)$  between  $u$  and  $y$  is finally computed:

$$G(j\omega) = \frac{\bar{\Phi}_{uy}(\omega)}{\bar{\Phi}_{uu}(\omega)} \quad (3.40)$$

In which  $j$  is the imaginary number and  $\omega$  the angular frequency in  $\text{rad s}^{-1}$ .

**3: Simulation - Dynamic model of the test bench** A dynamic model of the test bench was programmed with the models described earlier. It comprises only the relevant components:

- The CO<sub>2</sub> liquid line
- The CO<sub>2</sub> vapour line
- The condenser (27001)
- The CO<sub>2</sub> pump (12001) with its PI controller
- The flow control valve for cooling water at the central plant (11001) with its PI controller
- The evaporator (28001), the CO<sub>2</sub> flow control valve (3002) with its PID controller
- The flow control valve for water at the user substation (11001)

The simulated test bench was brought to the same stationary conditions that the test bench was in, prior to the start of the PRBS excitation.

**4: Simulation - PRBS excitation of valve (11001), recording of pressure (21002)** The same PRBS input signal than was applied to the real valve 11001 is applied to the simulated one. For numerical, it was in general necessary to use a smaller magnitude for the excitation signal, as the simulation appeared to be relatively unstable numerically.

**5: Simulation - Spectral analysis** The exact same procedure to the one done at step 2 with the experimental data was carried out for the signals generated by the simulation. It led to another estimation of the transfer function between the opening of valve 11001 the pressure in the network (21002) -  $G'(j\omega)$ . It is then possible to compare the results from the experiment and the simulation.

The results are presented at Fig. 3.8 - 3.9, for two different cases. Rigorously transfer functions apply only to linear time invariant (LTI) dynamic systems and therefore the functions  $G(j\omega)$  and  $G'(j\omega)$  obtained with the spectral analysis represent LTI systems that approximate the non-linear experiment and simulation around the considered operating point. At low frequency (left of the diagrams), when one compares the simulation harmonic response to the experimentally derived one it appears that the amplification at low frequency is for the experiment always around 20 dB or above, while the value from the simulation have higher variation and are in average lower. The difference comes from the higher amplitude of the excitation signal in the experiment than in most of the simulations. For instance, at Fig.3.8 the PRBS magnitude used experimentally was 8.8%<sup>4</sup> while the one used in the simulation was only 0.5%. Indeed, with a larger change in opening, the equilibrium pressure of the network will be further away from the value prior to the transient. It also takes a longer time to reach the new equilibrium pressure, which explains why the harmonic response starts to flatten earlier (at higher frequency) than that from the experiment. The high fluctuations at low frequency for the simulation make no physical sense, they are very likely due to a poor identification, resulting from a lack of sufficient excitation at these low frequencies, which again is probably caused by the small amplitude of the PRBS used. For angular frequencies higher than 0.066 rad s<sup>-1</sup> (periods below 95 s.) the evolution of the simulation and experimental harmonic response are similar, which means that the dynamic model of simulation captures the "fast" dynamics relatively accurately. Fig. 3.9 depicts a test at higher pressure (57.4 bar). The amplitude of the excitation signal was 8% for the experiment and 2% for the simulation. For the experimental part, although of almost the same value in term of excitation, the low frequency amplification is higher than the one observed at Fig. 3.8. It is due to the higher heat rate at which the system was operated. Indeed, for the same change of cooling water flow rate, at high load, the pressure will change more until the heating and cooling load of the user and central plant balance each other again.

The same kind of differences in the low frequency region are observed between the simulation and the experimental harmonic response. The similar behaviour of the two response at frequency higher than 0.066 rad s<sup>-1</sup> (periods below 95 s.) is also visible. Note that there seems to be a static gain difference of around 4 dB between experiment and simulation response. However, from a controllability standpoint this is not really an issue. The same analysis was carried out successfully for 15 different operating conditions. The low frequency discrepancy between the simulation harmonic response and the experimental harmonic response, was observed in all the 15 results. The low frequency gain obtained experimentally are comprised between 15 dB and 30 dB. The correspondence at higher frequency between experiment and

---

<sup>4</sup>the valve opening is comprised between 0.395 and 0.483.

### 3.9. Conclusion on the dynamic modelling and simulation

---

simulation was observed for the majority of the operating conditions, at least regarding the slope of the transfer functions. Some cases show a difference in amplitude that seems to be linked to the hysteresis of the CO<sub>2</sub> valve (3002) at the user, since the discrepancy is maximum around a period of 20 s.

Another spectral analysis was carried out, the input signal being in that case the opening of the CO<sub>2</sub> valve at the user (3002) and the output signal, the superheat at the evaporator (28001). An example of result is shown at Fig. 3.10. Again, at low frequency the transfer function is poorly identified for the simulation. This is also caused by the small amplitude of the excitation used. However, the major difference arise at higher frequency. The sharp valley observed at an angular frequency of 0.264 rad s<sup>-1</sup> (23.8 s) corresponds to the hysteresis observed with valve 3002. At higher frequencies it seems that the response is flat at around 5 dB. The simulation response is completely different, and reflects the fact that the valve modelled has no actuation time, contrarily to the real valve that needs 9 second to rotate 90°, and it has no hysteresis.

As a conclusion of these spectral analyses, the simulation showed that it could replicate the dynamic behaviour of the test bench, but the numerical difficulties render it relatively inappropriate in its current state. Also as the last analysis showed rather clearly, if the models do not correspond to the real components used, then the dynamics predicted might have nothing to do with reality.

There seems to be a correspondence between simulation and experimental results for the pressure. An attempt to replicate by simulation one of the pressure ramp discussed in the previous chapter (2.4.3) was carried out. The results are shown at Fig. 3.11 and 3.12 for the evolution of pressure, evaporator superheat, condenser subcooling and pressure difference. It appears clearly that the dynamics is not properly captured by the simulation model, as no drop in pressure difference, subcooling or excursion in superheat are observed with it. It can be concluded that the mass oscillation that was observed with the experimental facility is not represented by the model, which represents an unacceptable inaccuracy over the most important dynamic phenomenon observed with the test bench.

### 3.9 Conclusion on the dynamic modelling and simulation

A series of dynamic models have been developed for the various components of the network. The goal behind these models was twofold. First they were intended to help conceive the test facility, in particular its control. Second these models were intended to be validated by the experiment and then used in a simulation of a full scale CO<sub>2</sub> network. It required a great deal of effort over the whole duration of the project to develop these models. Concerning the first objective of helping develop the test bench control, the models proved valuable when used to simulate simple subsystems, in analyses rather similar to the free cooling substation discussed here. The second goal could only be very partly addressed. For what concerns the validation part of the models using the test facility, the models have proven cumbersome to put together in a model of a larger system (the test bench in this case.) It is due to the



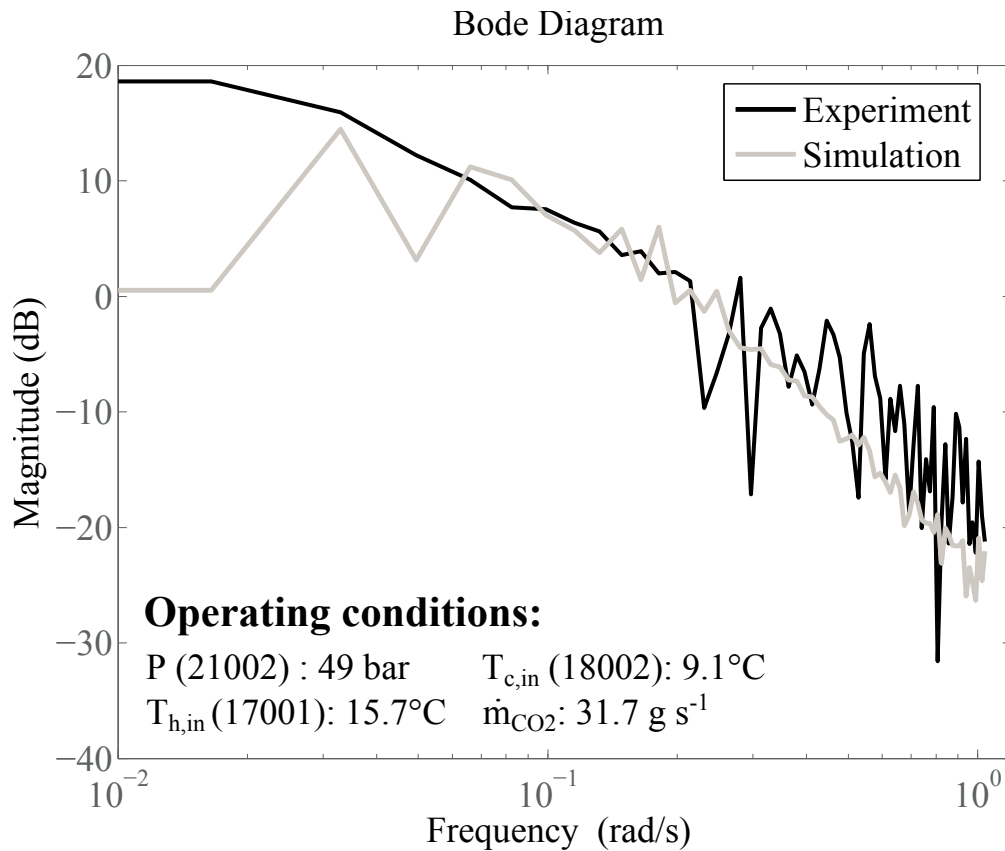


Figure 3.8 – Comparison experiment vs. dynamic simulation: Case 1. Bode diagram (magnitude) of the experimentally derived transfer function -  $G(j\omega)$  and the dynamic simulation derived one -  $G'(j\omega)$  - that relate the opening of valve (11001) to the pressure (21002). Both transfer function were evaluated through an identification using a PRBS excitation (freq. 1/3 s<sup>-1</sup>, 7 elements, 9 repetitions), followed by a spectral analysis. The operating conditions are described on the figure.

numerical instabilities that render very difficult the generation of exploitable results. However, some comparisons with the experimental facility have been done and have demonstrated a certain degree of similarity between simulation and experiment. However, the absence of hysteresis and motor valve dynamics in the model renders the dynamics of superheat of the experiment not comparable to that of the simulation. Moreover, the mass oscillation observed in the experiment, that causes the filling up or emptying of the condenser is not captured at all by the dynamic models presented here. As a result of their poor stability and their inability to represent some key dynamic behaviours, these models are currently unable to simulate an entire network.

The author has taken care not to include in the dynamic models too many parameters that cannot be known. Nevertheless, they remain probably too complicated for what they can do at the time of writing - Namely, help in the design process of the control of the various subsystems in a CO<sub>2</sub> network. If the task of dynamic simulation is to be carried on, these

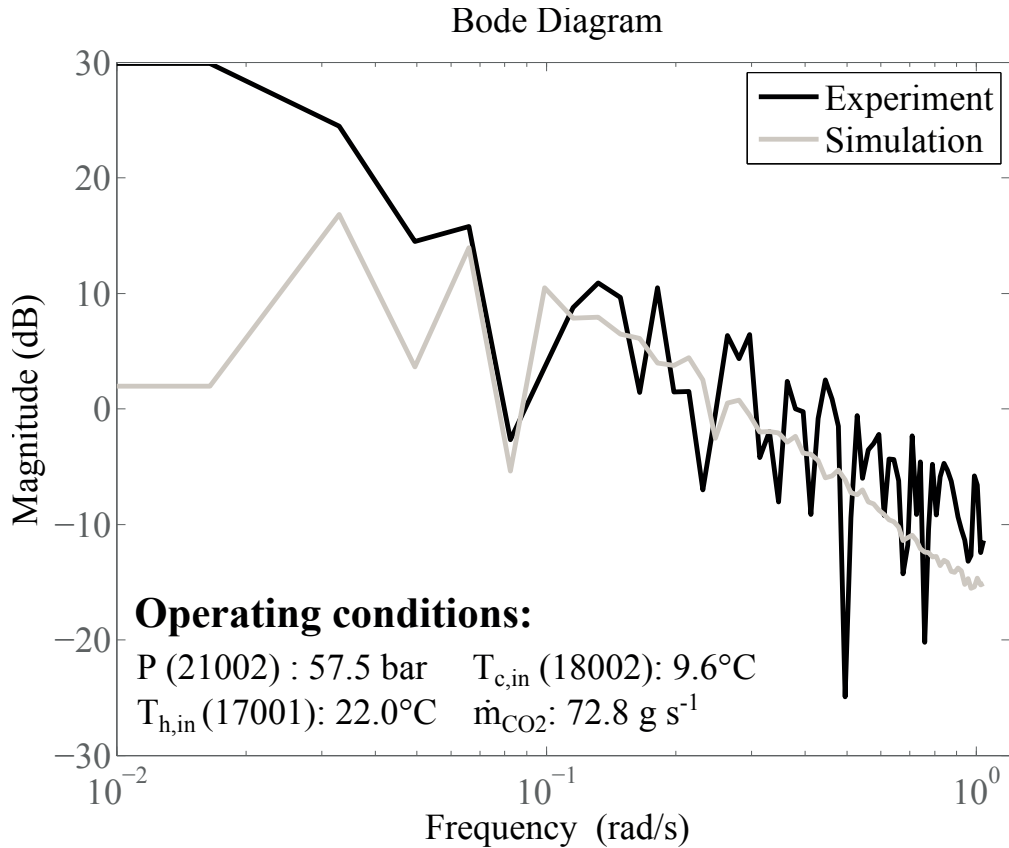


Figure 3.9 – Comparison experiment vs. dynamic simulation: Case . Bode diagram (magnitude) of the experimentally derived transfer function -  $G(j\omega)$  and the dynamic simulation derived one -  $G'(j\omega)$  - that relate the opening of valve (11001) to the pressure (21002). The operating conditions are described on the figure.

models must be rendered more stable and accurate or abandoned in favour of new ones. However it is also worth questioning the goal of simulating an entire network. Indeed such a model will definitely not bring more information on the energy consumption than a quasi-steady model, such as the one developed for the thermoeconomic analysis. It will also not capture the real problematic dynamic phenomena, like accidents (the failure of a fitting) or components that do not perform as expected (hysteresis of valve 3002). It will also be very time consuming and in the end won't bring more information on the control of the system than models of the subsystems would. As a result, future work should focus on the study of the subsystems of a CO<sub>2</sub> district heating and cooling network, starting by simulation of a heating user substation and of the central plant.

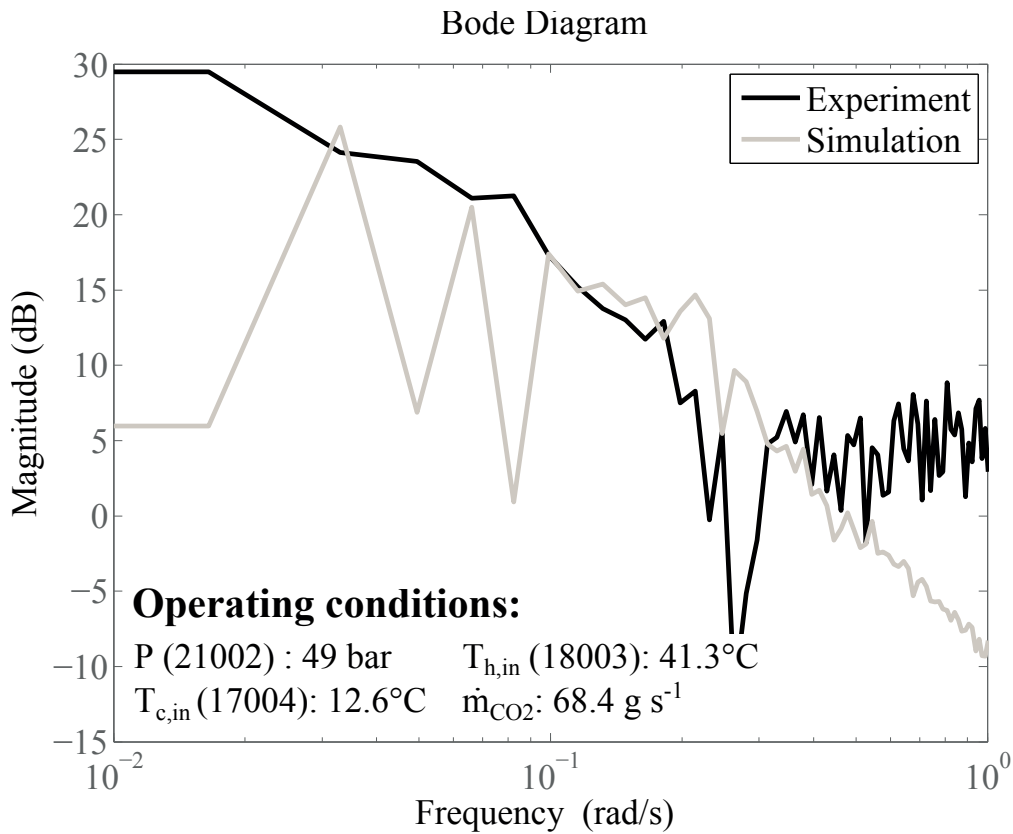


Figure 3.10 – Comparison experiment vs. dynamic simulation: Case 3. Bode diagram (magnitude) of the experimentally derived transfer function -  $G(j\omega)$  and the dynamic simulation derived one -  $G'(j\omega)$  - that relate the opening of valve (3002) to the superheat at evaporator (28001). The operating conditions are described on the figure.

### 3.9. Conclusion on the dynamic modelling and simulation

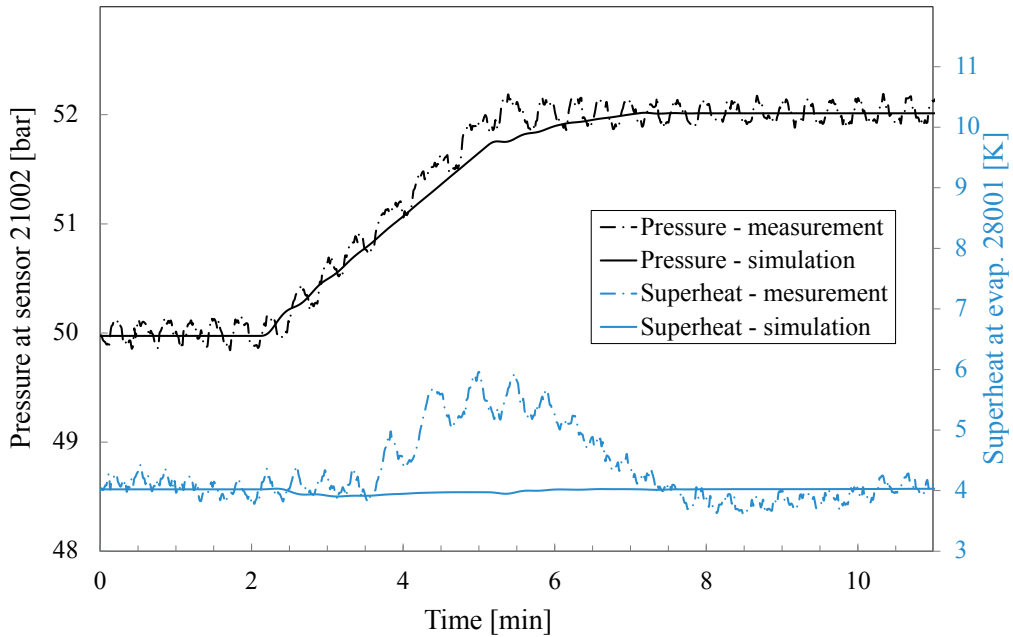


Figure 3.11 – Comparison of the evolution of pressure (21002) and on the superheat at the outlet of the evaporator, between experimental and simulation values. Change of the pressure setpoint from 50 to 52 bar during a 3 min. ramp.

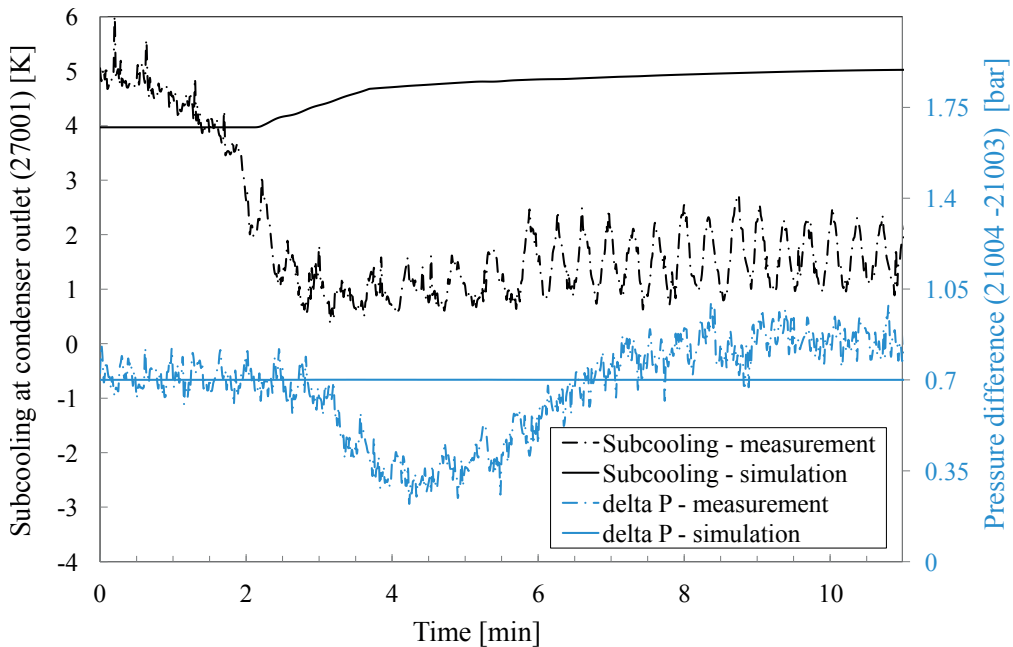


Figure 3.12 – Comparison of the evolution of the pressure difference (21004 - 21003) and on the subcooling at the condenser outlet, between experimental and simulation values. Change of the pressure setpoint from 50 to 52 bar during a 3 min. ramp.



## Conclusion

A thermoeconomic analysis was carried out in order to compare thoroughly different energy conversion technologies for the supply of heating and cooling services to an urban area in Geneva, Switzerland.

The urban area considered - known as "Rues Basses", roughly 1 km long and 200 m wide is located on the shore of lake Geneva, at its junction point with the Rhône river. The affectation of the buildings is mixed with roughly 23% of the heated floor being commercial, 60% office and 17% residential buildings. Five thermal energy services were considered as being used in this area, space heating, domestic hot water preparation, air conditioning, commercial refrigeration and the cooling of data centres. The area was separated in 32 building blocks, using the energy reference area and the affectation, the energy demand for each service in each block was computed based on an energy signature model.

The thermoeconomic analysis was carried out on seven different energy conversion technologies considered as options for the supply of the thermal energy services in the test case area. One, consisting in a combination of oil fired boilers and air cooled electrically driven chillers. These two technologies were chosen as they are representative of the current situation. Five of the conversion technologies studied were refrigerant based network, in which the evaporation/condensing of fluid is used to transfer heat across the network. The first three use CO<sub>2</sub>, one uses HFO R1234yf and the last one HFO R1234ze. Finally a concept of network similar to the refrigerant ones but using liquid water instead was added to the comparison. This last form of network was chosen as it represents the closest competing technology to refrigerant based networks. When the final energy consumption of the various technologies are compared, it can be concluded that all the network based technologies proposed reduce drastically the final energy consumption when compared to the currently used technology. Indeed, if any of the proposed networks were used instead of the current combination of boilers and chillers, the annual "on site" energy consumption would be reduced from a total of 66 GWh of heating oil and electricity, to less than 12 GWh of electricity only. In relative terms it represents a reduction of over 82% in final energy consumption. The least energy consuming technology technology is the R1234ze based network with 9.9 GWh of electricity consumed annually. However, the difference between the most and least electricity consuming network proposed is less than 20%, which is too narrow to determine which technology is the most promising.

An exergy analysis, done on a daily basis, was also carried out on the 7 conversion technologies.

## Conclusion

---

This analysis showed that the generalised use of heat pumping for the heating services is the main contribution to the higher performance of the networks compared to the currently used boilers and chillers. The annual exergy efficiency of the networks was shown to be comprised between 39.5% and 45%, while that of the boilers and chillers is less than 8%. An evaluation of the investment required for the 7 technologies showed that, the investment required to pursue with boilers and chillers would be 54.4 mio €, if all of them needed to be replaced at once. If one of the proposed networks was used instead the investment would range between 32.0 and 41.2 mio €. The major saving linked to the networks is the change from air cooled chillers to free cooling systems. In terms of investment, the cheapest network is the CO<sub>2</sub> network with an open cycle CO<sub>2</sub> heat pump at the central plant, while the most expensive is the cold water network. The difference in terms of investment comes essentially from the bigger pipes required and a more expensive central plant.

A profitability analysis, based on the net present value as a performance indicator was carried out and showed that, for the economic framework conditions used, the conventional technology of boilers and chillers is only marginally profitable after the 40 years lifetime considered. Conversely, all the proposed networks show good economic performances. The economic break-even times were shown to be comprised between 4 and 6 years and the profit generated in present value after 40 years are comprised between 75 mio € for the cold water network and 90 mio € for networks using CO<sub>2</sub>, R1234yf or R1234ze as a transfer fluid and having an open cycle heat pump at the central plant. However, once the price of purchasing the fluid is taken into account both the R1234yf and R1234ze networks become uninteresting. Furthermore, the uncertainty regarding the availability of these synthetic fluids in the long run finishes to render them impractical for use as a transfer media in district heating and cooling networks. Extra safety measures will necessarily apply to CO<sub>2</sub> when compared to water. Although the cost related to these extra measures was not directly accounted in the profitability analysis, it was shown that as long as the extra cost in present value remains below 25% of the initial investment, the CO<sub>2</sub> network should be more profitable than the cold water network.

The economic robustness of the boilers and chillers, the most promising version of the CO<sub>2</sub> network and the cold water network was evaluated based on a stochastic process based simulation. The result confirmed the economic benefit of the network based technologies, since both the CO<sub>2</sub> and cold water network reached a very high probability (>99%) of being economically profitable, while the combination of boilers and air cooled chillers has only a 36% probability of being so.

The last part of the comparison dealt with technical particularities of the CO<sub>2</sub> and cold water network, mostly in terms of potential for a higher compactness of the CO<sub>2</sub> network but also regarding the issue in terms of equipment readily available, where CO<sub>2</sub> is plagued by a scarce offer when compared to what is available for the cold water network.

An experimental facility aimed at demonstrating the functionalities of a CO<sub>2</sub> district heating was designed and built. Although a lab scale experiment, some characteristic sizes had to be comparable to those to be encountered in a real life pilot CO<sub>2</sub> network - hence the length



of the lab scale network of 100 m - which is around one order of magnitude smaller than a real network would be. The system could be built using exclusively off-the-shelf components which was one of the requirements. The technology of the components was also chosen according to what would likely be used in full scale network.

The design of the control, was focused on demonstrating that standard control schemes were applicable, that a high level of automation could be achieved and that it would lead to a system operating reliably without control inputs from an operator.

Tests in stationary regime showed that the system could be operated reliably between 48 and 59 bar, with superheat at the evaporator outlet stabilized at setpoint values comprised between 1 K and 8 K and for heat rates between 3.6 kW and 16.4 kW at the condenser of the central plant. Dynamic tests were also carried to study the behaviour of the system and of its control. It led to the conclusion that the controllability of the system was good, that it could cope reasonably well with step changes of setpoint and good for ramp changes.

Tests were also done in order to assess the risks linked with "liquid" and "gas" hammer, consecutive to a rapid stopping of the flow in the network. It resulted that only liquid hammer are possible and the overpressure generated is not incompatible with safe operation of a CO<sub>2</sub> network.

Based on the fact that a fully certified lab scale network could be built using exclusively off-the-shelf components and based on the tests realized with it. It can be concluded that there is at the moment no indication that a CO<sub>2</sub> based district heating and cooling network could not be built and operated reliably. However, with the current test facility, the automatic switching of the central plant from cooling to heating mode cannot be demonstrated. Future work should focus on realising such a demonstration as it is one of the key functionalities required.

A series of dynamic models have been developed for the various components of the network. The goal behind these models was twofold. First they were intended to help conceive the test facility, in particular its control. Second these models were intended to be validated using the experiment and then used in a simulation of a full scale CO<sub>2</sub> network. The first objective could be fulfilled as the models proved valuable when used to simulate simple subsystems during the design phase of the test bench. Regarding the second objective, dynamic simulation results have been compared to experimental results but cannot be considered a validation, a certain degree of similarity between simulation and experiment could be observed. However, the absence of hysteresis and motor valve dynamics in the model render the dynamics of superheat of the experiment not comparable to that of the simulation. Moreover, the mass oscillation observed in the experiment is not predicted at all by the dynamic model. It results that because of numerical instabilities and inability to capture key dynamic phenomena, these models are, in their current state, not capable of simulating an entire network. Future work should be done on those models to render them more stable and accurate. Finally, the simulation of a full network is probably not worthwhile. Too much effort would have to be put in realising it for no significant gain in knowledge. Instead, the focus should be on the study of the subsystems of the network, first on the heating users substations and the central plant.

## Conclusion

---

The two advanced networks discussed in this study that present the greatest potential are the CO<sub>2</sub> network equipped with an open cycle CO<sub>2</sub> heat pump at the central plant and a cold water network, sometimes referred to as an anergy network. Both will reach very similar efficiencies, around 40% annual exergy efficiency which is much higher than the 8% reached by the currently used boilers and air cooled chillers.

It also appears that there is some potential to exploit the higher compactness of the CO<sub>2</sub> network using an innovative layout and it could prove valuable if properly developed. If the potential of compactness can be realised, it would definitely render the CO<sub>2</sub> an interesting candidate in energy dense urban areas.

It could be demonstrated experimentally that a CO<sub>2</sub> based district heating and cooling network is relatively easy to control, which gives confidence in the fact that the technology can be made reliable. At the time of writing, the prime obstacle to the realisation of a full scale CO<sub>2</sub> network is safety/acceptability. It needs to be addressed thoroughly and future work must be aimed at proposing effective, realistic and cheap solutions to that issue. Eventually, in order to realise the potential of the technology, the development of CO<sub>2</sub> based district heating and cooling networks should be focussed on high energy density areas where the underground does not allow the use of a cold water network.

# A Centrifugal compressors

A preliminary design was carried out for the compressors of the heat pump at the central plant. Note that it was carried out for the three different working fluids considered, namely CO<sub>2</sub>, NH<sub>3</sub> and R1234yf. It assumes that the heat pump at the central plant is equipped with several variable speed centrifugal compressors equipped with vaneless diffusers operating in parallel. The methodology used is the following:

1. The desired inlet thermodynamic conditions, mass flowrate and pressure ratio are selected.
2. The values of specific speed -  $n_s$  - and specific diameter -  $d_s$  are selected on a  $n_s$  -  $d_s$  from [132] within the area of maximum efficiency for radial type compressors. The diameter and nominal frequency of rotation are then obtained.
3. Assuming some values for the following parameters all the compressors general geometry is defined:
  - Absolute inlet Mach number
  - Diffuser outlet to inlet diameter ratio
  - Geometrical outlet angle of the rotor blades
  - Number of rotor blades
  - Ratio of rotor disc clearance to impeller diameter
  - Ratio of blades tip clearance to blades height at impeller outlet
4. Using the geometry defined in 1-3, and the nominal frequency found in 2. The performances of the compressor are computed based on a velocity triangle approach using a code developed by Schiffman [133].
5. From point 4, and using the approach of Dyreby [134], the non-dimensional flow, work and efficiency coefficients are computed and an approximate compressor map is derived from them.

## Appendix A. Centrifugal compressors

---

For the three working fluids, the inlet thermodynamic state corresponds to  $T_{sat} = 2^\circ\text{C}$  and  $T = T_{sat} + \Delta T_{SH} = 4^\circ\text{C}$ . And the desired saturation temperature on the high pressure side was set at  $T_{sat} = 2^\circ\text{C}$ . As several compressor are assumed to be used in parallel, the mass flowrate used for each refrigerant is different, but was chosen such that when operating with only one compressor, running at its minimum mass flowrate<sup>1</sup> the three variants of heat pump would deliver a heat rate of around 2 MW to the CO<sub>2</sub> network. It means that roughly 4-5 compressors are necessary to reach the sizing capacity required for the test case area. The value used for both the tip clearance ratio and disc clearance ratio is 1/100. The same values are used for the three working fluids, since all three machines will operate at similar temperatures and assuming that the clearance requirement is mostly driven by the need to cope with thermal expansion. The result are shown at Fig. A.1 and A.2. It is clear from Figure A.1, that in spite of the required pressure ratio to be not that different, the three fluids lead to to very different rotational frequency and for R1234yf a slight improvement in efficiency. The maximum rotor peripheral velocity, necessary to reach the right end of the constant pressure ratio lines, poses no difficulties for CO<sub>2</sub> and R1234yf at around 250 and 200 m s<sup>-1</sup>, easily achievable with conventional aluminium alloy wheels, for ammonia however, the value is 590 m s<sup>-1</sup> and thus would likely require the use of a titanium alloy impeller instead. It is worth noticing that the very same thermodynamic properties of CO<sub>2</sub>, such as its high reduced pressure, high vapour phase density and low ratio of liquid to vapour density, that renders it an especially interesting fluid from the point of view of the network (See Table 1.5), are imposing the use of smaller compressors, less efficient, compressors and pose some difficulties for the realisation of an efficient heat pump cycle at the central plant.

---

<sup>1</sup>The minimum massflow achievable for a given rotational frequency is constrained by the surge limit.

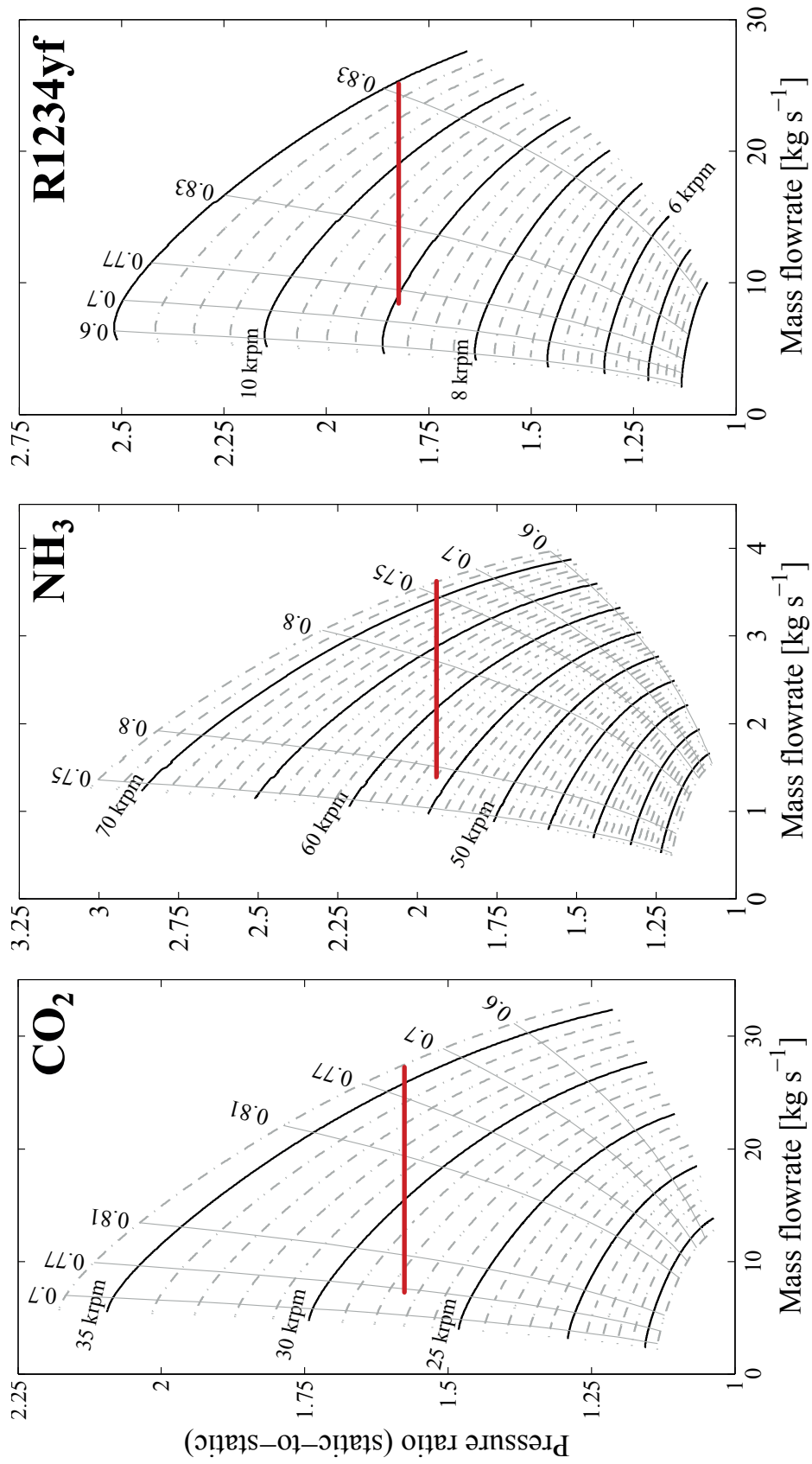


Figure A.1 – CO<sub>2</sub> network: Characteristics of the centrifugal compressors with vaneless diffusers proposed for the central plant's heat pump. The red lines represent typical operations at constant pressure ratio for an evaporation at 2°C and a temperature of the network at 20.5°C.

Appendix A. Centrifugal compressors

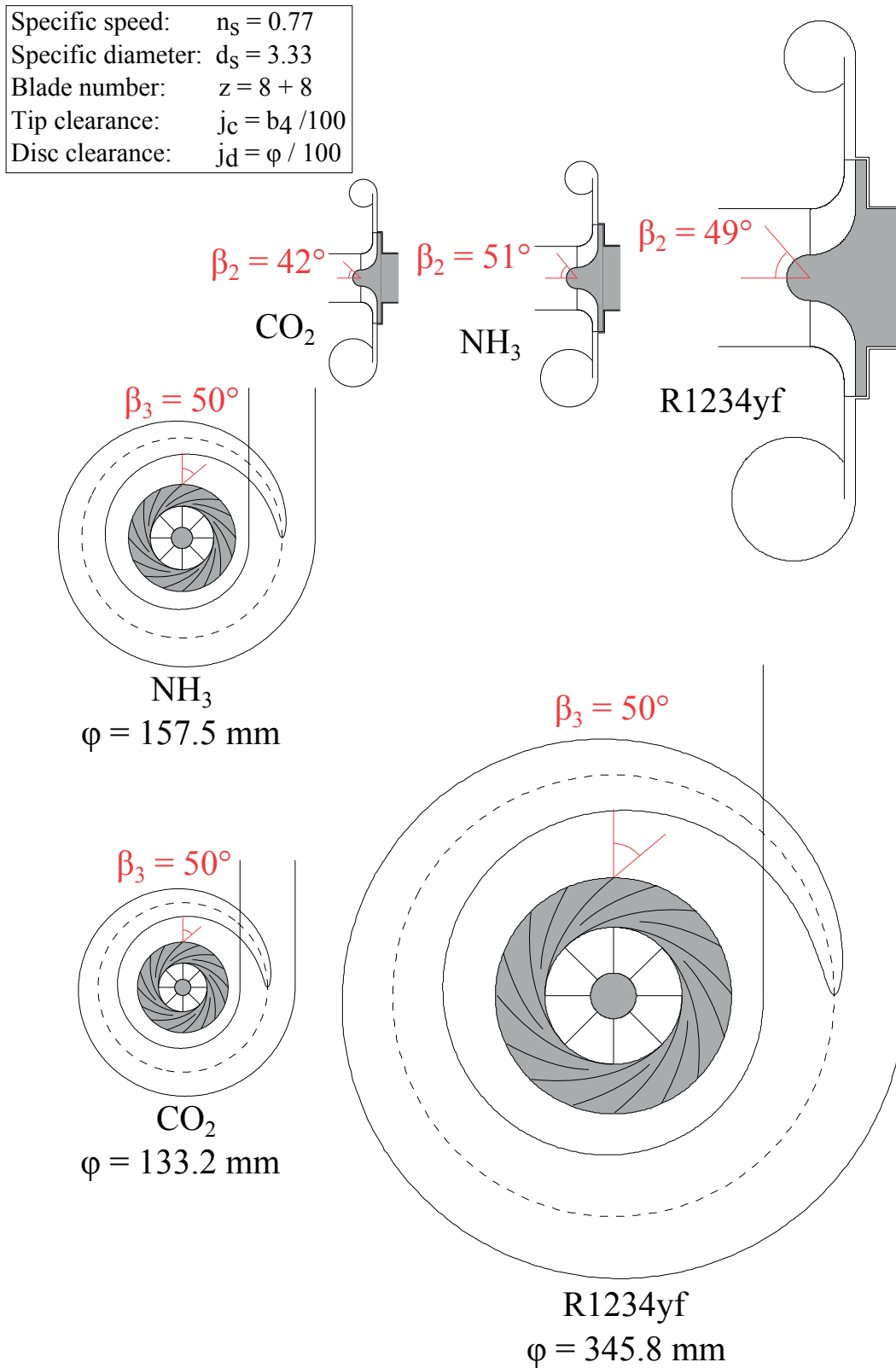


Figure A.2 – CO<sub>2</sub> network: Geometry of the centrifugal compressors with vaneless diffusers proposed for the central plant's heat pump of CO<sub>2</sub> based district energy networks. The three different compressors are represented on the same scale.

## B Cost functions

When possible, it was decided to rely on cost functions derived from pricing information that could be found in catalogues of various suppliers or in budgetary offers. For the decentralized heat pumps used for space heating and hot water preparation, it was found that a reasonable cost function could be derived, linking the nominal electric power of the compressor to the cost of the machine. Data from a total of 95 brine-water heat pumps were used. These data points and the cost function derived from them are shown at Fig. B.1. Note that the electric power used as a reference for the cost function corresponds to the standard test condition B0W55 [EN 14511]. This particular point was chosen as it corresponds to the highest electric power reported available for all the 95 machines surveyed.

The costs of the compressors at the central plant have been calculated using a cost function derived from catalogue prices. Data from a total of 832 compressors have been used. The data cover several type of volumetric compressor, from piston compressors used residential refrigeration to 300 kWe twin-screw compressors. A cost function relating catalogue prices to the suction volume flowrate, maximum suction pressure and maximum discharge pressure was derived from the data points. The data points and the cost function are shown on Fig. B.2. The cost of the booster compressors required on each vapour line, as well the cost of the compressors used for refrigeration were calculated using the same cost function.

A cost function was also derived from catalogue prices to compute the cost of the heat exchangers used in refrigeration and free cooling applications. It is based on data from 206 heat exchangers, all of them being either brazed plate or shell and tubes types. As brazed plate heat exchangers appear to be cheaper, it was chosen to fit the cost function on them only. The points and the cost function associated are shown on Fig. B.3.

Finally, another cost function was derived for centrifugal single stage, water pumps, in order to have a realistic evaluation of the cost the decentralized pumping scheme proposed for the cold water network. The cost function was derived from catalogue prices of 157 single stage, centrifugal water pumps. The sizing parameter chosen is the isentropic power at nominal



## Appendix B. Cost functions

---

conditions, defined as follows:

$$\dot{E}_s = \dot{V}_n \Delta P_n$$
$$\text{with: } \dot{V}_n = \dot{V}_{min} + 0.7(\dot{V}_{max} - \dot{V}_{min}), \quad \Delta P_n = f(\dot{V}_n) \quad (\text{B.1})$$

In equation B.1  $\dot{V}_{max}$  and  $\dot{V}_{min}$  are the *max* and *min* volume flowrate of the pump characteristics obtained from the manufacturer [lowara].  $\Delta P_n$  is the pressure differential at the nominal flowrate. It is an estimation based on a quadratic polynomial fit of the pump characteristics. The choice of the nominal flowrate is somewhat arbitrary, but was chosen since many of the 157 pumps surveyed had their maximum efficiency at around 70% of the flowrate range. The dataset and the cost function are visible at Fig. B.4.

## Cost of decentralized heat pumps

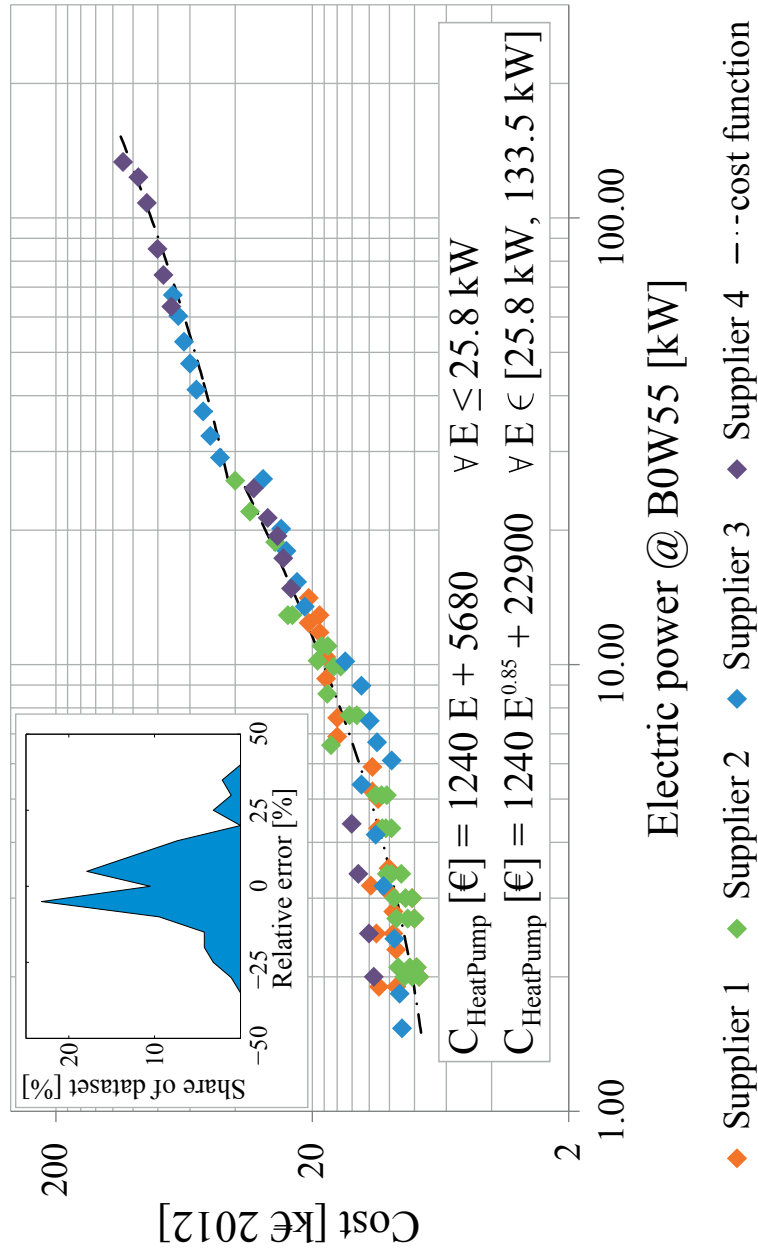


Figure B.1 – Cost function for brine-water heat pumps. The 95 data points on which it was derived are shown for the four different suppliers. An histogram of the relative error between predicted and real costs is also provided.

# Cost of compressors

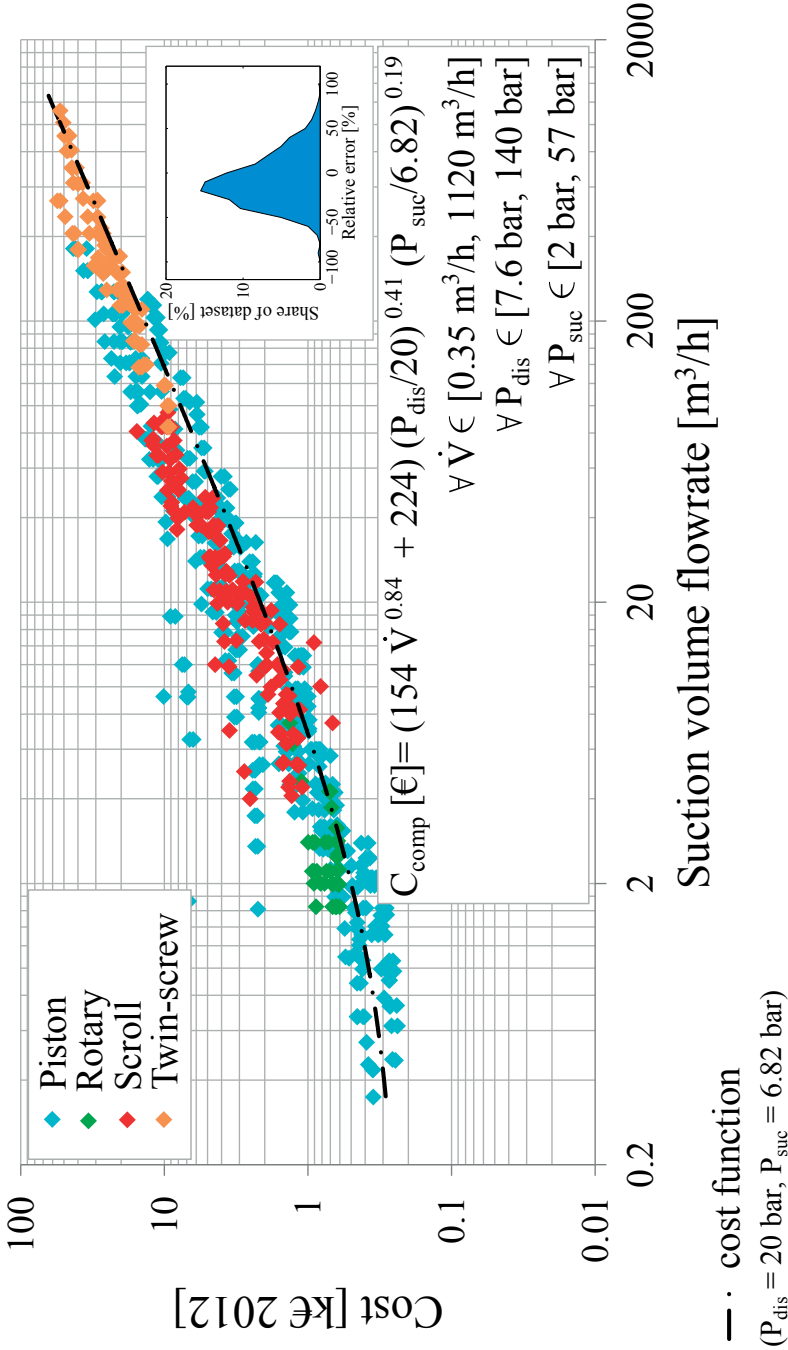


Figure B.2 – Cost function for the compressors. The 832 data points on which it was derived are shown for the four different types of machines included in the survey. An histogram of the relative error between predicted and real costs is also provided.

# Cost of heat exchangers

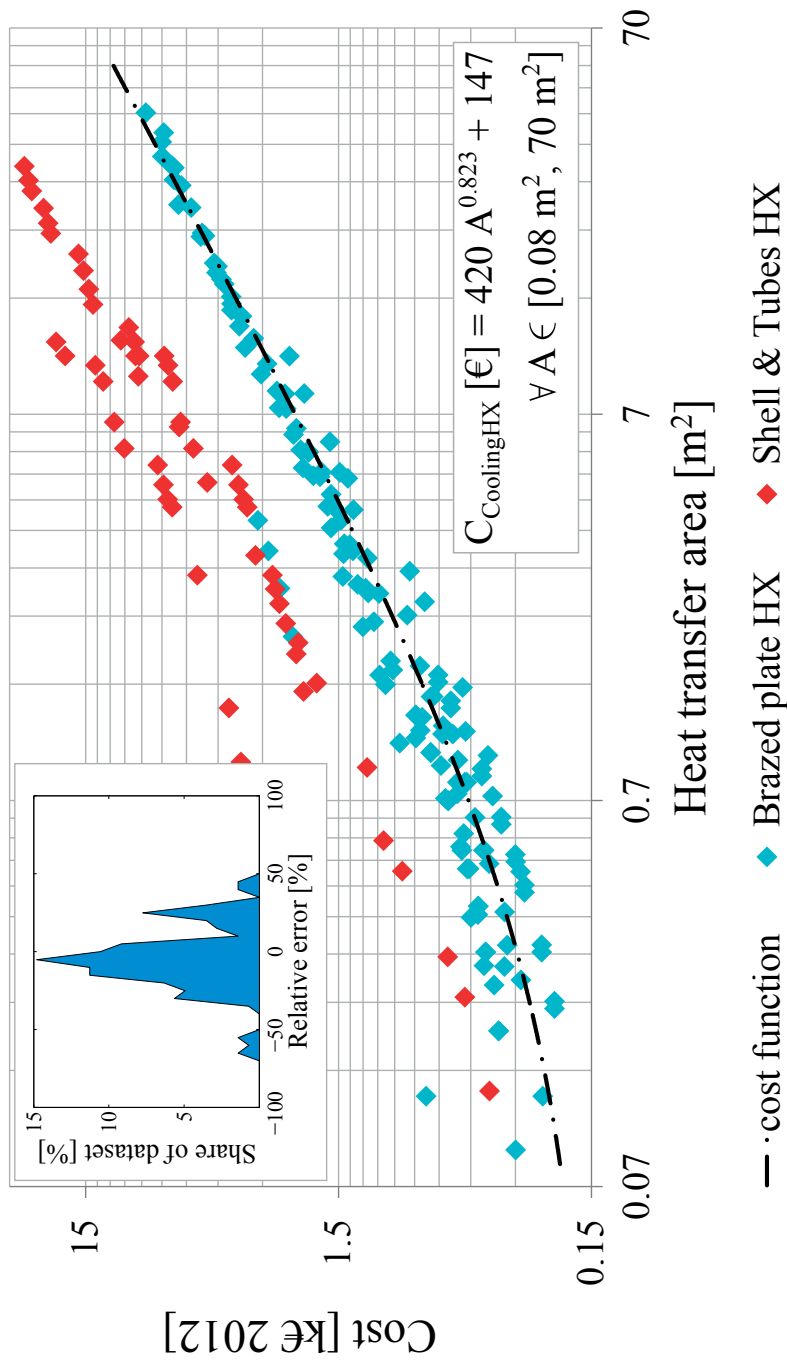


Figure B.3 – Cost function for the heat exchangers. The 206 data points are shown for the two types of heat exchangers surveyed. The cost function is fitted on the plate heat exchangers exclusively. An histogram of the relative error between predicted and real costs is also provided.

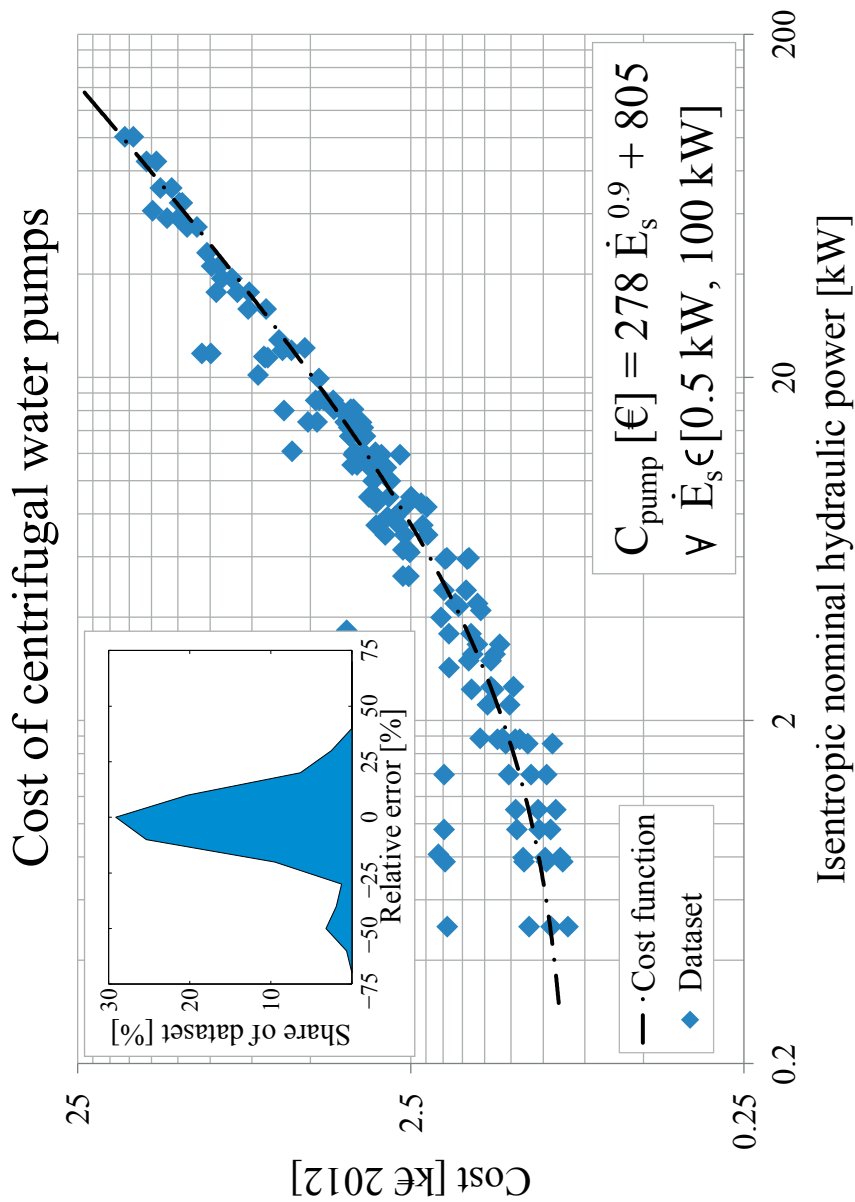


Figure B.4 – Cost function for the water pumps used in the cold water network. The 157 data points are visible as well as the cost function fitted from them. An histogram of the relative error between predicted and real costs is also provided.

## C Description of the safety concept

During the design phase of the test facility, it appeared necessary to clarify the responsibility of each participant since it was designed and operated by EPFL personnel, built by an external refrigeration company and installed in a building that belongs to SIG<sup>1</sup>, one of the two industrial partners of the research project. Eventually it was required to follow the procedure to get the european certification (CE mark) of the test facility. An external consultant experienced with the certification of refrigeration plants was contracted and help the EPFL team<sup>2</sup> getting the job done.

The procedure consisted in the following steps:

**1 - Preliminary risk analysis according to 2006/42/CE "machines":** A preliminary risk analysis was done in conformity with the "machines" directive of the european union [135]. The various potential damages and their probability of occurrence were evaluated in a heuristic way. Then prevention/protection measures were proposed and the residual risk was evaluated. As long as the residual risk remains too high (again based on a heuristic evaluation) additional measures must be adopted. The process is repeated until all the residual risks reach at least the acceptability threshold.

**2 - evaluation of the safety category according to PED EC 97/23:** The evaluation of the safety category had to be done according to the Pressure Equipment Directive (PED) EC 97/23 [78]. Since CO<sub>2</sub> is a fluid of group 2 according to the PED, the components of the test bench assimilable to vessels had to be checked against Table 2 (art 3, sec 1.1 (a) second indent) and those assimilable to piping,<sup>3</sup> had to be checked against Table 7 (art 3, sec 1.3 (a) second indent). In the present case the determining equipment is the heat exchanger at the central plant (27001), with  $P_s \cdot V = 320 \text{ bar l}$ . Making the test bench a Cat. II system. As a result, all the components connected to the system and falling under PED regulation had to have a certification for at least Cat. II. Once the PED category of

---

<sup>1</sup>Geneva's utility company

<sup>2</sup>To make it clear: The author and a student that was doing his master thesis.

<sup>3</sup>For instance plate heat exchangers are assimilated to vessels but shell and tube heat exchangers to piping.

## Appendix C. Description of the safety concept

---

the system is known, a particular certification module must be chosen, depending on the category, several choices are possible. In the present case a module "G" (EC unit verification) certification was done .

- 3 - Control chains with safety functionalities:** Based on the preliminary risk analysis and by applying the methodology of the standard ISO 13849 [79, 80] to determine the required performance level (PLr). Which in the present case was found to be "d". Some equipment are still characterized with an older metric - the safety integrity level (SIL). By correspondence, the SIL required for functional safety is SIL2. To ensure this level, all the components of control chain ensuring safety functionalities had to be at least PL: *d* or SIL2 certified.
- 4 - Ordinance on low voltage electric installations (OIBT):** The conformity of the test bench was also checked regarding electric safety [136]. The conformity of the wiring was checked by a certified inspector.
- 4 - Preparation of the documentation:** The documentation including operation manual, filling procedure, safety procedures, list of responsible persons... was prepared and sent to an official control body - SQS. To get the official certification.
- 5 - Pressure integrity test:** The last step consisted in testing the system resistance to 70.4 bar of nitrogen (1.1 time the service pressure) under the scrutiny of a representative of the control body, who delivered the authorisation to fill the system with CO<sub>2</sub> after the test succeeded.

The risk linked to pressure build-ups in the liquid lines was dealt with by installing check valves (used as safety valves) that would discharge in the vapour lines (See Fig. 2.1). Every section of liquid line that can be hydraulically isolated was connected to such a valve (150XX)<sup>4</sup>. The risk linked to pressure build-ups in vapour lines was dealt with by installing safety valves that discharge in the room. The risk associated with an excessive concentration of CO<sub>2</sub> in the room was dealt with by installing a CO<sub>2</sub> detector underneath the test bench<sup>5</sup>. If the concentration exceeds 5000 ppm (0.5 % Vol.):

- A sound alarm is triggered inside and outside of the room.
- A visual signal, installed inside the room, above the door is switched on. It instructs people to leave the room.
- A flashing light, installed inside the room, above the door, is switched on.
- A visual signal, installed inside the room, above the door, is switched on. It instructs people not to enter the room.

---

<sup>4</sup>The numbers refer to those used at Fig. 2.1.

<sup>5</sup>CO<sub>2</sub> is heavier than air at atmospheric pressure and temperature.



- 
- A flashing light, installed above the door, outside the room, is switched on.
  - The ventilation in the room is switched on at its highest speed setting.
  - The power supply of the test bench is switched off. As all electric and pneumatic valves are of the normally closed type, it triggers the sectioning of the network by valves 10XX and 20XX, the stopping of the heat supply (110XX) and it also stops all the pumps.
  - An alarm is relayed to the security lodge of the site. The security staff has instruction to send someone, to force the ventilation "on"<sup>6</sup>, contact the person responsible for the facility by phone (the author) and, as soon as the reading on the monitor<sup>7</sup> of the gas detector indicates less than 0.05 % Vol. check if there is someone in the room in need for help.

Additionally, the room being normally unoccupied, the operators are required to announce they will be working on the test bench upon arrival on site. When only one operator is in the room he is required to wear a *lone worker protection system*, that transmits an alarm to the safety lodge, when the system has been immobile for a certain period of time or when a shock is detected.

The risk associated with a rapid release of CO<sub>2</sub> in the room (catastrophic rupture of a component) was dealt by installing two pressure switches, one on the liquid and one on the vapour main line. If they are submitted to a pressure of less than 40.6 bar<sup>8</sup>, they open the electric circuit, shutting of the power supply. Consequently, it triggers the sectioning of the network by valves 10XX and 20XX, the stopping of the heat supply (110XX) and it also stops all the pumps.

The power supply of the gas detection and of the various alarm signals is a separate one and has a battery backup. It ensures that the same level of safety is maintained even during a power outage of a few hours.

---

<sup>6</sup>Switch installed outside next to the entrance of the room

<sup>7</sup>Also located outside next to the entrance of the room

<sup>8</sup>Lowest possible pressure when temperature of the chilled water is the coldest.



## Bibliography

- [1] World Bank Group, “Website of the world bank group, data on urban population.” <http://data.worldbank.org/indicator/SP.URB.TOTL.IN.ZS>.
- [2] B. A. Lewis J.O., Ní Hógáin S., “Building energy efficiency in european cities,” tech. rep., European Regional Development Fund - URBACT II, 2013.
- [3] T. Infrac AG, Prognos AG, “Analyse des schweizerischen energieverbrauchs 2000 - 2014 nach verwendungszwecken,” tech. rep., Swiss Federal Office of Energy SFOE, 2015.
- [4] J. F. Gibert, J-P., “Using geothermal waters in france: The district heating system of chaudes-aigues from the middle ages,” in *Stories From a Heated Earth: Our Geothermal Heritage*.
- [5] Euroheat and power, “Website of euroheat and power – statistical data on district heating and cooling for member states.” <http://www.euroheat.org/DHC---Statistics-4.aspx>.
- [6] H. Lund, S. Werner, R. Wiltshire, S. Svendsen, J. E. Thorsen, F. Hvelplund, and B. V. Mathiesen, “4th generation district heating (4gdh): Integrating smart thermal grids into future sustainable energy systems,” *Energy*, vol. 68, pp. 1 – 11, 2014.
- [7] A. D. Rosa and J. Christensen, “Low-energy district heating in energy-efficient building areas,” *Energy*, vol. 36, no. 12, pp. 6890 – 6899, 2011.
- [8] H. Tol and S. Svendsen, “Improving the dimensioning of piping networks and network layouts in low-energy district heating systems connected to low-energy buildings: A case study in roskilde, denmark,” *Energy*, vol. 38, no. 1, pp. 276 – 290, 2012.
- [9] IEA, “Linking heat and electricity systems,” tech. rep., International Energy Agency IEA, 2014.
- [10] N. L. Truong and L. Gustavsson, “Cost and primary energy efficiency of small-scale district heating systems,” *Applied Energy*, vol. 130, pp. 419 – 427, 2014.
- [11] M. Åberg, J. Widén, and D. Henning, “Sensitivity of district heating system operation to heat demand reductions and electricity price variations: A swedish example,” *Energy*, vol. 41, no. 1, pp. 525 – 540, 2012. 23rd International Conference on Efficiency, Cost, Optimization, Simulation and Environmental Impact of Energy Systems, {ECOS} 2010.

## Bibliography

---

- [12] B. Rezaie and M. A. Rosen, "District heating and cooling: Review of technology and potential enhancements," *Applied Energy*, vol. 93, pp. 2 – 10, 2012. (1) Green Energy; (2)Special Section from papers presented at the 2nd International Energy 2030 Conf.
- [13] P. A. Ostergaard and H. Lund, "A renewable energy system in frederikshavn using low-temperature geothermal energy for district heating," *Applied Energy*, vol. 88, no. 2, pp. 479 – 487, 2011. The 5th Dubrovnik Conference on Sustainable Development of Energy, Water and Environment Systems, held in Dubrovnik September/October 2009.
- [14] X. Pelet, D. Favrat, and A. Vögeli, "Performances of 3.9 MWTH Ammonia Heat Pumps within a District Heating Cogeneration Power Plant: Status After Eleven Years of Operation.," tech. rep., 1997.
- [15] P-A. Viquerat, "Utilisation des réseaux d'eau lacustre profonde pour la climatisation et le chauffage des bâtiments; bilan énergétique et impacts environnementaux: Etude de cas: le projet gln (genève-lac-nations) à genève," tech. rep., 2012. ID: unige:23016.
- [16] Y. Li, L. Fu, S. Zhang, and X. Zhao, "A new type of district heating system based on distributed absorption heat pumps," *Energy*, vol. 36, no. 7, pp. 4570 – 4576, 2011.
- [17] S. Winiger, S. Herkel, and G. Haroske, "Power generation using district heat: Energy efficient retrofitted plus-energy school rostock," *Energy Procedia*, vol. 48, pp. 1519 – 1528, 2014. Proceedings of the 2nd International Conference on Solar Heating and Cooling for Buildings and Industry (SHC 2013).
- [18] Groupe E, "Webpage of the group e utility company on the district heating network of la tour-de-peilz." <http://www.groupe-e.ch/cad-la-tour-de-peilz>.
- [19] M. G. T. Sulzer, "Eth zürich, honggerberg masterplan energie," in *Proceedings of 15. Schweizerisches Status-Seminar "Energie und Umweltforschung im Bauweisen"*, (Zürich, Switzerland), 2008.
- [20] Lauber IWISA AG, "Information leaflet on the "anerginetz" of west visp." [http://www.lauber-iwisa.ch/data/Ressources/1353872213-Projektblatt\\_Anergienetz\\_fix\\_Low.pdf](http://www.lauber-iwisa.ch/data/Ressources/1353872213-Projektblatt_Anergienetz_fix_Low.pdf).
- [21] EnAlpin AG, "Website of the company operating the "anerginetz" of naters." <http://www.enalpin.ch/unternehmen/fernwaerme/anergienetzners.php>.
- [22] C. Weber, *Multi-objective design and optimization of district energy systems including polygeneration energy conversion technologies*. PhD thesis, STI, Lausanne, 2008.
- [23] C. Weber and D. Favrat, "Conventional and advanced CO2 based district energy systems," *Energy*, vol. 35, no. 12, pp. 5070–5081, 2010.
- [24] S. Henchoz, C. Weber, and F. Marechal, "On a multi-service, CO2 based, district energy system for a better efficiency of urban areas," in *Proceedings of the World Engineering Convention*, (Geneva, Switzerland), 2011.

- [25] S. Henchoz, D. Favrat, and C. Weber, "Performance and profitability perspectives of a CO<sub>2</sub> based district energy network in geneva's city center," in *Proceedings of the 13th International Symposium on District Heating and Cooling*, (Copenhagen, Denmark), 2012.
- [26] S. Henchoz, C. Weber, F. Maréchal, and D. Favrat, "Performance and profitability perspectives of a CO<sub>2</sub> based district energy network in geneva's city centre," *Energy*, vol. 85, pp. 221 – 235, 2015.
- [27] Swiss Federal Office of Environment, "Liste des principaux fluides frigorigènes," tech. rep., 2014.
- [28] S. Henchoz, P. Chatelan, F. Maréchal, and D. Favrat, "Key energy and technological aspects of three innovative concepts of district energy networks," in *Proceedings Of the 28th International Conference On Efficiency, Cost, Optimization, Simulation and Environmental Impact Of Energy Systems*, (Pau, France), 2015.
- [29] L. Gerber, *Integration of Life Cycle Assessment in the conceptual design of renewable energy conversion systems*. PhD thesis, STI, Lausanne, 2012.
- [30] M. Rocco, E. Colombo, and E. Sciubba, "Advances in exergy analysis: a novel assessment of the extended exergy accounting method," *Applied Energy*, vol. 113, pp. 1405 – 1420, 2014.
- [31] DOE, "Technology readiness assessment guide," tech. rep., U.S. Department of Energy, 2011.
- [32] R. Romanowicz, "Reseau urbain de distribution de la chaleur et du froid employant le CO<sub>2</sub>," tech. rep., Geneva's Cantonal Office for Energy, 2011.
- [33] SIA, "L'énergie dans le bâtiment," tech. rep., Société suisse des ingénieurs et architectes, 1988.
- [34] L. Girardin, *A GIS-based Methodology for the Evaluation of Integrated Energy Systems in Urban Area*. PhD thesis, STI, Lausanne, 2012.
- [35] S. Hammarsten, "A critical appraisal of energy-signature models," *Applied Energy*, vol. 26, no. 2, pp. 97 – 110, 1987.
- [36] M. Mourshed, "Relationship between annual mean temperature and degree-days," *Energy and Buildings*, vol. 54, pp. 418 – 425, 2012.
- [37] OCEN, "Directive relative au calcul de l'indice de dépense de chaleur," tech. rep., Geneva's Cantonal Office for Energy, 2014.
- [38] SITG, "Le territoire genevois à la carte." [http://ge.ch/carte/pro/?mapresources=GEOTHERMIE%2CENERGIE\\_SOLAIRE%2CENERGIE&hidden=GEOTHERMIE%2CENERGIE\\_SOLAIRE](http://ge.ch/carte/pro/?mapresources=GEOTHERMIE%2CENERGIE_SOLAIRE%2CENERGIE&hidden=GEOTHERMIE%2CENERGIE_SOLAIRE).

## Bibliography

---

- [39] L. Borel and D. Favrat, *Thermodynamics and Energy Systems Analysis; From Energy to Exergy*. Lausanne: Presses Polytechniques et Universitaires Romandes PPUR, 2010.
- [40] Swiss Federal Council, “Ordinance on air pollution control.” <https://www.admin.ch/opc/en/classified-compilation/19850321/index.html>, 2010.
- [41] E. Schramek and H. Recknagel, *Taschenbuch für Heizung + Klimatechnik 07/08*. Oldenbourg Industrieverlag, 2007.
- [42] S. Henchoz, F. Buchter, D. Favrat, M. Morandin, and M. Mercangöz, “Thermoeconomic analysis of a solar enhanced energy storage concept based on thermodynamic cycles,” *Energy*, vol. 45, no. 1, pp. 358 – 365, 2012.
- [43] Eurovent Certification, “Certification programme of liquid chilling packages and heat pumps (lcp-hp).” [http://www.eurovent-certification.com/en/Certification\\_Programmes/Programme\\_Descriptions.php?lg=en&rub=03&srub=01&select\\_prog=LCP-HP](http://www.eurovent-certification.com/en/Certification_Programmes/Programme_Descriptions.php?lg=en&rub=03&srub=01&select_prog=LCP-HP).
- [44] European Commission, “Official journal of the european union - commission regulation no 813/2013.” <http://eur-lex.europa.eu/legal-content/EN/TXT/PDF/?uri=CELEX:32013R0813&from=EN>, 2013.
- [45] A. Mermoud, B. M. Lachal, W. Weber, and P.-A. Viquerat, “Hcr building : Measuring cooling installations and auditing for deep lake direct cooling network connectivity,” 333; 333.7-333.9, 2007. ID: unige:38784.
- [46] A. Mermoud, W. Weber, B. M. Lachal, and P.-A. Viquerat, “Un building: Measuring cooling installations and auditing for deep lake direct cooling network connectivity,” 333; 333.7-333.9, 2007. ID: unige:38785.
- [47] Alpha-Innotec, “Série alterra swc - pompes à chaleur sol/eau compacte - chauffage.” <http://www.alpha-innotec.ch/alpha-innotec/produits/pompes-a-chaleur/soleau/swc-102h3.html?L=2>.
- [48] Waterkotte EuroTherm, “Pompes à chaleur géothermiques - eco touch ail geo.” <http://www.waterkotte.ch/produits/pompes-a-chaleur/pompes-a-chaleur-geothermiques/eco-touch-ail-geo/?L=1>.
- [49] C. Weber, “CO2 based district energy system.” Patent. US2010018668, 2008.
- [50] M. Mohanraj, S. Jayaraj, and C. Muraleedharan, “Environment friendly alternatives to halogenated refrigerants—a review,” *International Journal of Greenhouse Gas Control*, vol. 3, no. 1, pp. 108 – 119, 2009.
- [51] Z. Yang and X. Wu, “Retrofits and options for the alternatives to hcfc-22,” *Energy*, vol. 59, pp. 1 – 21, 2013.

- [52] U. N. E. Programme, “Enabling a global phase-down of hydrofluorocarbons: discussion paper submitted by the european union,” in *Twenty-sixth meeting of the parties to the montreal protocol on substances that deplete the ozone layer*, (Paris, France), pp. 17–21, 2014.
- [53] Swiss Federal Council, “Ordonnance sur la réduction des risques liés à l’utilisation de substances, de préparations et d’objets particulièrement dangereux.” <https://www.admin.ch/opc/fr/classified-compilation/20021520/index.html#app29>.
- [54] Waterkotte EuroTherm, “Pompes à chaleur géothermiques - ds 6500.” <http://www.waterkotte.ch/produits/pompes-a-chaaleur/pompes-a-chaaleur-geothermiques/ds-6500/?L=1>.
- [55] Bitzer, “Screw compressors.” <https://www.bitzer.de/gb/en/products/Technologies/Screw-Compressors/>.
- [56] Schweizerische Normen-Vereinigung, “Refrigerant compressors - rating conditions, tolerances and presentation of manufacturer’s performance data,” Standard SN EN 12900, Winterthur, Switzerland, 2013.
- [57] NIST, “Reference fluid thermodynamic and transport properties database - REFPROP.” <http://www.nist.gov/srd/nist23.cfm>.
- [58] H. Recknagel, E. Sprenger, W. Hönnmann, and J.-L. Cauchepin, *Le recknagel : Manuel Pratique du Génie Climatique*. Paris, France, pyc ed., 1986.
- [59] S. Churchill, “Friction-factor equation spans all fluid-flow regimes,” *Chemical Engineering*, 1977.
- [60] Danfoss, “Danfoss turbocor technology.” <http://airconditioning.danfoss.com/products/compressors/turbocor/>.
- [61] Grundfos. <https://product-selection.grundfos.com/>.
- [62] xylect. [http://www.xylect.com/bin/Xylect.dll?IS\\_\\_NEXTPAGE=startup&IS\\_\\_NEXTPAGE=BDYHOME&IS\\_\\_AREA=SWITZERLAND&IS\\_\\_COUNTRY=SWITZERLAND](http://www.xylect.com/bin/Xylect.dll?IS__NEXTPAGE=startup&IS__NEXTPAGE=BDYHOME&IS__AREA=SWITZERLAND&IS__COUNTRY=SWITZERLAND).
- [63] R. Whitesides, “Basic pump parameters and the affinity laws.” <http://www.pdhonline.org/courses/m125/m125content.pdf>.
- [64] I. Koronaki, D. Cowan, G. Maidment, K. Beerman, M. Schreurs, K. Kaar, I. Chaer, G. Gontarz, R. Christodoulaki, and X. Cazauran, “Refrigerant emissions and leakage prevention across europe – results from the realskillseurope project,” *Energy*, vol. 45, no. 1, pp. 71 – 80, 2012.
- [65] M. Peters, T. Klaus D, and R. E. West, *Plant design and economics for chemical engineers*. 2003.

## Bibliography

---

- [66] V. Curti, *Modélisation et optimisation environnriques de systèmes de chauffage urbain alimentés par pompes à chaleur*. PhD thesis, Lausanne, 1998.
- [67] Swiss Federal Office for Statistics, “Swiss index for construction prices.” <http://www.bfs.admin.ch/bfs/portal/fr/index/themen/05/05/blank/key/baupreisindex/schweiz.Document.88739.xls>.
- [68] Swiss Federal Office for Statistics, “Prix moyens de l’énergie.” <http://www.bfs.admin.ch/bfs/portal/fr/index/infothek/lexikon/lex/0.Document.124153.xls>.
- [69] Swiss Federal Office for Statistics, “Prix moyens annuels du mazout.” <http://www.bfs.admin.ch/bfs/portal/fr/index/infothek/lexikon/lex/0.Document.88038.xls>.
- [70] A. v. Bassewitz, N. Jansen, and V. Liebel, “Flexible, pre-insulated polymer district heating pipes: A service lifetime study,” tech. rep., •, •.
- [71] Chemical Engineering, “Website of the journal of chemical engineering.” <http://www.chemengonline.com/pci-home>.
- [72] Swiss Federal Office for Statistics, “Hourly manpower costs per economical sector.” <http://www.bfs.admin.ch/bfs/portal/fr/index/themen/06/04/blank/data.html>.
- [73] Swiss Federal Office for Statistics, “Standard work hours in industry per economical sector.” <http://www.bfs.admin.ch/bfs/portal/fr/index/themen/03/02/blank/data/07.html>.
- [74] J.-B. Fressoz, *L'apocalypse joyeuse. Une histoire du risque technologique*. Paris, France: Le Seuil, 2012.
- [75] Schweizerische Normen-Vereinigung, “Refrigerating systems and heat pumps. safety and environmental requirements. basic requirements, definitions, classification and selection criteria,” Standard SN EN 378-1+A2, Winterthur, Switzerland, 2012.
- [76] Schweizerische Normen-Vereinigung, “Refrigerating systems and heat pumps. safety and environmental requirements. design, construction, testing, marking and documentation,” Standard SN EN 378-2+A2, Winterthur, Switzerland, 2012.
- [77] Schweizerische Normen-Vereinigung, “Refrigerating systems and heat pumps. safety and environmental requirements. installation site and personal protection,” Standard SN EN 378-3+A1, Winterthur, Switzerland, 2012.
- [78] European Commission, “Official journal of the european union - directive 97/23/ec on the approximation of the laws of the member states concerning pressure equipment.” <http://eur-lex.europa.eu/legal-content/EN/TXT/PDF/?uri=CELEX:31997L0023&from=EN>.



- [79] ISO, "ISO 13849-1:2006 - safety of machinery - safety-related parts of control systems - Part 1: General principles for design." [http://www.iso.org/iso/catalogue\\_detail.htm?csnumber=34931](http://www.iso.org/iso/catalogue_detail.htm?csnumber=34931).
- [80] ISO, "ISO 13849-2:2012 - safety of machinery – safety-related parts of control systems – Part 2: Validation." [http://www.iso.org/iso/iso\\_catalogue/catalogue\\_tc/catalogue\\_detail.htm?csnumber=53640](http://www.iso.org/iso/iso_catalogue/catalogue_tc/catalogue_detail.htm?csnumber=53640).
- [81] Swiss Federal Council, "Ordonnance sur les installations de transport par conduites." <https://www.admin.ch/opc/fr/classified-compilation/20000118/index.html>, 2000.
- [82] Swiss Federal Council, "Federal act on the protection of the environment." <https://www.admin.ch/opc/en/classified-compilation/19830267/index.html>, 1983.
- [83] Swiss Federal Council, "Ordinance on protection against major accidents." <https://www.admin.ch/opc/en/classified-compilation/19910033/index.html>, 1991.
- [84] Federal Office of Environment Switzerland, *Manuel I de l'ordonnance sur les accidents majeurs (OPAM): Aide à l'exécution pour entreprises utilisant des substances, des préparations ou des déchets spéciaux*. Bern, Switzerland, 2008.
- [85] Federal Office of Environment Switzerland, *Manuel II de l'ordonnance sur les accidents majeurs (OPAM): Aide à l'exécution à destination des entreprises utilisant des microorganismes*. Bern, Switzerland, 2013.
- [86] Federal Office of Environment Switzerland, *Manuel II de l'ordonnance sur les accidents majeurs (OPAM): Directives pour voies de communication*. Bern, Switzerland, 1992.
- [87] Federal Office of Environment Switzerland, *Methodikbeispiel für eine Risikoermittlung einer Flüssiggas-Tankanlage - Störfallverordnung*. Bern, Switzerland, 1996.
- [88] Federal Office of Environment Switzerland, *Rapport-cadre sur la Sécurité des installations de stockage d'hydrocarbures*. Bern, Switzerland, 2005.
- [89] Suisseplan Ingenieure AG, *Sécurité des installations de gaz à haute pression - Explications relatives au "rapport-cadre de l'estimation de l'ampleur des dommages et de l'étude de risque standardisées"*. Zürich, Switzerland, 2010.
- [90] Federal Office of Environment Switzerland, *La sécurité des patinoires artificielles - Ordonnance sur les accidents majeurs*. Bern, Switzerland, 1993.
- [91] T. Lewandowski, "Additional risk assessment of alternative of refrigerant r-1234yf." [http://www.sae.org/standardsdev/tsb/cooperative/crp\\_1234-4\\_report.pdf](http://www.sae.org/standardsdev/tsb/cooperative/crp_1234-4_report.pdf), 2013.
- [92] A. B. Pearson, *CO2 as a Refrigerant. (Digital or Paper version)*. France: IIF-IIR, 2014.
- [93] *District heating systems used in Western Europe*, ch. 2. Danfoss.

## Bibliography

---

- [94] Climatecenter, "Price of gas refrigerants r1234ze." [http://www.climatecenter.co.uk/en/brands/a-gas/a-gas-refrigerants-/CategoryDisplay?facet1=ads\\_f10018\\_ntk\\_cs%3AR1234ZE&storeId=10951&catalogId=11601&langId=44&categoryId=219161&pageView=detailed&pageSize=24&sortColumn=score&sortType=desc](http://www.climatecenter.co.uk/en/brands/a-gas/a-gas-refrigerants-/CategoryDisplay?facet1=ads_f10018_ntk_cs%3AR1234ZE&storeId=10951&catalogId=11601&langId=44&categoryId=219161&pageView=detailed&pageSize=24&sortColumn=score&sortType=desc).
- [95] SCS-tec, "Price of gas refrigerants r1234yf." [http://shop.scstec.de/product\\_info.php/info/p587\\_kaeltemittel-r1234yf--5-kg--mehrwegflasche.html](http://shop.scstec.de/product_info.php/info/p587_kaeltemittel-r1234yf--5-kg--mehrwegflasche.html).
- [96] Swiss Federal Council, "Message relatif au premier paquet de mesures de la stratégie énergétique 2050 (révision du droit de l'énergie) et à l'initiative populaire fédérale "pour la sortie programmée de l'énergie nucléaire"." <https://www.admin.ch/opc/fr/federal-gazette/2013/6771.pdf>, 2013.
- [97] S. Ross, *Simulation*. Elsevier Science, 2012.
- [98] Debrunner Acifer, "Indices de prix de produits de construction." [https://www.dkh.ch/da/media/da\\_home/produkte/unsere\\_sortiment/stahl\\_metalle/KBOB-Preisindizes-Baugewerbe.pdf](https://www.dkh.ch/da/media/da_home/produkte/unsere_sortiment/stahl_metalle/KBOB-Preisindizes-Baugewerbe.pdf), 2010.
- [99] Swiss Federal Office for Statistics, "Indice suisse des prix à la consommation." <http://www.bfs.admin.ch/bfs/portal/fr/index/themen/05/02/blank/data.Document.88060.xls>.
- [100] Swiss Federal Office for Statistics, "Bâtiments selon la catégorie de bâtiment, les cantons et l'époque de construction." <http://www.bfs.admin.ch/bfs/portal/fr/index/infothek/lexikon/lex/0.Document.21134.xls>.
- [101] Société Suisse des Ingénieurs et des Architectes, "Bases pour les calculs énergétiques des bâtiments." <http://shop.sia.ch/collection%20des%20normes/architecte/sia%20380/f/F/Product>, 2015.
- [102] Deutsches Institut für Normung, "Road and foot bridges; design loads." <http://www.din.de/en/wdc-beuth:din21:1813802>, 1967.
- [103] ISO-PLUS, "Design manual from isoplus for its district heating products.." <http://www.isoplus-pipes.com/en/download/design-manual/>.
- [104] Brugg pipesystems AG, "Leaflet on "stamant" double wall pipes from brugg pipesystems.." [http://www.pipesystems.com/domains/pipesystems\\_com/data/free\\_docs/STAMANT\\_SysBeschrbg\\_D\\_15sep09.pdf](http://www.pipesystems.com/domains/pipesystems_com/data/free_docs/STAMANT_SysBeschrbg_D_15sep09.pdf).
- [105] Shecco, "Guide 2012: Natural refrigerants - market growth for europe." <http://publication.shecco.com/publications/view/23>.
- [106] Shecco, "Guide 2013: Examples of nh3/co2 secondary systems for cold store operators." <http://publications.shecco.com/publications/view/20>.

- [107] Shecco, "Guide 2013: Natural refrigerants - market growth for north america." <http://publication.shecco.com/publications/view/6>.
- [108] Shecco, "Refrigerant circulation pumps – RC." <http://www.r744.com/products/view/184>.
- [109] Catpumps, "Liquid CO2 pumps - industrial duty liquid carbon dioxide pumps." <http://www.catpumps.com/products/liquid-co2-high-vapor-pumps.asp>.
- [110] Speck, "Speck-triplex high pressure plunger pumps in CO2-versions." <http://www.speck-triplex.de/en/co2-ausfuehrungen-en.html?search=>.
- [111] Catpumps, "5,7,15 PFR plunger pump service manual." <http://www.catpumps.com/products/pdfs/5-15FSvc.pdf>.
- [112] AlfaLaval, "CBXP27- brazed plate heat exchanger." <http://www.alfalaval.com/globalassets/documents/products/heat-transfer/plate-heat-exchangers/brazed-plate-heat-exchangers/cbxp27.pdf>.
- [113] Wilo, "Multicargo MC 605 (1 230 V)." [http://productfinder.wilo.com/en/FR/product/000000000028ae10001003a/fc\\_product\\_datasheet](http://productfinder.wilo.com/en/FR/product/000000000028ae10001003a/fc_product_datasheet).
- [114] Belimo, "Technical data sheet NRQ24A-SR." [http://www.belimo.ch/pdf/e/NRQ24A-SR\\_datasheet\\_en-gb.pdf](http://www.belimo.ch/pdf/e/NRQ24A-SR_datasheet_en-gb.pdf).
- [115] L. Cheng, G. Ribatski, J. M. Quibén, and J. R. Thome, "New prediction methods for CO2 evaporation inside tubes: Part I – A two-phase flow pattern map and a flow pattern based phenomenological model for two-phase flow frictional pressure drops," *International Journal of Heat and Mass Transfer*, vol. 51, no. 1–2, pp. 111 – 124, 2008.
- [116] L. Cheng, G. Ribatski, and J. R. Thome, "New prediction methods for CO2 evaporation inside tubes: Part II — An updated general flow boiling heat transfer model based on flow patterns," *International Journal of Heat and Mass Transfer*, vol. 51, no. 1–2, pp. 125 – 135, 2008.
- [117] W. Focke, J. Zachariades, and I. Olivier, "The effect of the corrugation inclination angle on the thermohydraulic performance of plate heat exchangers," *International Journal of Heat and Mass Transfer*, vol. 28, no. 8, pp. 1469 – 1479, 1985.
- [118] R. Longchamp, *Commande numérique de systèmes dynamiques: cours d'automatique*. Presses polytechniques et universitaires romandes, 2006.
- [119] C. Nicolet, *Hydroacoustic modelling and numerical simulation of unsteady operation of hydroelectric systems*. PhD thesis, STI, Lausanne, 2007.
- [120] S. Quoilin, R. Aumann, A. Grill, A. Schuster, V. Lemort, and H. Spliethoff, "Dynamic modeling and optimal control strategy of waste heat recovery organic rankine cycles," *Applied Energy*, vol. 88, no. 6, pp. 2183 – 2190, 2011.

## Bibliography

---

- [121] P. Haberschill, I. Guitari, and A. Lallemand, "Comportement dynamique d'une pompe à chaleur au CO<sub>2</sub> en cycles sous critique et transcritique," *International Journal of Refrigeration*, vol. 30, no. 4, pp. 732 – 743, 2007.
- [122] R. Shi, D. Fu, Y. Feng, J. Fan, and S. Mijanovic, "Dynamic modelling of CO<sub>2</sub> supermarket refrigeration systems," in *International Refrigeration and Air Conditioning Conference*, (Purdue, USA), 2010.
- [123] X. Jia, C. Tso, P. Jolly, and Y. Wong, "Distributed steady and dynamic modelling of dry-expansion evaporators: Modélisation du régime stable et du régime transitoire des évaporateurs à détente sèche," *International Journal of Refrigeration*, vol. 22, no. 2, pp. 126 – 136, 1999.
- [124] B. Li and A. G. Alleyne, "A dynamic model of a vapor compression cycle with shut-down and start-up operations," *International Journal of Refrigeration*, vol. 33, no. 3, pp. 538 – 552, 2010.
- [125] N. Liang, S. Shao, C. Tian, and Y. Yan, "Dynamic simulation of variable capacity refrigeration systems under abnormal conditions," *Applied Thermal Engineering*, vol. 30, no. 10, pp. 1205 – 1214, 2010.
- [126] D. Wei, X. Lu, Z. Lu, and J. Gu, "Dynamic modeling and simulation of an organic rankine cycle (ORC) system for waste heat recovery," *Applied Thermal Engineering*, vol. 28, no. 10, pp. 1216 – 1224, 2008.
- [127] gPROMS, "The gPROMS platform." <http://www.psenterprise.com/gproms/platform.html>.
- [128] F. P. Dewitt and D. P. Incropera, *Fundamentals of Heat and Mass Transfer*. John Wiley & Sons Inc, 1990.
- [129] Alfalaval, "CBXP52- brazed plate heat exchanger." <http://www.alfalaval.com/globalassets/documents/products/heat-transfer/plate-heat-exchangers/brazed-plate-heat-exchangers/cbxp52.pdf>.
- [130] LowFlow, "MK708 Series- fractional flow control valve." <http://www.lowflowvalve.com/sites/default/files/708.pdf>.
- [131] K. A. Bonvin, D., "Identification the systèmes dynamiques," 2008.
- [132] Barber-Nichols, "Pump chart." [http://www.barber-nichols.com/sites/default/files/wysiwyg/images/nsds\\_pump\\_chart.pdf](http://www.barber-nichols.com/sites/default/files/wysiwyg/images/nsds_pump_chart.pdf).
- [133] J. Schiffmann, *Integrated design, optimization and experimental investigation of a direct driven turbocompressor for domestic heat pumps*. PhD thesis, STI, Lausanne, 2008.

- [134] J. J. Dyreby, S. A. Klein, G. F. Nellis, and D. T. Reindl, "Modeling off-design operation of a supercritical carbon dioxide brayton cycle," in *Supercritical CO<sub>2</sub> Power Cycle Symposium*, (Boulder, Colorado), 2011.
- [135] European Commission, "Directive relative au machines et modifiant la directive 95/16/CE." <http://eur-lex.europa.eu/LexUriServ/LexUriServ.do?uri=OJ:L:2006:157:0024:0086:fr:PDF>, 2006.
- [136] Swiss Federal Council, "Ordonnance sur les installations électriques à basse tension." <https://www.admin.ch/opc/fr/classified-compilation/20012238/index.html>.



**Samuel Henchoz**  
Rue des Cordeires 13  
1124 Gollion CH.  
++41 +79 206 7271  
samuel.henchoz @epfl.ch

**Age:** 30  
**Sex:** Male  
**Nationality:** Swiss

I am interested in the **energy** domain, mostly in **thermal energy conversion**. I am an open-minded person, responsible and reliable. Furthermore I invest a lot of myself in everything I undertake.

## Education and Training

---

2008 – 2010      **Master EPF in mechanical engineering – Minor EPF in energy**  
2004 – 2008      **Engineering studies at EPFL**  
2001 – 2004      **Maturité (A-Levels) option Physics / maths at Gymnase de Morges**

## Employment

---

2010 - 2015      **Laboratory for industrial energy systems (LENI) – EPFL**  
PhD student in the program of Energy at EPFL. It covered many aspects from reasoning at a very fundamental level to hands on highly practical tasks. In the end it allowed me to develop skills in domain as various as project management, teaching and tutoring, automation, stochastic simulation, dynamic modelling and simulation, design of refrigerant systems, certification procedures, safety, district heating and cooling technologies, HVAC, and thermodynamics.

08.2009          **Laboratory for industrial energy systems (LENI) - EPFL**  
During this internship a test of a super-critical evaporator for a thermally driven heat-pump has been done. These series of tests have followed two semester projects, in which a model of the evaporator has been set up, the test bench has been designed/built up, and the experiment plan specified. That succession of project/internship allowed me to see many aspects of a problem, and to carry out a work from one end to the other. Furthermore it permitted me to work on a subject matter that has not been fully documented yet and in which industrials are more and more concerned about.

07 – 08.2008      **ENEFTECH / Laboratory for industrial energy systems (LENI) - EPFL**  
Internship during which an experimental small scale thermal power plant has been built. The part in which I contributed was the development of the plant control and data acquisition systems. The low performance of the technical equipment used asked for specially ingenious solutions to have a sufficiently good data acquisition.

2005 – 2015      **Theatre in Cossonay (CH)**  
Work as a film operator in a small town theatre. This job requires meticulousness, flexibility and reliability. It is also most satisfying as it is uncommon and improves my cinematographic culture.

## Projects

- 2010 – 2015      **CTI project on CO<sub>2</sub> district energy networks.**  
Project in collaboration with the engineering company Amstein & Walther Genève SA, and Geneva's utility company – SIG. The scope was on studying the potential of district heating and cooling network using CO<sub>2</sub> as a transfer fluid. My work included prospective studies regarding the energy and economic performance of the technology, but also the design and the supervision of the construction of an experimental facility and its testing. The facility was built at SIG and had to be fully certified (CE marking.) Dynamic simulation models were also developed
- 02 – 08.2010      **Thermoeconomic analysis of electricity storage concepts using thermodynamic cycles**  
In the context of my master thesis done at LENI and in collaboration with ABB Schweiz AG Corporate Research, a survey of the various possibilities for realizing electric energy storage plants based on thermodynamic cycles has been done. This survey allowed an identification of the most promising concepts both regarding technical feasibility and economic potential. Finally a multi-objective optimization (MOO) has been realized on the most interesting system.  
Three months were spent at ABB Schweiz AG Corporate Research – Baden-Dättwil. It gave me the opportunity to experience the work in a R&D department of a big company in a very stimulating multicultural environment and at the cutting edge of new technologies.
- 02 – 05.2010      **Prospective study for a small district heating in the village of Gollion**  
I carried out a prospective study during the late planning phase of a biogas plant in my village. The study was on determining whether it was possible to supply heating and domestic hot water to 5 buildings comprising 64 flats located 500 m away from the biogas plant. These buildings were to be built 6 months after the biogas plant, and the real estate company had planned to use a woodchips boiler to supply them with heat and domestic hot water. The study showed that the 426 MWh of annual heat demand could be provided almost exclusively with the cogeneration engine of the biogas plant through a 600 m district heating. This study served as a basis for an economic study conducted by Weinmann Energie, that convinced the biogas company to build the district network and the real estate company to accept using it for its buildings. The cogeneration plant and district heating operate since late 2011, a second cogeneration engine was added to the plant in 2013, two new multifamily housings have been connected and a second digester is being built.

## Publications

- S. Henchoz, C. Chatelan, F. Maréchal and D. Favrat.  
Key energy and technological aspects of three innovative concepts of District energy networks.  
*ECOS 2015, Pau, France, June 29-July 3, 2015.*
- S. Henchoz, C. Weber, F. Maréchal, and D. Favrat,  
*Performance and profitability perspectives of a CO<sub>2</sub> based district energy network in Geneva's city centre,*  
Energy, vol. 85, pp. 221 – 235, 2015.
- S. Henchoz, S. Gailledrat, J.-B. Carré and D. Favrat.  
*Dynamic Modeling and Simulation of Two-stage Compression Heat Pumps with Flash Economizer.*  
ECOS 2013, Guilin, PRC, July 16-19, 2013.
- S. Henchoz, F. Maréchal and D. Favrat.  
*Dynamic Modeling and Simulation of Two-phase Evaporators and Condensers in the context of a CO<sub>2</sub> Based District Energy Network.*  
ECOS 2013, Guilin, PRC, July 16-19, 2013.
- S. Henchoz, D. Favrat, and C. Weber,  
*Performance and profitability perspectives of a CO<sub>2</sub> based district energy network in Geneva's city center,*  
13th International Symposium on District Heating and Cooling, (Copenhagen, Denmark), 2012.
- S. Henchoz, F. Buchter, D. Favrat, M. Morandin, and M. Mercangöz,  
*Thermoeconomic analysis of a solar enhanced energy storage concept based on thermodynamic cycles,*  
Energy, vol. 45, no. 1, pp. 358 – 365, 2012.
- S. Henchoz, C. Weber, and F. Marechal,  
*On a multi-service, CO<sub>2</sub> based, district energy system for a better efficiency of urban areas,*



The World Engineering Convention, (Geneva, Switzerland), 2011.

**J. Demierre, S. Henchoz, D. Favrat,**

*Prototype of a thermally driven heat pump based on integrated Organic Rankine Cycles (ORC)*,  
Energy Volume 41, Issue 1, May 2012, Pages 10–17

**J. Demierre, S. Henchoz, D. Favrat,**

*#356 Prototype of a thermally driven heat-pump based on integrated organic Rankine cycles*,  
ECOS-2010, June 14-17 2010, Lausanne

## Awards

### **Prix Bombardier Transportation 2010**

Rewards the student of EPFL - Mechanical Engineering, having obtained the best grades over the whole Master.

### **Prix de l'Etat de Vaud 2010**

Rewards a Master Thesis at EPFL presenting an innovative solution favouring a more rational energy use.

## Competences

<b>Thermal energy:</b>	thermodynamics, heat transfer, energy integration, two-phase flows, modelling and optimisation of energy systems, thermal turbomachinery, CFD analysis.
<b>Hydro power:</b>	hydro power constructions, cavitation phenomena, transient in hydroelectric power plants, hydraulic turbomachinery, dams, CFD analysis.
<b>Automation:</b>	control of dynamic systems, PID controller, state-space controller, RST controller, analysis and identification of dynamic systems, control of electrical power-trains.
<b>Computer programming:</b>	MatLab, LabVIEW, VALI Modeller, Catia, Fluent, Star CCM+, C++
<b>Others:</b>	PED certification, optimisation, stochastic based simulation, dynamic modelling and simulation, data acquisition.

## Languages

<b>French</b> Native language	<b>English</b> Fluent (C2)	<b>German</b> Upper intermediate (B2)
----------------------------------	-------------------------------	--

## Interests

- Glider pilot between 2000 and 2010 at *groupe vaudois de vol à voile de Montricher*
- Actor between 2003 and 2014 in the theatrical company *Proz'Act*.
- Photography.